ESTIMATING EXPOSURE TO TRAFFIC-RELATED POLLUTION WITHIN A GIS ENVIRONMENT

Thesis submitted for the degree of
Doctor of Philosophy
at the University of Leicester

Cornelis (Kees) de Hoogh

March 1999

TABLE OF CONTENTS

APPENDICES

LIST OF FIGURES AND TABLES

Figures

Tables

ACKNOWLEDGEMENTS

The thesis you are about to read is the product of four years work. Without the help of the many people I met during this period, this would not have been possible.

Firstly and foremost, I would like to thank David Briggs. His support, patience, persistence, inspiration, enthusiasm and generosity made it an enjoyable and stimulating four years. Back in February 1995 he was brave enough to allow me back for the second time (after a 6 month placement) to the, at that time, Institute of Environmental and Policy Analysis (IEPA) in Huddersfield. Secondly I would like to thank Simon Kingham for his help and friendship during the Huddersfield period and beyond. He was, together with Dave, the initiator of this research.

In the mean time, David became Director of Research at the Nene Centre for Research (Northampton), subsequently leaving a trail of people who were to follow him. After Simon left Huddersfield as well (and IEPA ceased to exist) it was time for me to leave the hills behind me and descend on Northampton. I would like to thank all people at NCR, and in particular Maria, Lynn, Michelle, Charlotte and Emma, for supporting me throughout. John Gulliver and Dominic Tantram for helping me out on numerous occasions with computer related problems. To John McClatchey for keeping an eye on the quality of the work. And to John Wills, who as a friend, business partner and house mate, kept me going all the way.

The Sheffield case study was a collective effort and I would like to thank Jeremy Bullard and Paul Elliot (St Mary's Hospital Medical School and Imperial College of Science and Technology) and David Strachan (St George's Hospital Medical School) for their enthusiasm in completing the project. To Frank Price and Andy Elleker (Sheffield City Council) for providing me with the data.

And finally I would like to thank Nicky Seth, for putting up with me over the last half year, for her support and patience.

ABSTRACT

This thesis applies, evaluates and compares methods for estimating exposure to traffic-related pollution within a GIS environment. The methods were used in two contrasting case studies; Greater London and Sheffield, where they were selected on basis of data availability and resolution. The methods used in this research were CALINE3, DMRB, ADMS-Urban and ISC3 (air pollution dispersion models), kriging and co-kriging (spatial interpolation), SAVIAH (regression method) and traditional exposure indicators. Calculated estimates were validated by comparing them to monitored NO_2 data. In the Sheffield case study the best methods were then used to analyse relationships between traffic-related pollution and respiratory health.

Evaluation of the performance of the various methods found that none of the methods used in Greater London worked very well, although ISC3 and kriging tended to give more reliable results. In Sheffield DMRB and SAVIAH gave the best estimates of monitored pollution levels. Traditional exposure indicators were only used in Sheffield of which 'density of main roads within 150 metres', 'traffic flow within 150 metres' and 'HGV flow within 150 metres' provided the most reliable estimates. In general, the quality of all exposure measures was highly dependent on the quality of input data. This is largely due to the fact that most variation of traffic-related pollution occurs close to main roads. In Greater London the quality of data was clearly inadequate. In Sheffield, where data was of a higher quality, results were better. No substantial or significant associations were found between the exposure measures and health outcome in the Sheffield case study.

In Sheffield, this research also showed that passive sampling of NO_2 provided a reliable measure of relative levels of air pollution across an urban area. It also showed that none of the models were able to detect raised NO_2 concentrations due to accumulation of pollution from the city, as a result of wind direction.

The results of this research show that, although the methods used here can help in the investigation of relationships between traffic-related pollution and health, there is a major need to improve methods for modelling exposure to air pollution. An important development could be to link different models together within a GIS environment, in order to improve the ability to use available information and exploit the different capabilities of the models. In order to detect the effects of traffic-related pollutants on chronic health, estimates are needed across large populations. Linkage of the methods applied here, would be particularly useful to model spatial and temporal variations in these types of studies.

1 INTRODUCTION

1.1 RATIONALE

The impact of environmental pollution on public health has been of growing concern in recent years. World-wide, the premature death of millions of people - especially infants and children - and the ill health or disability of hundreds of millions more, can be attributed to contaminants in the human environment. These pollutants reach the human body through a range of pathways, via the water, food, air and soil (WHO 1992).

Particular concern is focused on the effects of air pollution on respiratory illness. Asthma, for example, has been on the increase across the world for the last 40 years. Over the last twenty years in the UK, there has been a 50% increase in the prevalence of childhood asthma and at least a ten-fold increase in hospital admissions for asthma amongst children. Currently, about 10% of children are diagnosed as having asthma, while a further 5% show asthmatic symptoms but have not been diagnosed. About 4-6% of adults have also been diagnosed as asthmatic. *Figure 1.1* shows trends in attack rates for asthma for England, Scotland and Wales. The number of undiagnosed asthma sufferers amongst adults is unknown, but is almost certainly substantial. The total cost of asthma to the UK is estimated at about £1 billion per annum (Committee on Medical Effects of Air Pollutants 1995).

At the same time there has been a world-wide increase in levels of road traffic. Between 1970 and 1990 in Latin America, for instance, the vehicle fleet grew by 250% to 37 million vehicles (Onursal and Gautam 1997); in Europe, during the same period, passenger car transport increased by 3.4% per annum (Stanners and Bordeau 1995). In the United Kingdom, the number of licensed motor vehicles increased by 210% between 1970 and 1996, to a total of 21 million cars. At the same time the use of cars has doubled since 1970 (see also *Figure 1.2*) (DETR 1997a).

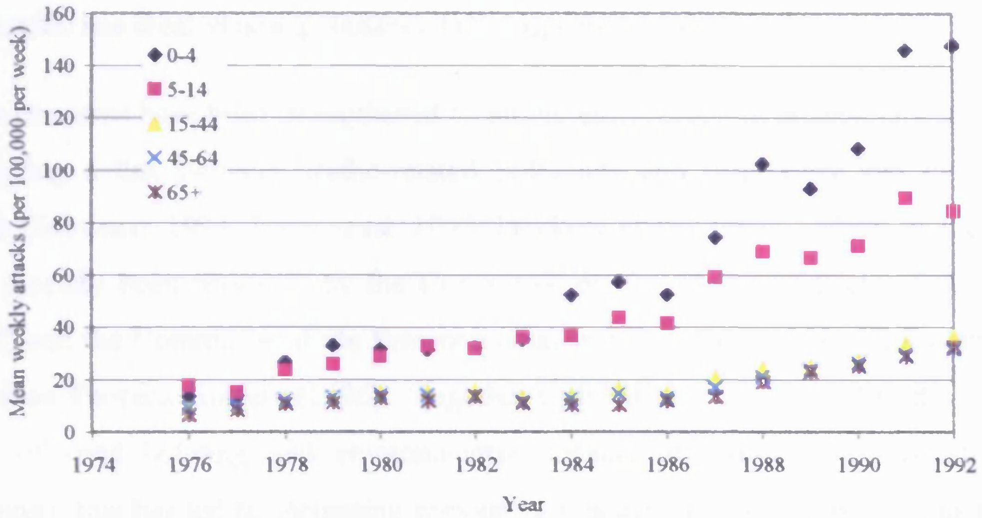

Figure 1.1: Mean weekly attack rates for acute asthma (per 100,000 per week) recorded by RCGP Weekly Return Service, both sexes, by age, England, Scotland and Wales, 1976-92 (Committee on Medical Effects of Air Pollutants 1995)

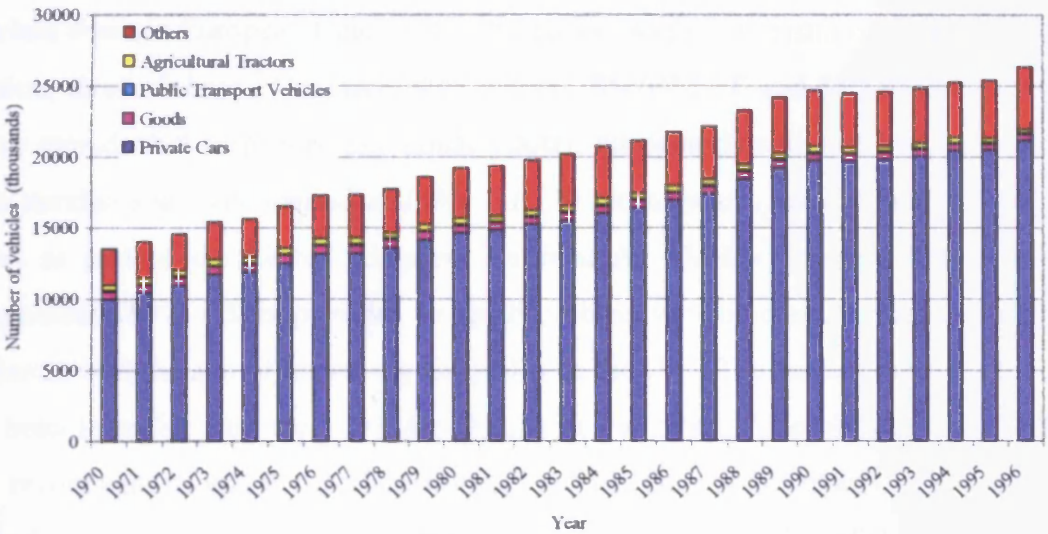

Figure 1.2: Motor vehicles currently licensed in Great Britain (1970-1996)(DETR 1997a).

Against this background, the exposure of people to traffic-related air pollution is a special concern. More than 1000 million people world-wide live in urban areas and are therefore potentially exposed to high levels of traffic-related pollution. In Europe, urban air pollution remains a problem despite great improvements in air quality: whilst industrial restructuring, technological innovation and pollution control has led to a reduction in levels of traditional pollutants, such as sulphur dioxide (SO_2) and black smoke, rapid growth in road traffic has created new pollutants, bringing new concerns.

These concerns have been strengthened by an increasing body of epidemiological evidence, suggesting a link between traffic-related pollutants and respiratory and cardiovascular health (Schwartz 1993, Pope *et al.* 1995, Dockery *et al.* 1993). Many of these studies have recently been reviewed by the Committee on the Medical Effects of Air Pollution (1995) and the Committee of the Environmental and Occupational Health Assembly of the American Thoracic Society (1996). Together with concern about road traffic congestion, costs of road building and environmental impacts of road traffic (including global warming), this has led to increasing pressure for policy action to control road traffic and reduce health risk.

One of the main strategies for reducing health risks and impacts on the environment has been the introduction of air quality standards. The UK air quality standards are based on those laid down in European Union (EU) Directives. Reflecting historic concerns about air pollution, three of these - Directives 80/779/EEC, 85/203/EEC and 85/210/EEC – refer to sulphur dioxide and suspended particulate matter, nitrogen dioxide and lead, respectively. These standards are summarised in *Table 1.1*. In recent years, these standards have been revised as part of the United Kingdom National Air Quality Strategy (Department of Environment 1997). This provides air quality objectives for concentrations of eight air pollutants, with the aim of improving air quality in the UK. The target objectives for 2005 have been formalised by the 1997 *Air Quality Regulations*. The objectives are derived from recommendations of the Expert Panel on Air Quality Standards (EPAQS). The standards of relevance to traffic-related pollutants are presented in *Table 1.2*, including recent announcements by the government have stated that those for NO_2 and PM_{10} would be relaxed (DETR 1998b).

The government's recent White Paper on the future of transport (DETR 1998a) takes this even further, by requiring local authorities to set up air quality management areas (AQMAs) where air quality standards are likely to be breached:

> "Local authorities have a duty to assess air quality in their areas to determine whether the objectives set out in the Strategy, and prescribed in the Air Quality

Regulations 1997, are likely to be met by 2005. Where a local authority considers that one or more of the objectives is not likely to be met, as a result of national measures alone, it must declare an air quality management area, covering the area where the problem is expected" (DETR 1998a p124).

Table 1.1: UK Air Quality Standards Based on EU Directives 80/779/EEC, 85/203/EEC and 85/210/EEC

Substance	Reference Period and Criteria	Limit Value [(a)] ($\mu g\ m^{-3}$)	Guide Value [(b)] ($\mu g\ m^{-3}$)
Sulphur dioxide	Median of daily mean Values over a year	80 (particulates >40) 120 (particulates <40)	-
	Arithmetic mean of daily mean values over a year	-	40-60
	98th percentile of daily mean values over a year	250 (particulates >150) 350 (particulates <150)	-
	24 hour daily mean value	-	100-150
Nitrogen dioxide	50th percentile of hourly mean values over a year	-	50
	98th percentile of hourly mean values over a year	200	135
Lead	Annual mean concentration	2	-
Suspended particulate matter (as measured by the gravimetric method)	95th percentile of daily mean values over a year	300	-
	Arithmetic mean of daily mean values over a year	150	-
Suspended particulate matter (as measured by the OECD black smoke method)	98th percentile of daily mean values over a year	250	-
	Arithmetic mean of daily mean values over a year	-	40-60
	Annual median of daily mean values over a year	80	-
	24 hour daily mean value	-	100-150

(a) Limit values must not be exceeded throughout the territory of the Member States during specified periods and under conditions laid down in the Directives.
(b) Guide values are intended to serve as long term precautions for health and the environment.

Table 1.2: NAQS Objectives

Substance	Concentration ($\mu g\ m^{-3}$)	Reference Period	Form of Compliance
Benzene	16	Running annual mean	100^{th} %ile
1,3-Butadiene	2.2	Running annual mean	100^{th} %ile
Carbon monoxide	11,700	Running 8-hour mean	100^{th} %ile
Lead	0.5	Annual mean	100^{th} %ile$^{(a)}$
Nitrogen dioxide	200	1 hour mean	99.8^{th} %ile$^{(a)}$
	40	Annual mean	
Ozone	100	Running 8-hour mean	100 $\mu g\ m^{-3}$ as 97^{th} %ile $^{(a)}$
PM_{10}	50	Running 24-hour mean	50 $\mu g\ m^{-3}$ as 90^{th} %ile $^{(a)}$
Sulphur dioxide	267	15 minute mean	267 $\mu g\ m^{-3}$ as 99.9^{th} %ile $^{(a)}$

(a) Objectives to be treated as provisional.

An action plan has to be drawn up for each air quality management area, after consultation with the public and organisations such as the local health authority, identifying measures which can help to achieve the air quality objective. The White Paper acknowledges that air quality management areas are likely to be places where most of the pollution comes from road transport.

The establishment of air quality management areas, monitoring of their effectiveness, and the assessment of health risks to air pollution clearly depend upon knowledge about the spatial distribution of traffic related pollution at a local scale. Data on air pollution are, however, extremely limited. Although the DETR (through NETCEN) maintains a national air quality monitoring network, the number of stations in this network remains relatively small. By 1998 there were only about 50 sites monitoring nitrogen dioxide (NO_2) on a continuous basis, and about 40 sites monitoring fine particulates. A national passive sampler network of about 1200 sites does exist for NO_2, but even this provides only a scanty framework on which to base air quality management areas. Local authorities do also carry out their own monitoring to a limited degree, but without information on likely hotspots, it is difficult to ensure that these are located most effectively.

In order to meet these policy requirements there is thus an urgent need for methods to model and map air pollution at a small scale. This is needed both to help identify air quality management areas or hotspots and to provide estimates of exposure for epidemiological studies and health risk assessment. Modelling air pollution at a small area scale nevertheless poses major challenges because of the local and short-term variations in air pollution. A number of recent developments in monitoring, dispersion modelling and spatial analysis, however, do provide the capability to produce detailed information on the spatial patterns of air pollution.

One of the most important developments in this context has been the introduction of Geographic Information Systems (GIS). A GIS brings together geographic information in a computer environment and provides tools to edit, query and analyse the data spatially. It thus provides the facility to create an environment in which air pollution models and assessment methods can be implemented and in which air pollution maps can be generated. GIS are now widely used as a basis for pollution modelling and mapping for epidemiological or policy applications. A range of uses of GIS for health-related analysis and applications are described by Gatrell and Löytönen (1998), Briggs and Elliot (1995) and Vine (1997). Teppo (1998), for example, uses GIS with cancer data in Finland, and Trinca (1998) describes GIS applications for environment and health in Italy. Dalbokova *et al.* (1999) used GIS to map the distribution of cancers in relation to air pollution hotspots and to analyse exposures to nitrate in drinking water in Bulgaria, while Vincze *et al.* (1999) explored unexpected relationships between iodide in drinking water and liver cirrhosis in Hungary. Gatrell and Dunn (1995) modelled the possible association between cancer of the larynx and incineration in north-west England within a GIS, and Kingham *et al.* (1995) used GIS as a framework for testing for clustering of health events. Wilkinson *et al.* (unpublished) obtained indicators using GIS to study the relationship between road traffic in north-west London and hospital admission with asthma in children. SEIPH (1997) and Briggs *et al.* (1997) also employed GIS techniques to model and map urban air pollution, in Greater London and Huddersfield respectively. GIS was also used by Wang and Stauffer (1995) to analyse the environmental impact in a traffic relief study, and by Souleyrette *et al.* (1992) to investigate the relationship between transportation and air quality in Las Vegas. The use of GIS is not confined to studies of air pollution. Other applications include hydrologic modelling (Moore 1996), integrated environmental impact modelling for oil and chemical spills (French and Reed 1996), atmospheric modelling (Lee and Peilke 1996), water quality modelling (Cronshey *et al.* 1996), and groundwater modelling (D'Agnese *et al.* 1996).

1.2 AIMS AND OBJECTIVES

The general aim of this thesis is:

to apply, evaluate and compare methods for estimating exposure to traffic-related pollution, within a GIS environment, as a basis for epidemiological and policy applications.

Within this context, the specific objectives are:

1. to review the available methods;
2. to apply selected methods in two contrasting areas;
3. to validate the methods against monitored data;
4. to evaluate the performance of the various methods in terms of their accuracy and ease of application;
5. to identify, on the basis of this analysis, the most robust and reliable methods;
6. to apply the preferred methods to analyse relationships between traffic-related pollution and respiratory health in a detailed case study; and
7. to consider the implications of the results for wider application for epidemiological purposes.

1.3 STRUCTURE OF THE THESIS

This Chapter has set the context within which this research has been conducted and defined the aims of the research. Following chapters are structured as follows:

- Chapter 2 presents a review of the literature on traffic-related air pollution and its links with health, and reviews methods for assessing and mapping exposure to air pollution.
- Chapter 3 describes the exposure assessment methods used in this research and describes results of piloting several of these methods as part of this study.

- Chapter 4 presents the case study in Greater London. It describes the application of the selected methods and presents results.

- Chapter 5 describes the case study in Sheffield. It describes the background to the study, outlines the methods and data sources used and presents results.

- Chapter 6 analyses and interprets the results from the two case studies, and attempts to test and compare the performance of the various methods as a basis for exposure assessment. For the Sheffield study area, it also presents an analysis of the relationship between the various exposure estimates and health outcome.

- Chapter 7 reviews the findings and conclusions of the research, considers their practical implications and presents suggestions for future work.

2 LITERATURE REVIEW

2.1 TRAFFIC-RELATED POLLUTION

2.1.1 Traffic growth

Traffic-related problems in cities across the world are caused by a variety of interrelated factors. Urban populations and household incomes have grown, leading to an increase in car ownership, causing in turn a demand for more roads. Increases in industrial and business activity have led to a rise in freight traffic both between and within urban areas. All these factors together have resulted in an increase in the impact of environmental pollution caused by road traffic (WRI 1996).

In the United Kingdom, length of roads increased from 322,484 kilometres in 1970 to 368,820 in 1996 (DETR 1997a). Over the same period, the number of licensed vehicles has grown steadily, almost doubling to a total of over 26 million vehicles, mainly as a result of increases in the number of private cars *(Figure 1.2)*. The use of vehicles has more than doubled since 1970 (*Figure 2.1*), again largely due to increases in the use of vehicles and taxis. *Figure 2.2* shows the passenger transport by different modes of transport. Vehicles and vans account for most of the growth in passenger kilometres: whilst these accounted for only 74% of total vehicle kilometres travelled in 1970, by 1996 their share had increased to 87%.

The increase of road traffic has led to a range of impacts in urban areas, including severe traffic congestion in many cities, increased energy consumption, increased air and noise pollution, and high levels of traffic accidents (WRI 1996). Congestion, for instance, costs the UK about £15 million per year (Bly and Dasgupta 1995) and road traffic has been identified as the main source of noise in the UK in two independent surveys (Royal Commission on Environmental Pollution 1995). Possibly the most important impact of road traffic, however, both socially and environmentally is air pollution. A recent study of the economic impacts of road traffic in Europe, for example, has suggested that health costs due to air pollution (in terms of hospital costs, lost days at work and health insurance costs) outweigh all other costs of road traffic combined (ApSimon, Imperial College 1997, pers. comm.)

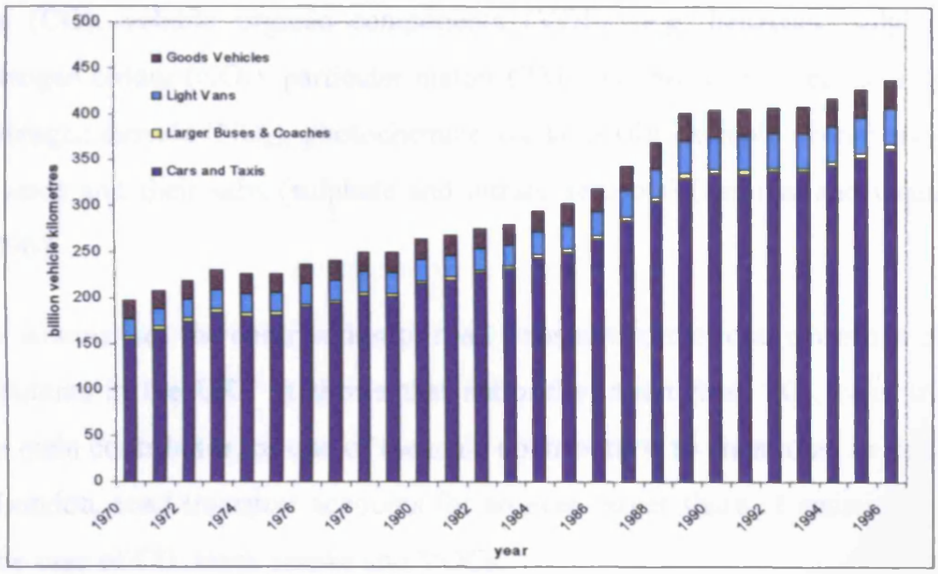

Figure 2.1: Road traffic by type of vehicle in Great Britain (1970-1996) (DETR 1997a).

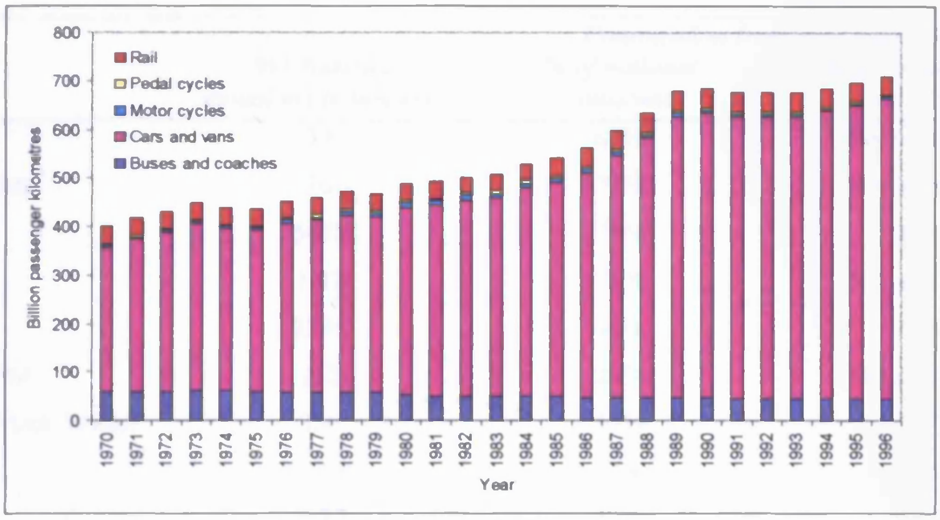

Figure 2.2: Passenger transport in Great Britain (1970-1996) (DETR 1997a)

2.1.2 Air pollutant emissions from motor vehicles

Air pollutants can be categorised into two groups: primary pollutants - those that are emitted directly into the atmosphere; and secondary pollutants – those that are formed in the atmosphere as a result of chemical reactions (such as hydrolysis, oxidation or photochemical reactions) with primary pollutants.

Primary pollutants emitted by motor vehicles include carbon dioxide (CO_2), carbon monoxide (CO), volatile organic components (VOCs, e.g. benzene), sulphur dioxide (SO_2), nitrogen oxides (NO_x), particular matter (PM) and lead (Pb). Secondary pollutants include nitrogen dioxide (NO_2), photochemical oxidants (for example ozone) and sulphuric or nitric acids and their salts (sulphate and nitrate aerosols) (Onursal and Gautam 1997; Elsom 1996).

Table 2.1 summarises the contribution of road transport to the total emissions of some of these pollutants in the UK. It shows that nationally, apart from SO_2, road transport is either the main contributor, or one of the main contributors, to emissions. In an urban area such as London, road transport accounts for an even larger share of emissions, well over 90% in the case of CO, black smoke and VOCs.

Table 2.1: Contribution from road transport to UK emissions (DETR 1997b)

		Contribution from road transport	
	1995 National emissions (k tonnes)	***% of national emissions***	***% of emissions in London***
Benzene*	39	67%	Not available
1,3-Butadiene*	10	77%	Not available
CO	5478	75%	99%
Lead	1.47	78%	Not available
NO_x	2295	46%	76%
Particles PM_{10}	232	26%	Not available
Black Smoke	356	50%	94%
SO_2	2365	2%	22%
VOC	2337	29%	97%

* 1994 estimates used

Many different factors nevertheless affect rates of emission from road traffic. One of the most important is traffic speed. *Figures 2.3* and *2.4* show the relationship between traffic speed and emission rates (expressed as ratios compared to a reference speed of 100 km/hr) for CO, CO_2, HC, NO_x and PM for light and heavy duty vehicles (Department of Transport 1994). These figures clearly show high emission rates for all pollutants at low speed, decreasing with higher speeds until a turning point after which the emission rate increases slightly again. The turning point differs between different pollutants but is generally around 60 to 80 km hr^{-1}. In urban areas, where traffic speeds are generally low, the emission rate of traffic related pollutants will thus tend to be relatively high. Notably, also, management schemes aimed at reducing traffic speed may actually increase rather than reduce levels of emission of many pollutants. By the same token, traffic congestion, which reduces traffic speeds and increases the length of time which vehicles are stationary, also increases emission levels. Another important factor is engine temperature. Cold engines have higher emission rates, with the result that short journeys tend to be more polluting than longer journeys. In recent years, the trend in Britain has been towards shorter journeys, as cars are used increasingly for shopping trips, personal business and the 'school run'. These now account for about two-thirds of all journeys and about 60% of total distance travelled. Journeys of less than 8 km now make up about 75% of all trips (Royal Commission on Environmental Pollution 1995).

Other important determinants of emission levels include engine and fuel design. The introduction of catalytic converters and the shift from petrol to diesel engined vehicles have been major factors in this context. Use of catalytic converters has undoubtedly helped to control emissions of some pollutants, such as NO_x, but the fact that they are less effective at low running temperatures (and may actually increase emissions in these conditions) has significantly limited their impact. Diesel engines are beneficial in that they emit lower levels of some pollutants, including CO_2 and NO_x, but conversely result in higher emissions of fine particulates. A major force for technological developments of these sorts is environmental policy. Vehicle emission standards set out in EU Directives are designed to restrict exhaust emissions. These Directives are amended from time to time. *Table 2.2* shows how emission standards for light duty vehicles have been tightened since the early 1980s (Department of Transport 1994).

Figure 2.3: Correction factor for traffic related pollutant emissions for light duty vehicles at speed other than 100 km hr-1 (Department of Transport 1994)

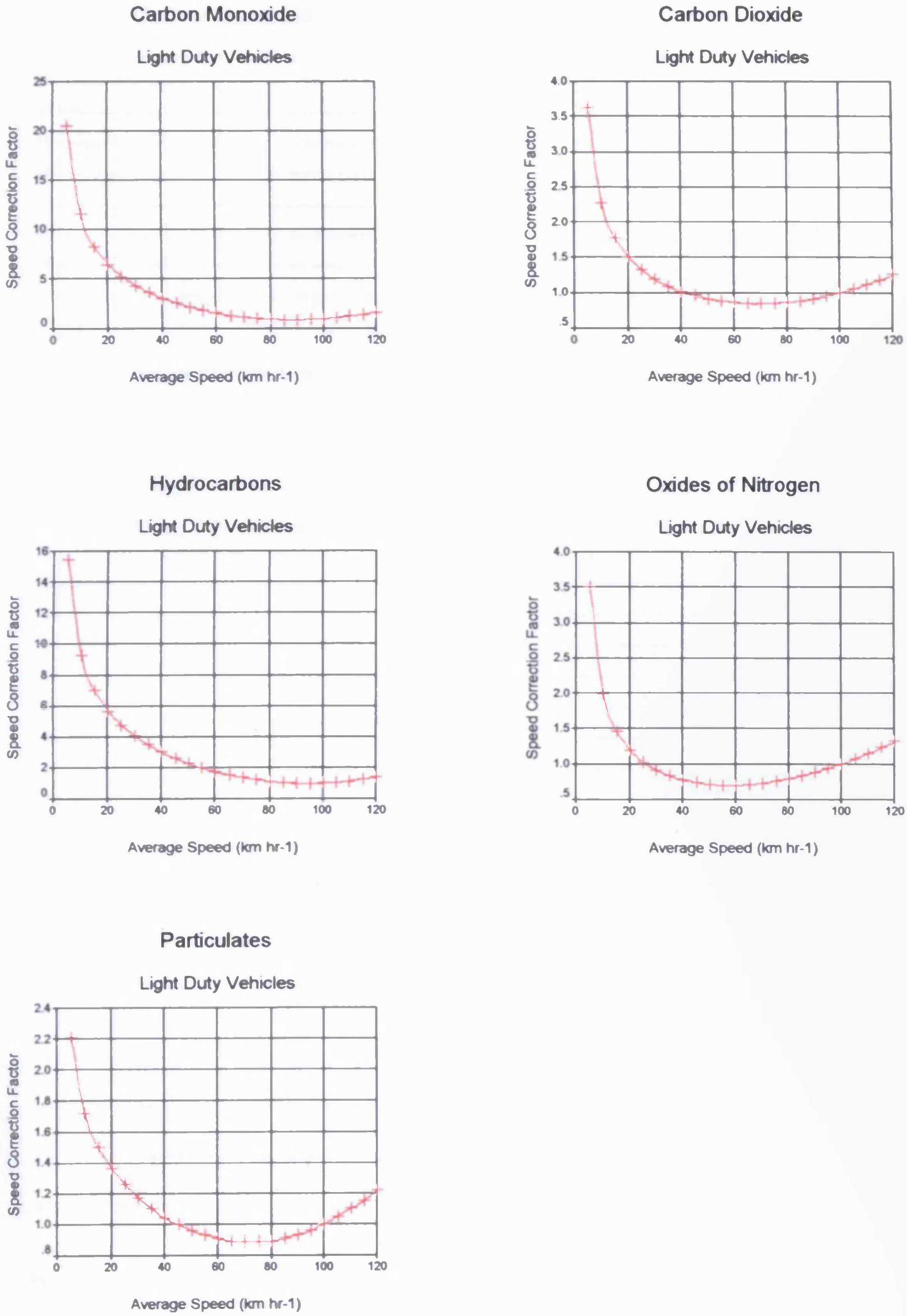

Figure 2.4: Correction factor for traffic related pollutant emissions for heavy duty vehicles at speed other than 100 km hr-1 (Department of Transport 1994)

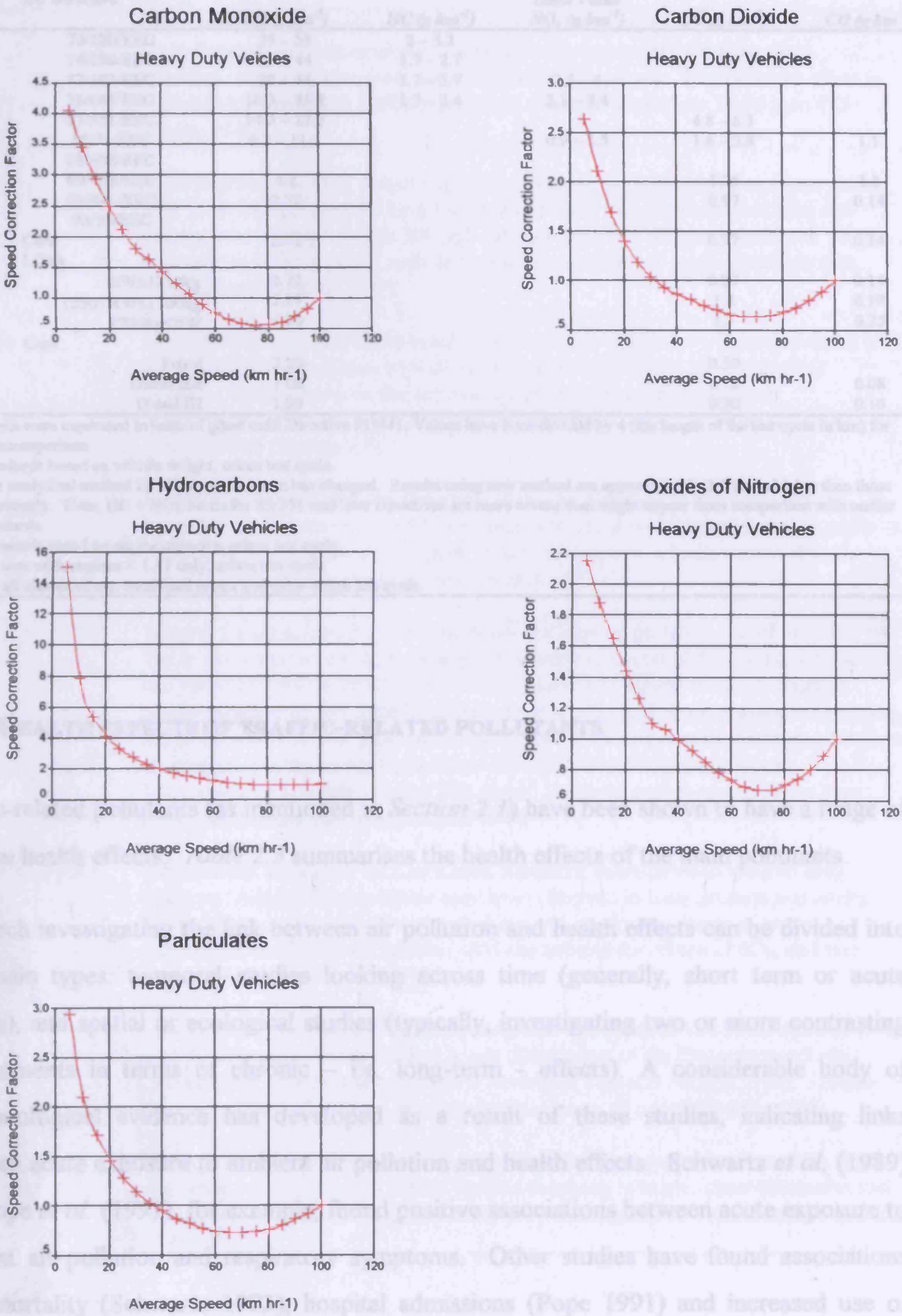

Table 2.2: Vehicle exhaust emission control history. Light duty vehicles (Department of Transport 1994)

Year	EC Directive		Limit Value			
		CO ($g\ km^{-1}$)	HC ($g\ km^{-1}$)	NO_x ($g\ km^{-1}$)	CO ($g\ km^{-1}$)	CO ($g\ km^{-1}$)
1970[a]	70/220/EEC	25 – 55	2 – 3.2			
1974[b]	74/290/EEC	20 – 44	1.7 – 2.7			
1977[b]	77/102/EEC	20 – 44	1.7 – 2.7	2.5 – 4		
1978[b]	78/665/EEC	16.3 – 35.8	1.5 – 2.4	2.1 – 3.4		
1983[b,c]	83/351/EEC	14.5 – 27.5			4.8 – 6.5	
1988[d]	88/76/EEC	6.3 – 11.3		0.9 – 1.5	1.6 – 3.8	1.1
	88/438/EEC					
1989[e]	89/458/EEC	4.8			1.25	1.1
1991[f]	91/441/EEC	2.72			0.97	0.14
1993[f]	93/59/EEC					
	Cars	2.72			0.97	0.14
	LCVs					
	RW≤1250kg	2.72			0.97	0.14
	1250<RW≤1700kg	5.17			1.4	0.19
	1700kg<RW	6.90			1.7	0.25
1994[f]	Cars					
	Petrol	2.20			0.50	
	Diesel IDI	1.00			0.70	0.08
	Diesel DI	1.00			0.90	0.10

(a) Limits were expressed in units of g/test until Directive 91/441. Values have been divided by 4 (the length of the test cycle in km) for intercomparison
(b) Standards based on vehicle weight, urban test cycle.
(c) The analytical method for HC measurements has changed. Results using new method are approximately 2.3 times higher than those previously. Thus, HC + NOx limits for 83/351 and later Directives are more severe than might appear from comparison with earlier standards.
(d) Standards based on engine capacity, urban test cycle.
(e) For cars with engines < 1.41 only, urban test cycle.
(f) For all classes of car, combined urban and extra-urban test cycle.

2.2 HEALTH EFFECTS OF TRAFFIC-RELATED POLLUTANTS

Traffic-related pollutants (as mentioned in *Section 2.1*) have been shown to have a range of adverse health effects. *Table 2.3* summarises the health effects of the main pollutants.

Research investigating the link between air pollution and health effects can be divided into two main types: temporal studies looking across time (generally, short term or acute studies), and spatial or ecological studies (typically, investigating two or more contrasting environments in terms of chronic – i.e. long-term - effects). A considerable body of epidemiological evidence has developed as a result of these studies, indicating links between acute exposure to ambient air pollution and health effects. Schwartz *et al.* (1989) and Pope *et al.* (1991), for example, found positive associations between acute exposure to ambient air pollution and respiratory symptoms. Other studies have found associations with mortality (Schwartz 1993), hospital admissions (Pope 1991) and increased use of asthmatic medication (Pope *et al.* 1991). Many of these studies have been recently reviewed by the Committee on the Medical Effects of Air Pollution (1995).

Table 2.3: Health effects of traffic-related pollutants

Pollutant	Health effects
CO	CO interferes with the absorption of oxygen by heamoglobin (Hb) (CO binds with Hb to form carboxyhaemoglobin (COHb) occupying oxygen-binding sites), increases cardiovascular disease and can affect the nerves. Threshold for effect is ~2% COHb, equivalent to 8hr exposure at moderate activity to 15-20 ppm CO (Elsom 1996).
NO_2	Acute exposure to NO2 causes respiratory disease, such as coughs and sore throat. NO2 probably worsens the lung function of people with chronic bronchitis and asthma at levels higher than 300 ppb (not confirmed by all studies) (Elsom 1996). Exposure to NO2 is linked with increased susceptibility to respiratory infection (Onursal and Gautam 1997)
Benzene	Benzene has toxic and carcinogenic effects. Toxic effects have been associated with the central nervous system as well as the hematological and immunological systems. Toxic effects on the nervous system have been observed with concentrations of 1,000 ppm or higher. Carcinogenic effects include leukemia (Onursal and Gautam 1997)
PAH	PAH are mutagenic and carcinogenic. They get absorbed in the lungs and the intestines and are metabolized in the human body. It is estimated that 9 in every 100,000 people exoposed to 1 $\mu g/m^3$ of benzo[a]pyrene, a PAH, over a lifetime, would develop cancer (Onursal and Gautam 1997)
Ozone	Adverse health effects of ozone can occur at exposure periods as short as 5min. Ozone can cause severe damage to lung tissues and impair defences against bacteria and viruses (Onursal and Gautam 1997). Short term effects of ozone begin at hourly averages of 200 $\mu g/m^3$ and include: eye, nose and throat irritation, coughing, throat dryness, thoracic pain and chest tightness. A decrease in pulmonary function in children and young adults has been reported at hourly average ozone concentrations between 160 and 300 $\mu g/m^3$. Long term exposure to ozone may reduce pulmonary function (Romieu 1990)
Particulate matter	PM has been associated with increased mortality, morbidity and reduced lung function. Adverse health effects have been observed in both children and adults. These effects are associated with coughing and respiratory diseases such as pneumonia, asthma and bronchitis. PM exacerbates the effects of SO_2, and vice versa (Onursal and Gautam 1997).
Lead	Lead causes impairment of brain development and function in infants and children, even at seemingly low blood lead levels (Committee of the Environmental and Occupational Health Assembly of the American Thoracic Society 1996). Effects have been detected at blood lead levels of less than 10 $\mu g/dl$ (Romieu 1990).
SO_2	SO_2 is associated with reduced lung function and increased risk of mortality and morbidity. Adverse health effects include coughing, phlegm, chest discomfort and bronchitis. SO2 exacerbates the effects of PM, and vice versa (Onursal and Gautam 1997)

Epidemiological studies looking at chronic effects across *space* in two (or more) contrasting environments - e.g., polluted/unpolluted cities, urban/rural areas - are less common. Recent examples are given by studies in Germany, contrasting symptom occurrence in the former West Germany with that in the former German Democratic Republic (Mutius *et al.* 1992), and the six cities study in the US which reported an association between particulate levels and mortality (Dockery *et al.* 1993). One problem with these studies, compared to the temporal studies, is that they are affected by major (and often unmeasured) ecological confounding by socio-demographic and lifestyle factors, as different populations are being compared. Recent advances in small area methodologies may offer help in reducing these difficulties (Elliott *et al.* 1992).

Various studies have been carried out to investigate the link between chronic exposure to traffic-related pollution and respiratory illness. *Table 2.4* gives an overview of some of these studies and summarises the key results. Five recent studies, which are indicative of these chronic investigations, will now be described in more depth.

In a recent Dutch study, Brunekreef *et al.* (1997) examined lung function in children living near major motorways. Six areas were chosen with homes located close to major motorways, carrying 80,000 to 152,000 vehicles per day. Exposure to traffic-related pollution was assessed, firstly, by measuring the distance (in metres) of home and school to motorway on 1:1,000 scale maps. Secondly the traffic density was classified, using weekday counts of motorway traffic for 1993. Thirdly, indoor PM_{10} (using low-volume impactors), black smoke (using PM_{10} filter reflectance) and NO_2 (using Palmes tubes) concentrations were measured in 12 of the 13 participating schools during two months. Lung function was measured using Vicatest-5 rolling seal spirometers. For each child the following parameters were recorded: Forced Vital Capacity (FCV), Forced Expiratory Volume (FEV), Peak Expiratory Flow (PEF) and Forced Expiratory Flow (FEF). Information on age, gender, parental respiratory symptoms, smoking in the home, pets, damp, ethnicity, number of persons in household, gas cooking, gas-fired and socio-economic status were obtained to allow for control on potential confounders. Truck traffic density was found to be related to FEV, PEF and FEF for children living within 1,000m of the motorways with estimated effects ranging from –2.5% for FEV to –8.0 % for PEF, per 10,000 trucks. Black smoke and automobile traffic density also tended to be negative,

Table 2.4 Literature investigating relationships between exposure to traffic pollution and respiratory illness.

Location	*Exposure estimate*	*Population*	*Ascertainment*	*Results*	*Reference*
Japan	Distance from main road: <20m, 20-50m and 50-150m	Age 4-11	Parental reporting	High prevalence of respiratory symptoms of roadside residents.	Murakami *et al.* 1990
Tokyo, Japan	Distance from road: 0-20m and 20-150m Measured NO_2	Females age 40-60	Self reporting	Exposure to automobile exhaust may be associated with an increased risk of certain respiratory symptoms	Nitta *et al.* 1993
Munich, Germany	Traffic flow on busiest road in school district: per 25,000 veh/day	Age 9-11	Parental reporting	High traffic flows diminish forced expiratory flow and increase respiratory symptoms in children.	Wjst *et al.* 1993
Birmingham, UK	Distance from road: <200m, 200m – 500m, > 500m Traffic flow: <24,000 v >24,000 veh/24h	Age 0-4	Hospital admissions	Children admitted to hospital for asthma are more likely to live in an area with high traffic flow along the nearest main road. It suggests that living along busy roads may have an adverse health effect of young children, especially those with asthma, but it did not show a causal association	Edwards *et al.* 1994
Bochum, Germany	Self-reported traffic index: "high" v "low"	Age 12-15	Self reporting	The results support a possible role of factors associated with automobile exhausts causing or exacerbating asthma symptoms and allergic rhinitis in children	Weiland *et al.* 1994
Stockholm, Sweden	Estimated outdoor NO_2	Girls: 4mths-4yrs Boys: 4mths-4yrs	Hospital admissions	The results suggest that exposure to combustion products containing NO_2 may be of particular importance for developing wheezing bronchitis in girls	Perhagen *et al.* 1995

Location	*Exposure estimate*	*Population*	*Ascertainment*	*Results*	*Reference*
Münster, Germany	Self-reported truck traffic: "constant" v "never"	Age 12-15	Self reporting	Results support that exposure to motor vehicle traffic is related to symptoms of asthma and allergic rhinitis in children, although misclassification due to self-reports of traffic exposure cannot be ruled out	Duhme *et al.* 1996
London, UK	Distance from road: <150m v >150m	Age 2-15	GP diagnosis	No increase in risk of asthma with living close to busy roads.	Livingstone *et al.* 1996
Haarlem, Netherlands	Modelled traffic pollution: "high" v "low" (model: CAR)	Age 0-15	Parental reporting	The results suggest that living along busy streets increases the risk of developing chronic respiratory symptoms in children.	Oosterlee *et al.* 1996
Six areas near motorways, Netherlands	Distance home/school from motorway Traffic density Measured NO_2/PM10 indoor and outdoor	Age 7-12	Parental reporting	The results indicate that the exposure to traffic-related air pollution, in particular diesel exhaust particles, may lead to reduced lung function in children living near major motorways	Brunekreef *et al.* 1997
London, UK	Distance from main road: >150m v <150m Traffic volume within 150m: >50,000 v <1,500 veh/day	Age 5-14	Hospital admissions	No association was found between risk of hospital admission for asthma or respiratory illness among children and proxy markers of road traffic pollution	Wilkingson *et al.* (unpub)
Huddersfield (UK), Amsterdam (NL), Prague (Czech Rep.) and Poznan (Poland)	Outdoor NO_2 levels calculated with the SAVIAH model.	Age 7-11	Parental reporting	No significant association were found between predicted outdoor air pollution at residence of child and respiratory symptoms	Elliot and Briggs 1998

whereas NO_2 was only negative with FEF. When the analysis was restricted to children living within 300m of motorways, the estimated effects of truck traffic density on forced vital capacity (FVC) and FEV increased. Similar increases were found for black smoke on all lung function parameters and for automobile traffic density and NO_2 on FEF. Stratified analysis on gender showed that the estimated effect of truck traffic density were stronger in girls than in boys. For example, the percentage change in FVC for girls living within 300 m of the motorway was –6.3 per 10,000 trucks and –8.4 per 10 $\mu g\ m^{-3}$ black smoke. For boys the same percentage changes were respectively –1.1 and 3.6.

A German study by Duhme *et al.* (1996) examined the association between self-reported symptoms of asthma and allergic rhinitis and self-reported exposure to motor vehicle traffic in adolescents in Munster, Germany. For this study, 13- to 14-year-olds were targeted in 36 schools. Questionnaires were handed out asking about symptoms of allergic rhinitis, socio-demographic characteristics, exposure to traffic in the residential street and additional factors. The health outcome was defined by questions about the occurrence of wheezing or whistling in the last 12 months and about problems with sneezing and runny or blocked nose without a cold or the flu. Information concerning traffic density on residential streets was obtained by two questions: one about the frequency of trucks passing through the street (never/seldom/frequently/constantly) and one about whether traffic noise would cause closure of the windows (yes, constantly/yes, frequently/yes, seldom/no, never). The sex- and age-adjusted prevalence odds ratios, contrasting the 'constant' against the 'never' categories for wheezing and allergic rhinitis ranged from 1.96 to 2.47 for truck traffic and 1.53 to 1.99 for traffic noise. The results may be affected by misclassification due to self-reports of traffic exposure.

Oosterlee *et al.* (1996) also investigated the possible higher prevalence of chronic respiratory symptoms of populations living along streets with high traffic density in Haarlem, the Netherlands. Busy traffic streets were selected from environmental traffic maps, showing estimated noise and air pollution levels of each street. Air pollution levels were estimated with the CAR model (see *Section 2.3.1.6* for description). For each street, parameters such as traffic composition, traffic density, local topography and meteorological conditions, were used. From the modelled map, streets were selected with NO_2 concentrations from 116 ug/m3 to 150 ug/m3 (calculated for the pavement nearest to the streets), corresponding with an estimated traffic density of 10,000 to 30,000 vehicles every 24 hours. From these streets, 673 adults and 106 children (0-15 years) were recruited. A control group of 812 adults and 185 children was also chosen living along quiet streets. Questionnaires were handed out containing questions about chronic cough, episodes of cough with phleghm, wheeze, dyspnoae, attacks of dyspnoae with wheeze and doctors diagnosis of asthma. Additional questions were asked about respiratory medication used and possible confounding variables such as lifestyle, living circumstances, housing conditions and habits. The prevalence of the symptoms for the children in the control group varied between 1.1% for chronic cough and 11.4% for wheezing ever. This compared to a higher prevalence for most of the symptoms in the exposed group, varying between 1.9% for periods of cough with phleghm and 25.5% for ever wheezing. Adjusted odd ratios were significant for wheeze (OR = 2.1) and for respiratory medication used (OR = 4.8). Risk ratios were found to be higher for girls than for boys. Significant adjusted odd ratios for girls were between 2.9 and 15.8, compared to no significant ratios for boys. In adults, no clear association was found with respiratory conditions. The study concludes that results suggest that living along a busy street increases the risk of developing chronic respiratory symptoms in children.

A cross-sectional study by Livingstone *et al.* (1996) investigated the association between the risk of asthma and living close to busy roads. The study took place at two adjacent general practices in Tower Hamlets, London, located near major roads. All eligible patients aged 2 to 64, who had computer consultations in the preceding year, were included. Cases had a computer record of asthma diagnosis and prescriptions of asthma drugs. Control subjects did not have a computer record of asthma diagnosis or prescriptions of asthma drugs. Data was collected from the records on age, sex, practice, smoking and residential postcode. Postcode grid references were obtained (10 m accurate for 92% of cases and 91% of controls) and the shortest distance to a busy road (1000 vehicles an hour at peak times) was calculated using ARCINFO. In children under 16 the unadjusted odds ratio for being treated for asthma when living 150 m or less from busy roads compared with more than 150 m from them was 0.94. In adults the odds ratio was 0.81. No significant difference was found between the odds ratios after adjusting for age, age group, sex and practice. This study showed no increase in risk of asthma associated with living close to busy roads. A weakness, acknowledged by the writers, is that the distance of residence from a busy road is a crude proxy for exposure to traffic related pollution.

The SAVIAH (Small Area Variation In Air quality and Health) project was a GIS-based study, which developed and tested methodologies for analysing the relationship between air pollution and health at the small area scale. Part of the study involved mapping traffic-related air pollution in the cities of Huddersfield (UK), Amsterdam (the Netherlands), Prague (the Czech Republic) and Poznan (Poland). NO_2 was used as a marker for traffic-related pollution except for Poznan where SO_2 was used as a marker. A description of the overall SAVIAH study is given by Elliot *et al.* (1995) and Elliott and Briggs (1998). Regression-based methods were used in each city to model and map mean annual NO_2 concentrations (Briggs *et al.* 1997). *Section 3.3.8* describes the regression-based methods in more detail. In each location, questionnaires were used to obtain information about children (age 7-11) living and going to school within the study areas. Response rate ranged from 63% in Amsterdam, where questionnaires were delivered directly to the home, to 88 to 96% in the other three areas where questionnaires were distributed through the schools. The questionnaires included a series of questions about symptoms and diagnosis of asthma and wheeze (both within the last 12 months and ever), personal and familial characteristics and domestic factors (e.g. smoking in the home, heating, pets). Logistic regression was used to investigate the relationships between predicted outdoor air pollution at residence of the child and respiratory symptoms. No significant associations were found.

The evidence of the association between chronic exposure to air pollution and health effects thus remains inconclusive. One of the difficulties these studies face is the fact that people are not a fixed point, but move around during long periods. Trying to find an exposure measure, accounting for these movements, is obviously a difficult task. Assumptions have to be made about general movements. The fact that the objects of study in most cases are school children makes this slightly easier as they have a more predictable lifestyle. Another problem in linking health to traffic-related pollution is the focus on outdoor pollution. In reality, however, people spend most of their time indoors and are exposed to a wide range of indoor sources. Farrow *et al.* (1997) investigated the time spent in the home of a sample population in the south-west of England. The results indicated that mothers, fathers and young infants spent an average of 18.4 (76.7%), 14.7 (61.3%) and 19.3 (80.4%) hours per day in the home, emphasising the potential importance of indoor air pollution.

These uncertainties in the risk estimates from chronic studies are highly important for environmental and health policy. They occur to a large extent because the individual, relative risk of long-term exposure to relatively low levels of air pollution is low; effects are thus masked by other factors (including noise in the data) and are difficult to detect. The total potential health burden across the population is nevertheless potentially large, for large numbers of people are exposed; even low levels of relative risk may thus translate into a high attributable risk across the population as a whole. The present lack of knowledge about chronic effects thus adds great uncertainty to attempts to quantify the environmental health impact of traffic-related air pollution.

The measurement of exposure is also important in relation to air quality management. As outlined previously, the National Air Quality Strategy in the UK obliges local authorities to identify areas of excessive pollution (relative to national air quality objectives) and to set up Air Quality Management Areas where these occur. Management strategies, such as traffic schemes, road closures or road pricing are then expected to be introduced to reduce levels of air pollution in these areas. So long as these areas are defined and managed in terms of short-term air pollution levels, however, they will only address problems of acute exposure. Indeed, many interventions may merely serve to reduce peak pollution levels, yet spread pollution over a wider area and longer period of the day, thereby adding to long-term exposures for large proportions of the population. Whether such measures have beneficial or adverse effects on public health will thus depend on the balance between acute and chronic effects. A more effective air quality strategy needs better information on these chronic effects.

One of the most important needs in this context is for improved methods to estimate chronic exposures to traffic related pollution. *Section 2.3* will give an overview of some of the available methods.

2.3 METHODS TO ESTIMATE EXPOSURE

As described in *Section 2.2*, human exposure of pollutants through air appears to be a major contributor to respiratory diseases, mortality and use of asthmatic medication. Air pollutants can enter or make contact with the human body by inhalation or by absorption through dermal contact. Exposure refers to both the concentration of a pollutant at the boundary between an individual and the environment and to the duration of contact between the two. The amount of the given pollutant absorbed is often described as the *dose*. The *dose* depends on the duration and intensity of the exposure, as well as the efficiency of absorption. The *target organ dose* is the amount that reaches the human organ where the relevant effect occurs (Corvalán *et al.* 1996).

It is difficult to measure exposure accurately. Personal monitoring would in principle be the most accurate method, and a growing body of data is becoming available based on this technique (e.g. Jantunen *et al.* in press). The method tends to be too costly, however, to be used in most large population studies. For this reason, epidemiological studies often use proxies to measure exposure. A range of different methods are available for this purpose. This section will review selected methods in terms of their theoretical background, their accuracy, their ease of use and their ability to be incorporated into a GIS.

2.3.1 Air pollution dispersion models

2.3.1.1 Introduction

Air pollution modelling is widely used as a tool in assessing the effects of processes when no air pollution concentrations can be measured. This is often the case with new facilities or the expansion of existing ones. A variety of models are available. The models are usually distinguished by type of source (point, line, area, or volume source), pollutant, transformations and removal, distance of transport, and averaging time. In its basic form a model requires two types of data: information on the source and meteorological data. The model then simulates the transport and dispersion of the pollutant mathematically. Depending on the model it might also simulate the chemical and physical transformations and removal processes. The model output is an air pollutant concentration for a certain time interval for a specific receptor location.

Temporal and spatial resolution and accuracy determine the complexity of the solution. Modelling becomes extremely difficult if emissions vary greatly, either in space and time, or when it is necessary to predict the time series of concentrations at specific locations. When, on the other hand, the interest is in the probability of occurrence of a specific concentration during a given period, for example a year, the modelling task is much less complicated. In general, long-period averages can be modelled more accurately than shorter averaging times (Harrison 1990), potentially making this approach especially applicable in long-term, chronic studies.

Air dispersion models can be divided into short range (0–~100km) and long range (~100km and greater) transport models. The most commonly used short-range transport model is the Gaussian plume model, which will be described later in this section.

The long-range transport models need to incorporate features which are unique for long range transport, including wet and dry deposition, large scale meteorological features and chemical reactions. There are two main types of long range transport models, Lagrangian and Eulerian models. The Lagrangian model follows the chemical and physical processes in an air mass pocket in time-intervals along so-called trajectories. Eulerian models look at the same processes, but at fixed points for specified time-intervals (Harrison 1990). Three long range transport models will be described in this section: the box model, the gradient transport models and the trajectory models.

Many dispersion models are based on Pasquill's stability categories. These categories describe the stability in the atmosphere in terms of categories of wind speed and cloud cover. *Table 2.5* shows the classification as used in the United Kingdom.

Table 2.5: Pasquill's stability categories

	Insolation			Night	
Surface wind speed (m s-1)	Strong	Moderate	Slight	Thickly overcast or ≥ 4/8 low cloud	≤3/8 cloud
<2	A	A-B	B	-	G
2-3	A-B	B	C	E	F
3-5	B	B-C	C	D	E
5-6	C	C-D	D	D	D
>6	C	D	D	D	D

Notes: Strong insolation corresponds to sunny midday in midsummer in England. Slight insolation occurs in similar conditions in midwinter. Night refers to the period from 1 hour before sunset to 1 hour after dawn. A is most unstable category and G the most stable. D is referred to as the neutral category and should be used, regardless of wind speed, for overcast conditions during day or night. (Harrison 1990)

2.3.1.2 *Gaussian plume model*

In the Gaussian plume model the plume has a Gaussian, or normal, distribution of concentration in the vertical (z) and lateral (y) directions. The concentration C at any point (x,y,z) is then given by (see also *Figure 2.5*):

$$C(x,y,z)=\frac{Q}{2\pi\sigma_y\sigma_z U}\exp\left[-\frac{y^2}{2\sigma_y{}^2}\right]\left\{\exp\left[-\frac{(z-H_e)^2}{2\sigma_z{}^2}\right]+\exp\left[-\frac{(z+H_e)^2}{2\sigma_z{}^2}\right]\right\} \tag{2.1}$$

C concentration (µg m^{-3})

Q pollutant mass emission rate (µg s^{-1})

U wind speed (m s^{-1})

x,y,z the along wind, crosswind and vertical distances (m)

H_e effective stack height

σ_y standard deviation of horizontal concentration in the plume (m)

σ_z standard deviation of vertical concentration in the plume (m)

When y = z = 0 the concentration calculated will be at ground level and the equation reduces to:

$$C(x)=\frac{Q}{\pi\sigma_y\sigma_z U}\exp\left[-\frac{H_e{}^2}{2\sigma_z{}^2}\right] \tag{2.2}$$

A few points of interest emerge from this equation. Firstly, the concentrations are directly proportional with the emission rate, which makes an accurate knowledge of Q essential in any application. Secondly, the maximum concentration will occur downwind and its distance will increase with increasing H_e. Also the maximum concentration will decrease with an increasing H_e (Adema 1989).

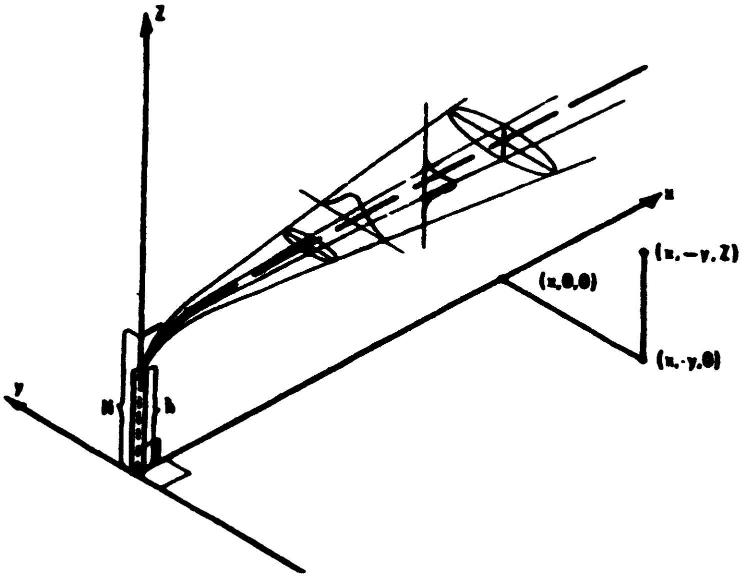

Figure 2.5: Co-ordinate systems showing Gaussian distribution in the horizontal and vertical direction. (Adema 1989)

The model just described is mainly used for point sources. To model a line-source with the Gaussian plume model, a line is considered as an infinite series of points. The concentration of a pollutant can then be calculated by integrating the Gaussian plume model over these points whilst assuming that the receptor and line-source are on the same level, with the following formula:

$$C = \frac{2q}{\sqrt{2\pi}\sigma_z U \sin\alpha} \tag{2.3}$$

where q is the line-source emission rate (μg m^{-1} s^{-1}) and α the angle of the wind direction and the direction of the line-source (see *Figure 2.6*) (Harssema 1987).

This is a very simplified line-source model, which does not account for parallel winds and cannot be used in situations where the wind speed is less than 1 m s^{-1}. When the line-source is a road, other complications arise, such as turbulence caused by moving cars, which will cause the pollution to disperse above the road before it is picked up by the wind. Air pollution dispersion models designed for line sources have attempted to solve these problems (see *Chapter 4*).

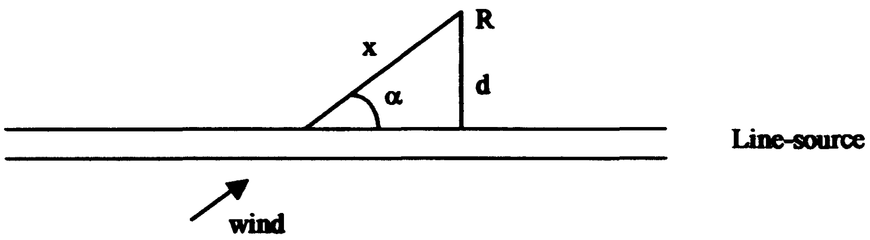

Figure 2.6: Line-source with wind direction; R = receptor, x = downwind distance source-receptor (m), d = perpendicular distance source-receptor (m), α = angle wind direction and line-source.

2.3.1.3 Box model

The box model assumes that emissions are instantaneously mixed up to the boundary layer height. This means that there is no vertical concentration gradient (Pul *et al.* 1996). Box models are useful for estimating concentrations, especially for first approximates (Boubel *et al.* 1994).

The concentration C, at a certain location, x, in the box is calculated by (Pul *et al.* 1996):

$$C = \frac{Qx}{uH} \quad (2.4)$$

where:

Q emission rate (μg s^{-1} m^{-2})

x distance over which diffusion take place (m)

u mean wind speed through vertical extent of the box (m s^{-1})

H mixing height (m)

2.3.1.4 Gradient transport models

The gradient transport models divide the atmosphere into grid cells. The atmosphere in each grid cell is assumed to be homogeneous and stationary. The change of concentration in the grid cell can be described on the basis of both the movement of air masses and turbulence in three dimensional space (Adema 1989).

The change of concentration with respect to time can be written as:

$$\frac{\delta C}{\delta t}+\left(U\frac{\delta C}{\delta x}+V\frac{\delta C}{\delta y}\right)=\frac{\delta}{\delta z}\left(K_z\frac{\delta C}{\delta z}\right)+\frac{\sum Q}{Az} \tag{2.5}$$

(1) (2) (3) (4)

where the following terms represent:

1. change of concentration in time
2. change of concentration as a result of the horizontal wind field (U is the direction of the wind, V is the horizontal crosswind)
3. change of concentration as a result of the vertical turbulence (K_z = diffusivity of vertical crosswind (eddies))
4. change of concentration as a result of emissions (ΣC = sum of all emission sources, A = area and z = height)

2.3.1.5 Trajectory models

A trajectory model moves an air mass pocket along with the mean wind speed. Emissions are added by each location over which the air mass pocket passes. The model can be source- or receptor-aimed. A source-aimed trajectory model considers the emissions from one specific source. The air mass pocket is assumed to follow the mean wind speed from this source and the model predicts where the pollutants will be deposited. A receptor-aimed trajectory starts at the receptor and calculates the course of the air mass pocket parcel back in time to investigate the origins of the emissions causing the pollution at the receptor (Boubel *et al.* 1994) (see also *Figure 2.7*).

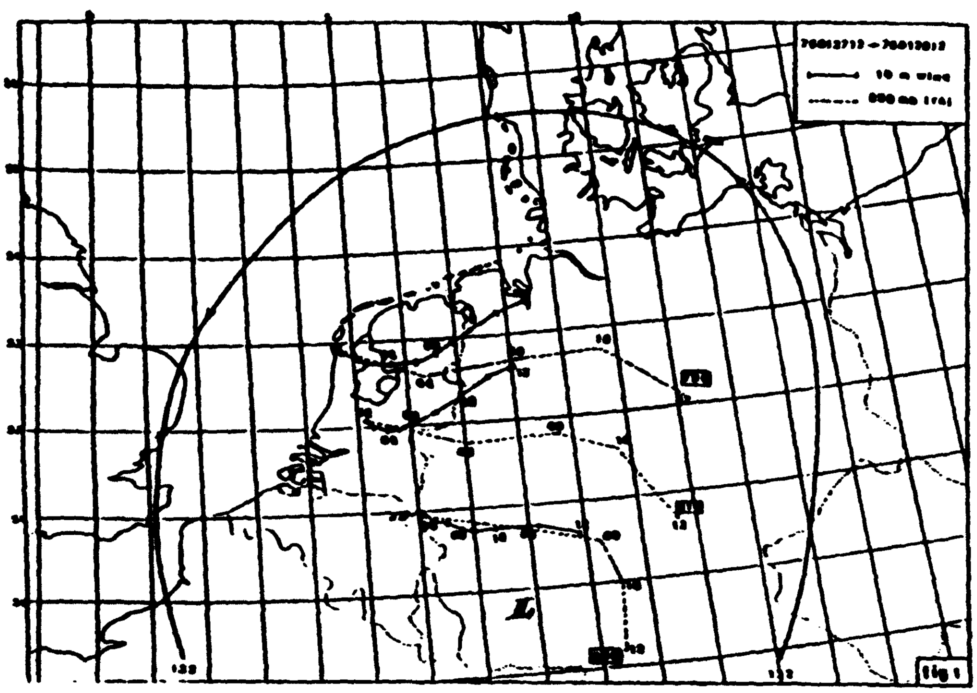

Figure 2.7: Example of a trajectory (Harssema 1987)

2.3.1.6 Air pollution dispersion models modelling traffic-related pollution

Several air dispersion models have been developed looking specifically at urban areas. Pul *et al.* (1996), presented a literature survey of existing urban air quality models. This was not intended to give a complete overview of urban air quality model but to provide some insight into the types of model used. The literature survey was therefore restricted to models published in the journal *Atmospheric Environment*. *Table 2.6* presents a slightly adapted version based on that presented in Pul *et al.* (1996). The table shows that most models were used to simulate the air pollution situation for a specific city and usually for short time periods, such as smog periods.

Several of the models listed in *Table 2.6* are worthy of especial note in relation to this research. In addition, several other models, not considered by Pul *et al.* (1996) are potentially important as a basis for mapping exposure to traffic-related pollution. These will be considered in more detail below.

Table 2.6: Overview of urban air quality models (from Pul et al. 1996)

Name	*Type*	*Scale*	*Input*	*Output*	*Reference*
No name	3D grid numerical model	30*40*7 stretched grid system covers an urban area of 40*60 km^2	Wind speed and direction, temp., area and point source emissions, and mixing height	Hourly SO_2 and 12-h average sulphate concentrations	Ku *et al.*, 1987a
UAM (Urban Airshed Model)	Photochemical box dispersion model	3D array of grid cells over urban area	Background concentrations, NOx and reactive HC emissions, meteorological data + modelled mixing layer height	1-hour average O_3 concentrations	Scheffe and Morris, 1993
No name	3D grid Lagrangian numerical photochemical model	Hor: 400*150 km, grid cells of 5*5 km, vert: 1525 m.	Emissions from 130 different source categories, wind speed, cloud cover, surface roughness	1-hour average O_3 and NO_2 concentrations	McRae, Goodin and Seinfeld, 1982 McRea and Seinfeld, 1983
State-Space model	Statistical adaptive state-space model coupled with Kalman filtering	Specific local area	One-day-lagged wind speed and persistence , daily Fe and Pb concentrations	Daily average Fe and Pb concentrations	Hernandez *et al.* 1992
No name	Statistical stepwise cluster analysis method	Specific local area	5-year average pollutant concentrations and source values	Annual average SO_2, NO_x and DF (Dust Fall) concentrations	Huang, 1992
No name	Numerical chemical plume model	Urban plume	NO_x, HC, CO and SO_2 concentrations	Sulphate particles and O_3 concentrations at the hour-of-day	Isaksen *et al.* 1978

Name	*Type*	*Scale*	*Input*	*Output*	*Reference*
No name	Lagrangian particle scheme that utilises wind and numerical fields from a numerical mesoscale model	Urban airshed	Wind speed, turbulence and emissions	Magnitude and spread of the urban plume	Pitts and Lyons, 1992
TEMPER	Bivariate temperature and persistence based regression model	Urban area	8 years of data from May to September from two monitoring stations	Daily maximum 1h average O_3 concentrations	Robeson and Steyn, 1990
ARIMA (Autoregressive Integrated Moving Average)	Univariate autoregressive integrated moving average model	Urban area	8 years of data from May to September from two monitoring stations	Daily maximum 1h average O_3 concentrations	Robeson and Steyn, 1990
No name	Univariate deterministic stochastic model	Urban area	8 years of data from May to September from two monitoring stations	Daily maximum 1h average O_3 concentrations	Robeson and Steyn, 1990
No name	Hybrid model combining Gaussian plume line source model with knowledge of a suitable parametric form of the probability distribution	Urban area	Vehicle patterns and emissions, basic meteorological measurements and historical concentrations	Seasonal extremes of 1-h average CO concentrations	Jakeman *et al.* 1991
No name	Hybrid model combining ATDL model with a two-parameter lognormal distribution	Area of 64 km^2 divided into 256 cells of 4*4 km	Daily average wind speed developed from 3-h values from wind dir. reduced to 16 point wind rose, and emissions	Daily average TSP concentrations	Simpson and Miles, 1990
No name	3D grid time-dependent finite difference model combined with puff model	3D array of grid cells situated over the urban area hor: 1*1km vert: 3 levels of 50, 50, 100m	Hourly data on emission, wind and dispersion conditions and background concentrations	1-h average SO_2, $PM_{2.5}$ and NO_x concentrations	Grønskei, *et al.* 1993

Name	*Type*	*Scale*	*Input*	*Output*	*Reference*
RAMS-CALGRID model (RAMS = Regional Atmospheric Modelling System)	Prognostic mesoscale model (RAMS) coupled with 3D grid Eulerian photochemical model (CALGRID)	Hor: 46*46 grid system cells of 4*4 km vert: 10 layers of variable thickness up to 2500m totally	Emission for a typical 24h period in Athens: all the necessary hourly meteorological data and other parameters required by CALGRID were produced by RAMS	Hourly O_3 concentrations	Pilinis *et al*, 1993
RAM	Gaussian plume model	Urban area	Wind speed, area emissions, mixing height and hourly surface observations	Hourly SO_2 concentrations	Ku *et al*., 1987b
No name	Box mode and a vertical cell model	Urban area	Time-dependent traffic emission rates for THC, NO and NO_2	Diurnal variation in O_3 concentration on a typical summer day	Zellner and Mussiopoulos, 1986
No name	Photochemical box model	Box over urban area Hor: city Vert: mixing height	Meteorological data, PBL height, emissions measured NO_x concentrations and NMHC/NO_x ratios	Continuous O_3 and PAN concentrations	Gladstone *et al.* 1991
PBM (Photochemical Box Model)	Photochemical box model	Box over urban area Hor: city Vert: mixing height	CO, NO_x and NMHC emissions resolved to hourly rates and distributed according to weekday/weekend hourly traffic patterns, meteorological parameters	1-h average CO, NO, NO_2 and O_3 concentrations	Jin and Demerjian, 1993
No name	Box model based on moving trajectory model	Box of 20*15 km * mixing height	Meteorological data (wind speed, temperature, solar radiation), NO_x, HCs and CO emissions and background concentrations	Continuous O_3, NO and NO_2 concentrations	Roemer, 1989

Name	*Type*	*Scale*	*Input*	*Output*	*Reference*
ATDL Model (Atmospheric Turbulence and Diffusion Laboratories)	Box model	Box over urban area	Area emissions, wind speed and stability parameters	Hourly particulates and SO_2 concentrations	Gifford and Hanna, 1973
CPBM (Canyon Plume Box Model)	Urban canyon box dispersion model	Urban street canyon	Traffic and pollutant data, modelled flow and turbulence (by sub-models).	½ hour NO_x, NO_2 and CO concentrations	Yamartino and Wiegand, 1986
CALINE (California Line Source Dispersion Model)	2D highway dispersion model based on gaussian plume methodology	Highway	Traffic parameters, street geometry, meteorology	½ or 1-h average of suspended particulates, NO_2 and CO Concentrations	Benson, 1992 Benson, 1979
CAR (Calculation of Air pollution from Road traffic) model	Simple parameterised street dispersion model	Close to streets	Background concentrations, traffic data, average wind speed, city radius, street type	Annual percentile values and average concentrations of non-reactive pollutants and NO_2	Eerens *et al.*, 1993
OMG (=Osaka Municipal Government)-VOLUME-SOURCE model	Micro-scale dispersion model for motor vehicle exhaust gas	Area extending 200m from the side of the road in an urban area	Emission rate and height; advection speed of plume; turbulence	Exhaust gas concentration	Kono and Ito, 1990b

Pul *et al.* (1996) describes the development of the Urban Air Quality Assessment Model (UAQAM). This model calculates the city-background concentrations of SO_2 and NO_x caused by the city emissions themselves. In the development of the UAQAM, three models were studied. The first, the Box model, which assumes an instantaneous mixing of emissions to the boundary layer height, is also described in *Section 2.3.1.3*. The second model, the Gifford and Hannah model (GH model) (Gifford and Hannah 1973) presents a simple description of the city background concentration for area sources based on the Gaussian Plume model. Thirdly, the two models were combined in the Box-GH model. The following input parameters were used for 16 cities across Europe: latitude, longitude, area and emissions for the city; temperature, wind velocity and cloud cover; and the regional SO_2 background concentration. The Box-GH and the GH models were found to be the most appropriate models for describing the city background concentrations of SO_2 and NO_x (r = 0.7 and 0.6 respectively for an hour-of-day basis).

The CAR model (Calculation of Air pollution from Road traffic) is a simple parameterised model to determine air quality alongside roads in cities (Eerens *et al.*, 1993). It was developed by the Dutch Environmental Ministry for use as a tool in local planning policy. The CAR model calculates the city background level, the local street emission, the local street traffic contribution and the annual average concentration or percentile of the pollutant. The model is annually updated and calibrated because it contains parameters which vary from year to year. Comparisons between CAR model results and measured data were made at sites from the Dutch National Air Quality Monitoring Network. The average, relative differences between the calculated and the measured values are -3±9% for CO, 8±19% for NO_x and 6±9% for NO_2. Similar results were found by Heida *et al.* (1989) who compared CAR model results with measurements at 10 streets in Amsterdam. They found errors of -10±12% for CO and 6±10% for NO_2. The results generally indicated that the CAR model is a reliable method for calculating traffic related air pollutants in urban streets.

The Design Manual for Roads and Bridges (DMRB) was designed as a screening model to help engineers and planners in road and bridge design (Department of Transport 1994). The model is based on Gaussian plume dispersion. As input, it needs peak hour traffic flow, vehicle speed and distance from road to receptor. It calculates concentrations of CO, NO_x, PM, CO_2 and HC. The model will be described in more detail in *Section 3.3.3*.

The Highway Air Pollution Model (HIWAY) is a Gaussian plume model which calculates concentrations of non-reactive pollutants. In the model a highway is simulated by a number of point sources with the contribution of all points computed by numerical integration of the Gaussian point source equation. Input parameters are emission rate, wind speed and source parameters (Zimmerman and Thompson 1974)

Tartaglia *et al.* (1995) describe the development and validation of an urban street canyon model. Estimations of CO concentrations due to road traffic were computed by integrating traffic, emission , meteorological and dispersion models. Three new dispersion models named Canyon/Box, Canyon/Gauss and Canyon were tested in Firenze (Italy); results were compared with measured CO concentrations. Results showed that the Canyon model was the most reliable.

SBLINE is a suit of models including ROADFAC (emission model), NOTLINE (Gaussian dispersion model) and CPD (street canyon dispersion model) which calculate temporal and spatial variations in airborne concentrations of gaseous pollutants emitted from motor vehicles (Namdeo and Colls 1996). It uses road link characteristics such as vehicle fleet structure, queue length and geometry. SBLINE was validated in Leicester by calculating CO concentrations and comparing them with observed CO concentrations. Results showed a correlation coefficient of $r = 0.82$ ($r^2 = 0.68$).

The CALINE suite of models are Gaussian line-source models, developed for the US-EPA for policy applications. Details of the model, including an outline of their history, are given in *Chapter 4*. Benson (1992) evaluated the latest versions of the model, CALINE3 and 4, and found modest improvements in accuracy when using the CALINE4 version. A statistical method was used to evaluate the CALINE3 and 4 performances relative to each other. Three highway monitoring sites, used in tracer studies for validation purposes, were used in a direct comparison between CALINE3 and 4. Both measured tracer gas, SF6, and CO concentrations were available. For two of the three studies the CALINE4 performance was clearly better. Results of the other tracer study proved to be inconclusive. Scatterplots of the CALINE4 results for two tracer studies indicated an r of

0.87 (n=599) and 0.51 (n=163). The first scatterplot showed that 85% of the CALINE4 concentrations were over-predicting the monitored concentrations. For the second tracer study, 90% of extreme over- and under-predictions occurred during sampling periods when either the wind speed was less than 1 m s^{-1} or the roadway angle did not exceed 15°. It was also found that CALINE4 performed significantly better than CALINE3 at wind speeds below 1 m s^{-1}.

ADMS-Urban is a relatively new dispersion model, developed by CERC of Cambridge (CERC 1998). It is one of the first air pollution dispersion models to use the boundary layer depth and the Monin-Obukhov length to describe the atmospheric boundary layer, and as such potentially offers great improvements in accuracy in rough terrain. As yet there have been relatively few attempts to apply and test the model under field conditions, or to compare it with other dispersion models. Preliminary studies by Bull (unpublished), however, suggest that the model performs rather badly close to roads. Similar effects have been noted in a recent study in Northamptonshire (Briggs *et al.* 1998). Further details on the model are given in *Section 3.3.5*.

Various studies have compared these and other urban air quality models with test data. Noll *et al.* (1978) compared HIWAY and the first two California line source models CALINE and CALINE2. They concluded that all three models over-estimated concentrations in parallel wind conditions and under-estimated concentrations in oblique and crosswind conditions. Similar results were shown by Rodden *et al.* (1982), who found that the models HIWAY, CALINE2, CALINE3, AIRPOL-4 (a model based on the Gaussian equation) and TRAPS IIM performed poorly in general.

Another evaluation study, by Rao *et al.* (1980), found that the GM (General Motors) model predictions were within a factor of two of the observed concentrations 87% of the time. The GM model uses the line-source approach, specifying one dispersion parameter as a function of wind-road orientation angle and distance from the source. It also considers plume rise over the road under very stable and light wind conditions. The other evaluated models, AIRPOL-4, HIWAY, CALINE2, DANARD, MROADS2 and ROADS performed poorly using the same data. The DANARD (Danard 1972), MROADS2 and ROADS models are two dimensional Eulerian models based on the mass conservation equation.

Rao, *et al.* (1989) compared the performance of three urban air pollution models - the RAM-model, the ATDL-model and a 3D grid numerical model - against observed hourly SO_2 ground-level concentrations. They concluded that the RAM and the ADTL model over-estimated the observed concentrations using stable diffusion coefficients. When using near-neutral diffusion coefficients, the ADTL model results were comparable to the 3D grid numerical model.

Burden *et al.* (unpublished) compared predicted NO_2 levels from CALINE4 and DMRB with monitored NO_2. The road co-ordinates of the M4/M5 intersection were retrieved from a 1:10,000 map of the area. Other roads in the area including slip roads were ignored as no traffic flows were available. Twelve-hour traffic counts and composition were obtained from the Avon Department and Engineering Department for the period between 7 a.m. and 7 p.m. in each direction. An emission factor of 4.6 g km^{-1} was used assuming an average speed of 100 km hr^{-1}. Background concentrations of nitric oxide and ozone were taken from the Bristol City Centre UK Automatic Urban Network monitoring site. A background NO_2 concentration was taken from a diffusion tube survey around the motorway (> 200m away). Meteorological parameters were obtained from available monthly averages during the study period. The correlation of the CALINE4 predicted values (r^2 = .704) against the monitored values was found to be better than the DMRB performance (r^2= .640). CALINE4 was found to under-predict in situations of low nitrogen dioxide and over-predict at higher levels. DMRB results were distorted because of the inability of the model to estimate background concentrations (outside a 200m buffer of the road).

Kono and Ito (1990a) compared estimated concentrations from the OMG VOLUME-SOURCE model with three line source dispersion models; the JEA (Japan Environmental Agency) model, the Tokyo model and the EPA HIWAY-2 model. The JEA dispersion model equations were derived from the Fickian diffusion equation. In this equation, the diffusion and wind speed are described as power-laws in terms of height above the ground. The JEA model includes three equations for three wind conditions and can be used for both rural open areas and urban areas. The Tokyo model is a modified version of the JEA model. The differences are that the Tokyo model is based on NO_x measurements near roads in Tokyo and the model also can be used for depressed and elevated roads. The

HIWAY-2 model is a revised version of the HIWAY model discussed earlier in this section. Data from seven line dispersion experiments were used in three cities across Japan using SF6 as tracer gas. Of the four models, the OMG VOLUME-SOURCE model provided the most accurate estimates. The HIWAY-2 model was in general more accurate than the JEA and the Tokyo models.

Two other recently developed models are also worthy of note. In 1991, the American Meteorological Society (AMS) and the Environmental Protection Agency (EPA) (US) initiated a collaboration to rebuild ISC (USEPA 1995) into a new model using the same new understanding of the atmospheric boundary layer. The working group, the AMS/EPA Regulatory Model Improvement Committee (AERMIC) was formed to develop the **AERMIC Model** (AERMOD) (Perry *et al.* 1994). At the time of the study described here, the model had not yet been made available and so could not be used. Another relatively new model is AIRVIRO which offers a complete air quality management system combining dispersion modelling for point, line, volume and area sources, air pollution monitoring and mapping tools all integrated in a GIS (Indic 1996). This model was potentially available for one of the case study areas used in this research, through collaboration with Sheffield City Council. The available version, however, could not easily be adapted to run for the relatively large number of receptors and short time periods required in this study, and was therefore not used.

To date, few epidemiological studies have used air pollution dispersion models to estimate exposure to traffic-related pollution. Pershagen *et al.* (1995) estimated outdoor NO_2 concentrations in rural areas using the CALINE4 model, while Oosterlee *et al.* (1996) used CAR to model areas of high and low traffic-related pollution. CALINE3 was also used by Collins (1997) as part of the SAVIAH study (see also *Sections 2.2, 2.3.3* and *3.3.8*).

2.3.2 Spatial Interpolation

2.3.2.1 Introduction

Interpolation is the procedure of predicting the value of properties at unsampled points, using measured values of existing point locations within the same area. Estimating the value of properties of sites outside the area covered by existing observations is called extrapolation. Interpolation is used to fit a surface through the data points.

According to Burrough (1986), spatial interpolation techniques can be divided into global (universal) and local fitting techniques. Global techniques (e.g. trend surface analysis, Fourier series) use all observations of the study area to fit a single, continuous surface. Local fitting techniques (e.g. Thiessen polygons, splines, weighted moving averages and geostatistical methods) estimate values from the nearest data points only.

2.3.2.2 *Trend surface analysis*

When a variation of a property occurs continuously over a landscape it is possible to model the surface by trend surface analysis. Trend surface analysis describes the large-scale systematic changes or trends, by fitting a surface through the data points using a smooth mathematical function. This is done by using a polynomial regression to fit a least-squares surface to the data points.

When a value z is measured along a line of points x_1, x_2, x_n, and, apart from minor variation, the value z increases linearly with its location, the long range variation can be described by the regression model (Burrough and McDonnel 1998):

$$z(x) = b_0 + b_1 x + \varepsilon \quad (2.6)$$

where b_0 is the intercept, b_1 the slope and ε the noise. More often z is not a linear function of x but a more complex polynomial model, e.g.:

$$z(x) = b_0 + b_1 x + b_2 x^2 + \varepsilon \quad (2.7)$$

This is a quadratic model. By increasing the terms, higher order polynomial models can be fitted.

When a value of z is measured on a set of x and y coordinates, the same polynomial functions can be fitted (respectively flat, linear and quadratic):

$$f\{(x,y)\} = \sum_{p}(b_0) \quad (2.8)$$

$$f\{(x,y)\} = \sum_{p}(b_0 + b_1 x + b_2 y) \quad (2.9)$$

$$f\{(x,y)\}=\sum_{p}(b_0+b_1x+b_2y+b_3x^2+b_4xy+b_5y^2) \tag{2.10}$$

where p is the order of the trend surface. A flat surface is zero order, a linear surface is first order and a quadratic surface is second order. *Figure 2.8* shows examples of trend surfaces for the first, the second and the third order.

Trend surface analysis is an appropriate technique when investigating a broad trend in a surface. However, when more complex data is investigated on a more local scale, trend surface analysis becomes increasingly inaccurate (Burrough and McDonnel 1998, Bailey and Gatrell 1995). The technique is very sensitive to edge effects. The edges of the surface tend to wave, to fit to the points in the centre of the area, resulting in extremely high or small values just outside the covered area when using second or higher order models. The model is also very vulnerable to extreme values. Because trend surfaces are smoothing functions, the surface rarely passes thorough the original data. When using higher order models, especially, the minimum and the maximum value of the surface can exceed the minimum and maximum value of the original data.

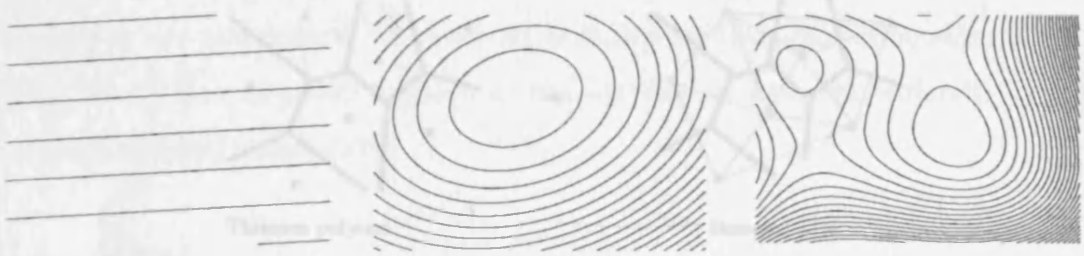

Figure 2.8: Examples of simple trend surfaces, respectively first order (linear), second order (quadratic) and third order (cubic)

The main use of trend surface analysis is in identifying outliers from a general trend (Burrough 1986). Anderson (1970) suggested that trend surface analysis could only be used as a mapping tool in describing generalised patterns of urban air pollution.

2.3.2.3 *Fourier Series*

Fourier series use a linear combination of sine and cosine waves to describe the one- or two-dimensional variation by modelling the observed variation (Burrough 1986) It is best used for data sets which feature periodicity, such as ocean waves. Fourier series are rarely incorporated in computing packages, and have not been used for air pollution modelling.

2.3.2.4 Thiessen (nearest neighbours) tesselation

Thiessen or Voronoi tesselation is an interpolation technique which is based on the assumption that the best information about an unsampled point lies with its nearest neighbour. It involves the construction of Thiessen polygons by triangulating the points in a Triangular Irregular Network (TIN) (Bailey and Gatrell 1995). An area is assigned to each sample point so that each location in that area is closer to its own sample point then to any other sample point (*Figure 2.9*).

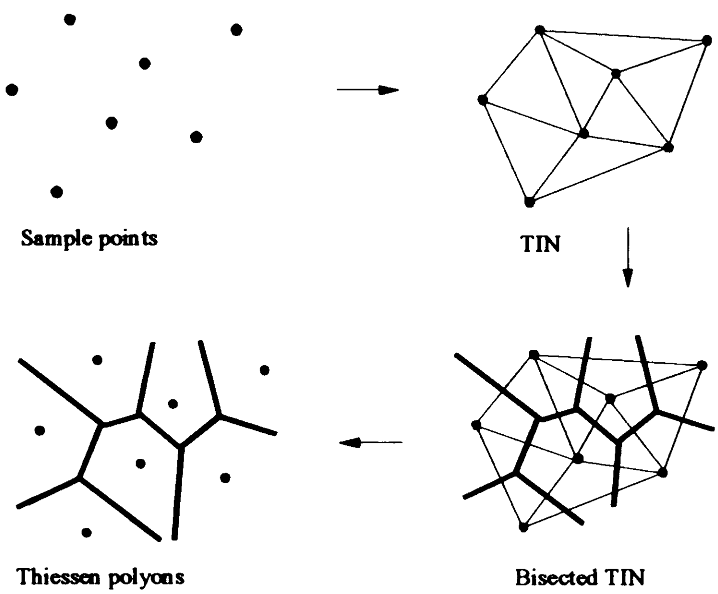

Figure 2.9: Generating Thiessen polygons by triangulating

The TIN as created can also be used to create isolines. Isolines are lines which join points of equal value (*Figure 2.10*).

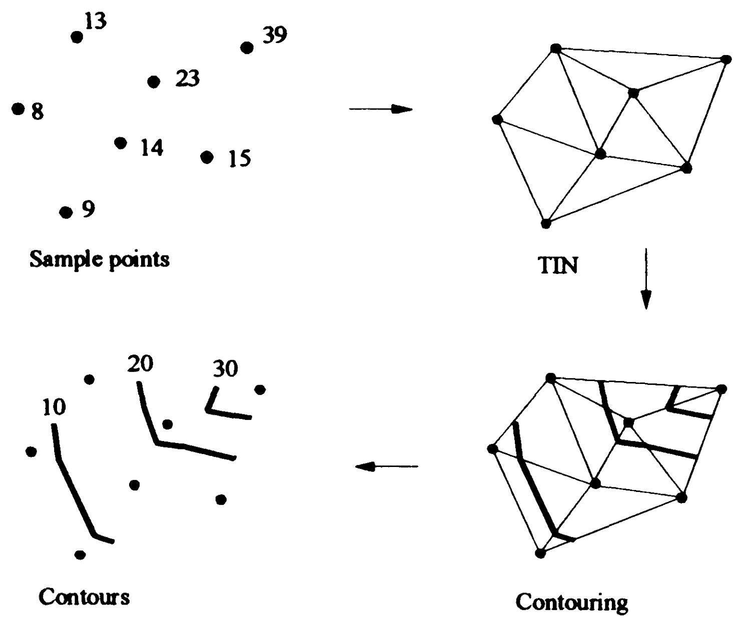

Figure 2.10: Generating contours or isolines using a TIN

Thiessen polygons are one of the most widely used GIS interpolation technique. This technique can be easily used with qualitative data, such as vegetation classes or land use, where the strange geometrical pattern of the boundaries are not critical, and where the variation within the polygon can be assumed to be homogeneous and isotropic. This technique is not appropriate, however, to gradually varying data in combination with a limited set of sample points because of the inability to estimate within-tile variability (Burrough and McDonnel 1998).

2.3.2.5 Splines

Splines originate from the pre-computer era, when curves were fitted with the eye using a flexible ruler (Burrough and McDonnel 1998). These curves have been converted into mathematical functions. The curves fit through a few data points exactly. The curves between the points vary continuously. Various spline functions can be applied, including linear, quadratic and cubic functions. The Laplacian spline method, one of the best developed spline interpolation techniques, allows smoothing of the data according to objective, error minimising criteria. The only restriction on the form of the interpolation function is that it has to satisfy a general, rotation invariant, minimum total curvature criterion. The method has not been widely used in the environmental sciences, but has been applied to model meteorological data by Hutchinson (1984), who noted that: "It works well with very irregularly spaced data points and, significantly, does not require estimation of a smoothing parameter." An example of a spline is shown in *Figure 2.11*.

Problems occur in applying splines to data which contain a natural variation and measurement error. In these cases, splines may produce extremely high or low values in some areas, creating local hollows and peaks. Thin plate splines are designed to remove these extreme local effects by replacing the exact spline surface with a locally smoothed average (Burrough and McDonnel 1998). Thin plate splines have been used for interpolating large areas in a quick and effective manner. Hutchinson (1996) found thin plate splines a flexible tool to interpolate mean rainfall in south-eastern Australia. Robeson and Willmott (1996) evaluated and compared thin plane splines with other interpolation methods in interpolating terrestrial air temperature averages.

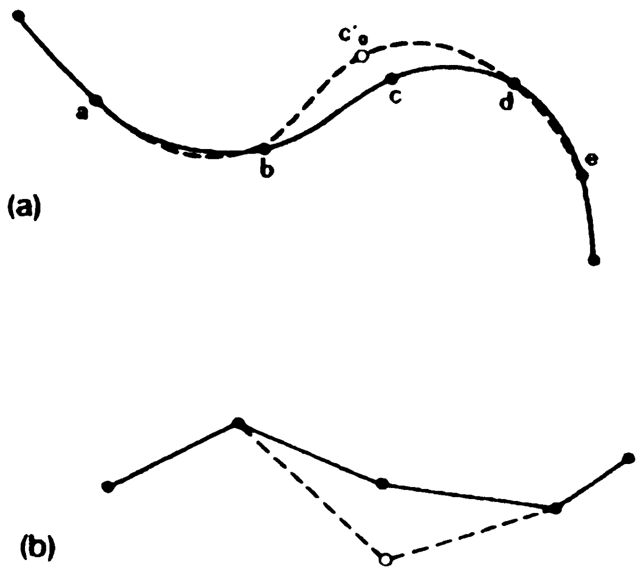

Figure 2.11: The local nature of splines. When one point is moved four intervals must be recomputed for a quadratic spline (a) and two for a linear spline (b) (Burrough 1986)

2.3.2.6 *Weighted moving averages*

Weighted moving averages assume that the value of an un-sampled point is the weighted average of sampled points in their neighbourhood. A commonly used weighted moving average is the inverse distance method.

Interpolated values using the distance weighted average will never exceed the highest or lowest values of the sampling points used. The best results are obtained when the sampling points are sufficiently dense with regard to the simulated local variation. If the sampling points are irregular or sparse, errors can occur in the estimated surface (Watson and Philip 1985). Weighted average methods have been widely used in environmental studies, especially in relation to land cover data (e.g. Hodgson 1991; Cornelius and Reynolds 1991). It seems to have been only rarely used, however, for pollution modelling.

2.3.2.7 Geostatistical models (kriging)

Kriging was first developed by Matheron (1971) for use in the mining industry. The theory of kriging is described in *Section 3.3.6*.

Geostatistical methods have been widely used in the soil and water research. Wartenberg *et al.* (1991) compared kriging with nearest neighbour interpolation and inverse distance squared weighting to derive individual estimates of exposure to contaminated groundwater. Kriging was found to be no better than the other two interpolation algorithms, though it was considerably more complex to use. Vauclin *et al.* (1993) used co-kriging to predict available water content (AWC) and water stored at 0.3 bar (pF2.5) in soil with the secondary variable sand content. They found co-kriging to be a promising tool in soil physics in estimating undersampled variables. Leenearts *et al.* (1989) used co-kriging to predict zinc concentrations, caused by flood events, with relative elevation as secondary variable. They found that co-kriging produced better estimates compared with ordinary kriging and linear regression. Stein *et al.* (1988) compared ordinary kriging and co-kriging in predicting moisture deficit (MD) in soil and found that co-kriging, using the mean highest water-table as a covariable, needed fewer MD sample points in order to obtain only a slightly less accurate prediction than using ordinary kriging on all the points. Knotters *et al.* (1995) compared the performances of ordinary kriging, co-kriging and kriging combined with regression, for the spatial interpolation of horizon depth with censored observations. Kriging combined with regression proved the best technique and had as an advantage that it needed fewer model parameters in its estimation than co-kriging. Ahmed and De Marsily (1987) compared a range of geostatistical methods (kriging combined with linear regression; cokriging; kriging with an external drift; and kriging with a guess field) for estimating transmissivity in water. Venkatram (1988) used simple kriging in spatial analysis of acid precipitation data in the eastern United States and Canada. Kriging explained 36% of the variance. This was improved to 55% by combining the simple kriging technique with deterministic modelling.

In recent years, several studies have used geostatistical methods to investigate and map air pollution. Lefohn *et al.* (1988), for example, showed that kriging could be used to estimate monthly means of the 7-h mean O_3 concentrations and the percentage of hourly concentrations below 0.07 ppm for a given month, when sufficient spatial coverage is available. Sally Liu and Rossini (1996) used kriging to predict outdoor 12h daytime ozone concentrations and compared them with actual home outdoor measurements. Their results indicated that kriging predictions were more accurate than using only the closest stationary ambient site measurements. Şen (1995) found the cumulative semivariogram (CSV) methodology a useful tool for describing qualitative regional features of air pollutant dispersion in the Istanbul area. Anh *et al.* (1997) also used the cumulative semivariogram in investigating the spatial variability of the air quality in Sydney. They concluded that the method was suitable to represent the spatial variability of a smoothed homogeneous and isotropic concentration field. Vincent and Gatrell (1991) used kriging to examine the spatial variability of radon gas in Lancaster, based on measurements from 391 homes. Their results suggested that use of additional co-variates (e.g. data on altitude or geology) was necessary to model radon concentrations. Kriging was also used as part of the SAVIAH study, to model air pollution from road traffic (Collins 1998b). The results were found to be less accurate than other methods, such as regression techniques, and were therefore not used to provide exposure assessments for comparison with health outcome. Indeed, to date there are few examples of the use of geostatistical techniques in epidemiological studies. One rare example is that by Wartenberg (1993), who applied kriging to investigate links between cancers and drinking water contamination and microwave radiation in Cape Cod, Massachusetts.

2.3.3 *Regression modelling*

2.3.3.1 *Introduction*

Regression modelling uses least square regression techniques to generate predictive models of the spatial surface of interest, using measured data on the dependent variable of interest and one or more covariates.

A regression equation is an equation for estimating a dependent variable (X_1) from independent variables (X_2 and X_3). The simplest regression equation of X_1 on X_2 and X_3 has the form:

$$X_1 = b_1 + b_2X_2 + b_3X_3 \tag{2.11}$$

where b_1, b_2 and b_3 are constants.

The least-square regression of X_1 on X_2 and X_3 has the equation (*2.11*) where b_1, b_2 and b_3 are determined by solving simultaneously the equations:

$$\begin{aligned} \Sigma X_1 &= b_1N + b_2\Sigma X_2 + b_3\Sigma X_3 \\ \Sigma X_1 X_2 &= b_1\Sigma X_2 + b_2\Sigma X_2^2 + b_3\Sigma X_2X_3 \\ \Sigma X_1 X_3 &= b_1\Sigma X_3 + b_2\Sigma X_2X_3 + b_3 \Sigma X_3^2 \end{aligned} \tag{2.12}$$

The technique is widely used in exploratory and explanatory surveys and is also a useful tool in classifying remote sensing imagery. Mattson and Godfrey (1994), used multiple regression combined with GIS in predicting road salt contamination in Massachusetts. The regression model gave a reasonably good fit to the data (r^2 = 0.67), but possibilities of collinearity in the independent variables, and evidence of heteroscedasticity in the data acted as warnings against oversimple interpretation of the results. They concluded that further validation was essential before the method could be used for policy purposes.

Si and Harrison (1997) used regression modelling to predict hourly NO_x and NO_2 concentration in the urban air in London. Hourly measurements of NO_x and NO_2 at two central London monitoring sites (Central London Laboratory and Bridge Place) over two years (June 1989-May 1990, June 1991-May 1992) were used in the model. Hourly values of O_3 were taken from four monitoring sites, distributed in four different directions outside

London. Data on wind speed and boundary layer depth was obtained from the London Weather Centre, and a box model was developed to reflect the daily and day-to-day variations in NO_x source strength. Two regression models were created: an ordinary least squares (OLS) model and a first-order autoregression (AR) model. The OLS model violated the independence assumption. It was thought that errors were introduced in the emission factor when the wind speed is low. The results of the AR model was capable of predicting NO_2 (r = 0.83) and NO_x (r = 0.65) when the explanatory variables were available.

Another study in predicting nitrogen oxide using regression analysis was undertaken by Inoue *et al.* (1986a and 1986b). Hourly NO_x concentrations were measured in Chiba City (Japan) from April 1977 to March 1978, at a site where the influence of cars was dominant. Data on traffic volumes and weather conditions were obtained. A regression model was constructed using explanatory variables and composite variables. The models created were found to be applicable in predicting hourly NO_x concentrations; however, results suggest that it might be difficult to apply the models to predictions of two hours or more.

Few epidemiological studies have used regression modelling to provide estimates of exposure to environmental pollution. The main example is in the SAVIAH study (Elliot and Briggs 1998, Briggs *et al.* 1997), where a regression-based model was derived by regressing measured NO_2 concentrations against indicators of traffic volume, land cover and topography (see also *Section 2.3.3* and *3.3.8*). This was then used to estimate mean annual NO_2 concentrations for a fine (10 metre) grid across the study area. Exposures for ca. 4600 children for whom data on respiratory illness had been obtained were then estimated by dropping the place of residence and/or school onto the resulting pollution map.

2.3.4 *Indicators*

Indicators are indirect measures of exposure based upon location and the source-activity relationship. Examples, in relation to exposure to traffic-related pollutants, are traffic volume, distance to road and road density. Distance to road, for instance, gives a measure of the distance between the subject's location (house, school) and the nearest road. The closer the road, the more the subject will tend to be exposed to pollutants which are generated by the traffic using that road. The source in this example is the road, and the activity the traffic.

Indicators such as these have been widely used in epidemiological studies of the relationship between traffic-related air pollution and health (see *Table 2.4*). Recent studies, for example, have examined the possible association of respiratory symptoms and hospital admissions for asthma with: proximity of residence to major roads (Livingstone *et al.* 1996, Nitta *et al.* 1993, Murakami *et al.* 1990); measures of traffic density in the surrounding area (Wjst *et al.* 1993, Brunekreef *et al.* 1997, Wilkinson *et al.* unpub., Edwards *et al.* 1994); and self-reported traffic levels (Weiland *et al.* 1994, Nitta *et al.* 1993 and Duhme *et al.* 1996).

Exposure indicators have various advantages over more direct measures of exposure (e.g. modelled pollution levels). One is their ease of compilation. Using GIS, it is a relatively simple task to derive measures of distance from the nearest road, road density within a specified buffer zone around the place of residence, or total traffic volume on surrounding roads. The data needed to generate such estimates are also simple and readily available. For these reasons, the technique can be easily applied in large population studies and to most urban areas.

Several disadvantages nevertheless occur in using indicators. Indicators are very general and loosely defined. The relation between the indicator and the exposure of interest is often far from clear, and in many cases is not linear: levels of pollution are likely to fall relatively rapidly in the first few metres away from a road source, for example, then level off at greater distances. Nor do they take account of the meteorological and other factors which might affect patterns of pollution and exposure across an urban area. Indicators are also non-specific: they do not relate to any specific pollutant and thus do not help to distinguish the causative agents. In addition, the lack of standardisation of these measures means that results from different studies often cannot easily be compared. Partly for these reasons, perhaps, results from these studies have tended to be inconclusive.

2.4 CONCLUSION

This Chapter has reviewed literature on traffic-related pollution and the health effects from these pollutants. It showed that although there is strong evidence for an acute effect, the link between chronic exposure to air pollution and health effects remains inconclusive. The present lack of knowledge about chronic effects adds great uncertainty to quantify the environmental health impact to traffic-related pollution.

This Chapter then reviewed a number of methods which can be used to estimate exposure to traffic-related pollutants. It identified four main approaches to exposure assessment: dispersion modelling, spatial interpolation, regression modelling and the use of exposure indicators. The review shows that only a few of the many existing air pollution dispersion models have been used in epidemiological studies. Similarly, few epidemiological studies have used spatial interpolation or regression modelling for providing exposure estimates to traffic-related pollution. Most studies in the past have relied on the traditional exposure estimates, such as distance from the nearest road or road density within a specified buffer zone.

In *Chapter 3* a few of these methods will be examined more closely, prior to applying selected methods in the field.

3 SELECTION AND DEVELOPMENT OF METHODS

This chapter starts by identifying the two study areas (*Section 3.1*) used in this research. In *Section 3.2* and *3.3*, it then describes the selected methods and how they were implemented in the GIS.

3.1 CASE STUDIES

Two case studies in two different areas were chosen to test and evaluate the performance of some of the methods described in *Chapter 2*. Greater London was the first choice. The area was selected for a number of reasons. It is the largest city in the UK, with a resident population of over 6 million people (about 10% of the national population). It is thus a major source of air pollution and faces major problems of air pollution. Data are readily available on air quality, emissions and the road network (see *Section 4.3*), allowing the methods used to be implemented and validated. In addition, the city has been the location of a number of important previous studies of the relationship between air pollution and health (e.g. Livingstone *et al.* 1996; Wilkinson *et al.* unpub.). During the research, the possibility also arose to undertake a similar study in Sheffield, as part of a Department of Health/MRC-funded project (see *Section 5.1*). The Sheffield case study provided the opportunity to apply the methods in contrasting conditions from Greater London (different topography, smaller size) and to explore relationships between the resulting exposure estimates and health outcome.

During selection and implementation of the methods, several of the methods were also piloted in the Kensington and Chelsea area, using local data obtained from the Royal Borough of Kensington and Chelsea.

In each area, a number of different methods were investigated and compared. These included simple exposure indicators, dispersion modelling and spatial interpolation techniques. The methods used in Greater London and Sheffield varied, depending on data availability, spatial resolution of the data and availability of the methods. The following sections describe the various methods used.

3.2 INDICATORS

3.2.1 Description

As *Chapter 2* has shown, several non-pollutant indicators have been used in epidemiological studies in the past, as measures of exposure to traffic-related pollution. The following indicators were selected for use in this research:

- distance to nearest road
- road density within 150m
- traffic volume within 150m

These were selected to represent a range of source-related indicators, including one measure of proximity to the nearest road, one of road density and one of level of traffic flow. The distance of 150m was chosen as a basis for measuring the road density and traffic volume indicators because it was the most commonly used distance in the literature reviewed (Livingstone *et al.* 1996, Murakami *et al.* 1990, Wilkinson *et al.* unpub.). The first two indicators (distance to nearest road and road density) were calculated for two different sets of roads: main roads (i.e. those defined as roads greater than 4m wide) and all roads (main and minor roads). The traffic flow was calculated for both 'all motor vehicles' and 'heavy goods vehicles (HGV)'.

3.2.2 Implementation

The indicator 'distance to nearest road' was calculated using the NEAR command in ARC. This command searches for the closest road near the point and calculates its distance. The indicator 'road density within 150m' was calculated in ARC using an AML written by the author (see *Appendix 3A*). For every given point, a 150m buffer was created using the BUFFER command, which was then intersected with the roads coverage concerned. With the STATISTICS command, the road length of the intersected roads was calculated. The indicator 'traffic volume within 150m' was calculated in the same way, expect that in the STATISTICS command the road length was multiplied by the traffic flow. Thus:

Traffic volume = traffic flow x road length

3.3 MODELLING TECHNIQUES

3.3.1 NO_2 as an indicator for traffic-related air pollution

3.3.1.1 Introduction

Modelling of exposure to traffic-related pollution was undertaken using nitrogen dioxide (NO_2) as the target pollutant. NO_2 is not, of itself, a pollutant of major concern in terms of its health effects. Although it is a respiratory irritant, it rarely reaches concentrations sufficient to exacerbate asthma or other respiratory symptoms in the ambient environment. Nevertheless, it was selected as the target pollutant for a number of reasons.

Firstly, as shown in *Section 2.2*, NO_2 is strongly related to traffic volume. *Table 2.1* showed that road transport contributes 46% to NO_x emissions nationally and 76% in London. It thus provides a reliable marker for traffic-related pollution, especially in urban areas.

Secondly, although, as noted NO_2 is rarely directly implicated in health effects, it does show consistent correlations with pollutants of more immediate health concern. As *Figures 2.3* and *2.4* show, for example, the relationship with traffic speed is similar for NO_x and fine-particulates, for both light and heavy duty vehicles. NO_2, as the major component of the NO_x fraction in the ambient air, thus provides a better predictor of particulate concentrations than other pollutants, such as CO.

Thirdly, NO_2 has been widely used as a marker for exposure to traffic-related pollution in previous health-related studies: for example in studies by Brunekreef *et al.* (1997), Oosterlee *et al.* (1996), Pershagen *et al.* (1995), Nitta *et al.* (1993), Murakami *et al.* (1990) and Nakai *et al.* (1995).

Finally, measuring NO_2 is relatively cheap and easy, and data on NO_2 concentrations are widely available. In particular, the development of simple, passive sampling devices

(Palmes *et al.* 1976) has meant that dense networks of sampling can be established, providing detailed data on spatial patterns of air pollution within a city. The national diffusion tube network operated by NETCEN, for example, includes about 1200 sites, compared to a mere 40-50 sites in the national particulate network. The cheapness of passive samplers also meant that they could be used to conduct purposely-designed surveys, as part of this research.

3.3.1.2 Sources of NO_2

Nitrogen oxides include nitric oxide (NO), nitrogen dioxide (NO_2), nitrous oxide (N_2O), dinitrogen trioxide (N_2O_3) and nitrogen pentoxide (N_2O_5). They are produced by natural processes, including lightning, volcanic eruptions, forest fires and bacterial action in the soil and by human activity during combustion processes of fossil fuels, especially by non-nuclear power stations and motor transport (Onursal and Gautam 1997). NO and NO_2, collectively known as NO_x, are the most important nitrogen oxides in the context of pollution studies. The other nitrogen oxides are not known to have any biological significance (Elsom 1987).

Table 3.1 shows the main emission sources of oxides of nitrogen in the United Kingdom. The highest contributor (49%) is from motor vehicles. (Note that this represents a slightly different estimate from that reported in *Table 2.1*). Nearly 25% is contributed by non-nuclear power stations.

Overall, emissions of nitrogen oxides into the air in the United Kingdom are estimated to have increased slowly from 1970 to 1989, since when they have declined to 1970 levels. This is notwithstanding a doubling in traffic volume since 1970 (*Figure 2.2*). The reduction in the unit emission rate is largely due to the introduction of new engine and emission control technologies, in part as a result of government policy. However, if no further measures are taken, it is expected that there will be a slow increase in pollution after 2010 as traffic levels continue to grow (DETR 1995).

Ambient ground level concentrations of nitrogen dioxide will generally be influenced more by emissions from motor vehicles than by power stations. The tall stacks of power stations will disperse the pollution effectively before it reaches ground levels (Department of the Environment 1996). It can therefore be assumed that in towns, where most people live and where consequently the highest risk of exposure exists, near-ground NO_2 concentrations will be largely derived from motor vehicles.

Table 3.1: Estimated United Kingdom emissions of oxides of nitrogen by emission source, 1994, thousands tonnes per year (Department of the Environment 1996)

Source	Estimated Emissions*	Percentage of Total**
Power Stations (fossil fuelled)	526	24
Domestic	69	3
Commercial/Public service	34	2
Refineries	45	2
Iron and Steel	48	2
Other Industrial Combustion	128	6
Non Combustion Processes	5	-
Extraction and distribution of Fossil fuels	109	4
Road Transport		
Petrol	653	29
Diesel	442	20
Other Transport	151	7
Waste Treatment and Disposal	4	-
Agriculture	3	-
Total	2218	100

* Rounded to the nearest thousand tonnes
** Rounded to nearest 1%

3.3.1.3 *Chemistry of NO_2*

Nitrogen oxide (NO), and to a lesser extent nitrogen dioxide (NO_2), are formed at high temperatures during combustion processes, by oxidation of nitrogen in the air and from nitrogenous components in fuel.

The main process by which NO is converted into NO_2 in the atmosphere is by interaction with ozone (O_3):

$$NO + O_3 \leftrightarrow NO_2 + O_2 \tag{3.1}$$

This reaction is a photo-stationary state, which means it only takes place in daylight. In the presence of hydrocarbons, NO_2 is then transformed photochemically to NO and atomic oxygen (O):

$$NO_2 + \text{energy} \rightarrow NO + O \tag{3.2}$$

Oxygen then combines with the atomic oxygen to form ozone:

$$O_2 + O \rightarrow O_3 \tag{3.3}$$

It can therefore be seen that nitrogen dioxide is a product of a reaction between ozone and the nitrogen oxide emitted from car exhausts. Ozone itself is formed by the action of sunlight on nitrogen dioxide. The proportion of NO converted into NO_2 and the reaction rate depend on the concentration of O_3 available and the concentration of NO to be oxidised. Where there is a large source of NO, the limiting factor on the production of NO_2 will be the available O_3. At the stage where all the available O_3 has reacted with NO, no more NO_2 will be produced even at much higher NO concentrations. In city centres, supplies of ozone quickly run out, halting the production of NO_2. Only when the remaining NO drifts away to the suburbs or rural areas does more ozone become available for oxidation. At city centre roadside locations, therefore, 5-40% of the NO_x typically consists of NO_2, at urban background sites 30-80% and in rural areas 70-100% (Elsom 1996).

3.3.1.4 Measuring NO_2

Measuring NO_2 concentrations can be done with either automatic or non-automatic monitoring techniques. For reasons of cost and convenience, this research uses the non-automatic or passive technique.

The principle underlying passive techniques of monitoring is the molecular diffusion of gas in a stationary air layer. This diffusion is described in Fick's law (Hartog 1995):

$$J = \frac{D * A(C - C_0)}{L} \tag{3.4}$$

where:

J mass flux of gas ($\mu g\ s^{-1}$)

D diffusion coefficient of gas in air (m^2 s^{-1})

A reaction area of sampler (m^2)

C external gas concentration in air (μg m^{-3})

C_0 equilibrium concentration at reaction surface (μg m^{-3})

L diffusion length (m)

A wide range of passive sampling devices have been developed over the last twenty years, including both tube- and badge-type devices (van Reeuwijk *et al.* 1998). In this research the Palmes diffusion tube (Palmes *et al.* 1976) was used. The design of the tube is shown in *Figure 3.1*. The sampler consists of a polyeurethane tube, 82 mm in length, with a metal reaction grid, or membrane, at one end. The reaction grid is coated with T.E.A. (Tri Ethanol Amine, $C_6H_{15}NO_3$), which acts as an absorbent for NO_2 in the atmosphere. The open end of the tube is capped prior to use, and again immediately afterwards for storage and shipment to the laboratory. NO_2 concentrations are analysed in the laboratory using spectrophotometry.

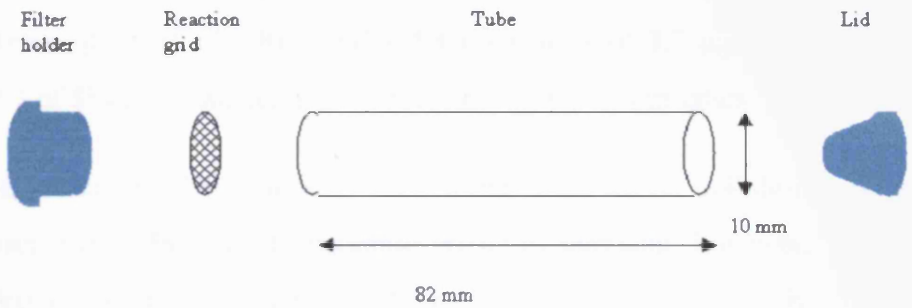

Figure 3.1: Sketch of the Palmes-tube

The main advantages of the NO_2 diffusion tube, as mentioned earlier, are its low cost and easy application. This is especially important when one is interested in the spatial coverage of an area, and thus where a number of sites is needed to provide spatial coverage. The most important disadvantage is its poor temporal resolution. The detection limits of the sampler mean that it must be exposed for several days (typically 10-30) to provide a reliable measure of ambient concentrations. The tubes thus provide data only on relatively long-term average NO_2 levels, and cannot measure short-term peaks. Sampling problems caused by meteorological conditions and interference of other pollutants are other possible disadvantages. These may lead to significant bias in the measurements. Heal and Cape (1997), for example, examined the chemical interferences in the measurements of NO_2 with passive diffusion tubes, using a numerical evaluation model. By comparing passive diffusion tube NO_2 measurements with continuous monitor results, they found NO_2 overestimates of 28% at urban sites in the summer and 8 to 14% at rural sites and at urban sites in the winter, when using the diffusion tube. The overestimation was caused by the chemical reaction between NO and O_3 inside the diffusion tube. Similar results were found by Gair and Penkett (1995), in a study of the effects of wind speed and turbulence on the performance of diffusion tubes. They found that NO_2 concentrations were overestimated by up to 40% when using the diffusion tubes, apparently because turbulence at the face of the sampler caused by wind shortened the effective diffusion path along the tube.

The relatively low precision of passive samplers compared to chemiluminescent methods may also be a problem. This is often assessed by using duplicate tubes. Atkins *et al.* (1986) and Goldsmith (1986) report coefficients of variation between duplicate tubes of 5-8%. Van Reeuwijk *et al.* (1998) found a detection limit of 3.7 $\mu g\ m^{-3}$ and a coefficient variance (CV) of 8% from duplicate NO_2 diffusion tubes, in four cities.

Despite these limitations, NO_2 tubes are now widely used for air pollution monitoring and exposure assessment. In order to minimise errors in sampling, however, strict field and laboratory procedures are necessary, and were employed in this research. These include use of duplicate tubes at all sites, repeat surveys at different times of the year (to allow for meteorological and other factors), strictly controlled and consistent deployment times (to reduce effects of differences in diffusion rate or possible saturation of the reaction grid), and careful siting of the samplers (to avoid the effects of local emission sources or turbulence).

3.3.1.5 Modelling techniques

A number of different modelling techniques were used in this study. These included dispersion models, spatial interpolation techniques and regression mapping methods.

Four dispersion models were investigated:

- ***CALINE3*** - because it is one of the most frequently used models in relation to traffic-related pollution (Onursal and Gautam 1997);
- ***DMRB*** - because it provides a relatively simple and widely used technique, which is often employed in the UK for environmental assessment of local traffic schemes;
- ***ISC3*** - which represents an early, area-source dispersion model; and
- ***ADMS-Urban*** - a new generation line dispersion model, which is now being widely promoted as a local authority standard for air pollution assessment.

Two geostatistical techniques were used:

- ***Kriging*** - the most widely used of the geostatistical techniques, and which has been employed on a number of occasions to map air quality (Lefohn *et al.* 1988, Vincent and Gatrell 1991, Şen 1995, Ahn *et al.* 1997 and Collins 1998b); and
- ***Co-kriging*** - a more recently developed method with potential for estimating air pollution (Sally Liu and Rossini, 1996)

In addition, an empirical regression-mapping method was used:

- the so-called ***SAVIAH*** model, which was developed as a basis for mapping small area variations in traffic-related air pollution in Huddersfield, UK (Briggs *et al.* 1997).

The following sections give a brief description of the models and describe how they were implemented in ARCINFO.

3.3.2 CALINE3

3.3.2.1 Description

The development of CALINE by the California Department of Transport (CALTRANS) was a direct result of the US National Environmental Act in 1969. The original version of CALINE was released in 1972 but was soon replaced by CALINE2, in 1975. This second-generation model was able to predict pollution levels in parallel wind conditions and for depressed sections.

Research to validate CALINE2 concluded that, in specific meteorological conditions (stable, parallel wind conditions), CALINE2 overpredicted pollution levels by two to five times. Because these specific meteorological conditions were often used for worst case scenarios a new model, CALINE3, was developed in 1979 which overcame these problems (Benson 1979). Since then, CALTRANS have developed CALINE4, although this has not yet been approved by the EPA for general usage (Onursal and Gautam 1997).

CALINE3 is an air pollution dispersion model for line sources based on the Gaussian plume model. It can be used to estimate concentrations of non-reactive pollutants from traffic. The input variables needed for the model are source strength, meteorology, site geometry and site characteristics.

CALINE3 divides the road network around a receptor into links. Each link is assumed to be straight with a constant width, height, traffic volume and emission factor. For each link, CALINE3 calculates the contribution to the receptor. The total exposure is calculated by summing all the contributions of all links. The receptor distance is measured perpendicular to the link. Emissions from the link are assumed to disperse in a Gaussian manner downwind from the link. The regions directly over the width of the link, and three metres on either side of the link, are defined as the mixing zone and are assumed to be characterised by uniform emissions and turbulence. The distance of three metres either side of the link takes into account the horizontal dispersion caused by the vehicle wake effect. Vertical dispersion curves are used to calculate the contribution to a receptor. The curves are defined by parameters derived from the mixing zone, as defined by Pasquill (Pasquill 1974).

In its distributed form, CALINE3 can handle a maximum of 20 links, 20 receptors and 384 different meteorological conditions in one run.

CALINE3 takes into account links with a receptor to up a distance of 10 km. To reduce processing times, it was decided in this study to select only sources/links within a 200m radius of the receptor. The Department of Transport (1994) uses 200 m as a cut off point in the Design Manual for Roads and Bridges, and it is widely accepted that dispersion models such as CALINE are relatively inaccurate at distances greater than this.

CALINE4 is an updated and expanded version of CALINE3. While the models use different methods for developing the horizontal and vertical dispersion curves, the final results differ very little by air quality modelling standards. The main differences are in the areas of improved input and output flexibility and expanded capabilities (Benson 1989). Comparison of CALINE3 and CALINE4 showed that the later model gave only modest improvements in accuracy (Benson 1992).

3.3.2.2 Piloting

CALINE3 and CALINE4 were compared in an early stage of this research, in the Royal Borough of Kensington and Chelsea.

Data on air pollution levels originated from a feasibility study, undertaken by the local authority, of the health effects of air pollution on the residents of the Royal Borough. As part of the air pollution study, NO_2 was monitored at 57 sites during two sampling periods (19-6-95 to 19-7-95, and 26-10-95 to 26-11-95) in the Lots Road area and the Worlds End Estate, using NO_2 diffusion tubes.

The Kensington Borough also provided detailed traffic counts at eight locations in the study area for the year 1994. Hourly traffic counts were recalculated into 24-hour average traffic counts. For links without any traffic information a traffic volume was imputed by interpolation between neighbouring links. This traffic data was then attached to the road coverage in ARCINFO. Meteorological data for the two survey periods were obtained from the Meteorological Office for the London Weather Centre.

Modelled results from both CALINE3 and CALINE4 were compared with monitored data for the 57 sampling sites, using correlation analysis. Correlations were relatively weak for both models for both survey periods (*Table 3.2*). In part, at least, this may reflect inadequacies in the air quality data: unfortunately, the surveys had not used duplicate tubes, and sample sites often seem to have been poorly chosen and were highly variable in height above ground. Overall, however, CALINE3 was seen to perform better than CALINE4. Taken together with results reported by Benson (1992), this suggested that little, if anything, would be gained by using the CALINE4 model; CALINE3 was thus chosen because of its ability to handle more hours of meteorological data in one run.

Table 3.2: Pearson correlation coefficient (r) of CALINE3 and CALINE4 predictions against monitored data.

	CALINE3	*CALINE4*
Survey1	0.344	0.032
Survey2	0.245	0.130

3.3.2.3 Implementation

In its distributed form, CALINE3 consists of a set of Fortran files and is designed to run as a stand-alone package under DOS. A DOS-executable file (rcaline3.exe) was obtained from Trinity Consultants. This executable file allowed CALINE3 to be run using previously prepared input files, without having to use the time consuming interface, which comes with the stand-alone package.

In order to link the rcaline3.exe file to ARCINFO, an AML (Arc Macro Language) program was written in ARCINFO 7.1, which writes one CALINE3 input file for each specified receptor. The AML buffers the selected receptor point with a 200m radius and intersects the resulting areas with the road network in order to pick out the road links used in the CALINE3 run. A second AML was also written to read the separate output files and calculate the mean NO_2 for each receptor for the defined period (see *Appendix 3B*).

CALINE3 uses a user-defined emission factor for each road link. In this research an emission factor of 4 g mile^{-1} (2.5 g km^{-1}) was used. This represents the upper limit of the range of emission factors suggested for the UK by the Department of Transport (1994), and within the range of values previously computed for the UK by Gilham *et al.* (1992) and Europe (Commission on the European Communities 1995). A relatively high value was used to reflect the slow speeds and high proportion of heavy duty vehicles found in urban areas such as London and Sheffield. It should be noted, however, that the relationship between emissions and concentrations in the CALINE3 model is linear, so that any error in this emission factor will produce a proportional error in the modelled concentrations; it will not affect the spatial pattern of pollution.

3.3.3 DMRB

3.3.3.1 Description

The Design Manual for Roads and Bridges (DMRB) was developed by the Department of Transport to guide engineers and planners in road and bridge design. It contains a model, which assesses the environmental impact of roads and bridges. The model is based on a series of graphs derived from a Gaussian dispersion model, developed by the UK Transport Research Laboratory. The main purpose of this model is quickly to assess the environmental impact of existing or proposed road schemes and to see whether more detailed air quality assessments are required (Department of Transport 1994).

The model is a screening model and does not take into account the actual meteorological conditions, emissions and photochemical processes at a specific point. The wind speed is assumed to be 2 m s^{-1}, and emission rates are derived from national figures. Variables needed for input are peak hour traffic flow, traffic speed and distance of the receptor from the centre of the road. NO_x concentrations are modelled from the peak hour traffic flow and can be converted to 98th percentile of hourly average NO_2 concentrations by reading from an appropriate graph (see *Figure 3.2*).

DMRB is at the moment of writing under further development. The new DMRB methodology is expected to be released in December 1998 and will include modifications to the air quality module. The main change is that the new methodology uses annual mean traffic counts rather than peak hour traffic counts as an input parameter to the model. This is designed to counter problems encountered with the original model, when peak flows fall outside the morning and early evening peak hours. By using annual mean traffic counts it is thought the model will represent a more realistic scenario (Dispersion Modellers Group meeting, 29 November 1998).

In this research, the original DMRB model was used.

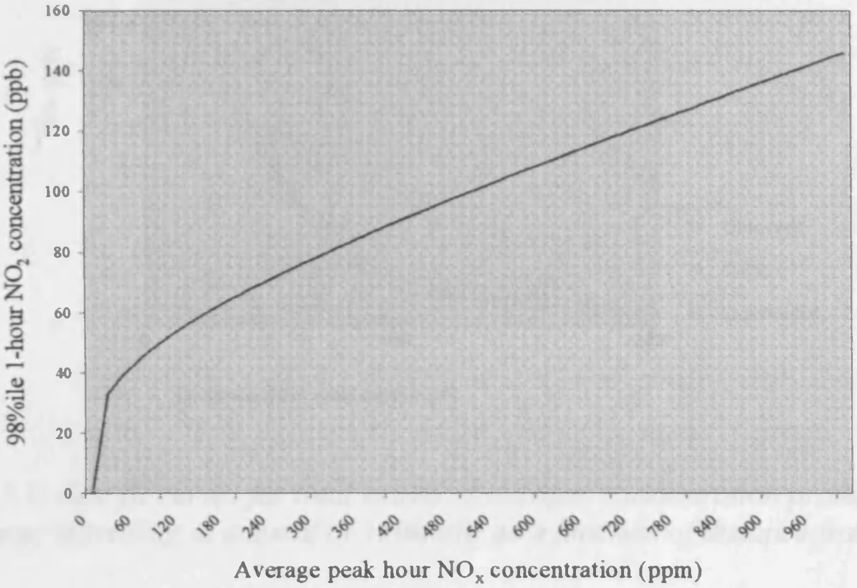

Figure 3.2: 98th percentile of 1 hour average nitrogen dioxide concentration as a function of total oxides of nitrogen in the peak traffic hour.

3.3.3.2 Implementation

In order to link DMRB to ARCINFO, an AML was written in ARCINFO (see *Appendix 3C*).

The two graphs in DMRB, describing NO_x against distance from road centre and the 98%ile 1-hour NO_2 against average peak hour NO_x, were first transformed into equations which could be used in the AML. To accomplish this, the tables from these graphs (see *Appendix 3D*) were imported into SPSS where the best-fit curves were estimated.

The best fit curves for NO_x concentration versus distance from road are shown in *Figure 3.3*, and are as follows:

For Distance (d) $\leq$ 47.5: $NOx = 219.738 - 4.519d + 0.032d^2 - 0.00008d^3$ (cubic) (3.5)

For Distance (d) > 47.5: $NOx = 166.886 * e^{-0.0199d}$ (exponential) (3.6)

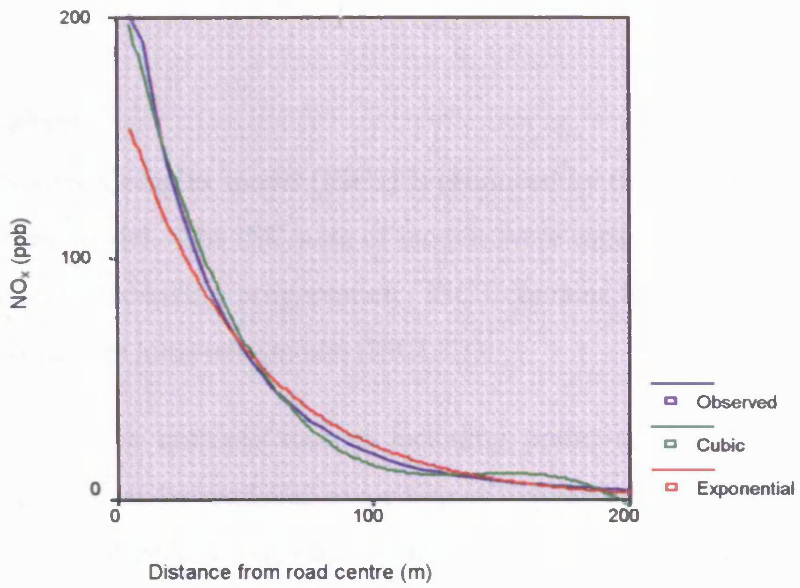

Figure 3.3: Best fit curves for total oxides of nitrogen concentration produced by 1000veh/hour travelling at a speed of 100km/hr as a function of distance from a road.

The best-fit curves for the 98%ile 1-hour NO_2 concentrations (98%NO_2) against the average peak hour NO_x concentrations (PHNO_x) were as follows (*Figure 3.2*):

For PHNOx (x) < 20: $98\%NO2 = 1.65x$ (3.7)

For $20 \leq$ PHNOx (x) ≤ 200: $98\%NO2 = 26.298 + 0.3712x - 0.0014x^2 + 2.9E\text{-}6x^3$ (3.8)

For PHNOx (x) > 200: $98\%NO2 = 49.11 + 0.0984x$ (3.9)

All curves described in *Equations 3.5 – 3.9* had $r^2 > 0.98$, indicating a near perfect fit. These equations were implemented in the AML. The AML creates a 200m buffer around the receptor point, which is then intersected with the road network. The variables traffic flow, traffic speed and distance to receptor are derived from the selected road links. With these variables the 98%ile 1-hour concentration NO_x (ppb) is calculated. The 98%ile 1-hour concentration can be converted into an annual mean by dividing it by a factor of 2.4 (HMIP, 1993)

3.3.4 ISC3

3.3.4.1 Description

The Industrial Source Complex model (ISC3) is produced by the US-EPA and is based on the Gaussian plume model. The ISC suite of models were especially developed to support the EPA's regulatory modelling programmes. ISC3 contains two models, the short-term model (ISCST3) and the long-term model (ISCLT3).

Both models can handle multiple sources including point, area, volume and open pit sources. Line sources can be modelled as a string of volume or area sources. The models also include a range of options such as building downwash effects and urban and rural dispersion parameters. The short-term model has additional options including a COMPLEX option, which takes account of receptors located in complex terrain, and dry and wet deposition algorithms.

Receptors in both models can be defined as grids (Cartesian or polar) or as specific points.

The meteorological parameters needed in the short-term model are hourly records of flow vector, wind speed, temperature, stability category, rural mixing height and urban mixing height. The long-term model uses joint frequency distributions of wind speed class, by wind direction sector, by stability category, known as STAR (STability ARray) summaries (USEPA, 1995).

3.3.4.2 Implementation

Only the long-term program was used in this study. The FORTRAN code was compiled in C++ in order to use it in a UNIX environment in combination with ARCINFO. AMLs were written to automate input to the model and to convert output into ARCINFO coverages for further analysis (see *Appendix 3E*).

3.3.5 ADMS-Urban

3.3.5.1 Description

The Atmospheric Dispersion Modelling System for urban environments (ADMS-Urban) was developed by the Cambridge Environmental Research Consultants Ltd (CERC) and the UK Meteorological Office (CERC 1998). It is an air quality system, which takes account of traffic, domestic and industrial pollution. The traffic model contains a chemistry model for NO_2, SO_2 and O_3, a street canyon model and a traffic emission database. ADMS-Urban has an interactive interface, ArcView, for data entry and display of model output.

ADMS-Urban contains several advanced options, such as modelling the effect of buildings and/or the effect of complex terrain on dispersion of pollutants. It also uses an up-to-date understanding of the atmospheric boundary. This is described by boundary layer depth, h, and the Monin-Obukhov length, L_{mo}, rather than by the Pasquill stability categories (CERC 1998).

The Monin-Obukhov length is defined as:

$$L_{MO} = \frac{-u*^3}{\kappa \cdot g \cdot F_{\theta_0} / \left(\rho \cdot c_p \cdot T_0\right)} \tag{3.10}$$

where

$u*$	friction velocity at earth's surface (m/s)
κ	von Karman constant (0.4)
g	gravity acceleration
F	surface heat flux
p	density of air
c_p	specific heat capacity of air
T_0	surface temperature

In unstable conditions, the Monin-Obukhov length is negative. All the turbulence in the boundary layer is generated convectively (by wind). Mechanical (friction at the earth's surface) turbulence has no great impact. In stable conditions, however, the process is reversed. All the turbulence is mechanically generated giving the Monin-Obukhov length a positive value. The developers claim that research has shown that using these variables much improves model performance.

Data requirements for the Monin-Obukhov length are demanding, and often cannot be satisfied by the available meteorological stations. In these cases, it is possible to use cloud cover or the surface sensible heat flux as proxies. The extent to which these degrade the performance of ADMS-Urban is unknown.

In this study, only the line model in ADMS-Urban is used. This model needs the following input data:

- traffic composition (type, count, speed)
- traffic emissions (hourly, monthly)
- road geometry (location, width)
- receptor (location, elevation height)
- complex terrain information
- meteorological data (see above)

This data can be added manually or it can be imported by the emission inventory database stored in Access. In one run, ADMS-Urban can calculate concentrations at 20 receptor points for 1000 road sources and 10 pollutants. In this study it is used under Windows NT.

3.3.5.2 Implementation

ADMS-Urban is already implemented in ArcView and there was therefore no need for any special alterations. At the time of this research, however, CERC had not finished writing the hill module, which allows for the effects of a complex terrain on dispersion, in ADMS-Urban. A beta-release of the module was received from CERC, but it was noted that this module was not fully tested at that time (Alistar Lester, CERC, pers. comm.) and was therefore not used.

3.3.6 Kriging

3.3.6.1 Description

Kriging is an optimal method for interpolation developed by Matheron (1971) originally for use in the mining industry. Since then, kriging has been widely applied to ground water mapping, soil mapping and other related fields. Only recently has it been used in the field of environmental pollution mapping (see *Section 2.3.4*)

The method is based on the assumption that the property of interest is too irregular to be modelled by a smooth mathematical surface but is better described by a stochastic surface (Burrough and McDonnel 1998). Kriging depends on assumptions known as the 'regionalized variable theory', which assumes that the spatial interpolation of the z-values is spatially homogeneous (stationary) throughout the surface, or, stated more simply, that sites which are close together tend to be more similar than those which are further apart.

An essential first step in kriging is analysing the spatial dependency in the data by the generation of a variogram. The variogram is created from the sample data by plotting the semi-variance, *y(h)*, against the distance between the samples *(h)*. The semi-variance is defined as (Burrough, 1986):

$$\hat{y}(h) = \frac{1}{2n}\sum_{i=1}^{n}\{z(x_i) - z(x_i + h)\}^2 \tag{3.11}$$

where n is the number of pairs of observations of the values of attribute z separated by distance $\boldsymbol{h}$.

Sample spacing, $\boldsymbol{h}$, is also called the lag. In many cases, the sample sites are irregularly distributed. This would mean that, for an exact vector $\boldsymbol{h}$, too few pairs of data would be available to create the variogram. This problem is solved by putting a tolerance on $\boldsymbol{h}$, so it becomes the lag $\boldsymbol{h}$, thus providing more pairs for the analysis. This approach was used here.

For a stationary spatial process the variogram would have a distinctive shape, as shown in *Figure 3.4*.

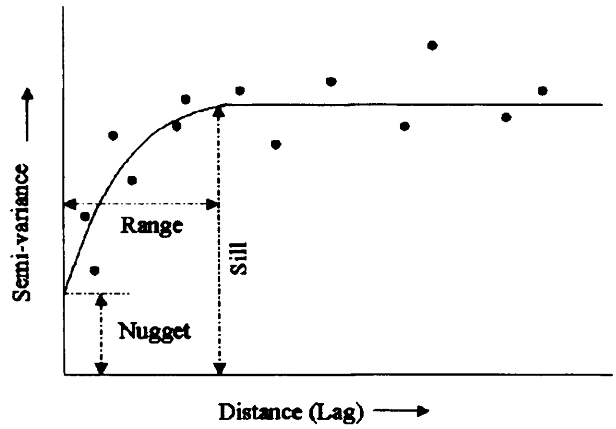

Figure 3.4: The variogram

Assuming a stationary spatial process, points close together would have a similar value, so the semi-variance would be small (points at the same location would have the same value, so semi-variance would be 0). Points further apart would have a greater difference so the semi-variance would be larger. At a certain distance, the samples become independent of each other. The semi-variance at which this happens is called the *sill (c)* and the distance is called the *range (r)*.

The shape of the semivariogram departs from this idealised form in many cases. The distribution thus needs to be modelled, by fitting an appropriate curve to the semiovariogram, using least squares or weighted least squares techniques (McBratney and Webster 1986). Spherical, gaussian, exponential and linear models are often applied.

In practice, points close together can often have quite dissimilar values due to randomness in the data. This is called the nugget effect. It means that the model does not go through the origin. A variogram with pure nugget effect lacks any spatial dependency. In a variogram this would show up as a horizontal line, intersecting the semivariance at some point above zero.

Where there is spatial trend in the data, the shape of the semiovariogram may not be the same in all directions; spatial dependency is then said to be anisotropic. To explore these directional effects, variograms can be calculated for different directions. In practice, very few studies have considered anisotropy, and previous applications of kriging for air quality analysis have tended to assume isotropy (Anh *et al.* 1997, Lefohn *et al.* 1988, Sally Liu and Rossini 1996). For broader scale analyses, where there may be strong regional trends in the data (e.g. relating to prevaling wind directions), this assumption is liable to be false. For local-scale (e.g. urban) analyses, however, the assumption is likely to hold true. Neither Wu (1998) nor Collins (1998a), for example, found any directional effects in using kriging to map traffic-related air pollution data in Huddersfield. In this research, therefore, the data were assumed to be isotropic.

With the information from the variogram, an empirical model can be derived, which can be used to predict the value of a variable at a point where a measurement is not available. This process is referred to as kriging.

Kriging is a method of estimation by local weighted averaging (Oliver and Webster 1990):

$$\hat{z}(x_0) = \sum_{i=1}^{n} \lambda_i \cdot z(x_i) \tag{3.10}$$

where $\hat{z}(x_0)$ is the estimate and λ_i are the weights, summing up to 1. The weights are derived from the modelled variogram.

The term 'kriging' summarises a set of methods, including simple kriging, ordinary kriging, universal kriging, block kriging and co-kriging. The most widely used techniques are ordinary and universal kriging. Ordinary kriging is the method described in *Equation 3.10* with the weights of λ_i summing up to 1. Ordinary kriging is an extended version of simple kriging in that it uses a location-dependent mean within the search neighbourhood rather than a fixed mean over the whole area. Ordinary kriging takes no account of regional trends in the data. It is therefore a local and exact interpolator. Universal kriging estimates values in the presence of a regional trend (drift). Block kriging estimates values for areas as opposed to points, while in co-kriging, secondary variables are used to help calculating the estimates (see *Section 3.3.7*) (Bailey and Gatrell 1995 and Deutsch and Journel 1992).

3.3.6.2 Implementation

The program used for ordinary kriging was GSLIB (Geostatistical Software Library) produced by Stanford University (US). The source code comes on two floppy disks together with the manual: 'GSLIB, Geostatistical Software Library and User's Guide' (Deutsch and Journel 1992). The source code, which is written in Fortran 77, was compiled in a UNIX environment.

The program *gamv2m* was used to create the variogram. The best model was then fitted with *vmodel* and the resulting variogram plotted using *vargplt*. The model was then cross-validated using *xvok2dm*. Cross-validation is a method which takes out each point in a dataset and, using the rest of the points, estimates the value of the removed point. The programs used are all part of the GSLIB-software.

3.3.7 Co-kriging

3.3.7.1 Description

Often when sampling the primary variable, other, so-called 'secondary variables' are also sampled. Where these are co-variates of the variable of interest, they may be used to help predict conditions at unsampled sites. It is this principle which underlies co-kriging (Bailey and Gatrell 1995). Co-kriging is thus an extension of ordinary kriging to include additional, non-locational variables.

Whereas in kriging, a variogram is used to analyse the spatial dependency for one variable, in co-kriging a cross-variogram is used for two variables. The natural sample estimator of the cross-variogram, given n pairs of observations (x_i, y_i) at sample sites s_i, is:

$$2\hat{y}_{YX}(h) = \frac{1}{n(h)} \sum_{s_i - s_j = h} (y_i - y_j)(x_i - x_j) \qquad (3.13)$$

3.3.7.2 Implementation

Co-kriging is available as part of the GSLIB (Geostatistical Software Library) package described above. Again, the source code, which is written in Fortran 77, was compiled in a UNIX environment.

The program *gamv2m* (GSLIB-program) was used to create the variograms and cross-variograms of the first and secondary variable. *Vmodel* (GSLIB-program) was then used to fit a model and *vargplt* (GSLIB-program) to plot the resulting (cross-) variograms. GSLIB did not have a program to cross validate the model, so an AML was written (see *Appendix 3F*). In the AML, a point was taken out of the dataset in order to run the GSLIB-program *cokb3dm* for the omitted point. *Cokb3dm* performed the co-kriging and provided an estimate and estimate variance. This was repeated for every point in the dataset.

3.3.8 SAVIAH

3.3.8.1 Description

In Section 2.2 the SAVIAH study (Elliot and Briggs 1998) was described. This section will give a more detailed description of that part of the SAVIAH methodology which provides measures of outdoor air pollution.

As part of the SAVIAH study in Huddersfield, NO_2 monitoring was carried out during 4 surveys (June 1993, October 1993, February/March 1994 and May/June 1994), using Palmes diffusion tubes. In the latter three surveys, tubes were exposed for two weeks at 80 core sites. An additional 8 reference sites were monitored continuously on a monthly basis over the study period. These 8 reference sites provided independent measurements of the annual mean NO_2 and were used for validation purposes.

Regression modelling was carried out by regressing measured NO_2 concentrations at fixed site locations against indicators of traffic volume, land cover and topography. In brief the methods used to generate the Huddersfield equation were as follows (Briggs *et al.* 1997):

- Computation of a weighted traffic volume factor (TVOL) for the 300 metre buffer around each monitoring site. Daytime traffic volumes were estimated for 20m zones around each sample site up to 300 metres, using the FOCALSUM command in ARCINFO. In SPSS, multiple regression analysis was carried out using the results of each 20m band against the modelled mean of each sample site. The best-fit combination gave two bands, weighted as follows: 0-40m (weight = 15) and 40-300m (weight = 1).

- Computation of a compound land cover factor (LAND) for the 300m buffer around each monitoring site. The area of each land use type was estimated for 20m zones around each sample site up to 300 metres, using the FOCALSUM command in ARCINFO. In SPSS, multiple regression analysis was carried out using the results of each 20m band against the modelled mean of each sample site. The best-fit combination was a single band (0-300m), comprising two land use types: high-density housing (HDH) and industry (Ind). Weights were identified by examining the slope coefficients. This gave a weight of 1.8 for HDH and 1.0 for Ind.
- Stepwise multiple regression analysis was rerun using the two compound factors (TVOL and LAND), together with altitude and sample height, against the modelled mean nitrogen dioxide.

The original equation to predict the mean NO_2 ($\mu g\ m^{-3}$) was as follows (Briggs *et al.* 1997):

$$\mathrm{MEANNO2} = 11.83 + (0.00398\mathrm{TVOL}_{300}) + (0.268\mathrm{LAND}_{300}) - (0.0355\mathrm{RSALT}) + (6.777\mathrm{SAMPHT}) \quad (3.14)$$

where:

TVOL_{300} = $15*\mathrm{Tvol}_{0\text{-}40} + \mathrm{Tvol}_{40\text{-}300}$ (vehicle km/hr)

LAND_{300} = 1.8*High Density Housing$_{0\text{-}300}$ + Industry$_{0\text{-}300}$ (hectares)

RSALT = 1/sin(Altitude) (m)

SAMPHT = Sampleheight (m)

Since its initial development in the Huddersfield area, the SAVIAH model has been successfully applied to other study areas in the UK. Wills (1998), for example, used the SAVIAH model in Hammersmith and Ealing (West London) to obtain NO_2 concentrations at receptors which then were compared with health data. Estimated NO_2 concentrations were validated against measured NO_2 concentrations using Palmes diffusion tubes at 11 monitoring sites across the study area. Results showed a correlation coefficient of r=0.87 for the 11 sites.

When applying the original Huddersfield equation in Sheffield, as part of this research, unexpectedly high values for the altitude factor (1/sin(ALTITUDE)) were found for some of the receptors. Re-examination of the data showed that this was due to instability in this variable, at values outside the range of altitudes found in the Huddersfield data set. In order to derive a more stable equation, the original Huddersfield data were therefore reanalysed and a new regression equation developed using alternative transformations of altitude. The best-fit model for the 80 core sites was as follows:

MEANNO2 ($\mu g\ m^{-3}$) =

49.732 + (0.003705 * TVOL) + (0.232 * LAND) - (5.673 LOGALT) - (22.424 * 1/SAMPLEHT) (3.15)

where:

TVOL = $15Tvol_{0-40} + Tvol_{40-300}$ (vehicle km/hr)

LAND = 1.8High Density $Housing_{0-300}$ + $Industry_{0-300}$ (hectares)

LOGALT = Log10(Altitude) (m)

SAMPLEHT = Sampleheight (m)

This gave a correlation coefficient of 0.78 (r^2 = 0.6) and a standard error of the estimate of 6.06 $\mu g\ m^{-3}$.

With the new equation, a new NO_2 pollution map was created for Huddersfield. The coverage, which contains information about traffic volumes (TRAFFOL), was converted into a 10m grid using the LINEGRID command in GRID. The value assigned to the TRAFFOL grid was the daytime hourly traffic volume included in the TRAFFOL coverage. The GRID-command FOCALSUM was then used to calculate values of all the variables for each grid cell across the study area. Two TRAFFOL coverages were produced: one based on a 40m radius buffer, the other on a 300m radius buffer. The traffic volumes for the 40m buffer were then subtracted from those for the 300m buffer, to produce estimates of TRAFFOL in the 40-300-metre buffer.

From the landcover coverage (LANDCOV), two separate coverages were created - high-density housing and industry. The two coverages were then converted into 10m grids using the POLYGRID command in GRID. Again, FOCALSUM was used to compute 300m buffers for both the coverages.

The altitude of the study area was stored in the HUDD_DTM grid. The sample height for all receptors was set to 2 metres.

The CALC command in GRID was then used to create the new NO_2 pollution map by weighting and summing the five coverages thus produced.

As already noted, the regression equation fitted well to the measured NO_2 concentrations for the 80 sites on which it was based, with $r^2 = 0.60$ (*Figure 3.5* and *Table 3.3*). Further validation was carried out by comparing the modelled results with measured concentrations (not used in the model construction) for the 8 reference sites. This gave $r^2 = 0.72$, and SEE = 4.72 $\mu g\ m^{-3}$ (*Figure 3.6* and *Table 3.3*)

Table 3.3: Performance of regression map: r^2 and standard error of estimate for 80 core sites and 8 reference sites.

Number of sites	***r***	***r square***	***Adjusted r square***	***Std. error of the estimate***
80	.777	.604	.599	6.06
8	.849	.720	.673	4.72

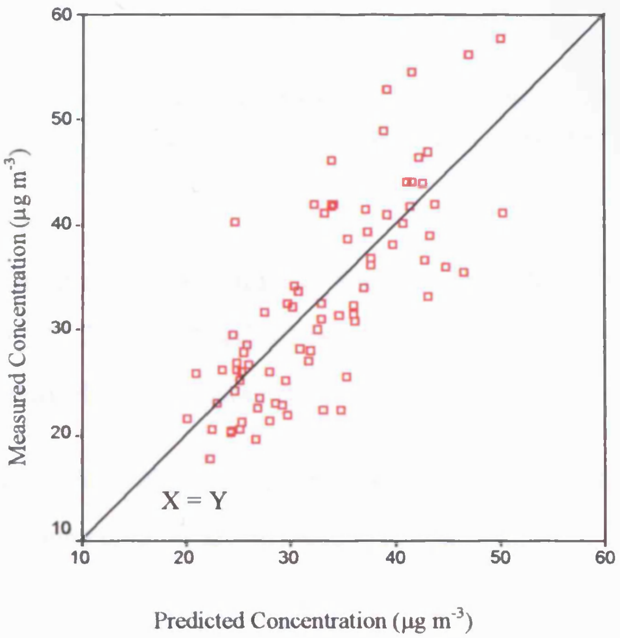

Figure 3.5: Predicted mean annual concentration NO_2 versus monitored concentrations at 80 core sites, Huddersfield (1993/1994)

Since correcting the SAVIAH equation, it has successfully been used in Northampton as part of an EPSRC-funded project (Briggs *et al.* 1998). NO_2 concentrations predicted from the revised SAVIAH model were compared with monitored NO_2 concentrations at 39 monitoring sites, for which passive samplers had been used during five two-week surveys. The results gave $r^2=0.58$ (SEE=5.58 µg m^{-3}) (Briggs, 1998, pers. comm.).

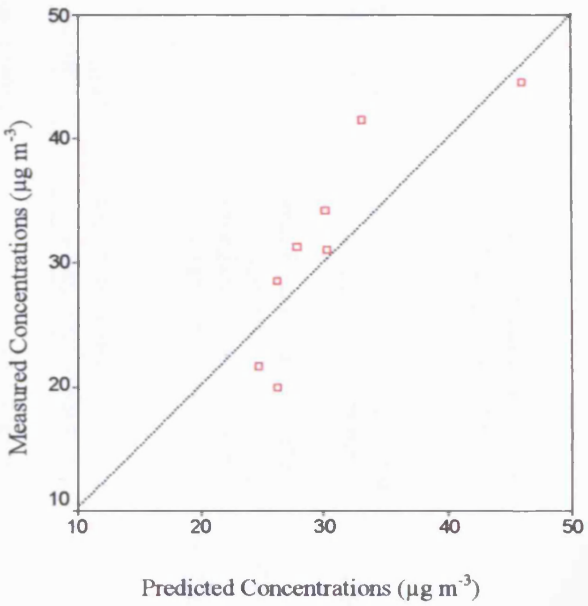

Figure 3.6: Predicted mean annual concentration from the regression map versus monitored concentration at 8 reference sites, Huddersfield (1993/1994).

3.3.8.2 Implementation

To apply the revised Huddersfield equation to Sheffield, an AML (Arc Macro Language) was written in ARCINFO. This AML calculates the NO_2 estimate for every given point in the study area using vector data (see *Appendix 3G*).

For every given point the following procedure was followed. First, a 40m buffer and a 300m buffer (polygons) was created around each receptor point. A check was then made to ascertain whether there were any roads (road coverage roads3) within these buffer zones. Depending on the outcome, the INTERSECT command in ARC was used to intersect the road coverage with either or both the 40m buffer and the 300m buffer. With the STATISTICS command, the weighted sum of length by traffic volume was calculated

Table 3.4: Data requirements for selected methods plus limiting factors

	Traffic data	***Emission data***	***Met. data***	***Road network***	***Local topography***	***Monitored data***	***Running times***[1]	***Limiting factor***	***Comments***
Indicators	✓			✓			n.a.	Accuracy of road data + location of monitoring sites	Relatively easy to obtain data in a GIS
Air pollution dispersion models									
CALINE3[2]	✓	✓	✓	✓			±2½ min, 10 links	Accuracy of road data + location of monitoring sites	
DMRB[3]	✓	✓		✓			±1½ min, 10 links	Accuracy of road data + location of monitoring sites	
ISC3[3]		✓	✓				n.a.		
ADMS-Urban[2]	✓	✓	✓	✓	✓[4]		±17 min., ±600 links	Accuracy of road data + location of monitoring sites	Preparing the input data file was a time consuming process
Spatial Interpolation									
Kriging[2]						✓	n.a.	Amount of sampling sites	
Co-kriging[2]	✓			✓		✓	n.a.	Amount of sampling sites	
Regression model									
SAVIAH[3]	✓			✓	✓[5]		±2½ min	Location of monitoring sites	

[1] 1 receptor for 2 weeks hourly met data
[2] running on UNIX SPARC Workstation
[3] running on NT Windows
[4] Terrain heights
[5] Terrain heights, industrial and high density housing areas

for the selected roads. If no roads were found within the buffers, the Tvol0-40 and Tvol40-300 variables were automatically set to nil.

Next, checks were made to determine whether there were any high density housing areas or industrial areas within 300 metres of each point using the NEAR command.

Test runs showed that, if the high density or industrial area was between 297 and 300 metres away from the receptor, the AML would crash. The reason was that an intersection of the 300m buffer with, for example, an industrial area 298 metres away, would result in too small an area which would generate a mathematical error in ARCINFO. It could be assumed that negligible errors would occur in setting the distance to 297 metres.

The sum of the area was then calculated, using the STATISTICS command.

All the resulting variables were then used to calculate the NO_2 estimate in $\mu g\ m^{-3}$.

3.4 CONCLUSIONS

This chapter has described the study areas used in this research, and outlined the three indicators and seven modelling methods which were selected for analysis. *Table 3.4* summarises the data requirements for each of the methods, indicates the run-times for a single receptor for a two week averaging time, and identifies the major limiting factors likely to affect their accuracy. The decision of which method to use in each of the case studies (described in the next two chapters) was made in the light of these data requirements, processing times and potential limitations. It should also be noted that monitored data has been used for all methods for validation purposes, but, except for kriging and co-kriging, is not a necessary input data requirement.

4 THE GREATER LONDON CASE STUDY

4.1 INTRODUCTION

In this chapter the Greater London area is used as a case study for estimating exposure to traffic-related pollution. Several selected methods were applied and validated against measured data. Greater London is a large area and obtaining detailed data would inevitably be costly, and would be prohibitive not only in this study but for many epidemiological investigations. In order to examine the application of the available techniques across a large urban area, the case study was therefore designed to make use of freely available data as much as possible.

4.2 STUDY AREA

4.2.1 Description

London is the capital city of Great Britain, located in southeastern England, and is situated at the head of the Thames River estuary, west of the river's mouth on the North Sea. Hills to the north and the south from the Thames rise to 200 metres to form the Thames river basin. The City of London and 32 surrounding boroughs form the Greater London metropolitan area (see *Figure 4.1*), which covers 1579 km^2. The 13 inner boroughs are Camden, Hackney, Hammersmith and Fulham, Haringay, Islington, Kensington and Chelsea, Lambeth, Lewisham, Newham, Southwark, Tower Hamlets, Wandsworth, and the City of Westminster. The 19 outer boroughs are Barking and Dagenham, Barnet, Bexley, Brent, Bromley, Croydon, Ealing, Enfield, Greenwich, Harrow, Havering, Hillingdon, Hounslow, Kingston upon Thames, Merton, Redbridge, Richmond upon Thames, Sutton, and Waltham Forest.

Around 1940, Greater London reached a peak population of 8.61 million. Since then, the population has declined to 6,680,000 in 1994, as a consequence of migration to new towns and further afield, beyond the Green Belt. The Green Belt has also restrained the further

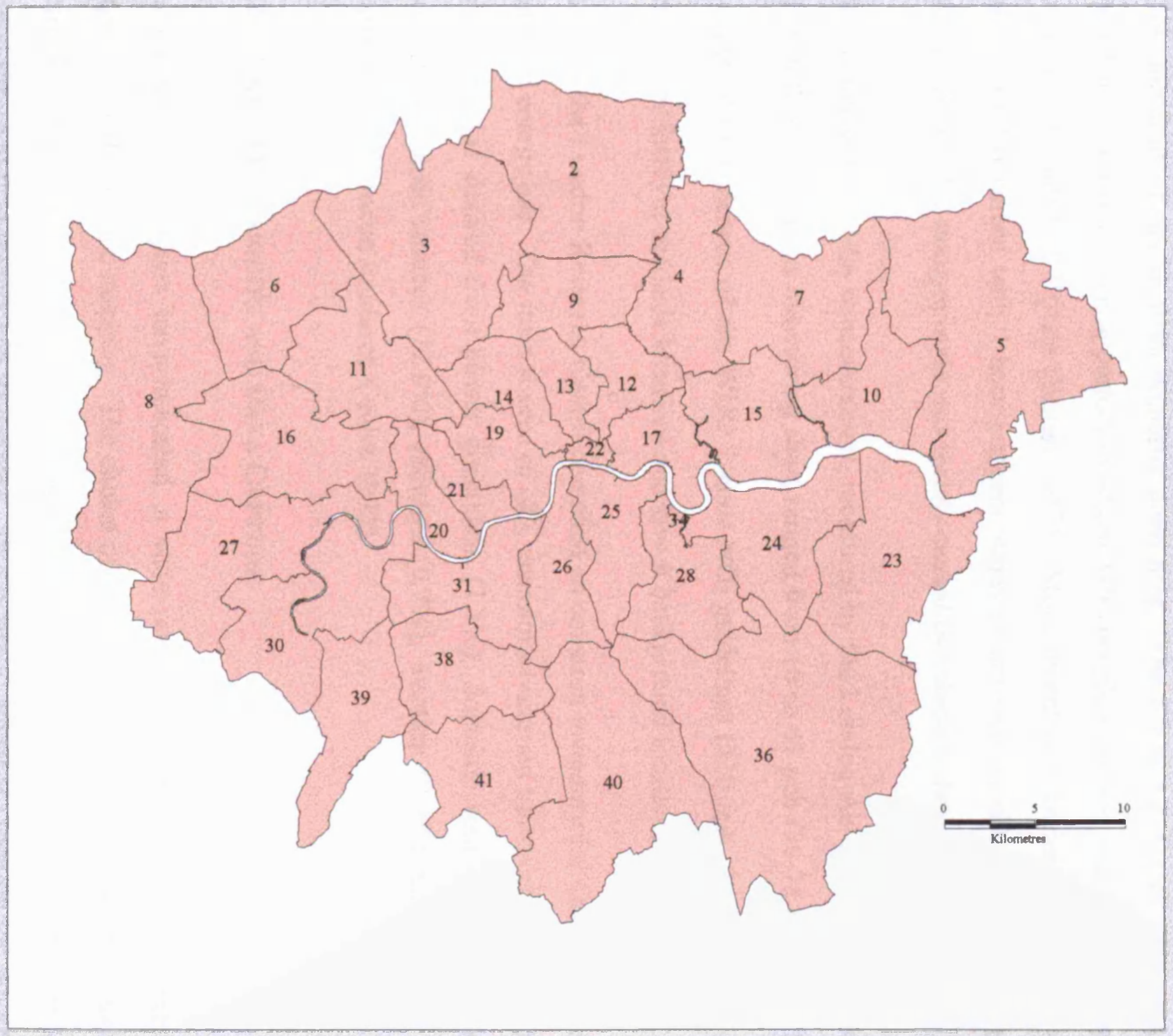

Figure 4.1

Study Area of Greater London

2. Enfield
3. Barnet
4. Waltham Forest
5. Havering
6. Harrow
7. Redbridge
8. Hillingdon
9. Haringey
10. Barking and Dagenham
11. Brent
12. Hackney
13. Islington
14. Camden
15. Newham
16. Ealing
17. Tower Hamlets
19. Westminster City of
20. Hammersmith and
21. Kensington and Chelsea
22. City Of London
23. Bexley
24. Greenwich
25. Southwark
26. Lambeth
27. Hounslow
28. Lewisham
30. Richmond Upon Thames
31. Wandsworth
36. Bromley
38. Merton
39. Kingston upon Thames
40. Croydon
41. Sutton

outward spread of the continuous built-up area and provides valuable recreational space for the Londoners. It has, however, contributed to the rapid expansion of population in outer London. The completion of the M25 in 1986, the route of which lies almost completely within the Green Belt, has led to more pressure for development within the Green Belt (van Zandvoort *et al.* 1995).

4.2.2 London and traffic-related pollution

London has historically often been related with bad air quality. The London smog of 1952 was the worst smog period after the Second World War, and was mainly caused by low-level emissions of smoke from domestic open fires. The Clean Air Act of 1956 was an immediate result of this smog period, in which 4700 people died, and was the first step in air pollution control in Britain (Elsom 1987). More recently, in December 1991, a bad smog period occurred with 1-hour concentrations of nitrogen dioxide reaching 425 ppb (808 $\mu g\ m^{-3}$). This smog episode was mainly caused by vehicle emissions (Elsom 1996).

The annual average NO_2 concentrations, measured by the London Air Quality Network in 1995 at their continuous monitoring sites, ranged from 16 to 41 ppb (30-78 $\mu g\ m^{-3}$). The number of exceedences of the WHO 1-hour NO_2 guidelines (110 ppb; 200 $\mu g\ m^{-3}$) was great (over forty) at roadside locations and low at background locations (SEIPH 1996).

In 1990, the London Research Centre compiled an emission inventory for Greater London based on energy use. The main source of NO_x emissions was road transport (75.9%). The remainder was derived from power generation (1.1%), domestic sources (6.4%), small industrial/domestic sources (12.9%), railways (0.7%), aviation (2.9%) and transport by water (0.1%) (London Research Centre 1993).

4.3 DATA AVAILABILITY AND DATA CAPTURE

As the previous chapters have indicated, a wide range of techniques are available for exposure modelling and mapping. The choice of which technique(s) to use in any situation depends upon a number of factors, including the purpose of the analysis, resource limitations, and data quality and availability. In this study, aimed at covering the whole of

London, data availability was inevitably a determining factor, for as noted it would be prohibitively costly to obtain new data through purposely designed field studies. The aim was also to investigate the utility of the available methods under the constraint of readily available data.

For this reason, a detailed search was carried out to assess the availability of relevant data for the Greater London area. This section describes the data sources identified and explains how the data were obtained and integrated into the GIS.

4.3.1 NO_2 monitoring data

Measured data on nitrogen dioxide concentrations are required both as a means of validating the methods used in this analysis, and as a basis for spatial interpolation. For London, as elsewhere in the UK, relatively few automatic monitoring sites are available; a dense network of sites does exist, however, as part of the national NO_2 diffusion tube network. This was set up in 1993 when AEA Technology's National Environmental Technology Centre (NETCEN) started to coordinate a large scale survey, funded by the Department of Environment, using passive diffusion tubes. These diffusion tubes are operated by Local Authorities throughout the UK. The number of sites in the Greater London area was 66 in 1993, 87 in 1994 and 80 in 1995. The sites are classified as kerbside, intermediate and background sites according to following definition:

- Kerbside (K) 1-5m from a busy road.
- Intermediate (I) 20-30m from the same or an equivalent road.
- Background (B) >50m from any busy road.

Each tube is exposed for a period of one month. Data from the network are stored on the Internet, which gives access to monthly and annual values, referenced by geographical co-ordinates. The data for the NO_2 diffusion tube network was therefore retrieved from AEA Technology's website, and a coverage created in ARCINFO. *Figure 4.2* shows the type and location of the NO_2 monitoring sites. The x – and y-coordinates of the site locations given in the AEA dataset are only accurate to 100 metres. Hence a sampling site could me as much as 140 metres out of place ($\sqrt{(100^2 + 100^2)}$).

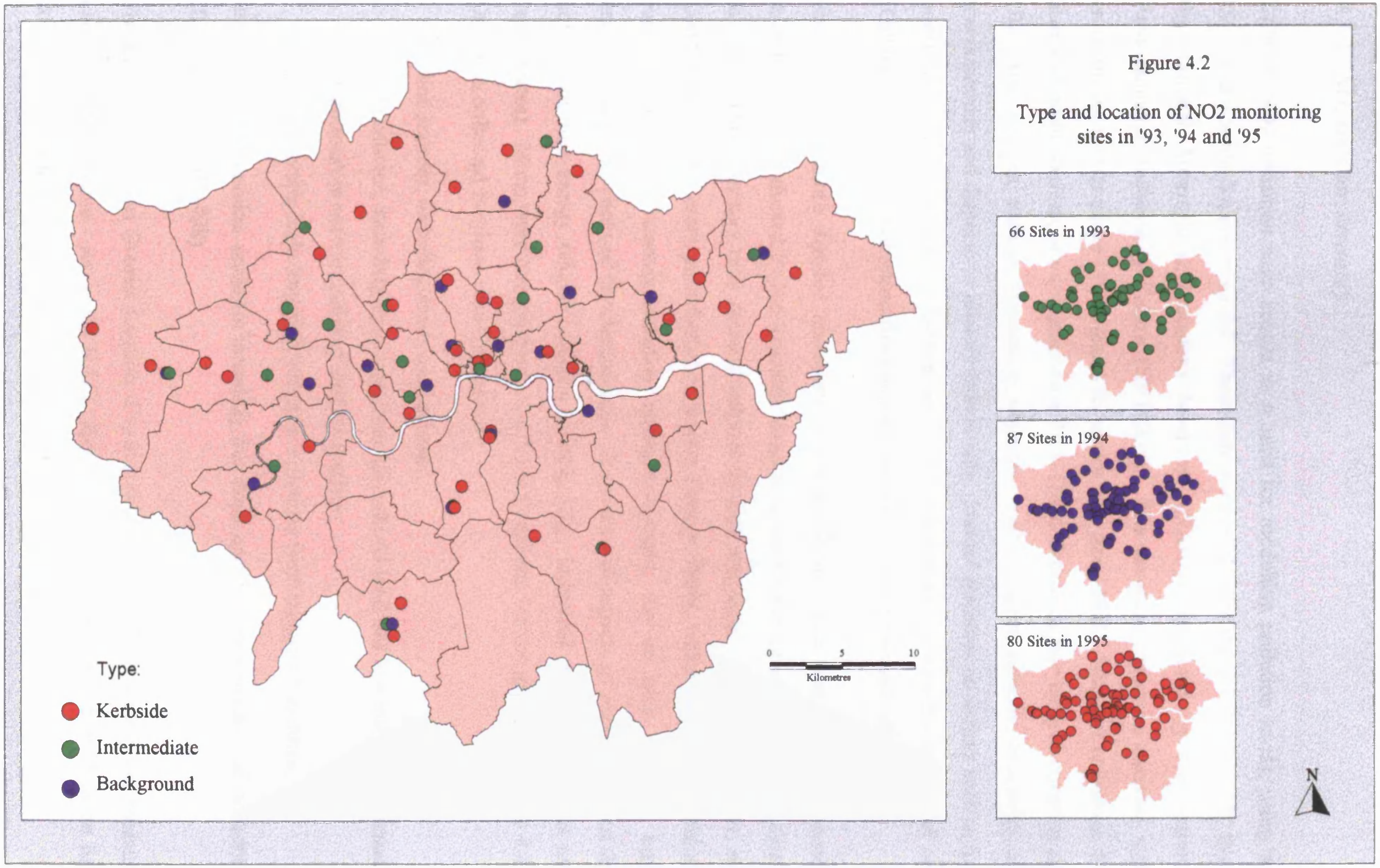

Figure 4.2

Type and location of NO2 monitoring sites in '93, '94 and '95

4.3.2 NO_x emission inventory

Data on NO_x emissions were sought as a basis for modelling pollution levels, using the ISC3 area-source dispersion model. These data are available for the whole of the UK from the National Atmospheric Emissions Inventory (NAEI), conducted by the National Environmental Technology Centre (NETCEN). The inventory provides national total emissions of a wide range of pollutants for every year since 1970. Maps of emissions, for area and point sources, are compiled on a 10 x 10km Ordnance Survey grid covering the UK. Area sources, such as domestic combustion, road transport, agricultural activity, are too numerous and disperse to identify individually. Instead statistics on factors such as fuel consumption and kilometres travelled are used to derive an estimate for each grid cell (Gillham *et al* 1992). Emissions from major point sources are estimated individually.

For London, a more detailed inventory is also available. The first London emission inventory was conducted by the Scientific Branch of the former Greater London Council, in 1979. This inventory only covered sulphur dioxide emissions. In 1993, however, the London Research Centre published the London Energy Study, which estimated emissions for a range of pollutants, including nitrogen dioxide, for an area of 1940 km^2, encompassing the whole of Greater London. It covered all aspects of energy use, but did not include non-energy related emission sources (e.g., industrial process emissions and landfill sites). Maps were compiled on a 1 x 1 km Ordnance Survey grid (see *Figure 4.3*). Data was collected for three types of sources:

- line sources, including roads and railways;
- area sources, including emissions from agricultural land and low intensity emissions from sources such as building heating systems;
- point sources, including high intensity emissions from industrial facilities;

Since then, the London emission inventory has been updated on a number of occasions (Buckingham *et al.* 1998).

For an area as large as Greater London, it is inevitably impossible to identify and measure every emission source. As in the NAEI, therefore, the survey is based on data on fuel consumption, vehicles kilometres travelled or other measures of activity relating to

Figure 4.3

Emission inventory NOx

Greater London, 1992

emissions. Emissions are then estimated using emission factors (London Research Centre 1993) as follows:

Emission rate = activity rate x emission factor (4.1)

Emissions inventories of this type inevitably suffer from a number of inaccuracies (Henriques and Briggs 1998). These include errors in both the emission factors used (often based on laboratory data or manufacturer's data) and the source activity data (which often have to be disaggregated from relatively large administrative units). For this study, the relatively coarse spatial units of the inventory (1 x 1 km) also represents a significant source of error, for it means that local scale variations in emissions (< 1 km) cannot be detected. For traffic-related pollutants, which typically show marked variations over small distances, this may be of considerable importance.

Emissions data from the London inventory were obtained from NETCEN in a text format and converted into an ARCINFO grid using the GENERATE command. *Figure 4.3* shows the emissions of NO_x in tonnes km^{-2} in Greater London.

4.3.3 Road data

Data on the road network were needed as a basis for dispersion modelling, using line source models and for calculation of the proxy exposure indicators. Data was obtained from the Bartholomews Greater London 1:5,000. database, which was licensed under the CHEST-agreement. The database was stored in an ARCINFO export file and contained several layers, such as building polygons, boundaries, roads, railways, landuse, etc. Only the roads layer (_RDS) was retrieved from the database. The export file was imported into ARCINFO using the IMPORT command. The main roads, used in this study, are shown in *Figure 4.4*.

4.3.4 Traffic counts

Data on traffic volumes were needed as a basis for dispersion modelling and computation of the traffic-related indicators. Traffic counts for all major roads in the Greater London

Figure 4.4

Main roads in Greater London

were obtained from the Department of Transport. The majority of traffic counts were based on observed counts made after 1992, and were scaled up using national scaling factors to reflect flows in 1995. The traffic counts were stored in separate text files for each of the 33 Boroughs in London. Every road link had a separate sheet and consisted of the following information (see also *Appendix 4A*):

- observed flow;
- estimated annual average flow 1995 (daily, weekday, 24hr, 16hr, 12hr);
- categories of vehicles (cycles, cars and taxis, bus and coach, etc);
- coordinates for start and end point of link;
- speed limit.

An AML was then written in ARCINFO to convert the text files into a line-coverage for each Borough. From the text file, the x- and y-coordinates of the start and end point of the link were extracted and were written to an input file. This input file was then used to create the line-coverage using the GENERATE command. Next, the categories 'All motor vehicles' and '% HGV' were extracted from the text file, and stored in a Look Up Table (LUT) in INFO. The LUT-table was then attached to the line-coverage using the JOINITEM command. This process was repeated for all the 33 text files of all the London Boroughs. With the APPEND command these 33 line-coverages were compiled to give a single road coverage (see *Figure 4.5*).

4.3.5 Meteorological data

Meteorological data for both Heathrow meteorological station and the Central London meteorological station for the years 1993, 1994 and 1995 were bought from the Meteorological Office. The data was provided in ISC3 format and included hourly values of temperature, wind direction, wind speed, urban mixing height and stability category. Monthly summaries are given in *Figures 4.6* to *4.9*.

These Figures show similar values and trends for both the meteorological stations. This suggests that mean monthly weather patterns do not vary greatly across the Greater London area. In order to facilitate modelling, it was therefore decided to use the data from the Central London site for the whole study area.

Figure 4.5

Daily traffic flows in Greater London

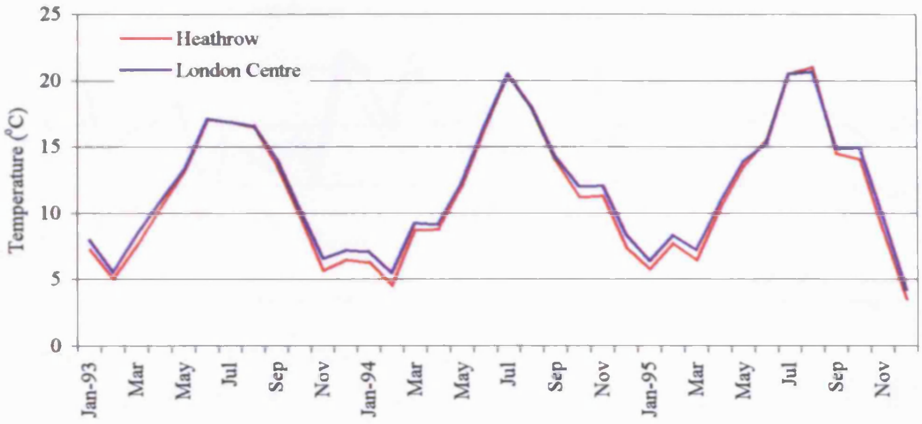

Figure 4.6: Monthly average temperature (°C) during the years 1993, 1994 and 1995 measured at Heathrow and London Centre Meteorological Stations.

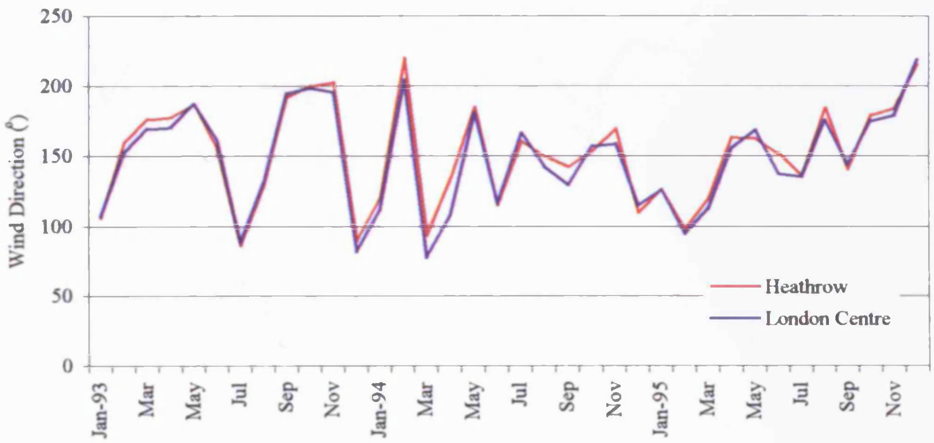

Figure 4.7: Monthly average wind direction (towards which the wind is blowing) during the years 1993, 1994 and 1995 measured at Heathrow and London Centre Meteorological Stations.

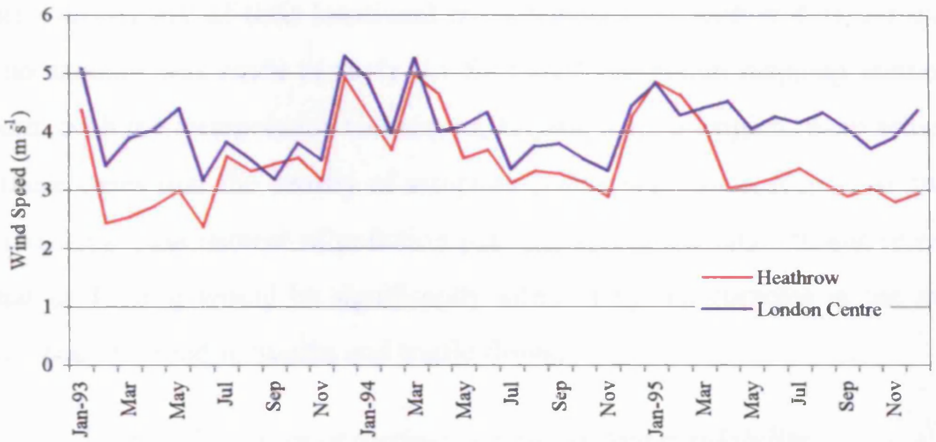

Figure 4.8: Monthly average wind speed (m s^{-1}) during the years 1993, 1994 and 1995 measured at Heathrow and London Centre Meteorological Stations.

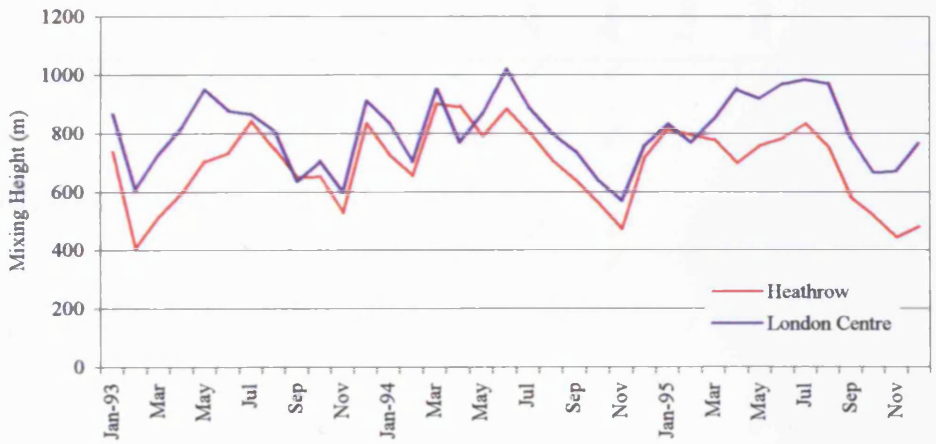

Figure 4.9: Monthly average mixing height (m) during the years 1993, 1994 and 1995 measured at Heathrow and London Centre Meteorological Stations.

4.4 SELECTION OF METHODS

Table 4.1 shows the data requirements for the methods identified in *Chapter 3*, and lists those methods selected for use in the Greater London case study. As can be seen, the decision was made to omit a number of techniques, either because the required data were not available, or because they were not considered to be of sufficiently high spatial resolution.

The lack of topographic and landuse data, the limited number of pollution monitoring sites, and the spatial inaccuracy of their locational co-ordinates (see *Section 4.3*), for example, meant that no attempt was made to apply the SAVIAH regression mapping method. On the other hand, both the interpolation techniques, kriging and co-kriging, were selected. It was felt in these cases that the density of sampling points was just sufficient to provide a relatively coarse-scale assessment of pollution patterns across the city. It was recognised, however, that co-kriging would be significantly affected by inaccuracies in the available covariate data (i.e. the road networks and traffic flows).

Table 4.1: Choice of methods based on data availability

	Traffic data	***Emission data***	***Met. data***	***Road network***	***Local topography***	***Monitored data***	***Used***
Available for Greater London	✓	✓	✓	✓		✓[1]	
Indicators	✓			✓			-
Air pollution dispersion models							
CALINE3	✓	✓	✓	✓			✓
DMRB	✓	✓		✓			✓
ISC3		✓	✓				✓
ADMS-Urban	✓	✓	✓	✓	✓		n.a.
Spatial Interpolation							
Kriging						✓[1]	✓
Co-kriging	✓			✓		✓[1]	✓
Regression model							
SAVIAH	✓			✓	✓		-

[1] Inaccurate to up to 140 metres (see *Section 4.3.1*).

Inaccuracies in the road and traffic data were also likely to affect the performance of the line-source models, CALINE3 and DMRB, both of which depend on the distance from receptor points (monitoring sites) to road. Nevertheless it was decided to attempt to apply both these method in order investigate the effects of these inaccuracies on model performance. ISC3 was chosen because it provided an area-source model, which could use coarser spatial emission data; as described above, these data were available through the

London emissions inventory. ADMS-Urban became available only later in this research, so the model was not used for the London case study.

Limitations in the accuracy of the available road network data also meant that no attempt was made to calculate the exposure indicators for the Greater London area.

4.5 RESULTS

4.5.1 CALINE3

Because of the long data preparation and processing times involved, it was decided to run CALINE3 only for one year, using the 1993 meteorological data: for 66 receptors and one year of 1-hourly meteorological data processing took approximately 69 hours (66 * 2.5 min * 25 two-week periods). An example of a CALINE3 input file is shown in *Appendix 4B*.

The road coverage created from the traffic count text files was used as line sources for the model. However, as a result of the way in which this traffic coverage was constructed in ARCINFO, the roads did not follow the actual road network, as defined by the Bartholomews dataset. In the traffic coverage, all road links were straight between the coordinates of the start and end point of the link. As only the roads within a 200 metre buffer from the monitoring points were needed, buffer polygons of 200 metre radius were created around the monitoring sites, using the BUFFER command. The traffic coverage was then intersected with the buffers, using the INTERSECT command. Next, the straight line links within the buffer zones were manually adjusted in ARCEDIT, using the Bartholomew's road dataset as a background coverage (see *Figure 4.10*) The re-adjusted road coverage was then used in the CALINE3 AML. A background value for NO_2 of 31 ppb was used in the CALINE3 input file, reflecting the annual mean of the urban background site, London Bloomsbury, in 1994 (AEA 1994).

Relationships between the predicted and monitored NO_2 concentrations were analysed using both Pearson and Spearman's correlation. The Pearson correlation coefficient was .325 ($p=0.053$) and the Spearman correlation coefficient was .128 ($p=.459$) ($n=36$). *Figure 4.11* shows the plot of the observed versus the modelled concentrations.

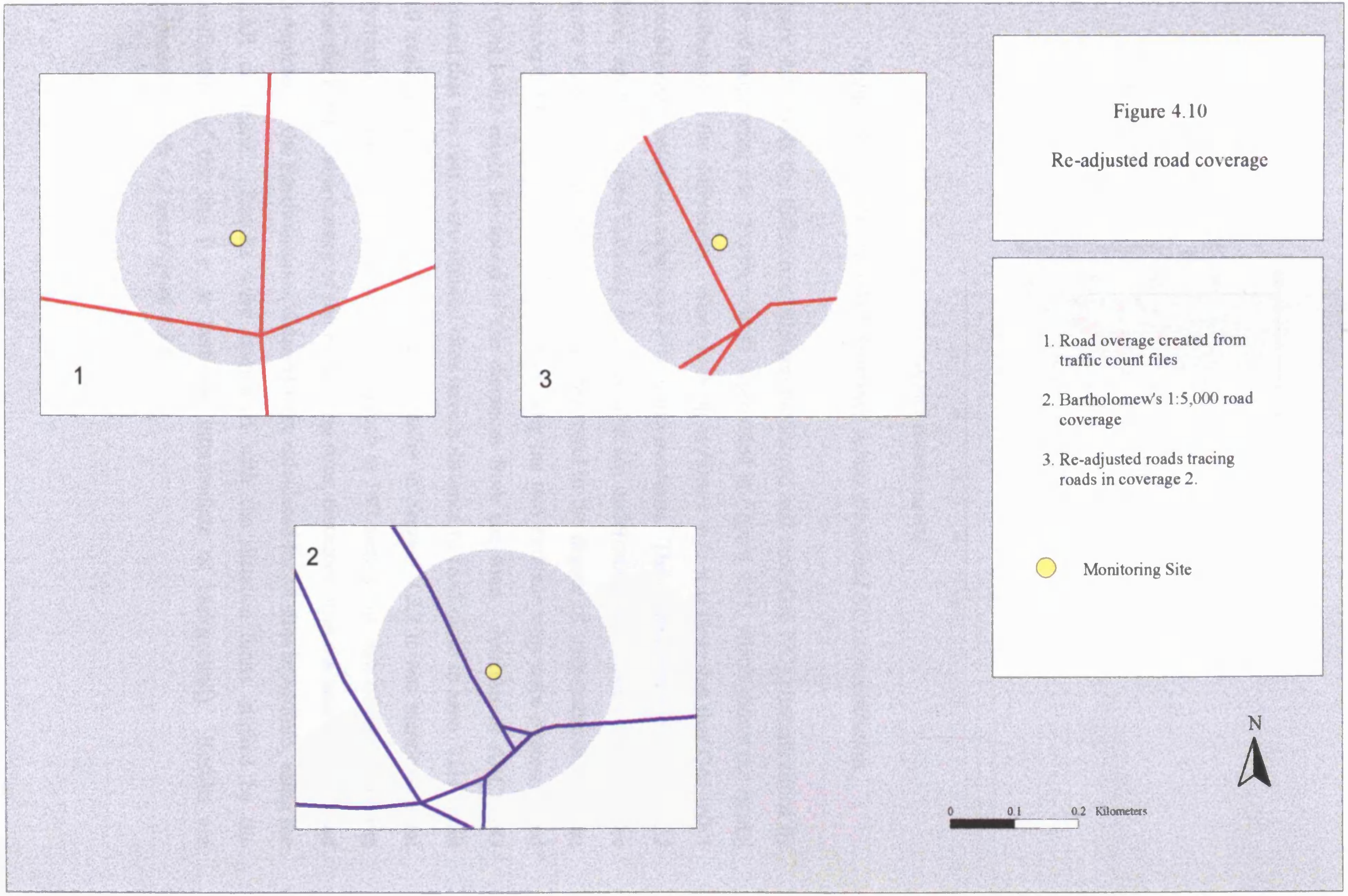

Figure 4.10

Re-adjusted road coverage

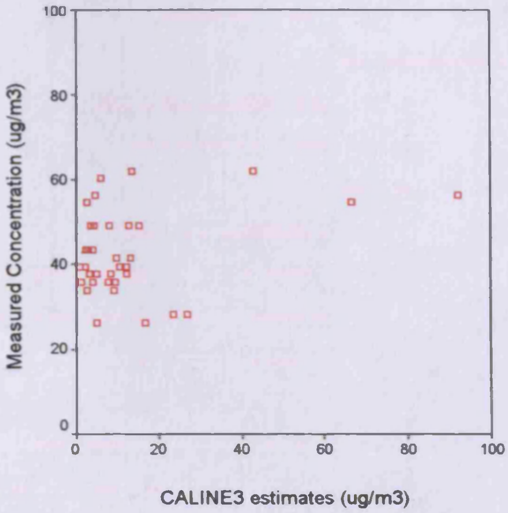

Figure 4.11: CALINE3 NO_2 estimates versus measured NO_2 concentration.

Figure 4.12 plots the difference between monitored and modelled NO_2 concentrations by type of monitoring site. Further detail is provided in *Figure 4.13,* which shows the spatial distribution of the differences. When looking at *Figure 4.11* it is clear that that CALINE3 generally underestimates monitored NO_2 concentrations. This is confirmed in *Figure 4.12* where, apart from two kerbside sites, all sites are underestimated. Spatial analysis (see *Figure 4.13*) does not reveal a recognisable trend in the degree of underestimation of the monitored NO_2 concentrations. A reason why the two kerbside sites were overestimated by CALINE3 might be found in the distances from the road. Analysis in ARCINFO showed that the two overestimated sites have a distance to road close to zero. This might well explain their high estimated values. Earlier in *Section 4.3.1* it was mentioned that monitoring sites could be mislocated by as much as 140 metres. In view of these concerns about the locational accuracy of the monitoring sites, distances from the nearest main road (as depicted in the Bartholomews dataset) were calculated for all sites in ArcInfo, using the NEAR command. Results were compared with the distance limits implied by the classification of the site (i.e. as kerbside, intermediate or background). Results are presented in *Table 4.2* and *Figure 4.14*.

Figure 4.12: Difference between monitored and modelled NO_2 concentrations using CALINE3 by type of monitoring site

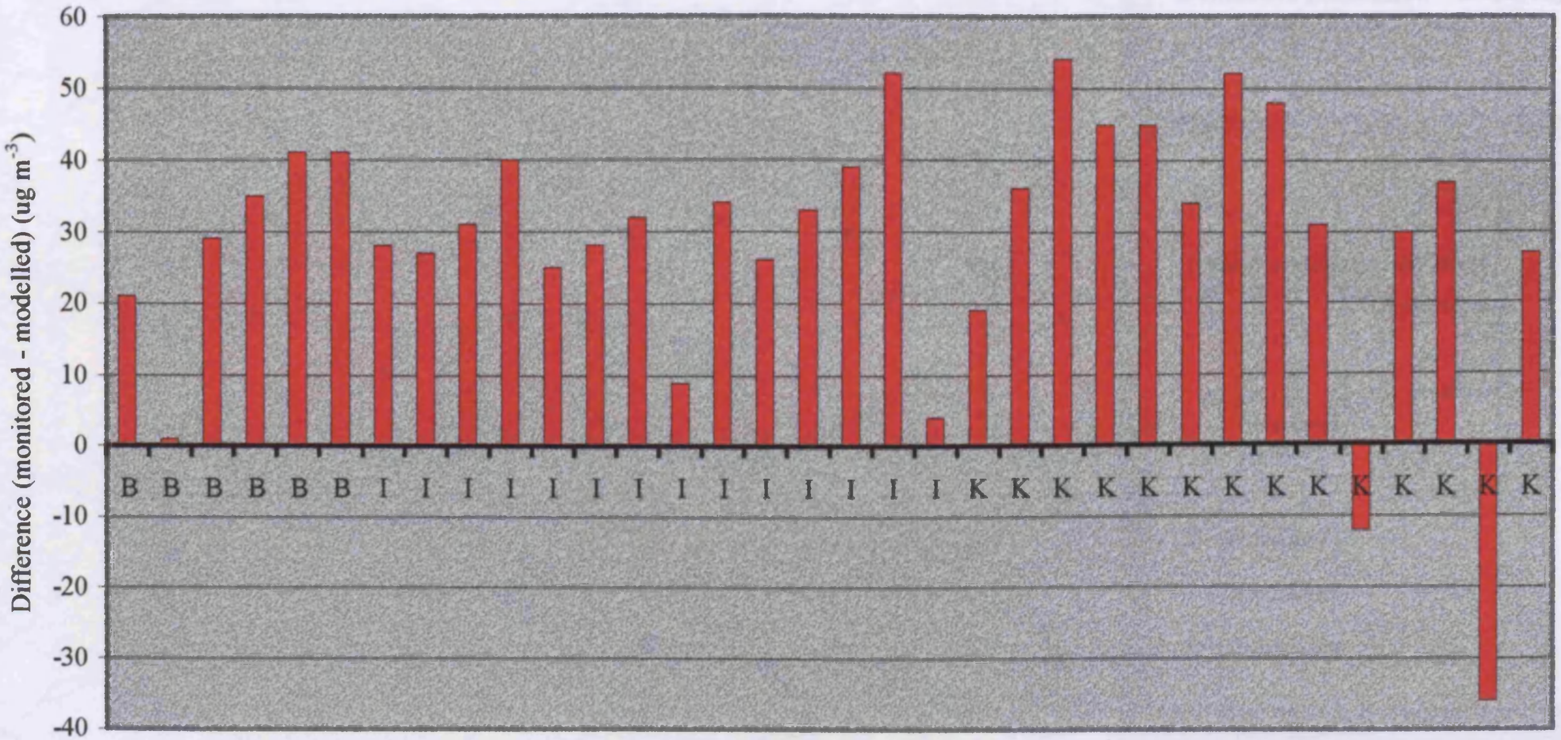

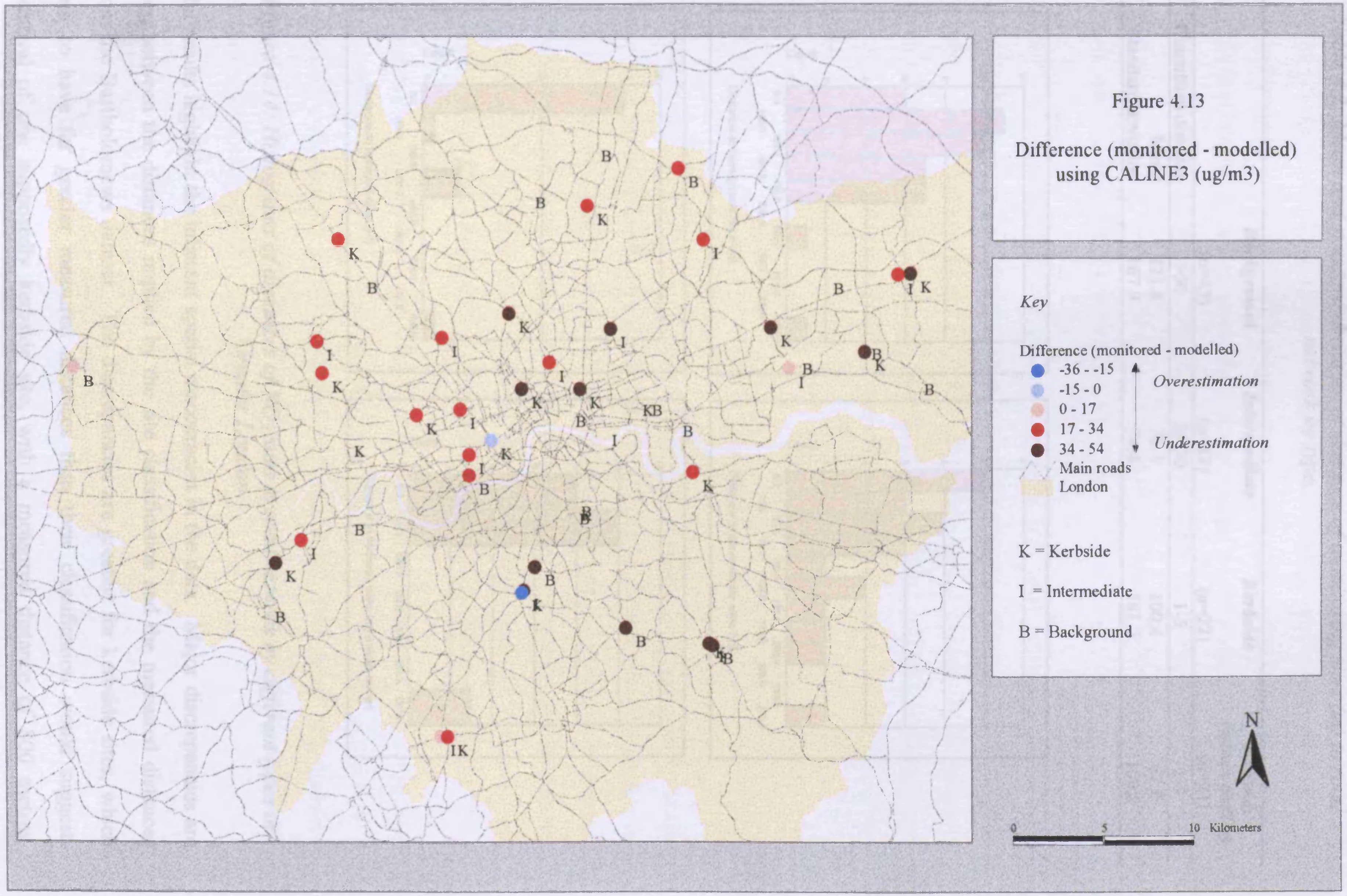

Figure 4.13

Difference (monitored - modelled) using CALINE3 (ug/m3)

Table 4.2: Mean and standard deviation of distance of monitoring sites (m) to road network by type.

	Background (n=43)	***Intermediate*** (n=22)	***Kerbside*** (n=22)	***Kerbside (minus outlier)*** (n=21)
Classified distance	>50	20-30	1-5	1-5
Mean	221.8	78.3	100.4	67.8
Standard deviation	187.9	74.4	181.7	100.8

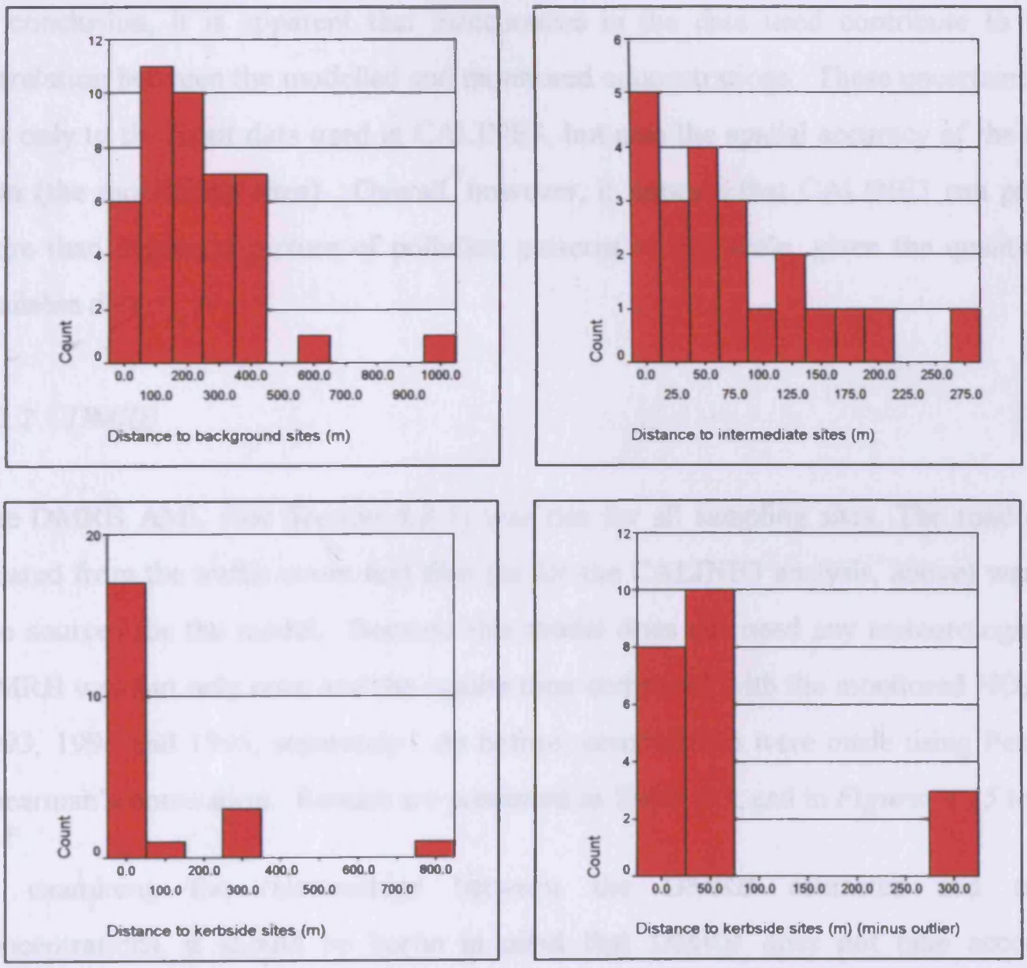

Figure 4.14: Histograms of distances of NO_2 sites to road network by different types in Greater London

The results highlight the inherent spatial inaccuracies in the data. Major discrepancies are seen between the distances implied by the site classification and the measured distances from the Bartholomews dataset. The discrepancies are greatest for kerbside sites, which tend to have far greater measured distances than their classification would suggest. Removal of one supposedly kerbside site, with a measured distance of 800 metres, improves the distribution slightly, but does not resolve the problem. The poor relationship between site classification and measured distance undoubtedly contributes to the relatively poor performance of the CALINE3 model. Errors in the Bartholomew's road network may also have an effect, though given the spatial resolution of these data, these are not felt to be serious. Another source of error is likely to be gaps in the traffic count data (which defined so-called 'main roads'). This may have meant that some roads, used in classifying the sites, were not included in the analysis here.

In conclusion, it is apparent that inaccuracies in the data used contribute to the poor correlation between the modelled and monitored concentrations. These uncertainties relate not only to the input data used in CALINE3, but also the spatial accuracy of the reference data (the monitoring sites). Overall, however, it appears that CALINE3 can provide no more than a general picture of pollution patterns at this scale, given the qualities of the available data.

4.5.2 DMRB

The DMRB AML (see *Section 3.3.3*) was run for all sampling sites. The road coverage created from the traffic count text files (as for the CALINE3 analysis, above) was used as line sources for the model. Because this model does not need any meteorological input, DMRB was run only once and the results then compared with the monitored NO_2 data for 1993, 1994 and 1995, separately. As before, comparisons were made using Pearson and Spearman's correlation. Results are presented in *Table 4.3*, and in *Figures 4.15* to *4.17*.

In examining the relationships between the DMRB estimates and monitored concentrations, it should be borne in mind that DMRB does not take account of a background concentration in the calculated concentrations. The model will therefore inherently tend to underestimate actual concentrations by this amount. *Table 4.3* shows the performance of the DMRB estimates.

Figure 4.16 maps the error of estimate (monitored – modelled) from the model for 1995. This suggests a weak spatial pattern in the performance of the model. In the centre of London, it tends to overestimate concentrations; outside this area it tends to

Table 4.3: Performance of DMRB estimates; Pearson and Spearman correlation coefficients.

		1993 (*n=41*)	*1994* (*n=55*)	*1995* (*n=51*)
DMRB	Pearson	.277 (p=.080)	.281 (p=.038)	.233 (p=.100)
	Spearman	200 (p=.210)	.367 (p=.006)	309 (p=.027)

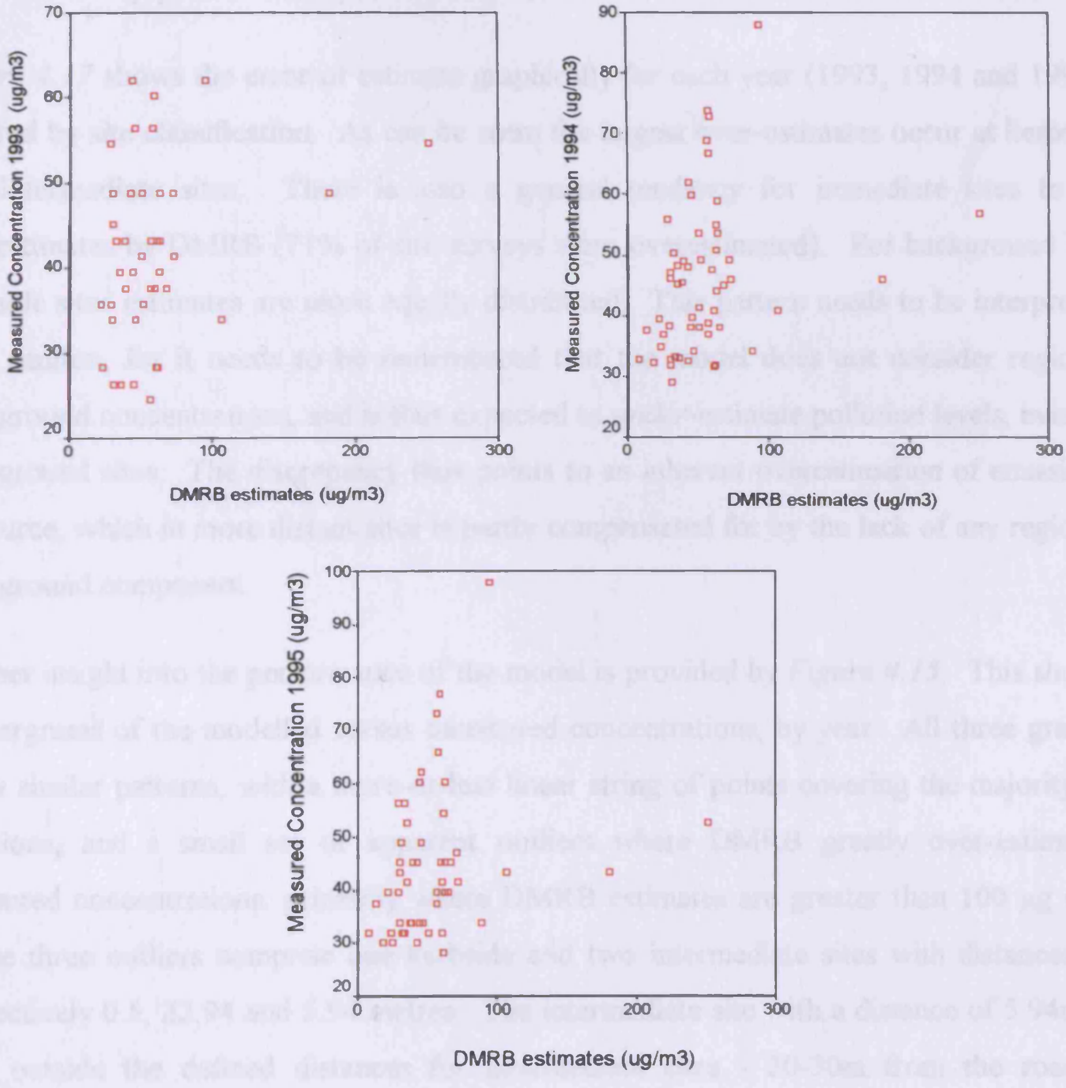

Figure 4.15: DMRB estimates versus measured concentrations in 1993, 1994 and 1995.

underestimate. This pattern might reflect a number of factors. One possibility is that the traffic data are of variable quality across the city (due to the differing density of count points and the different types of roads). Another possibility is that it reflects meteorological factors: as noted, DMRB does not take account of meteorological conditions, but the effect of these might be expected to vary across the city, as a function of the heat island effect. Equally, differences in urban morphology might be expected to have an effect on model performance, though in this case it is surprising that the model *over*-estimates in central London, where street canyons are more common; these would be expected to trap pollution and possibly cause the model to underestimate concentrations.

Figure 4.17 shows the error of estimate graphically for each year (1993, 1994 and 1995), ordered by site classification. As can be seen, the largest over-estimates occur at kerbside and intermediate sites. There is also a general tendency for immediate sites to be overestimates by DMRB (71% of site-surveys were overestimated). For background and kerbside sites estimates are more equally distributed. This pattern needs to be interpreted with caution, for it needs to be remembered that the model does not consider regional background concentrations, and is thus expected to *under*-estimate pollution levels, even at background sites. The discrepancy thus points to an inherent overestimation of emissions at source, which in more distant sites is partly compensated for by the lack of any regional background component.

Further insight into the performance of the model is provided by *Figure 4.15*. This shows scattergrams of the modelled versus monitored concentrations, by year. All three graphs show similar patterns, with a more-or-less linear string of points covering the majority of locations, and a small set of apparent outliers where DMRB greatly over-estimates measured concentrations: primarily where DMRB estimates are greater than 100 $\mu g\ m^{-3}$. These three outliers comprise one kerbside and two intermediate sites with distances of respectively 0.5, 22.94 and 5.94 metres. The intermediate site with a distance of 5.94m is well outside the defined distances for intermediate sites - 20-30m from the road – suggesting that it is wrongly located on the basis of the site co-ordinates. The distances of the other kerbside and intermediate sites from the road, however, correspond with their

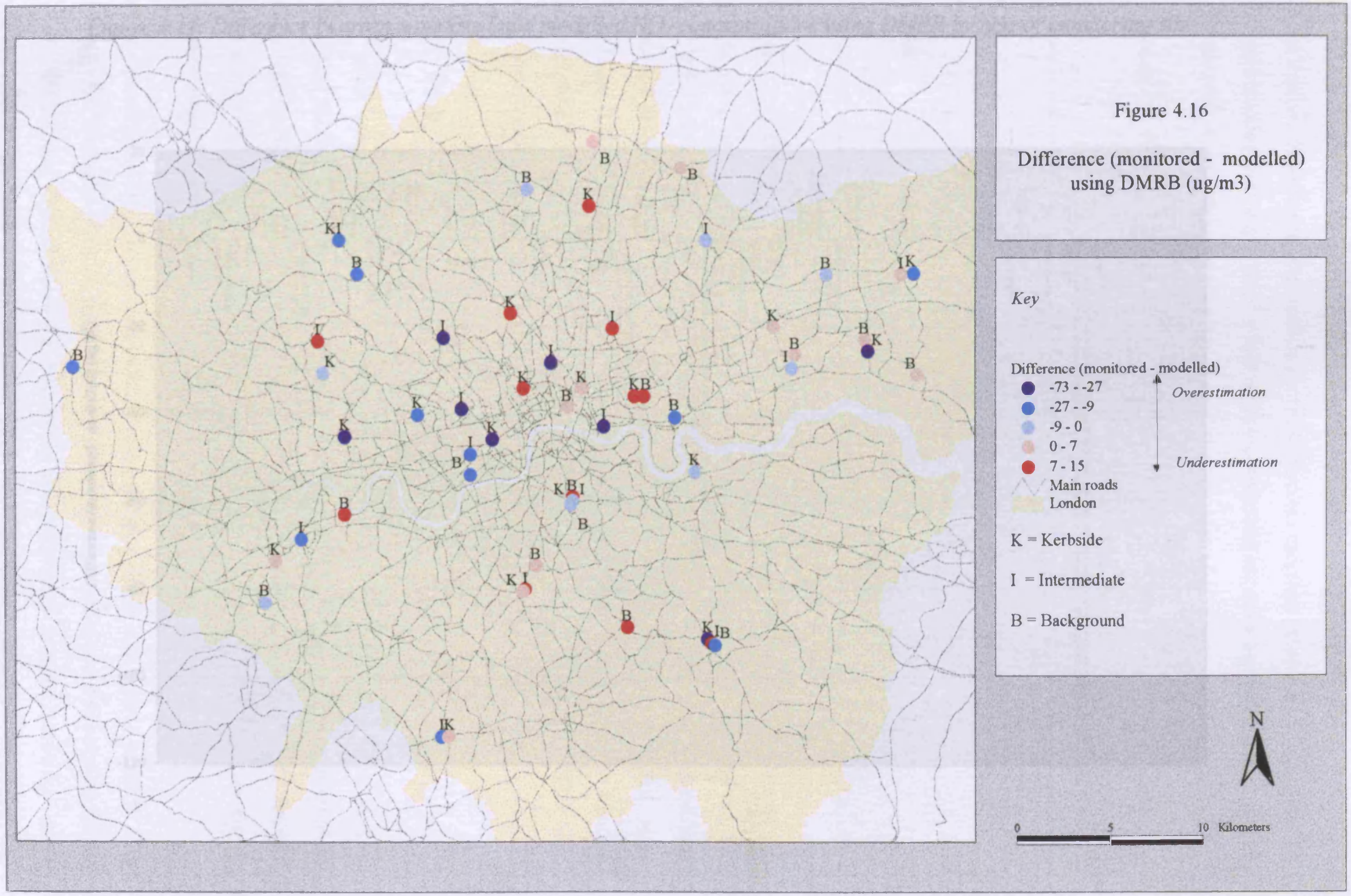

Figure 4.16

Difference (monitored - modelled) using DMRB (ug/m3)

Figure 4.17: Difference between monitored and modelled NO_2 concentrations using DMRB by type of monitoring site

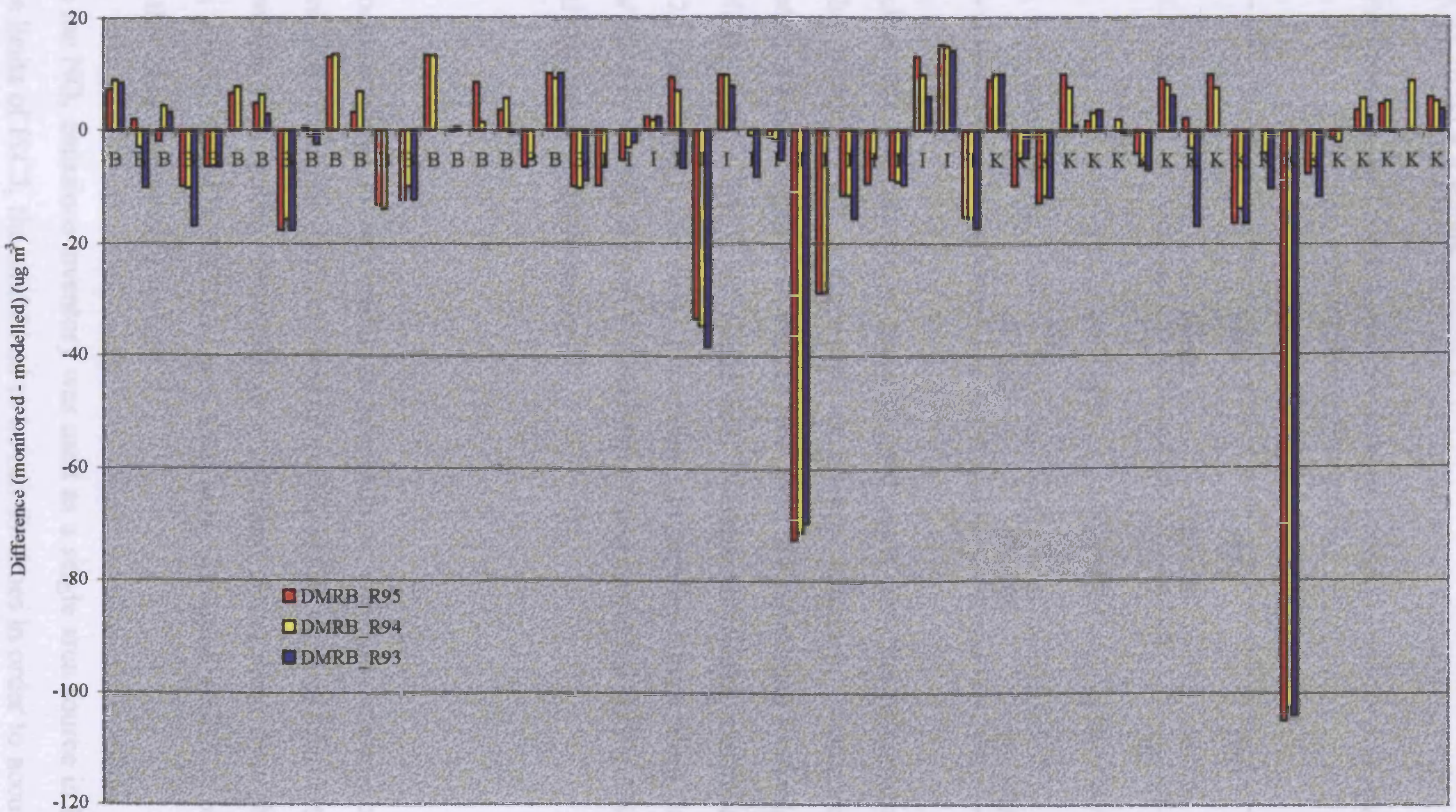

classification. No general explanation for these outliers can thus be provided. Removal of the outliers also has only a small effect on the correlation between modelled and observed concentrations, as *Table 4.4* shows.

Table 4.4: Performance of DMRB estimates without outliers; Pearson and Spearman correlation coefficients.

		1993 (n=41)	***1994 (n=55)***	***1995 (n=51)***
DMRB	Pearson	.255 *(p=.122)*	.431 *(p=.001)*	.382 *(p=.007)*
	Spearman	.176 *(p=.292)*	.362 *(p=.008)*	.293 *(p=.043)*

Overall, it is clear that inaccuracies in the data used again limit the performance of the model (and the ability to test it rigorously in Greater London). Compared to the CALINE3 model, the performance is similar: for 1993 the Spearman's correlation was 0.200 for DMRB, against 0.128 for CALINE3; Pearson correlation coefficients were 0.277 and 0.325 respectively. No firm conclusions can thus be drawn about the relative performance of the two models, except that the lack of meteorological data in DMRB does not seem greatly to impair its performance.

4.5.3 ISC3

The ISC3 model employs a very different approach to the two line-source models described above. This is a point- and area-source model, which takes as input estimated or measured emissions, then models dispersion as a Gaussian plume away from the source. The long-term version of ISC3, ISC3LT, was used here. As noted earlier, it was run in London using the 1 km^2 emissions inventory.

Every 1km^2 in the NO_x emissions inventory was used as a single area source in ISC3. To keep within the limits of ISC3, the model had to be run six times in order to account for all 1564 area sources. Locations of the monitoring sites were used as point receptors. After the six runs, concentrations calculated for each run were added together to estimate the

Table 4.6: Performance of ISC3 estimates: Pearson and Spearman correlation coefficients.

		1993	*1994*	*1995*
		(n=66)	*(n=87)*	*(n=80)*
ISC3	Pearson	.343 *(p=.005)*	.330 *(p=.002)*	.270 *(p=.014)*
	Spearman	.313 *(p=.010)*	.441 *(p=.000)*	.451 *(p=.000)*

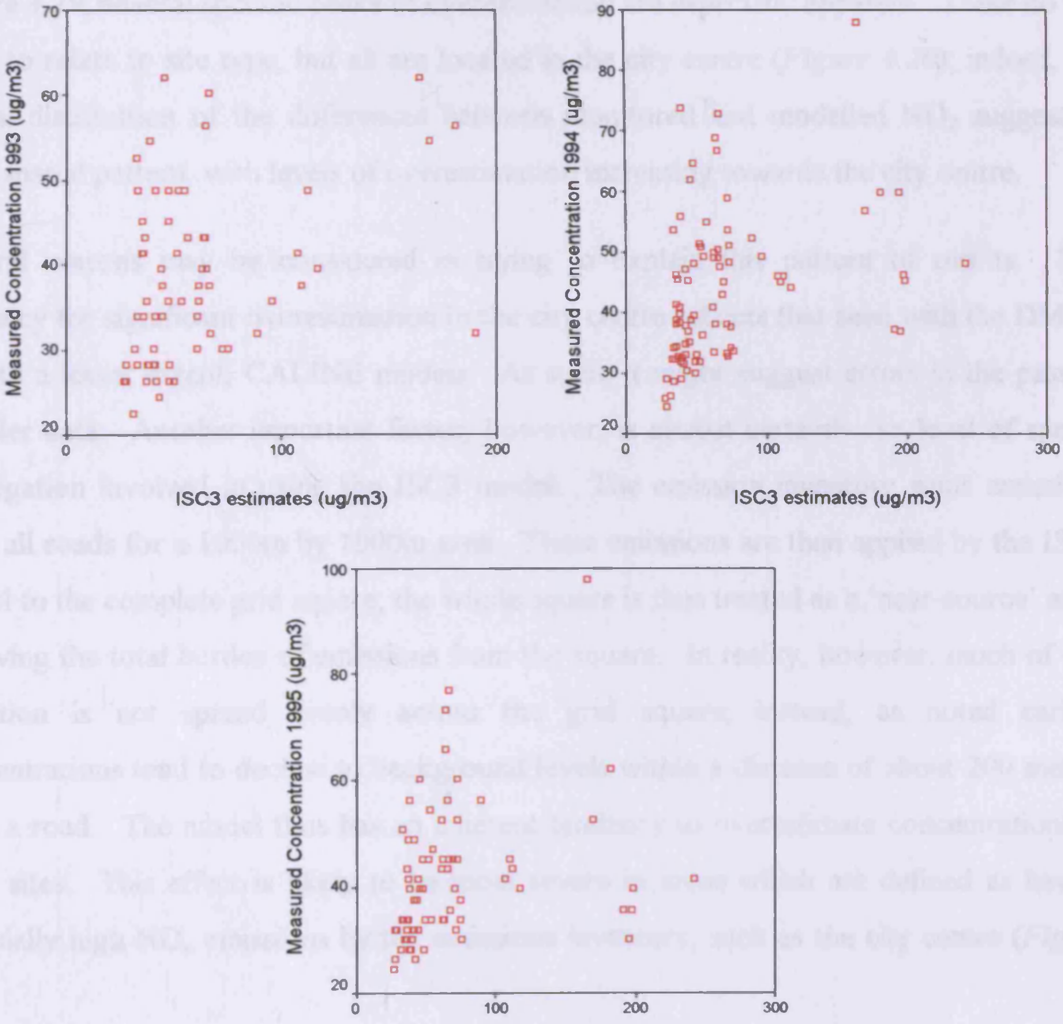

Figure 4.18: ISC3 estimates versus measured concentrations in 1993, 1994 and 1995

Differences between monitored and modelled NO_2 concentrations are shown in *Figure 4.19*, where they are plotted against the type of monitoring site. Further detail is provided in *Figure 4.20*, which shows the spatial distribution of these differences.

The correlation of the ISC3 estimates versus the observed NO_2 concentrations is again weak, though considerably better than that achieved with either the DMRB or CALINE models. ISC3 also tends to overestimate the observed values, and the scattergrams of estimated versus observed concentrations show marked heteroscedasticity (perhaps because of a small group of sites where especially high concentrations are predicted). In *Figure 4.19*, several specific peaks of overestimation are especially apparent. These do not seem to relate to site type, but all are located in the city centre (*Figure 4.20*); indeed, the spatial distribution of the differences between monitored and modelled NO_2 suggests a clear spatial pattern, with levels of overestimation increasing towards the city centre.

Several reasons may be considered in trying to explain this pattern of results. The tendency for significant overestimation in the city centre reflects that seen with the DMRB and, to a lesser extent, CALINE models. As such, it might suggest errors in the passive sampler data. Another important factor, however, is almost certainly the level of spatial aggregation involved in using the ISC3 model. The emission inventory sums emissions from all roads for a 1000m by 1000m area. These emissions are then applied by the ISC3 model to the complete grid square; the whole square is thus treated as a 'near-source' area, receiving the total burden of emissions from the square. In reality, however, much of this pollution is not spread evenly across the grid square; instead, as noted earlier, concentrations tend to decline to background levels within a distance of about 200 metres from a road. The model thus has an inherent tendency to overestimate concentrations at most sites. This effect is likely to be most severe in areas which are defined as having especially high NO_x emissions by the emissions inventory, such as the city centre (*Figure 4.3*).

Another factor is the inclusion in the emissions model of non-traffic related emissions. Although these would, in principle, contribute to the measured concentration, many of these sources are likely to be high level sources (e.g. industrial stacks). High level

Figure 4.19: Difference between monitored and modelled NO_2 concentrations using ISC3 by type of monitoring site

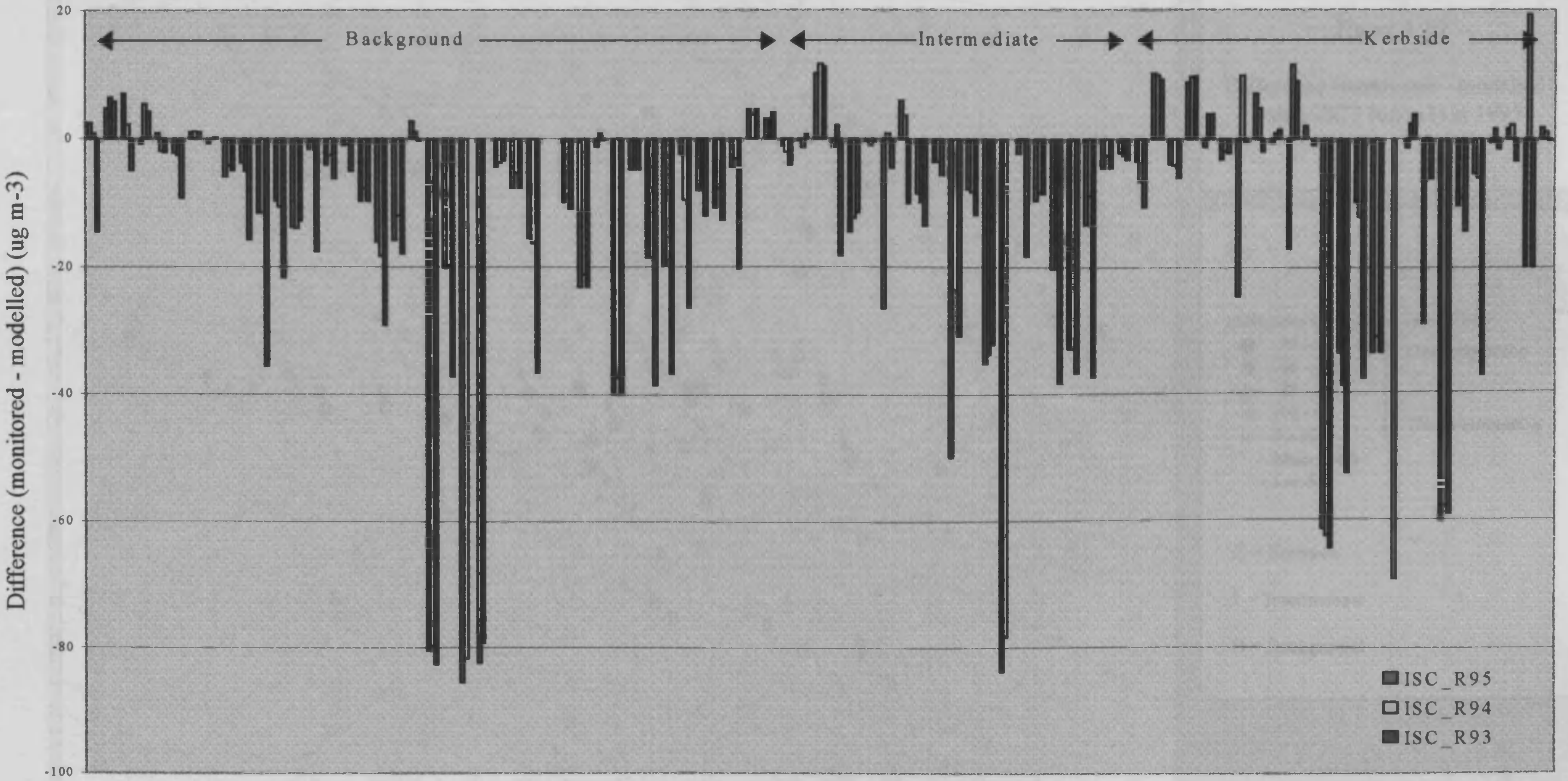

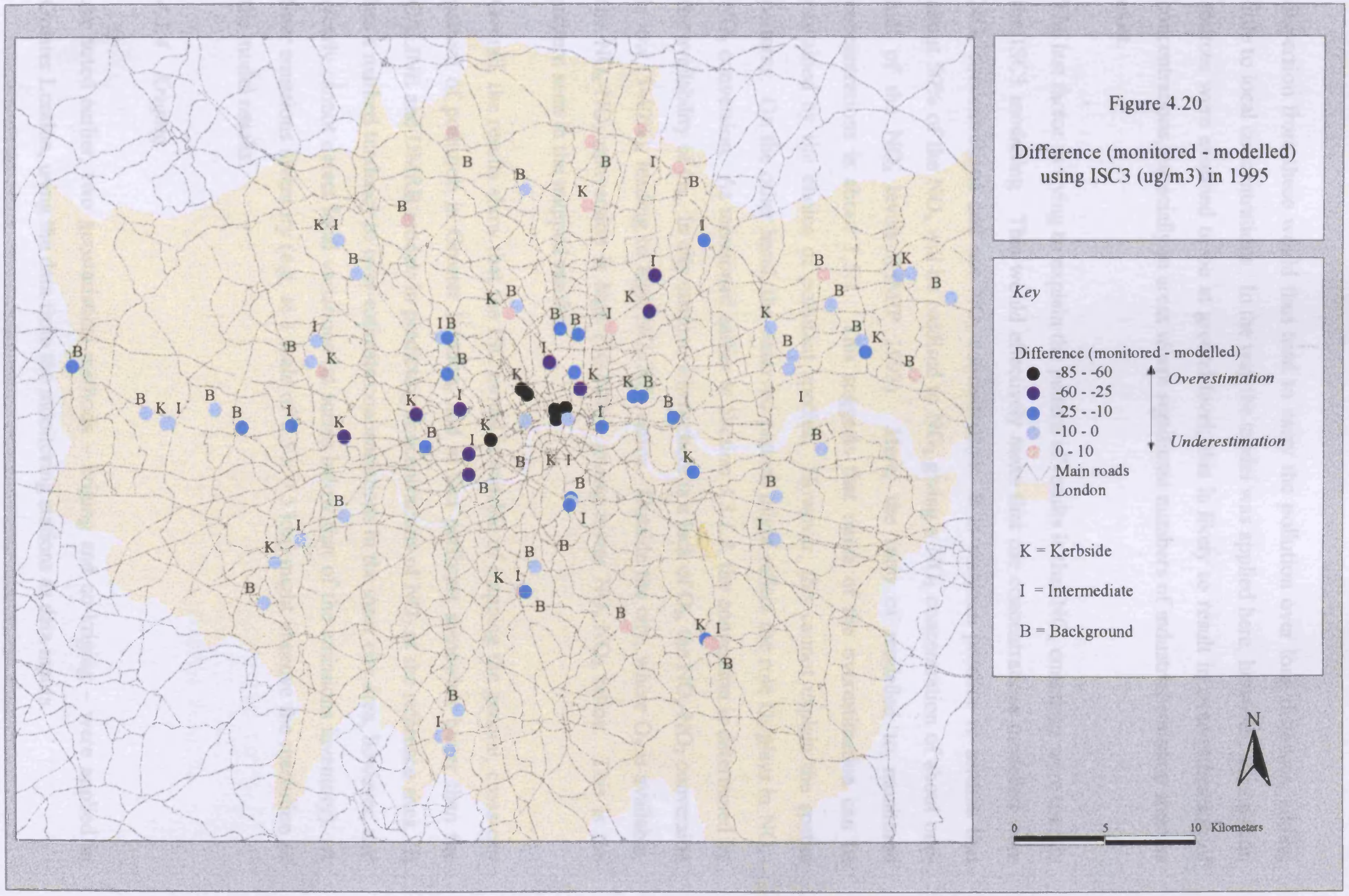

Figure 4.20

Difference (monitored - modelled) using ISC3 (ug/m3) in 1995 dispersion from these would thus tend to carry the pollution over long distances, adding little to local concentrations. In the way the model was applied here, however, all emission sources were assumed to be at ground level; this is likely to result in over-estimation of concentrations, especially in areas where significant numbers of industrial emission sources exist.

The last factor in trying to explain the pattern of results is that NO_x emissions were used in the ISC3 modelling. This would effectively mean that the concentrations modelled were NO_x concentrations and not NO_2 concentrations. It is common practice to assume that about 50% of the NO_x will be oxidised to NO_2 giving a NO_2 concentration of about one-half of the NO_x levels (HMIP 1993). Here, the ratio of modelled to monitored concentrations is about 1.5:1. This suggests that much of the overestimation can be explained by the choice of pollutant species. However, this cannot explain the spatial patterns. On the other hand, the observed pattern might reflect the role O_3 plays in NO_x-NO_2 conversion. As mentioned earlier in *Section 3.3.1.3*, the conversion is determined by the availability of O_3. In city centres, where there is a lack of O_3, the NO_x-NO_2 conversion is low (5-40%), leading to high NO_x:NO_2 ratios. Outside the city, where O_3 is available, the NO_x-NO_2 conversion is high (30-80%), giving lower NO_x:NO_2 ratios. This is the pattern seen in the mapped results.

Overall, the results show that the ISC model is capable of mapping the general, cross-city pattern of pollution in Greater London, and in fact performs somewhat better than the CALINE and DMRB models in predicting concentrations of NO_2 at the reference sites. It has a marked tendency to over-estimate concentrations in the inner city area, however, and clearly cannot detect local variations (at scales below that of the emissions inventory). A finer emissions inventory (e.g. at a scale of 0.5 x 0.5 km) might improve the resolution of the model results.

4.5.4 Kriging

As noted earlier, two geostatistical methods – kriging and co-kriging – were applied in Greater London, using the data from the monitoring stations as data inputs.

For ordinary kriging, variograms were created for the three years of monitoring data (1993, 1994 and 1995) both for the complete data sets (i.e. kerbside, intermediate and background sites) and for background sites only. Results are shown in *Figure 4.21*.

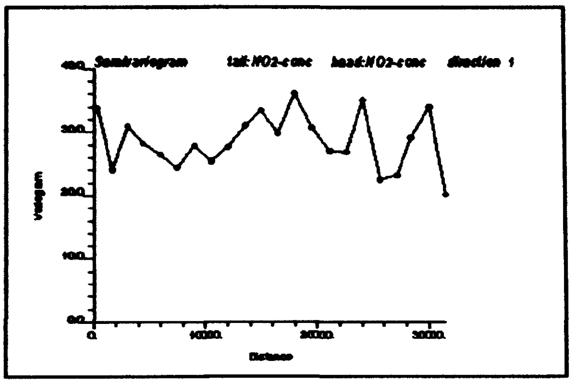

1. Variogram 1993 (all) NO_2

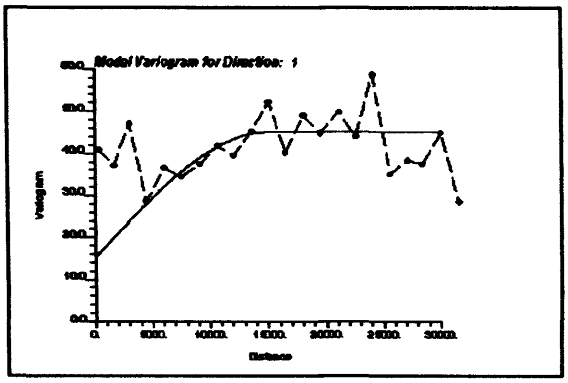

2. Variogram 1994 (all) NO_2

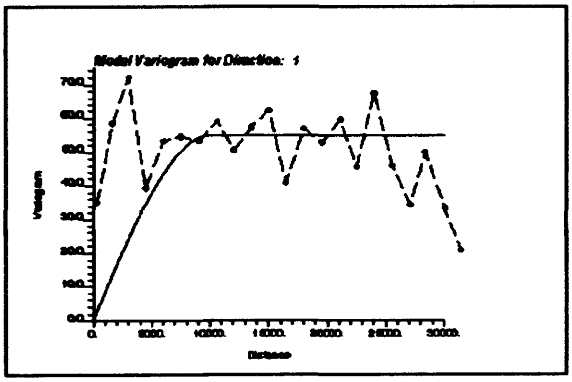

3. Variogram 1995 (all) NO_2

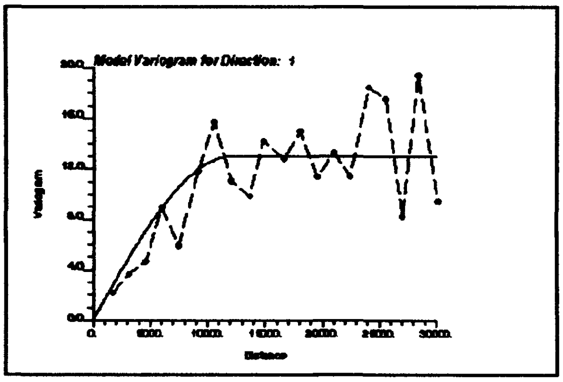

4. Variogram 1993 (back) NO_2

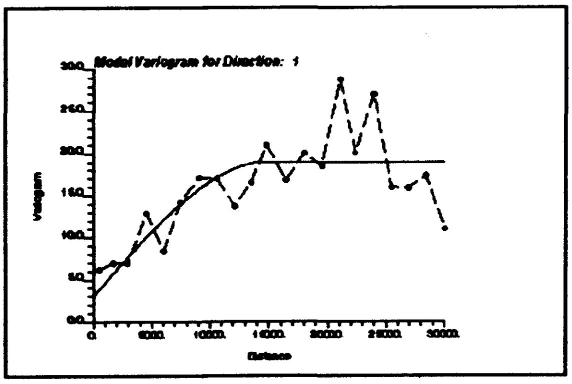

5. Variogram 1994 (back) NO_2

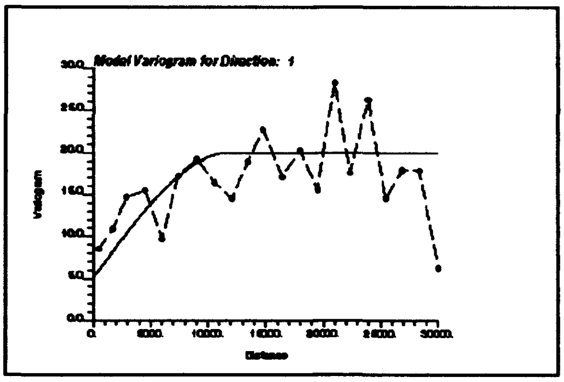

6. Variogram 1995 (back) NO_2

Figure 4.21: Variograms used in kriging for Greater London

As can be seen, the plot of the variogram for all the sites in 1993 was completely horizontal, indicating that there was no spatial dependency in the data. The plots of the 1994 and 1995 variograms for all sites showed some weak spatial dependency. Spherical models were fitted to the 1994 and 1995 data.

In the case of the background sites, the spatial dependency appeared to be stronger in all years. Again, spherical models were fitted to the data, giving some suggestion of a sill at a lag of about 1200-1500 metres.

The performance of the kriging models was tested by cross-validation, as outlined in *Section 3.3.6.2*. Results are shown in *Table 4.7* and *Figure 4.22*. *Figure 4.23* shows the errors of estimate plotted by site type, and *Figure 4.24* shows the spatial distribution of the errors of estimate, from the full data set.

Table 4.7: Results of correlation of monitored NO_2 versus kriging estimates using cross-validation.

	Pearson Correlation Sig. (2-tailed)	*Spearman Correlation Sig. (2-tailed)*	*Variogram (Range, sill, nugget)*
1994 (n=83) all sites	.449	.508	15000, 30, 15
	(p=.000)	*(p=.000)*	*(variogram 2, Fig 4.21)*
1995 (n=81) all sites	.429	.514	10000, 55, 0
	(p=.000)	*(p=.000)*	*(variogram 3, Fig 4.21)*
1993 (n=31) background	.573	.478	12000, 13, 0
	(p=.001)	*(p=.006)*	*(variogram 4, Fig 4.21)*
1994 (n=43) background	.710	.719	15000, 16, 3
	(p=.000)	*(p=.000)*	*(variogram 5, Fig 4.21)*
1995 (n=43) background	.684	.673	12000, 15, 5
	(p=.000)	*(p=.000)*	*(variogram 6, Fig 4.21)*

Levels of correlation between the kriging estimates and the monitored NO_2 concentrations for all sites are relatively low for both 1994 and 1995, reflecting the weak spatial dependency in the data. Correlations are much stronger for the background sites, especially for 1994 and 1995 (Pearson r = .710 and .684, respectively). This difference in performance is to be expected. It reflects the fact that background sites are likely to be much less influenced by roads (>50m away from busy road), with the result that they represent a much smoother surface, which is more effectively modelled by ordinary

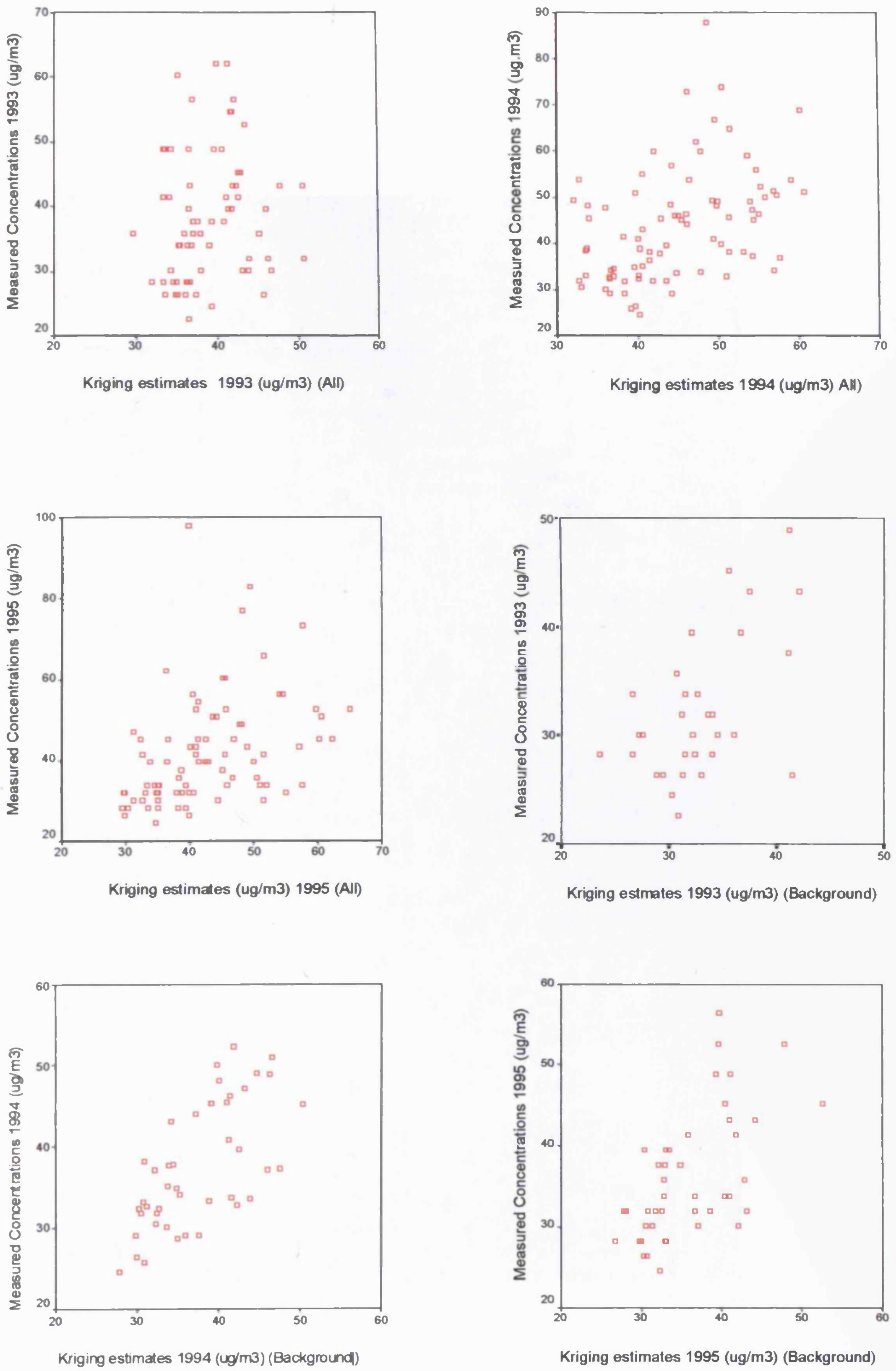

Figure 4.22: Kriging estimates versus measured concentrations in 1993, 1994 and 1995 (for All sites and for Background sites).

Figure 4.23: Difference between monitored and modelled NO_2 concentrations using kriging by type of monitoring site

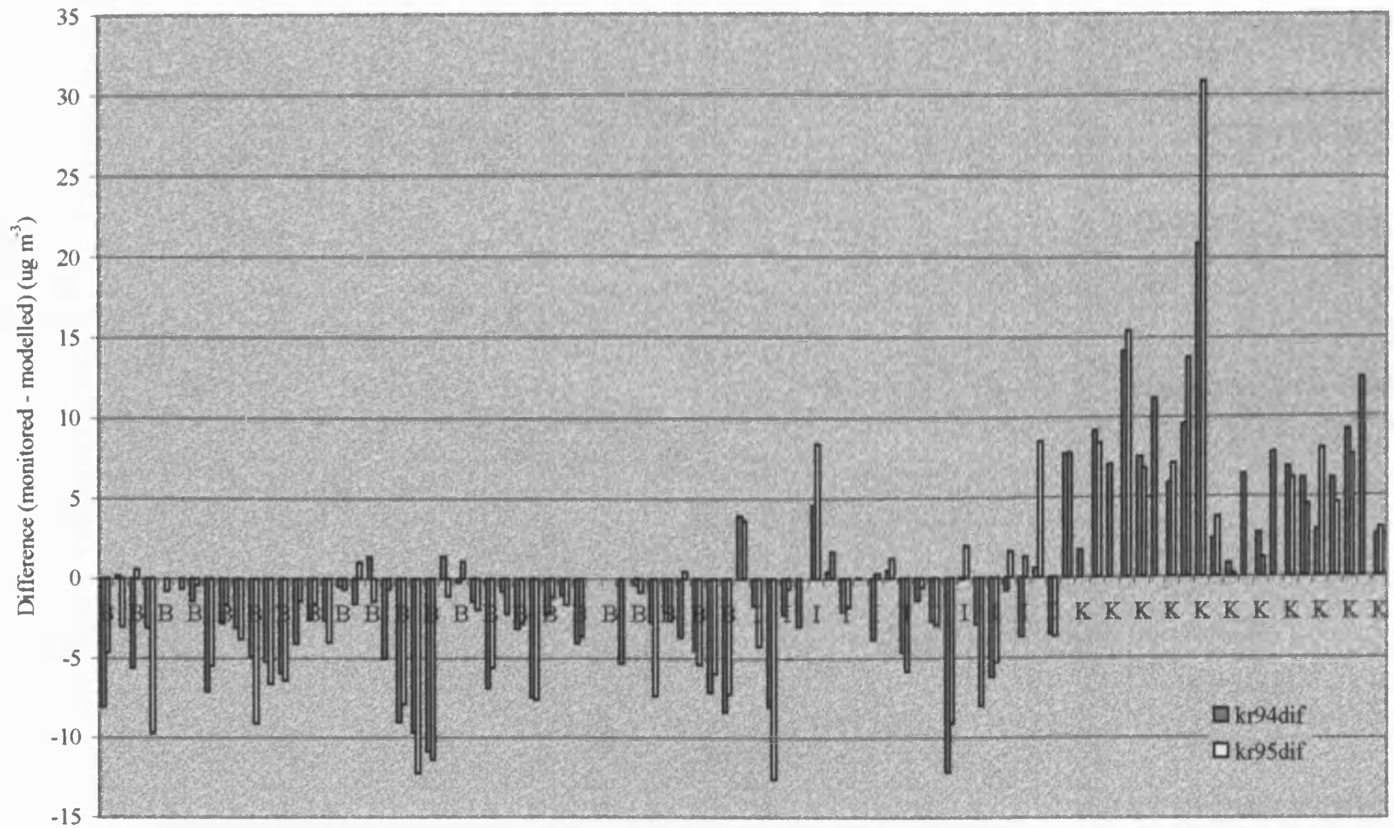

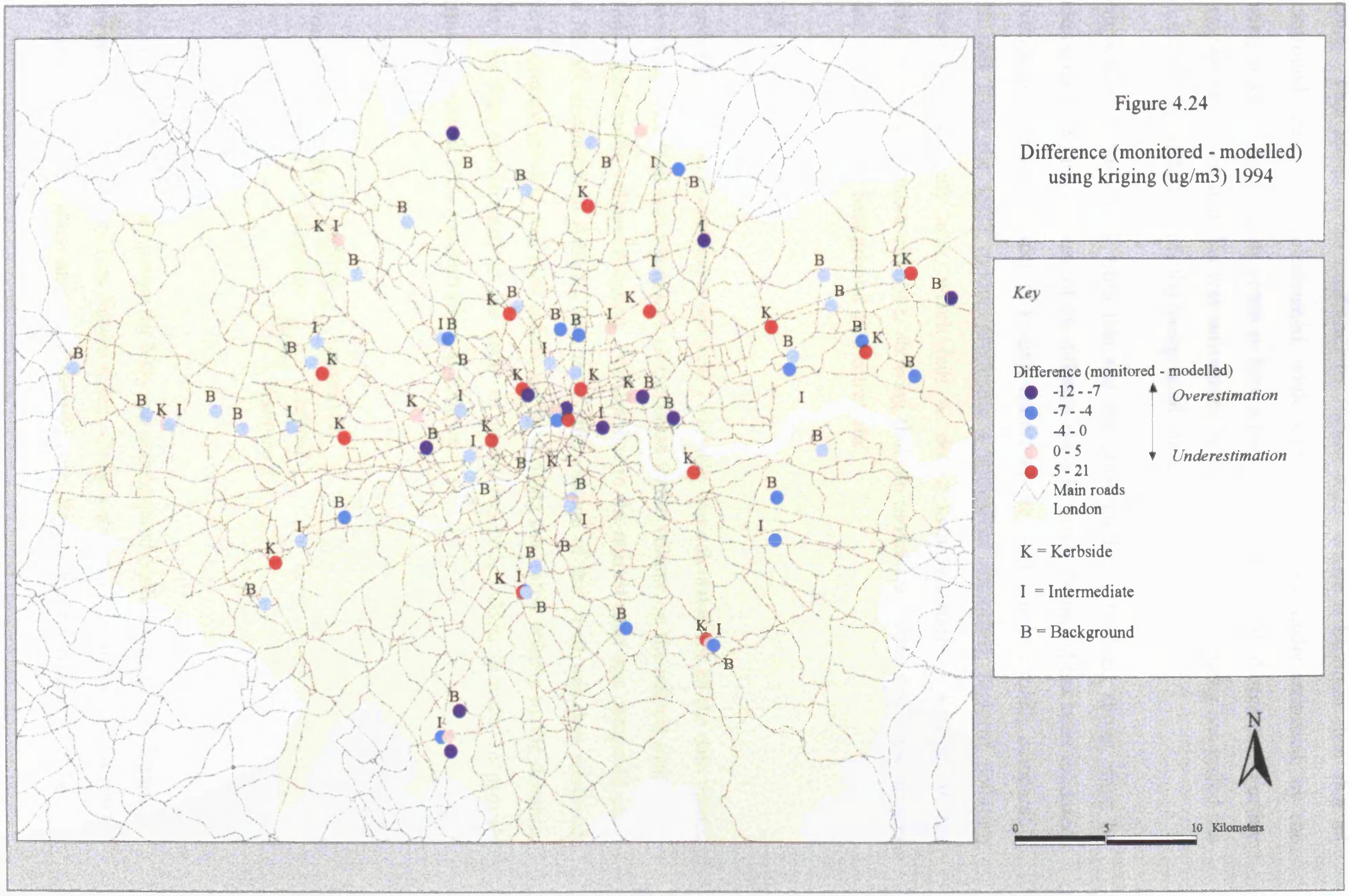

Figure 4.24

Difference (monitored - modelled) using kriging (ug/m3) 1994 kriging. This seems to be confirmed by *Figure 4.23*, where it becomes clear that all background sites are over-estimated, while kerbside sites are under-estimated, by the kriging model. One kerbside seems to have a particularly large error of estimate. Further examination showed that this was surrounded by background sites: kriging has pulled the value of the kerbside towards the background values.

Comparison of the results from this and the other methods, outlined above, must be undertaken with care, because of the different ways in which the model has been validated. Nevertheless, the performance of kriging against all sites seems to be broadly comparable with that from the ISC3 model, producing a somewhat smoothed, regional pollution surface for the study area, which fails to detect local variations. Kriging on the background sites is more effective, showing that the model can better detect the simpler spatial patterns in the background concentrations.

4.5.5 Co-kriging

In order to perform co-kriging a secondary variable was calculated for all the data points. The variable selected was a measure of the mean traffic volume on the nearest main road: standardised traffic volume/distance. The distance to the nearest road was computed using the NEAR command in ArcInfo, and the traffic volume of that road was then retrieved. The secondary variable was than calculated by dividing the traffic volume by the distance. This was then standardised to the mean of monitored NO_2 values, in order to provide output in terms of NO_2 concentration, as follows:

$$secondary\_variable = \frac{traffvol}{distance} * \frac{meanNO_2}{mean\left(\frac{traffvol}{distance}\right)} \tag{4.1}$$

Variograms and cross-variograms for NO_2 and standardised traffic volume over distance were calculated and plotted (see *Figure 4.25*). Cross-variograms for all the sites in 1993, 1994 and 1995 did not show any spatial dependency. Similarly, the variograms of the standardised traffic volume over distance lacked any spatial dependency. This suggests that co-kriging with this secondary variable is unable to model the spatial variation across the full range of sites.

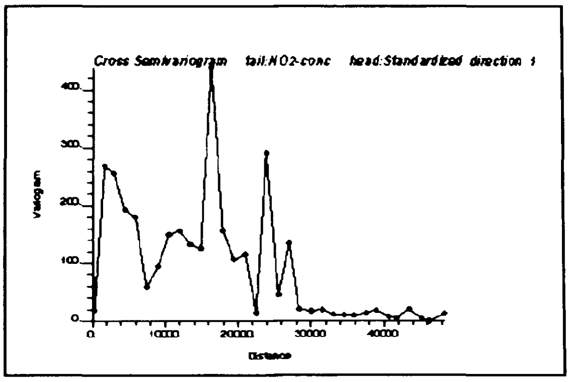

1. Cross-variogram 1994 (all) NO_2/St. Traffvol.

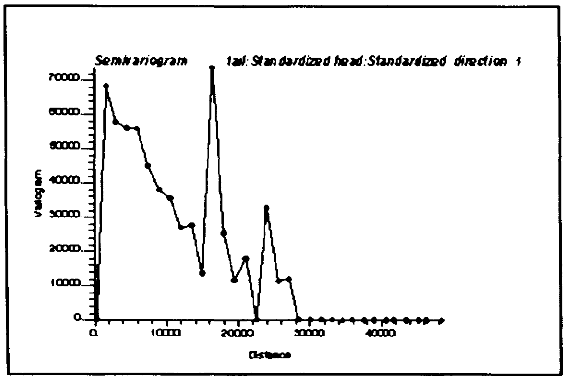

2. Variogram 1994 (All) St. Traffvol.

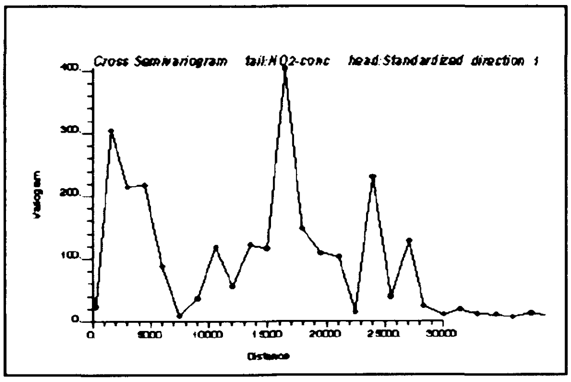

3. Cross-variogram 1995 (all) NO_2/St. Traffvol.

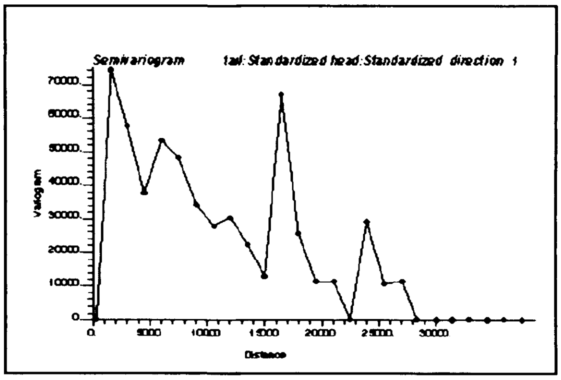

4. Variogram 1995 (All) St. Traffvol.

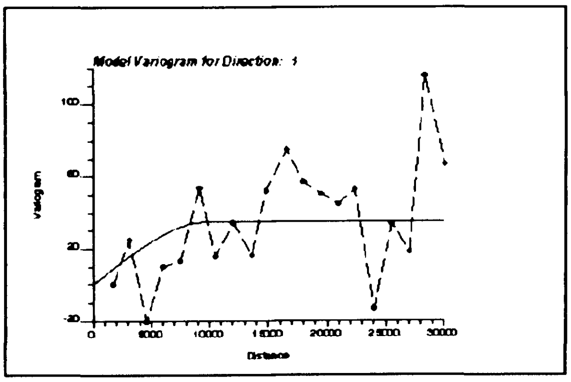

5. Cross-variogram 1993 (back) NO_2/St. Traffvol.

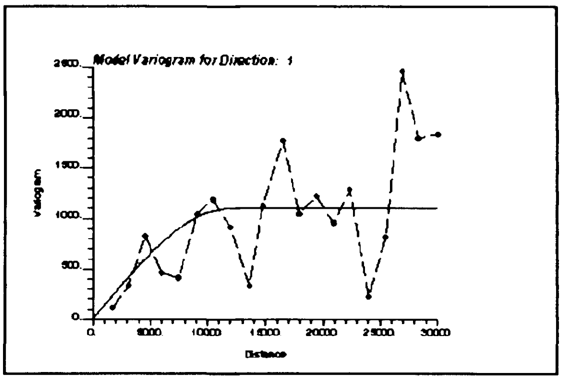

6. Variogram 1993 (Back) St. Traffvol.

Figure 4.25: Cross-semivariograms and variograms used in co-kriging in Greater London

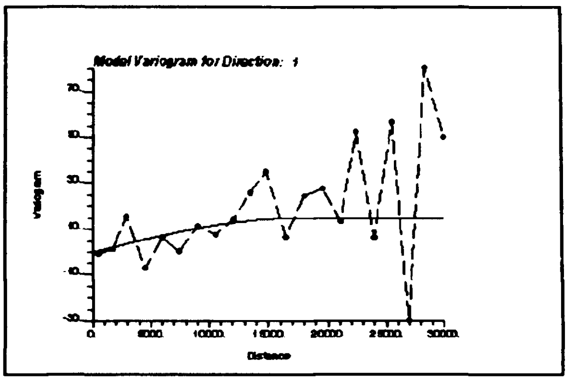

7. Cross-variogram 1994 (back) NO_2/St. Traffvol.

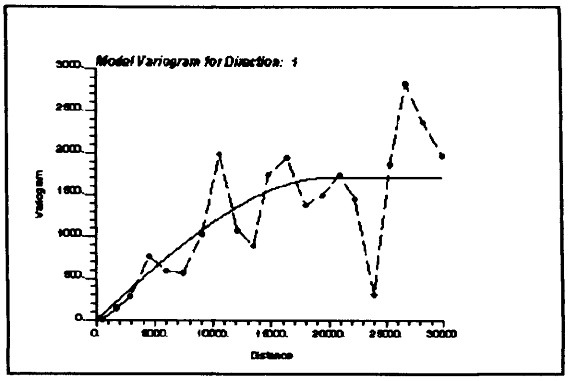

8. Variogram 1994 (Back) St. Traffvol.

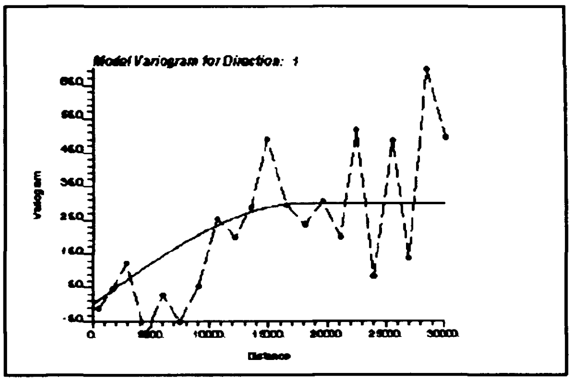

9. Cross-variogram 1995 (back) NO_2/St. Traffvol.

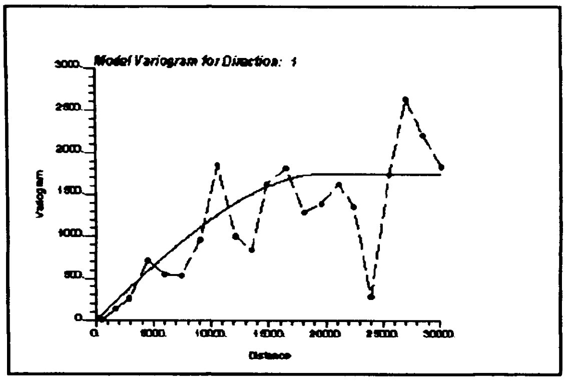

10. Variogram 1995 (Back) St. Traffvol.

Figure 4.25: Cross-semivariograms and variograms used in co-kriging in Greater London (continued)

Plots of the cross-variograms for the background sites in 1993, 1994 and 1995, however, showed some spatial dependency as did the variograms for standardised traffic volume over distance. Spherical models were fitted through the variograms and cross-variograms. The AML, specially written to perform the cross-validation, was then run for the background sites in 1993, 1994 and 1995. Results of the correlation between the co-kriged estimates and the monitored NO_2 data are shown in *Table 4.8* and *Figure 4.26*. The correlation coefficients are broadly similar to those obtained for the background sites by ordinary kriging. For these sites, therefore, the inclusion of a secondary variable (standardised traffic volume of nearest road over distance to nearest road) does not explain any of the spatial variation, and co-kriging is unable to improve on the performance of ordinary kriging.

Table 4.8: Results of correlation of monitored NO_2 versus co-kriging estimates using cross-validation.

	Pearson Correlation Sig. (2-tailed)	***Spearman Correlation Sig. (2-tailed)***	***Variogram and cross-variogram (aa,cc,n)***
93 (n=31) background	.585 *(p=.001)*	.506 *(p=.004)*	10000, 35, 0 (cross-variogram) *(nr. 5 in Fig 2.25)* 12000, 1100, 0(variogram) *(nr. 6 in Fig 2.25)*
94 (n=43) background	.703 *(p=.000)*	.704 *(p=.000)*	18000, 15, 0 *(nr. 7 in Fig 2.25)* 20000, 1700, 0 *(nr. 8 in Fig 2.25)*
95 (n=43) background	.675 *(p=.000)*	.663 *(p=.000)*	18000, 30, 0 *(nr. 9 in Fig 2.25)* 20000, 1750, 0 *(nr. 10 in Fig 2.25)*

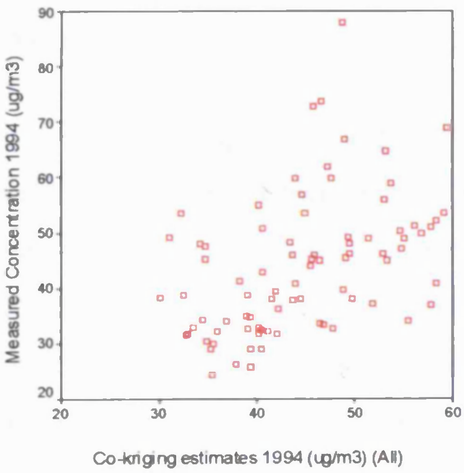

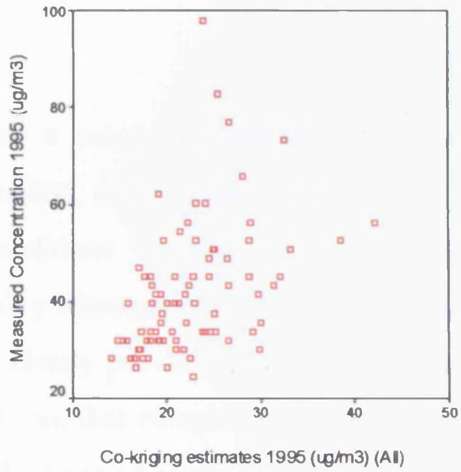

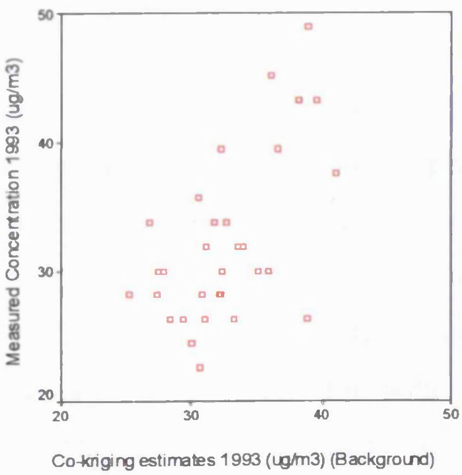

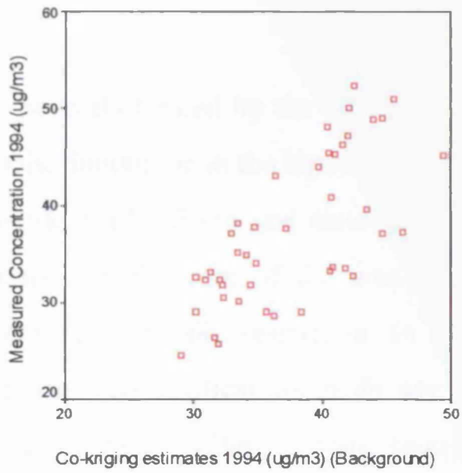

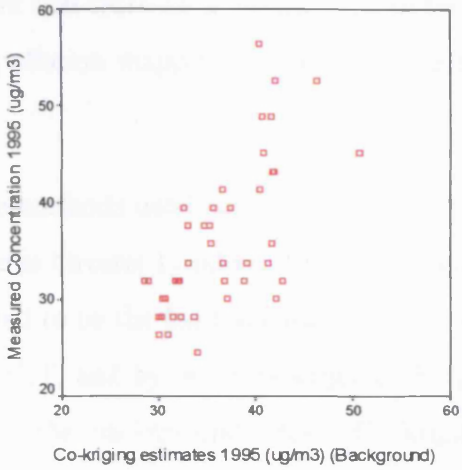

Figure 4.26: Co-kriging estimates versus measured concentrations for 1993 (Background), 1994 and 1995 (All + Background)

4.6 CONCLUSION

This Chapter has attempted to apply and compare a range of methods for pollution mapping and exposure assessment across Greater London, using existing data sources. As such, the study was designed to simulate conditions encountered by city-wide epidemiological studies or attempts to map Air Quality Management Areas across a large city, based on readily available data. This analysis clearly provides a major challenge to any pollution model or mapping method, for it requires that complex pollution surfaces, over a large geographic area, can be modelled on the basis of relatively sparse and often relatively poor quality data.

The results show that the methods used here are all severely limited by the quality of the available data. In the case of the line dispersion models, limitations in the input data - e.g. the spatial resolution and accuracy of the road network, traffic flows and meteorological data (where used) – are clearly significant constraints. In the case of the area-source models, the spatial resolution of the emissions inventory is equally restrictive. In many ways more serious, however, for both these and the geostatistical methods are the inaccuracies in, and the sparseness of, the monitored data. The analysis suggests significant locational inaccuracies in the data used here. This clearly weakens the use of these data either to test and validate the models, or as a basis for spatial interpolation of the pollution levels. It is evident that these data would need to be greatly improved if they are to be used as a basis for pollution mapping and exposure assessment across Greater London.

Within these constraints, all the methods used here showed the ability to model the broad-scale, regional pollution surface in Greater London. Measured against the monitored data, the line dispersion models tended to be the least accurate. Better estimates were provided by the area source model, ISC3LT, and by ordinary kriging. Kriging was most effective, however, when applied only to the background sites. Co-kriging, using a measure of traffic volume on the nearest main road as the secondary variable, failed to improve on ordinary kriging.

5 THE SHEFFIELD CASE STUDY

5.1 INTRODUCTION

This chapter describes a second case study, undertaken in Sheffield, aimed at applying and comparing different methods for assessing exposure to traffic-related pollution.

Sheffield was selected for this purpose for a number of reasons. The opportunity to carry out the case study arose because of funding from the Department and Health and Medical Research Council for a project entitled *Relationship of asthma and allergic rhinitis to local traffic density and ambient pollution modelled at a small area level.* This study was a collaboration between the Nene Centre for Research (Nene University College Northampton), the Department of Public Health Sciences (St George's Hospital Medical School) and the Department of Epidemiology & Public Health (St Mary's Hospital Medical School and Imperial College of Science and Technology). A key part of the project was the assessment of exposure to traffic-related pollution of a sample of ca. 18000 children, for whom data on respiratory symptoms had previously been acquired. It thus provided an ideal opportunity to apply and evaluate the methods being investigated, within a full epidemiological study. In the process, it allowed associations between the exposure measures and various respiratory health outcomes to be assessed.

In addition, Sheffield provided a useful adjunct to the London case study for a number of other reasons. It differs from Greater London both in terms of size and topography. It provided the opportunity to undertake purpose-designed air pollution monitoring, as a basis for implementing and validating several of the methods. It also permitted the use of more detailed data, and a wider range of environmental data, than available for London. It thereby avoided some of the uncertainties and limitations inherent in both the reference data and the input data used in London.

5.2 BACKGROUND OF SHEFFIELD HEALTH STUDIES

The Sheffield case study is built upon two previous studies carried out in the town (Strachan and Carey 1995, Strachan *et al.* 1996). These investigated a group of children who were born between 1975 and 1980 and who attended schools in Sheffield, with the aim of determining the effects of various risk factors of childhood allergic illness. The following sections briefly describe these earlier studies and outline the way in which these were developed within the new study, funded by the DoH/MRC.

5.2.1 Sheffield Allergy Study

The Sheffield Allergy Survey was carried out in 1991 and included all secondary school children aged 11-16 in Sheffield at the time (Strachan and Carey 1995, Strachan *et al.* 1996). A questionnaire survey enquiring about symptoms related to asthma, allergic rhinitis and eczema was circulated to the parents of 23,054 children; 18,023 questionnaires were returned (79% response). Two indicators of the severity of wheezing were included in the questionnaire: the frequency of attacks and the occurrence of wheezing sufficient to limit the speech to no more than one or two words between breaths. The child's gender, date and place of birth, as well as detailed information relating to many respiratory and allergic conditions, were also obtained from this questionnaire.

Analysis at the level of school demonstrated a highly significant ($p>0.001$) heterogeneity in the prevalence and severity of wheeze, and the prevalence of doctor-diagnosed asthma, hay fever and eczema (Strachan and Carey 1995, Strachan *et al.* 1996).

The aim of the initial study was to link responses to birth records using additional information, including address and postcode of residence. Subsequently, two additional studies were conducted, the case-control study and the skin prick test, as described below.

5.2.2 Case-control study

In 1993, 763 children with more severe wheezing (12 attacks in the last year, or one or more attacks limiting speech), 763 school-matched controls who had never wheezed, and 359 children with milder forms of wheezing were selected from the initial survey for inclusion in a case-control study. Questionnaires were sent out to the parents of these children enquiring about indoor environmental risk factors, including cooking and heating fuels, parental smoking, pet ownership, bedding, dampness and mould growth. The response rate was 75%.

The data was used to investigate the effects of the home environment on the risk of severe asthma during adolescence (Strachan and Carey 1995). Positive associations were found between severe wheeze and non-feather bedding and the ownership of furry pets. Attempts were made to adjust for children who influenced their exposure to pets or bedroom environment because of their allergic condition. The study concluded that either there is a previously undiscovered risk factor associated with foam pillows, or that inadequate adjustment was made for the avoidance of feather bedding.

5.2.3 Skin prick test

In the same year (1993) skin prick tests were performed on 727 children from 14 of the 36 schools used in the first questionnaire survey. The allergens used were house dust mite, mixed grass pollen and cat fur together with positive (histamine) and negative (saline) controls. The parents of these children were also mailed the same indoor environment questionnaire as in the case-control study. The aims of this study were to assess early life influences on the development of allergic sensitisation through linkage to health visitor records. It was concluded that the first month of life and the first postnatal exposure to allergen are not critical periods during which a protective effect is determined (Strachan *et al.* 1996).

5.2.4 Relationship of asthma and allergic rhinitis to local traffic density and ambient pollution modelled at a small area level

In 1995, funding was obtained for a further study, aimed at investigating the small area variations in the prevalence and severity of wheezing illness and other allergic disorders amongst children in Sheffield, and their relationship to estimates of exposure to traffic related air pollution (Strachan *et al.* 1998). This study provided the second case study undertaken here. The data from the two questionnaires - from the Sheffield Allergy

Survey and the Case-control Study - was used together with address and postcode of residence of the children to provide measures of health outcome. Data on exposures was obtained for children in the survey, as part of this research, using a range of methods.

Seven exposure measures were selected, which were estimated for each place of residence, as follows:

- distance to nearest road
- distance to nearest main road
- road density within 150m
- main road density within 150m
- traffic flow within 150m
- HGV flow within 150m
- NO_2 concentration obtained from pollution modelling (using a range of techniques)

These methods were chosen because of their wide use in similar research (see *Chapter 2*).

The exposure estimates were then correlated with the respiratory symptoms at the individual level by logistic regression, adjusting for age, sex and deprivation.

Analysis of the relationship between health outcome and the exposure measurements, was carried out by Jeremy Bullard, from Imperial College of Science and Technology. Results of this analysis will be summarised in *Section 5.6*. The estimates of the exposure measurements using indicators and various modelling techniques were carried out as part of this thesis.

Comparing exposure estimates from a large number of measures with health outcome is undesirable, for two important reasons. The first is that analysis is time-consuming and costly. The second is that multiple analyses of this type are likely to generate false-positive associations: simply by chance, some measures are likely to show correlations, which might then be interpreted as meaningful relationships. To avoid this, it is important to select exposure indicators with care, taking account both of underlying aetiological assumptions and the quality of the available data. In this case, it was therefore decided to restrict analysis of relationships between health outcome and exposure to only a few exposure measures. These were selected by comparing predicted exposure scores with measured pollution data at a sample of reference sites. Data on NO_2 was obtained through a purposely-designed monitoring programme across Sheffield, using passive samplers.

5.3 STUDY AREA

Sheffield is England's fourth largest city and is located in the county of South Yorkshire, at the junction of the Don River and four of its tributaries, at the southern foot of the Pennines. Sheffield has been a major steel-manufacturing centre, known especially for its stainless steel products, notably cutlery. The city is located in an important coal-mining region and has iron and brass foundries and manufactures a range of products including steel tools and other metal products, processed foods, and glass. Much of this industry was, however, closed during the 1980s, with the result that it now has a much more diversified industrial base. During the late 1980s and early 1990s, it underwent considerable redevelopment. The population in 1991 was a little over half a million (OPCS 1991).

The actual study area included all urban areas of Sheffield (see *Figure 5.1*) and covers an area of approximately 137 km^2. As shown in *Figure 5.1*, most of Sheffield's industrial area is situated in the north-east of the study area, between the city centre and the M1 motorway. There are also smaller industrial areas to the north-west and just south of the city centre. In the study area, the altitude ranges from 31m in the east to 311m in the west.

In 1995 Sheffield introduced a rapid light transit system (the Supertram), which runs along two lines and has a total length of 30km of track. One line runs from the city centre to Meadowhall Regional Shopping Centre (near the M1) and the other line runs from Middlewood through the city centre towards Halfway Mosborough. Although these have had a significant effect on road traffic in recent years, at the time of the health survey the system was not in operation.

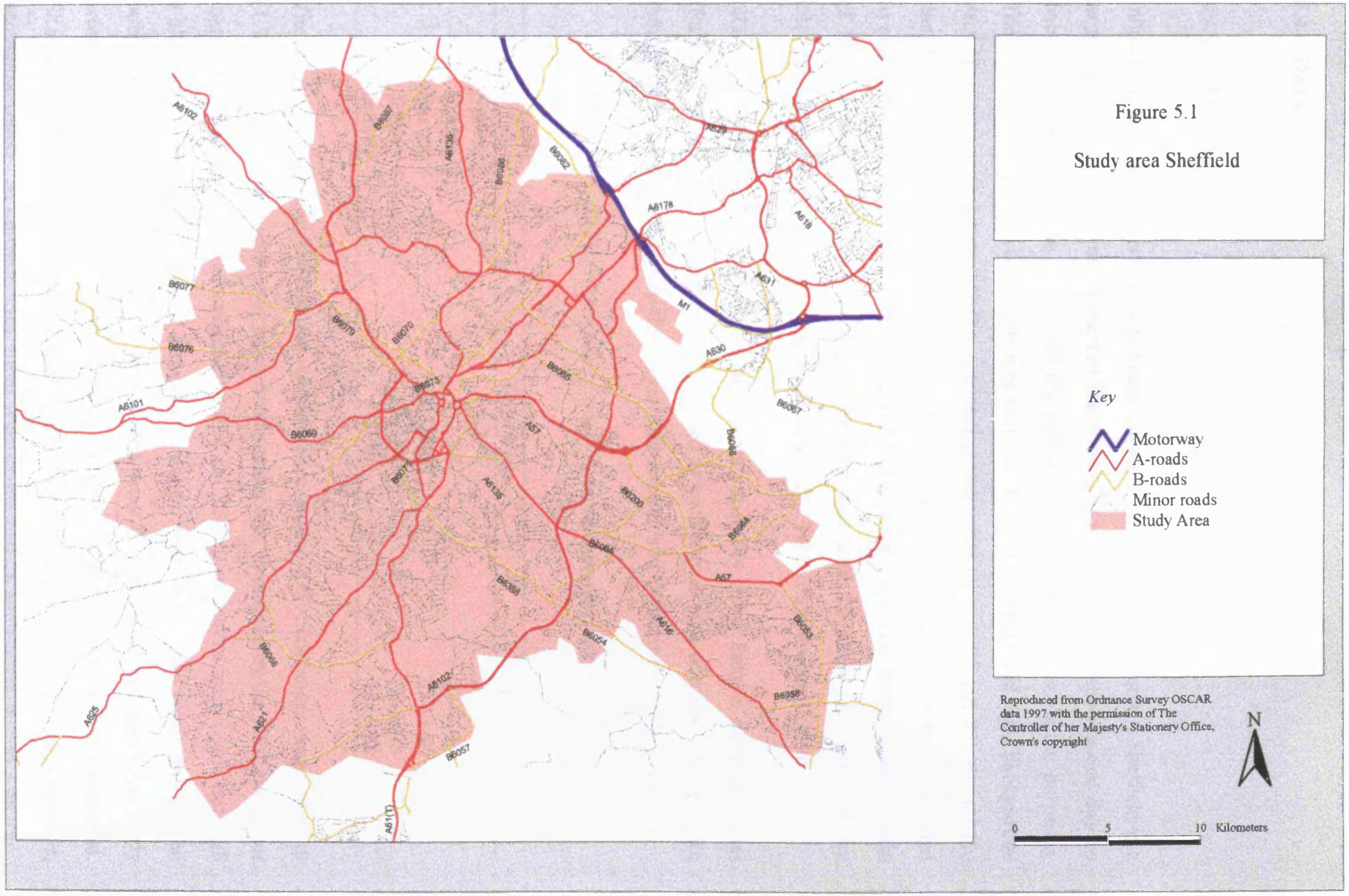

Figure 5.1

Study area Sheffield

5.4 DATA

5.4.1 NO_2-monitoring

Initially 26 sites were selected for pollution monitoring, for logistic reasons. Sheffield is a large area and 26 sites was considered the maximum that could be visited in one day by one person, whilst on the other hand the number was sufficient for validation purposes. The 26 sites were defined to provide nine kerbside, nine intermediate and eight background sites. During survey 1, loss of tubes occurred at three sites (nos. 6, 23 and 25); these were therefore relocated to safer sites in subsequent surveys. After survey 1, it was also decided to add two new intermediate sites (nos. 2 and 14) in order to provide better representation of these areas. The remainder of the surveys thus used 28 sites: nine kerb, eleven intermediate and eight background sites (*Figure 5.2*). Table 1 shows dates of surveys.

NO_2 concentrations were measured at 2-weekly periods using Palmes diffusion tubes (Palmes *et al.* 1976). Two tubes were exposed at each site on each occasion. Tubes were purchased from and analysed by the Kirklees Environmental Department in Huddersfield.

Table 5.1: Dates of the NO_2 monitoring periods

	Start date	***End date***
Survey 1	15-7-97	29-7-97
Survey 2	9-9-97	23-9-97
Survey 3	11-11-97	25-11-97
Survey 4	14-1-98	28-1-98
Survey 5	4-3-98	18-3-98

The 28 sites were initially selected by reference to the OS Landranger map no. 110 (1:50,000). Kerbside areas were chosen near main roads, as defined by the OS Landranger map. Intermediate areas were selected within ca. 20-200 metres of main roads but well within urban areas. Background areas were chosen away from main roads and on the outskirts of urban areas. All three sets of area were equally distributed inside the study area. All these 28 areas were visited and a suitable location for the samplers identified. Sites were selected which were well away from significant point sources (e.g. chimneys, ventilation units). At kerbside sites, tubes were positioned on lamp-posts, within 3 metres

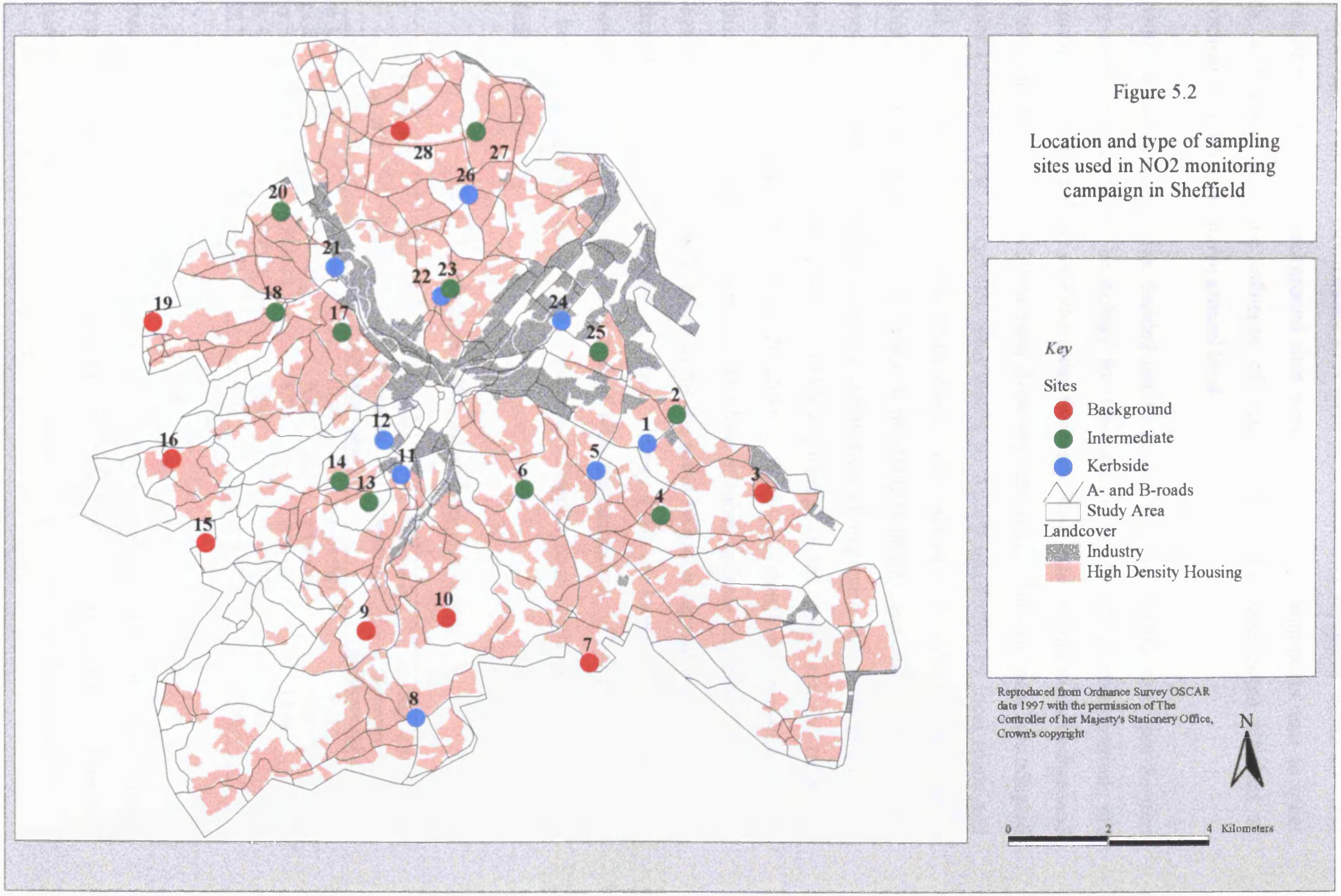

Figure 5.2

Location and type of sampling sites used in NO2 monitoring campaign in Sheffield of a main road. Tubes at intermediate sites were positioned on lamp-posts within 20 - 200 metres of a main road. Background sites were positioned on lamp-posts near to quiet roads, and away from the influence of main roads. All tubes were attached at approximately 3.5 metres above ground level.

It should be noted that it was decided not to follow the site classification (see *Section 4.3.1*) used by the AEA Technology for this study. In the AEA classification, the background sites are defined as >50m away from any busy road; in this study background sites were defined as being >200m away from any busy road. This protocol was adopted in order to ensure that background sites would be wholly unaffected by local roads and would measure true background concentrations. The limit of 200 metres was selected to be consistent with the limit to modelling in the DMRB model, and also is close to the distance of 150 metres widely used for calculation of exposure indicators in previous studies (see *Chapter 2*). To provide complete coverage of the study area, the range for intermediate sites was extended to 20-200m. *Table 5.2* shows the statistics of the monitoring campaign by survey period. The loss of tubes became less after the first two surveys. Survey 3 has the highest values for the mean NO_2 concentration and the average coefficient of variation (CVs) between tubes. Survey 4 has the lowest standard deviation between sites and also the smallest range of NO_2 concentrations. *Figure 5.3* shows the CVs between duplicates for all the 5 surveys. Despite some high values, CVs were generally +/- 10%.

Table 5.2: Statistics NO_2 monitoring campaign

	Mean NO_2 ($\mu g\ m^{-3}$)	***Range ($\mu g\ m^{-3}$)***	***Standard Deviation between sites***	***Number of tubes lost***	***Average CV between duplicate tubes***
Survey 1	42	20-74	10.43	6 (n=52)	9.21
Survey 2	39	18-78	9.41	6 (n=56)	5.89
Survey 3	53	26-84	8.10	3 (n=56)	12.54
Survey 4	47	29-74	6.61	4 (n=56)	7.65
Survey 5	44	21-82	8.91	2 (n=56)	5.98

Estimates of mean annual pollution at each of the 28 sites were made by using a fixed-effect model, with terms for measurement error and site and survey effects. This was necessary to fill up the gaps created by of loss of tubes (see *Table 5.2*). *Appendix 5A*

Figure 5.3: Coefficients of variance (CVs) for tubes

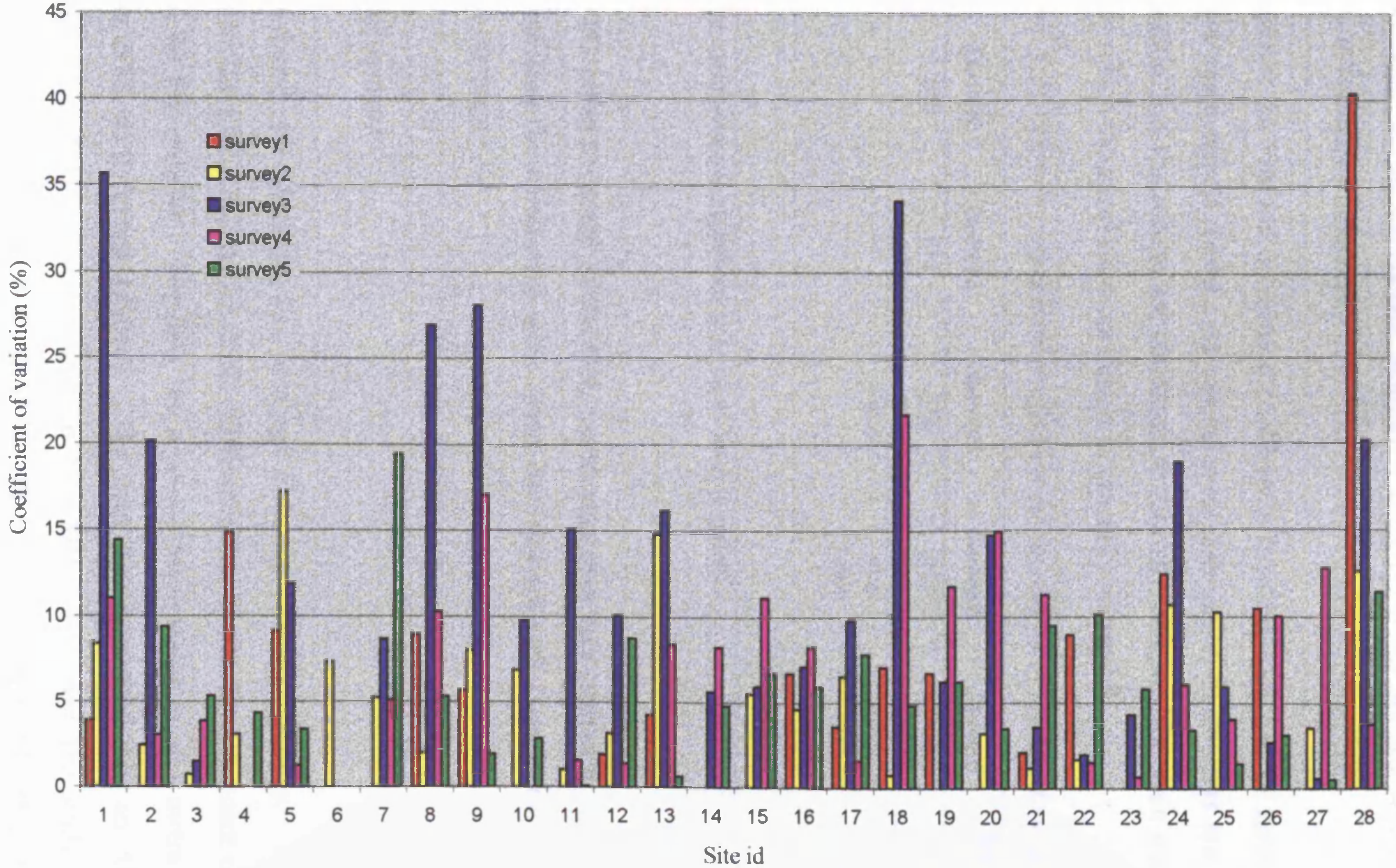

shows the results of the NO_2 monitoring and the results of the fixed effect model. The calculations were made by Jeremy Bullard (Imperial College, London) and the modelled values were used in all subsequent analysis. *Figure 5.4* shows the 2–weekly NO_2 concentrations during the 5 surveys.

Table 5.3 shows the Pearson correlation coefficients between each pair of surveys, using data from the fixed effects model. As can be seen, correlation coefficients are generally high, suggesting that the results are consistent across all surveys. The main exception is survey 3, for which the correlation coefficient is generally below 0.8.

Table 5.3: Pearson correlation coefficient of the results of the fixed model.

	Survey1	***Survey2***	***Survey3***	***Survey4***	***Survey5***	***Mean of 5 surveys***
Survey1	1.000	.946	.710	.845	.939	.964
Survey2		1.000	.770	.841	.907	.967
Survey3			1.000	.774	.688	.845
Survey4				1.000	.807	.912
Survey5					1.000	.942
Mean of 5 surveys						1.000

All correlation coefficients are significant at the 0.01 level (2-tailed).

An ARCINFO point coverage of the NO_2 monitoring sites was created in ARCEDIT, by manually digitising the monitoring sites, using the road network (see *Section 5.4.2*) as a background coverage.

5.4.2 *Road network*

The road network for Sheffield was obtained from the Ordnance Survey. The Asset-Manager from the OSCAR product family (Ordnance Survey Centre Alignment of Roads) was chosen for this purpose. The data has a co-ordinate resolution of 1 metre and was delivered in NTF v2.0 format (digital). The data was converted into an ARCINFO coverage using the NTF converter supplied by ESRI. To cover the study area the following 5x5 km tiles were needed: SK39SW, SK39SE, SK49SW, SK28NE, SK38NE, SK38NW, SK48NW, SK28SE, SK38SW, SK38SE, SK48SW and SK37NW.

Four types of roads are distinguished in the OSCAR road network: motorways, A-roads, B-roads and smaller roads. For the analysis it was evident that use of the main roads

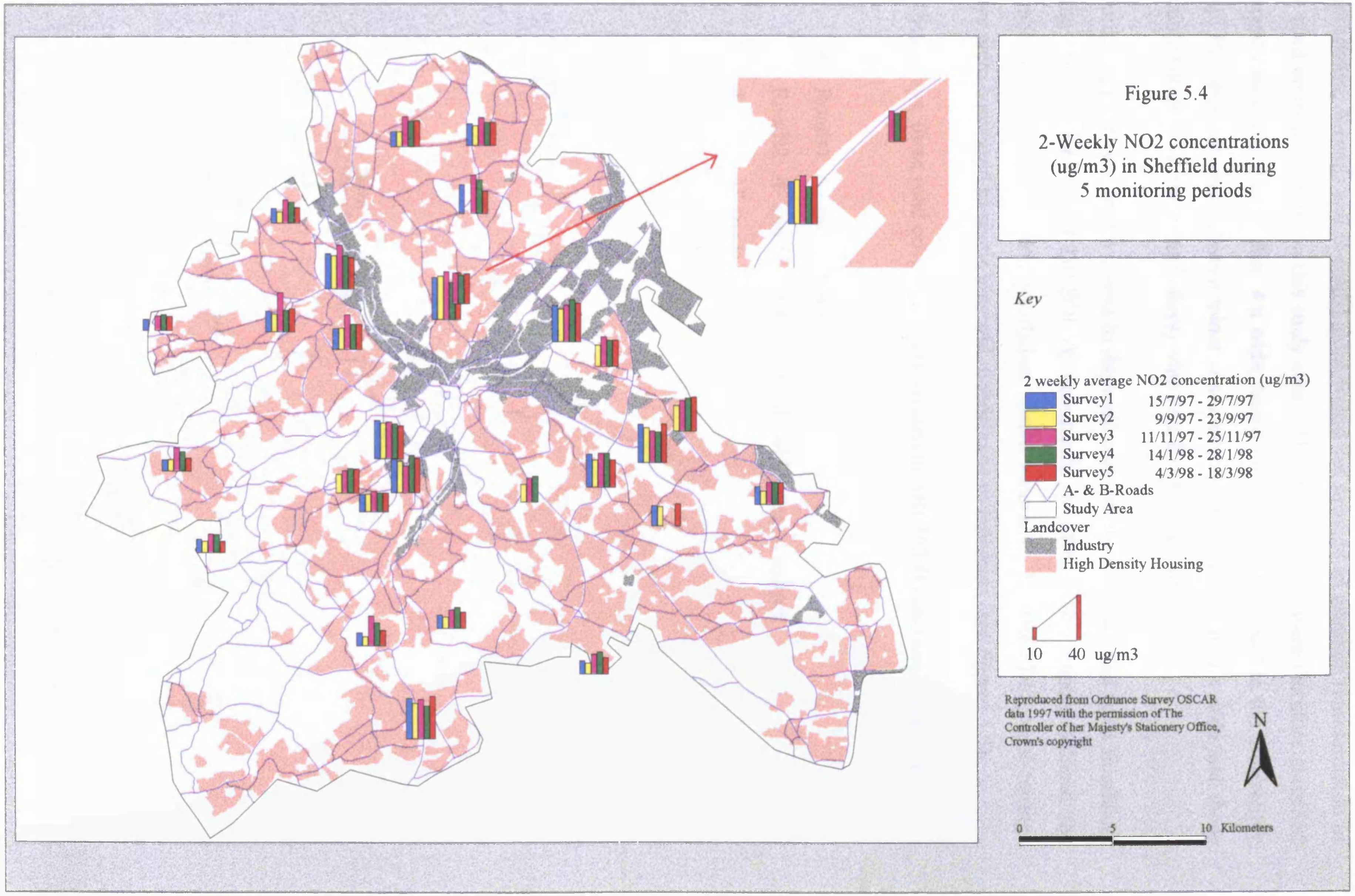

Figure 5.4

2-Weekly NO2 concentrations (ug/m3) in Sheffield during 5 monitoring periods (motorways, A-roads and B-roads) alone would not provide an accurate representation of the road emission sources in this study area. The smaller roads were therefore classified manually as roads greater than 4m wide, based on the definition used in the Landranger map: this distinguishes between minor roads which are greater than 4m wide and those (mainly cul-de-sacs, tracks and alleys) which are less than 4m wide.

In order to attach the traffic counts to this road network the coverage had to be simplified, using the ARCEDIT and DISSOLVE commands in ARC. This greatly reduced the number of arcs whilst retaining sufficient spatial accuracy. In ARCEDIT, dual-carriage ways were converted to single arcs and roundabouts to crossings (see *Figure 5.5*).

In these ways, three road coverages were created in ARCINFO (also see *Figure 5.6*):

- Roads1: A- and B- roads
- Roads2: A- and B- roads and roads wider than 4 metres
- Roads3: All roads

Figure 5.5: Example of road coverage before and after editing in ARCINFO

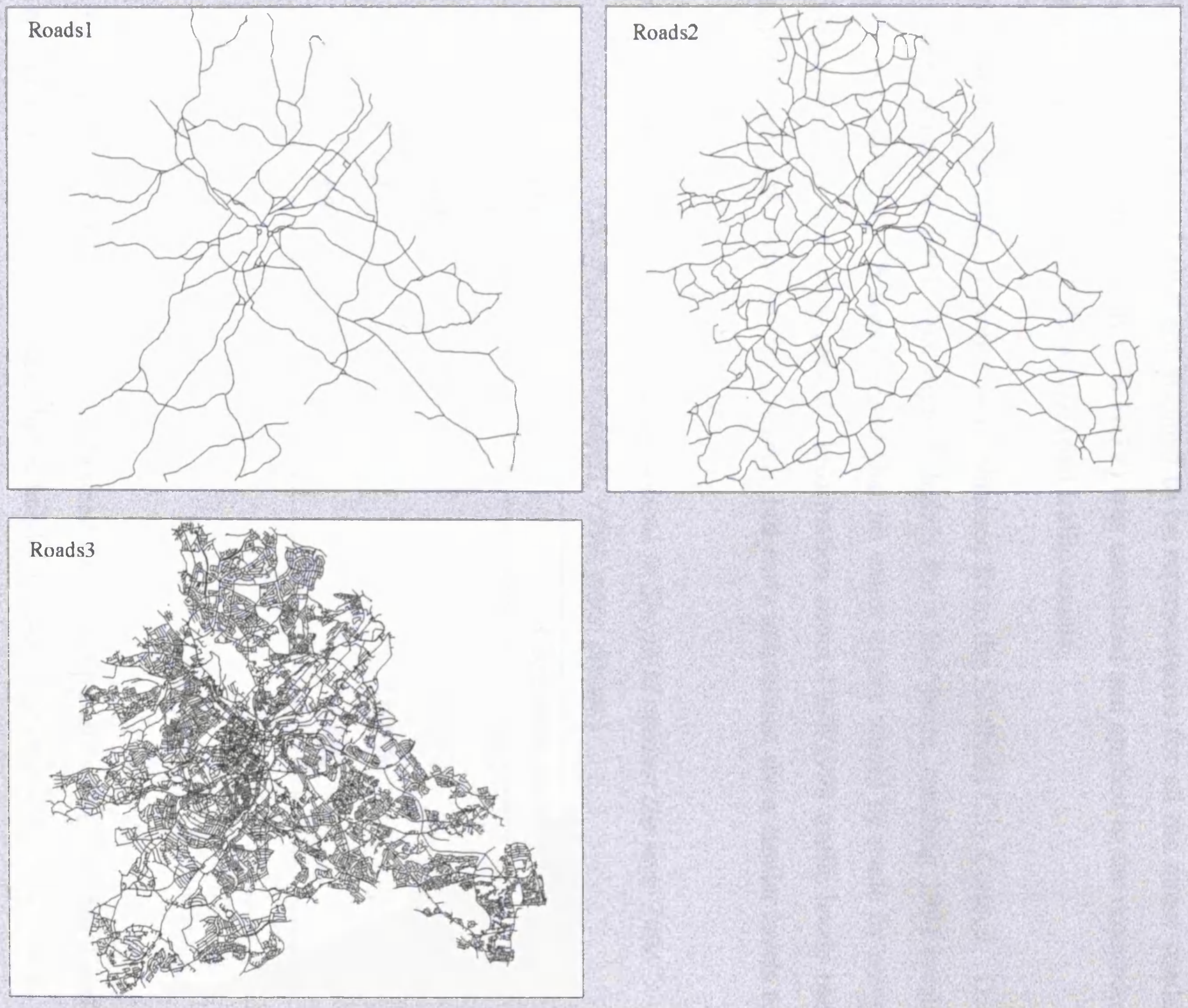

Figure 5.6

Different road coverages used in the analysis

Key

Roads1: A- and B- roads

Roads2: All roads wider than 4m

Roads3: All roads

N

0 5 10 Kilometers

5.4.3 *Traffic counts*

Traffic count data was obtained from the Department of Transport of Sheffield City Council. The data consisted of 24-hour average 1996 traffic count estimates (total traffic and percentage of Heavy Good Vehicles (HGV)) derived from 1995 GMTU day and month factors, for most of the main roads in the Sheffield area. The data was supplied in an Excel file and was geo-referenced by road name (*Appendix 5B)*. This data was manually linked to the road coverage in ARCINFO. Road links without any traffic information were assigned values by interpolation from traffic data of neighbouring roads. For the minor roads, very few counts were available. From the few minor roads with available traffic counts, which were assumed to be representative for all the minor roads, an average of 250 vehicles per day (5% HGV) was calculated and applied to the remainder of the minor roads. *Figure 5.7* shows the road traffic counts.

Correction factors for traffic volumes were obtained from the Sheffield City Council. The traffic reached a peak in 1991, then dipped slightly for a few years, reaching 1991 levels again in 1996 (*Table 5.4*). It was decided that no major errors would be made by using 1996 traffic counts for the study period. Information about 1997/1998 traffic levels had not been published at the time of this research, but early indications show similar levels to 1996.

Table 5.4: Correction factors for traffic volume in Sheffield against the year 1996. (Sheffield City Council, 1998, pers. comm.)

Year	***Correction factor***
1991	0.990
1992	0.974
1993	0.976
1996	1.000

5.4.4 *Terrain heights*

Terrain heights in the Sheffield area were obtained from the Ordnance Survey. The Land-Form PANORAMA is a 1:50,000 scale digital height dataset. The Digital Terrain Model

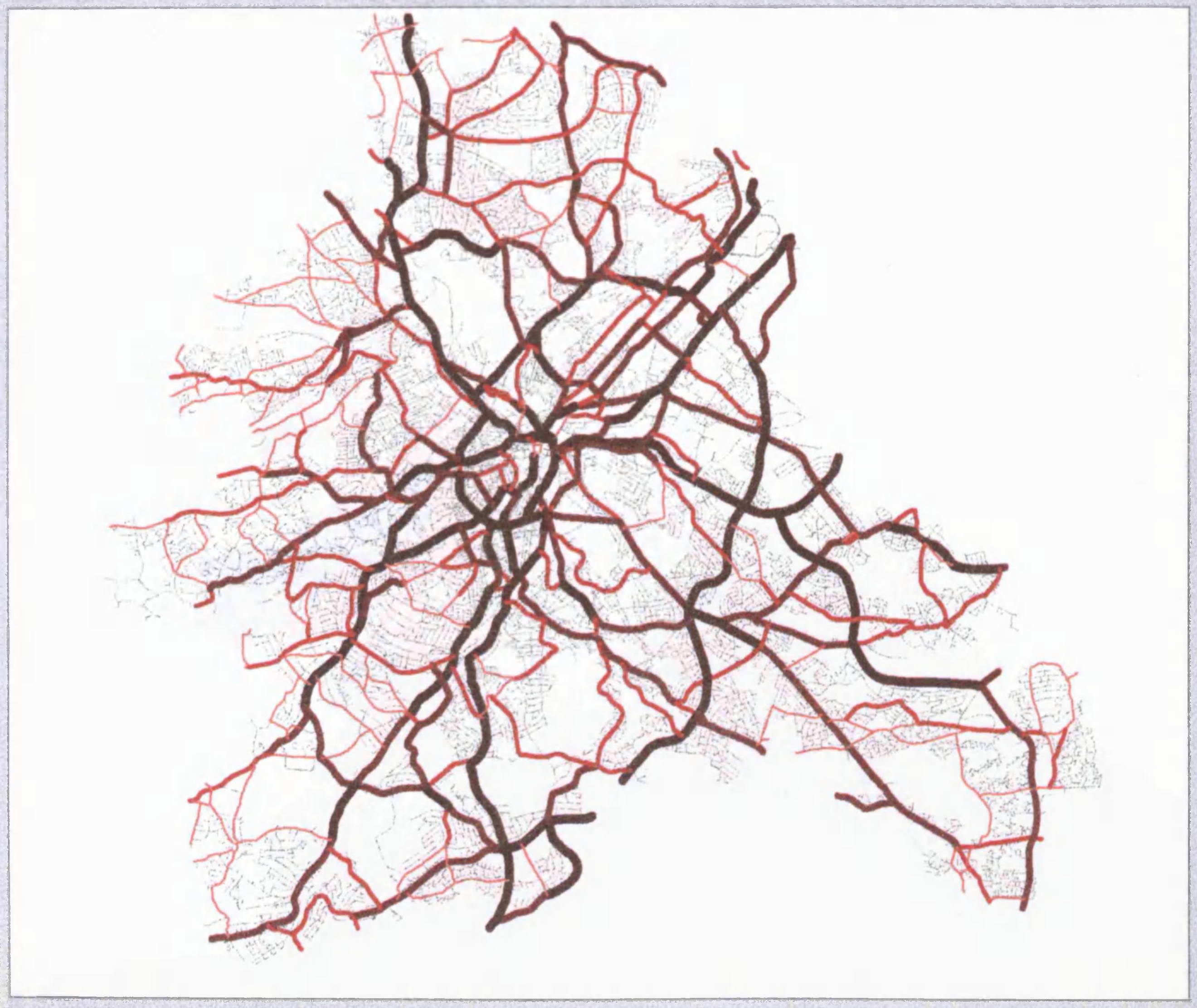

Figure 5.7

Daily traffic flows in Sheffield

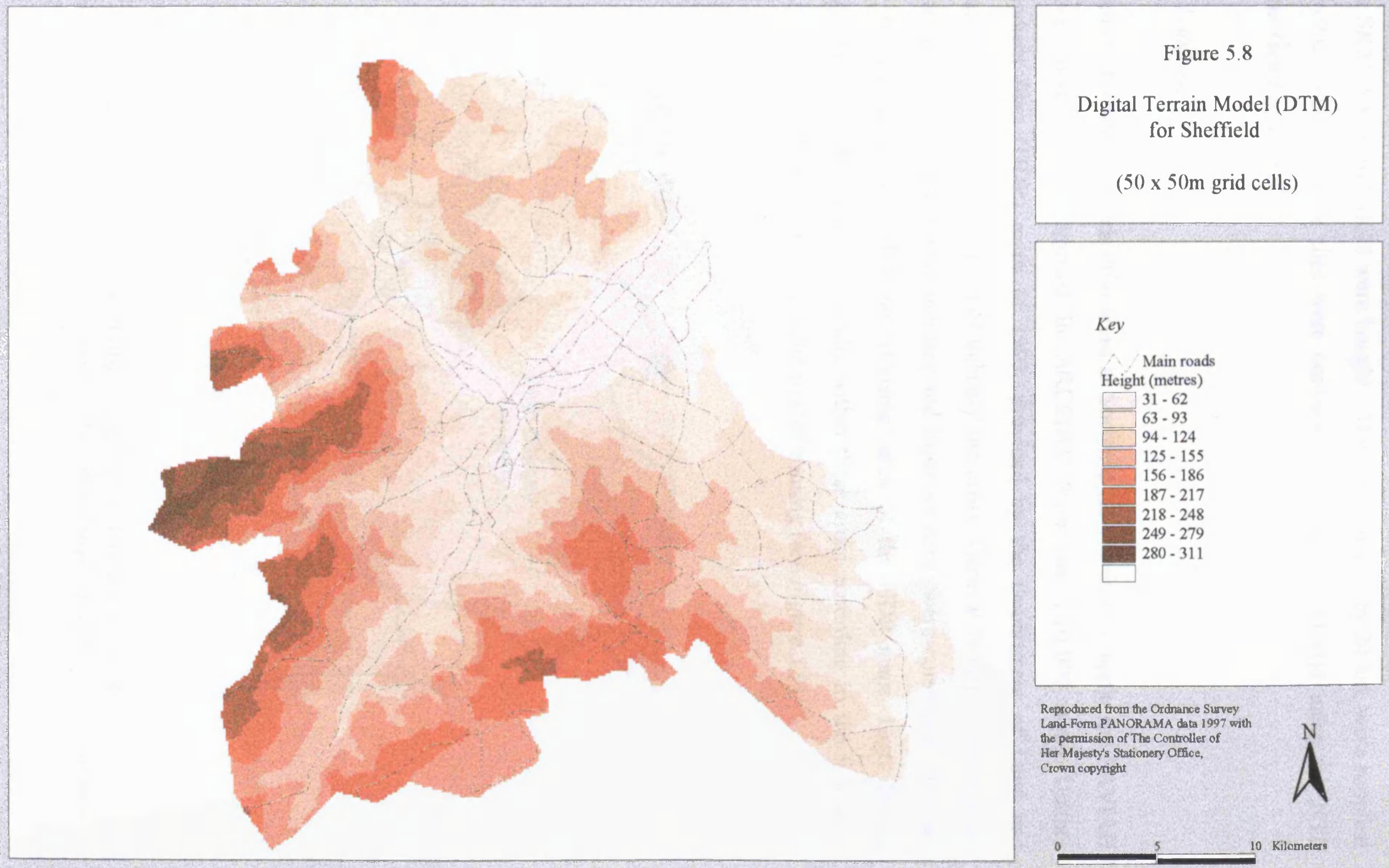

Figure 5.8

Digital Terrain Model (DTM) for Sheffield

(50 x 50m grid cells)

(DTM) consists of a grid of height values at 50 metre intervals. To cover the study area the tiles SK26, SK28 and SK48 were bought. The tiles, each 20 by 20 km, were supplied in NTFv2.0 format. These tiles were converted into ARCINFO grid using the NTF converter (see *Figure 5.8*).

5.4.5 Land use

High density housing and industrial areas in Sheffield (as required to apply the SAVIAH regression model) were digitised in ARCEDIT from ten 1:10.000 scale Unitary Development Plan (UDP) maps of 1993, provided by the Department of Land and Planning, Sheffield City Council. For industry the areas 'General Industry with Special Industries (A and B)' and 'Fringe Industry and Business Area' were combined. All high density housing occurred within the 'Housing' area of the UDP maps. High density housing areas were distinguished visually within these areas according to the following criteria: a) small gardens, b) more than one row of housing (see *Figure 5.9*).

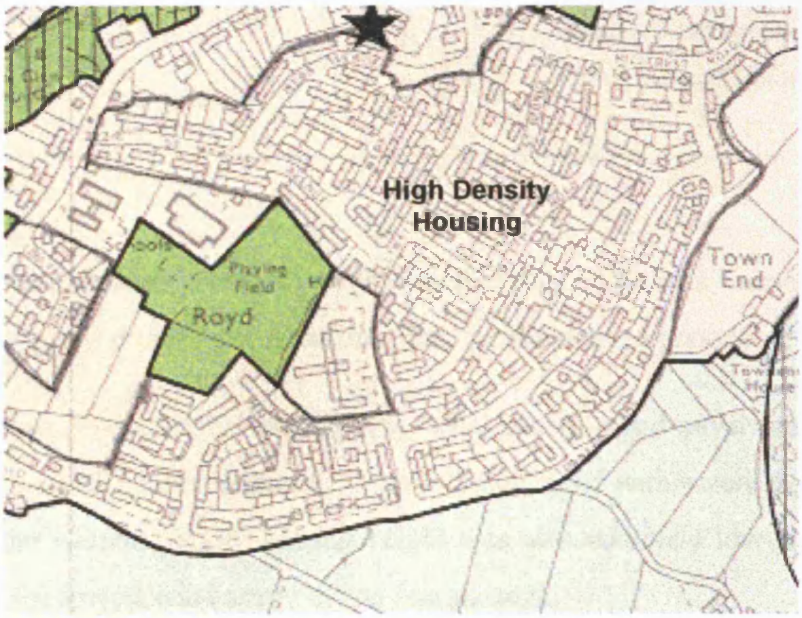

Figure 5.9: Example of defining High Density Housing in Sheffield
Source: UDP-map, Sheffield City Council, 1993, made and printed by the Ordnance Survey

5.4.6 *Meteorological data*

Meteorological data for the five surveys was purchased from the UK Meteorological Office. The data was supplied in both ADMS format and ISC3 format. An AML was written automatically to convert the ISC3 format into a format read by CALINE3. *Table 5.5* shows the meteorological parameters used in ADMS-Urban and ISC3.

Table 5.5: Meteorological parameters for ADMS-Urban and ISC3.

Hourly meteorological data	
ADMS-Urban	***ISC3***
Station Number	Station Number
Year	Year
Julian Day Number	Month
Hour (GMT)	Day
Temperature (0.1 deg C)	Hour (GMT+1)
Wind Speed (m s-1)	Flow Vector (ten of degree. from true North)
Wind Direction (direction wind is coming from)	Wind Speed (m s-1)
Precipitation (0.1 mm)	Ambient Temperature (K)
Total Cloud Amount (Oktas)	Stability Class
	Rural Mixing Height (m)
	Urban Mixing Height (m)

Both datasets were obtained from Leeds Weather Centre. This was the nearest station to Sheffield, which could provide the necessary data for the desired periods.

Figure 5.10 shows averages for temperature, wind speed, cloud cover and urban mixing height plus the sum of the precipitation. Survey 3 coincided with a very dry period, while survey 5 was the wettest period. Mixing height was also relatively low during survey 3, which also had the lowest wind speed of the five surveys.

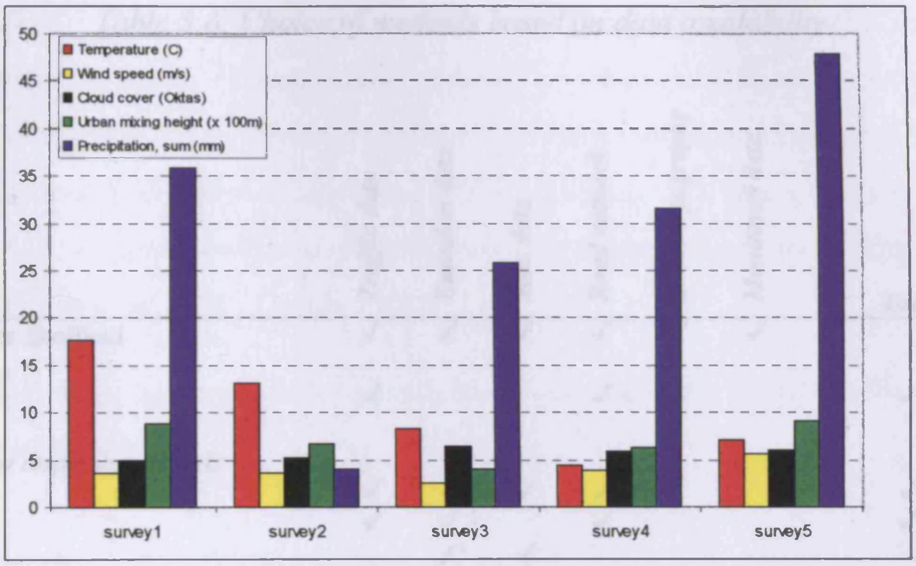

Figure 5.10: Averages of temperature, wind speed, cloud cover and urban mixing height plus the sum of the precipitation during the 5 surveys.

Wind directions over the 5 surveys are shown in *Appendix 5C*, in the form of wind roses. As this shows, during the first, second and the fifth survey period the predominant wind direction was from the west; during the third survey it was predominantly from the east. The fourth survey had a less clear wind pattern, with winds coming from both the east and the west.

5.5 SELECTION OF METHODS

As with the Greater London case study, the range of methods which could be applied in Sheffield was restricted by data availability. *Table 5.6* shows the data requirements for the methods initially considered for application in this research, and (see also *Table 3.4* in *Section 3.3*) and identifies those used in the Sheffield case study.

As this shows, the spatial accuracy of both the road data and the NO_2 monitoring data, and the measurement accuracy of traffic volumes, was considered sufficient in this case to calculate all the exposure indicators.

Table 5.6: Choice of methods based on data availability

	Traffic data	*Emission data*	*Met. data*	*Road network*	*Local topography*	*Monitored data*	*Used*
Available for Sheffield	✓	✓	✓	✓	✓	✓	
Indicators	✓			✓			✓
Air pollution dispersion models							
CALINE3	✓	✓	✓	✓			✓
DMRB	✓	✓		✓			✓
ISC3		✓[1]	✓				-
ADMS-Urban	✓	✓	✓	✓	✓		✓
Spatial Interpolation							
Kriging						✓[2]	-
Co-kriging	✓			✓		✓[2]	-
Regression model							
SAVIAH	✓			✓	✓		✓

[1] emssion data did not contain an emission inventory
[2] insufficient amount of monitoring sites

In *Chapter 4*, it was found that one of the possible reasons for the poor performance of CALINE3 and DMRB in the London study was the inaccuracy in the locations of the monitoring sites. The data in this case was of considerably higher quality than in Greater London. In order to provide a more rigorous test of these methods, therefore, both CALINE3 and DMRB were applied. In addition, since the London study a new dispersion model - ADMS-Urban – had become available (*Chapter 2*). This was therefore also included in this case study. No emission inventory was available for the Sheffield area, so the area-source dispersion model, ISC3, could not be used.

Despite the apparent large number of monitoring sites available in the Greater London case study, the performance of kriging and co-kriging on all sites was found to be poor (though better results were obtained for background sites). Suggested reasons were the large spatial variation in NO_2 concentrations, especially close to main roads, without any clear spatial dependency. In the Sheffield case study, only 28 monitoring sites were available. This was felt to be insufficient for kriging, and the methods were therefore not applied.

All the necessary data was available to use the SAVIAH-method. Using this method also had the advantage that it allowed a direct comparison with results from the similar analysis of links between chronic exposure to traffic-related air pollution and childhood respiratory illness in Huddersfield (Elliot and Briggs 1998). This study had shown that the SAVIAH-method gave a good prediction of NO_2 concentrations, often out-performing other methods (Briggs *et al.* 1997, Collins 1998a).

The selected methods were used to calculate exposure measures for all the 28 sites in the NO_2 monitoring survey.

5.6 RESULTS

5.6.1 Indicators

Six exposure indicators were calculated using the AMLs as described in *Section 3.2*:

- distance to the nearest main road (road1, as shown in *Section 2.1*)
- distance to nearest road (road2)
- density of main roads within 150 metres (road1)
- density of roads within 150 metres (road2)
- total traffic flow (vehicle metres) within 150 metres
- HGV flow (vehicle metres) within 150 metres

Figures 5.11, 5.12 and *5.13* show relationships between these indicators and monitored NO_2 at the sample sites. *Table 5.7* summarises Spearman and Pearson correlation coefficients for these variables. *Figure 5.11* shows the relationship with measured NO_2 concentration, using a log scale for distance; this both improves visualisation of the sampling points and also reflects the anticipated non-linear relationship between distance from road and measured concentration.

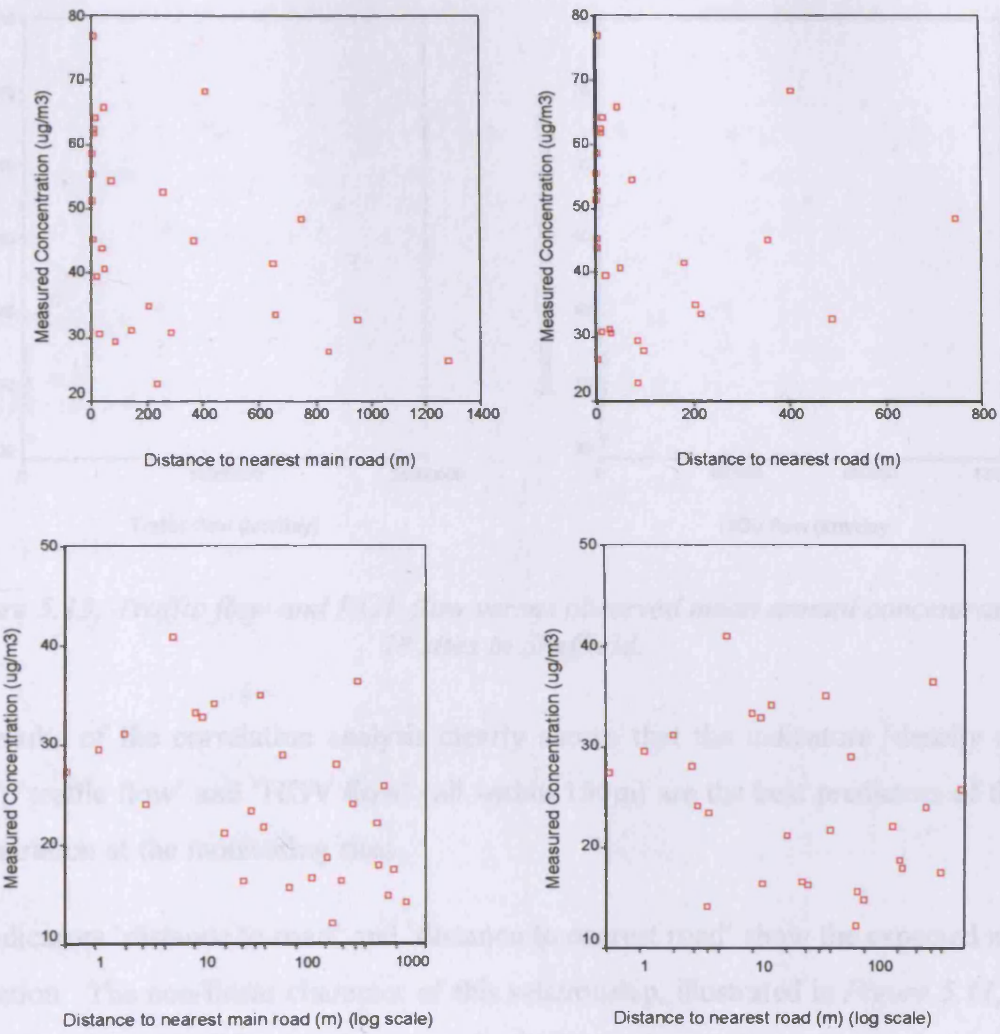

Figure 5.11: Distance to nearest main road and road versus observed mean annual concentration at 28 sites in Sheffield.

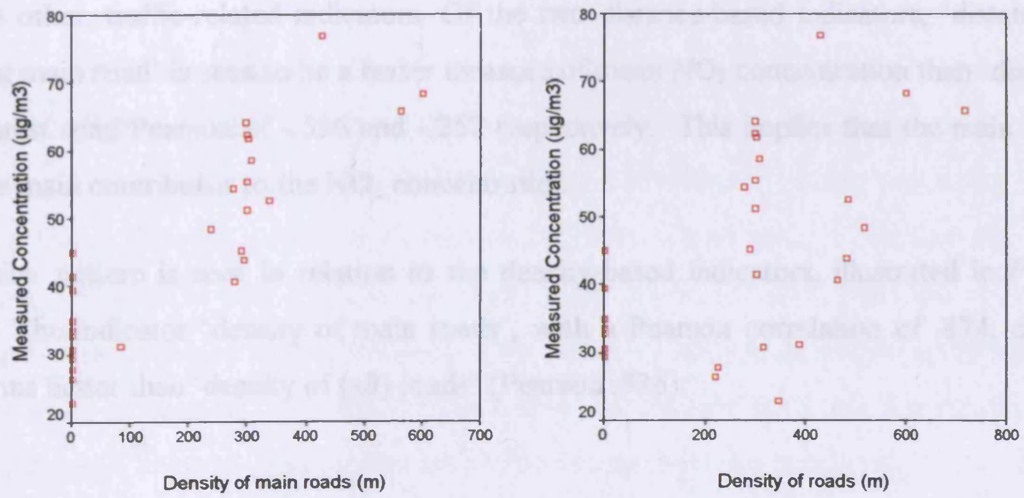

Figure 5.12: Density of main roads and roads within 150m versus observed mean annual concentration at 28 sites in Sheffield.

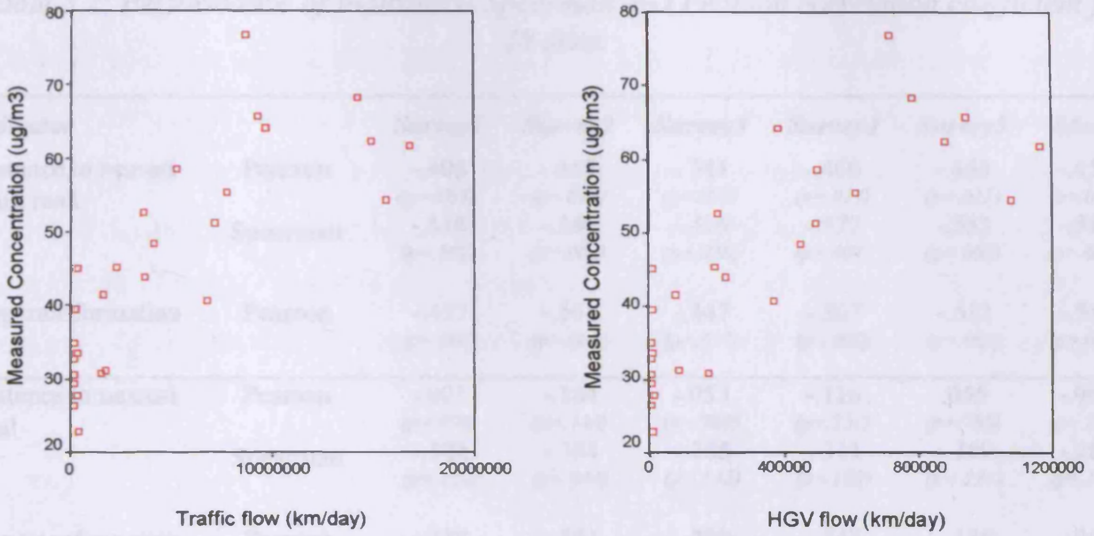

Figure 5.13: Traffic flow and HGV flow versus observed mean annual concentration at 28 sites in Sheffield.

The results of the correlation analysis clearly shows that the indicators 'density of main roads', 'traffic flow' and 'HGV flow' (all within 150m) are the best predictors of the NO_2 concentration at the monitoring sites.

The indicators 'distance to road' and 'distance to nearest road' show the expected negative correlation. The non-linear character of this relationship, illustrated in *Figure 5.11*, is also demonstrated by the difference between the Spearman's and Pearson correlations. Log-transformation of the data improves the Pearson correlation coefficient for all surveys and the mean, but the distance measures still show lower correlations with measured NO_2 than do the other, traffic-related indicators. Of the two distance-based indicators, 'distance to nearest main road' is seen to be a better measure of mean NO_2 concentration than 'distance to nearest road Pearson of -.556 and -.257 respectively. This implies that the main roads are the main contributor to the NO_2 concentration.

A similar pattern is seen in relation to the density-based indicators, illustrated in *Figure 5.12*. The indicator 'density of main roads', with a Pearson correlation of .874, clearly performs better than 'density of (all) roads' (Pearson .536).

Table 5.7: Performance of indicators: Spearman and Pearson correlation coefficient for 28 sites.

Indicator		***Survey1***	***Survey2***	***Survey3***	***Survey4***	***Survey5***	***Mean***
Distance to nearest main road	Pearson	-.405 (p=.033)	-.447 (p=.017)	-.341 (p=.076)	-.460 (p=.014)	-.455 (p=.015)	-.453 (p=.016)
	Spearman	-.516 (p=.005)	-.546 (p=.003)	-.416 (p=.028)	-.577 (p=.001)	-.553 (p=.002)	-.541 (p=.003)
Log transformation	Pearson	-.497 (p=.007)	-.564 (p=.002)	-.447 (p=.017)	-.567 (p=.002)	-.512 (p=.005)	-.556 (p=.002)
Distance to nearest road	Pearson	-.001 (p=.998)	-.184 (p=.348)	-.053 (p=.769)	-.116 (p=.558)	.055 (p=.780)	-.062 (p=.752)
	Spearman	-.301 (p=.120)	-.384 (p=.044)	-.285 (p=.142)	-.311 (p=.107)	-.199 (p=.331)	-.285 (p=.142)
Log transformation	Pearson	-.228 (p=.243)	-.351 (p=.067)	-.230 (p=.238)	-.247 (p=.206)	-.134 (p=.496)	-.257 (p=.187)
Density of main roads (within 150m)	Pearson	.876 (p=.000)	.815 (p=.000)	.715 (p=.000)	.822 (p=.000)	.820 (p=.000)	.874 (p=.000)
	Spearman	.865 (p=.000)	.816 (p=.000)	.741 (p=.000)	.836 (p=.000)	.777 (p=.000)	.875 (p=.000)
Density of roads (within 150m)	Pearson	.604 (p=.001)	.490 (p=.008)	.387 (p=.042)	.459 (p=.014)	.522 (p=.004)	.536 (p=.003)
	Spearman	.546 (p=.003)	.394 (p=.038)	.350 (p=.068)	.374 (p=.050)	.448 (p=.017)	.460 (p=.014)
Traffic flow (within 150m)	Pearson	.847 (p=.000)	.794 (p=.000)	.595 (p=.001)	.699 (p=.000)	.778 (p=.000)	.807 (p=.000)
	Spearman	.882 (p=.000)	.819 (p=.000)	.675 (p=.000)	.741 (p=.000)	.825 (p=.000)	.854 (p=.000)
HGV flow (within 150m)	Pearson	.858 (p=.000)	.794 (p=.000)	.560 (p=.002)	.741 (p=.000)	.825 (p=.000)	.820 (p=.000)
	Spearman	.878 (p=.000)	.805 (p=.000)	.648 (p=.000)	.750 (p=.000)	.847 (p=.000)	.852 (p=.000)

The two traffic flow indicators (***traffic flow within 150 metres*** and ***heavy goods vehicle flow within 150 m***) perform generally similarly (see also *Figure 5.13*); ***heavy goods vehicle flow***, however, tends to give slightly higher correlations with monitored NO_2 concentration, both for individual surveys and for the overall mean. The fact that these measures are slightly less strongly correlated with monitored NO_2 than the equivalent density measure (***density of main roads within 150 m***) is somewhat surprising; it suggests that inclusion of data on road traffic volume does not improve the predictive capability of the roads data. This may suggest that the traffic volume data are inaccurate.

For all the exposure indicators measured, the level of correlation varies to some extent between surveys. Highest correlations are found for survey 1, followed by surveys 5 and

2. The lowest correlation tends to occur for survey 3. One possible reason for this difference is shown by the monitoring data (see *Table 5.2*). As noted earlier, the at-site standard deviations for survey 3 (i.e. the variations between duplicate tubes) are considerably greater than for other surveys. The reasons for this are unknown. They may, however, suggest inaccuracies in the monitored data for this survey, for example due to a faulty batch of tubes, errors during laboratory analysis or problems during storage and transport. Other possible reasons for the between-survey differences in the correlations are explored in *Chapter 6*.

5.6.2 CALINE3

CALINE3 was used to estimate NO_2 concentrations at the 28 monitoring sites. The model was run for each of the 5 different survey periods. An emission factor of 4.0 grams mile^{-1} (2.4 g km^{-1}) was used (see also *Section 3.3.2.2*). Links within the 200-metre buffer of a site were selected from the *roads2* coverage of Sheffield. This resulted in six of the 28 monitoring sites not being included in this analysis, for these were background sites which were more than 200-metres from any road in the *roads2* coverage.

Figure 5.14 shows the relationship between the CALINE3 estimates and the monitored NO_2 concentrations, and *Table 5.8* summarises the Pearson and Spearman correlation coefficients.

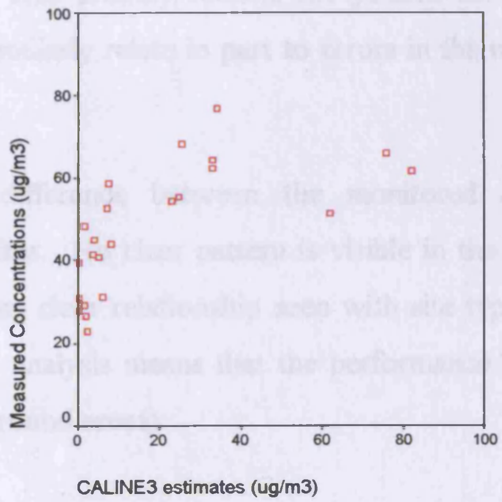

Figure 5.14: Average of CALINE3 estimates over the 5 surveys versus observed annual concentration at 22 sites in Sheffield.

Table 5.8: Performance of the CALINE3 estimates: Pearson and Spearman Correlation Coefficient.

	Survey1	Survey2	Survey3	Survey4	Survey5	Mean
CALINE3						
Pearson	.718	.693	.291	.646	.694	.657
	(p=.000)	(p=.000)	(p=.178)	(p=.001)	(p=.000)	(p=.001)
Spearman	.758	.804	.668	.738	.685	.832
	(p=.000)	(p=.000)	(p=.000)	(p=.000)	(p=.000)	(p=.000)

The standard error of estimate (from the Pearson correlation) was 11.76 μg m^{-3} for the average of the 5 surveys. Spearman correlation coefficients tend to be slightly higher than Pearson coefficients, implying some degree of non-linearity in the data. This is also seen in *Figure 5.14*, where the scattergram is clearly curved. A steep curve is noticeable in the monitored NO_2 concentration range from 20 to approximately 50 μg m^{-3}, after which the curve seems to flatten in the range from 50 to 80 μg m^{-3}. Also noticeable is that CALINE3 tends to underestimate at the majority of sites, except for two kerbside sites (no. 1 and 24) and one intermediate sites (no. 23). Overestimation for these three sites was consistent throughout the 5 surveys. The analysis for these sites was rechecked and found to be correct. The sites was therefore investigated in more detail, but no reason for the overestimation could be found.

The results are reasonably consistent for all surveys, except for survey 3: while surveys 1, 2, 4 and 5 have Pearson correlation coefficients between .646 and .718, for survey 3 the coefficient is only .291. This broadly reflects the pattern for the exposure indicators, outlined above, and may similarly relate in part to errors in the monitored data for survey 3.

Figure 5.15 maps the difference between the monitored and the modelled NO_2 concentrations at the 28 sites. No clear pattern is visible in the distribution of over- and under-estimates. Nor is any clear relationship seen with site type (though the loss of six background sites from the analysis means that the performance of the method cannot be reliably assessed for background areas).

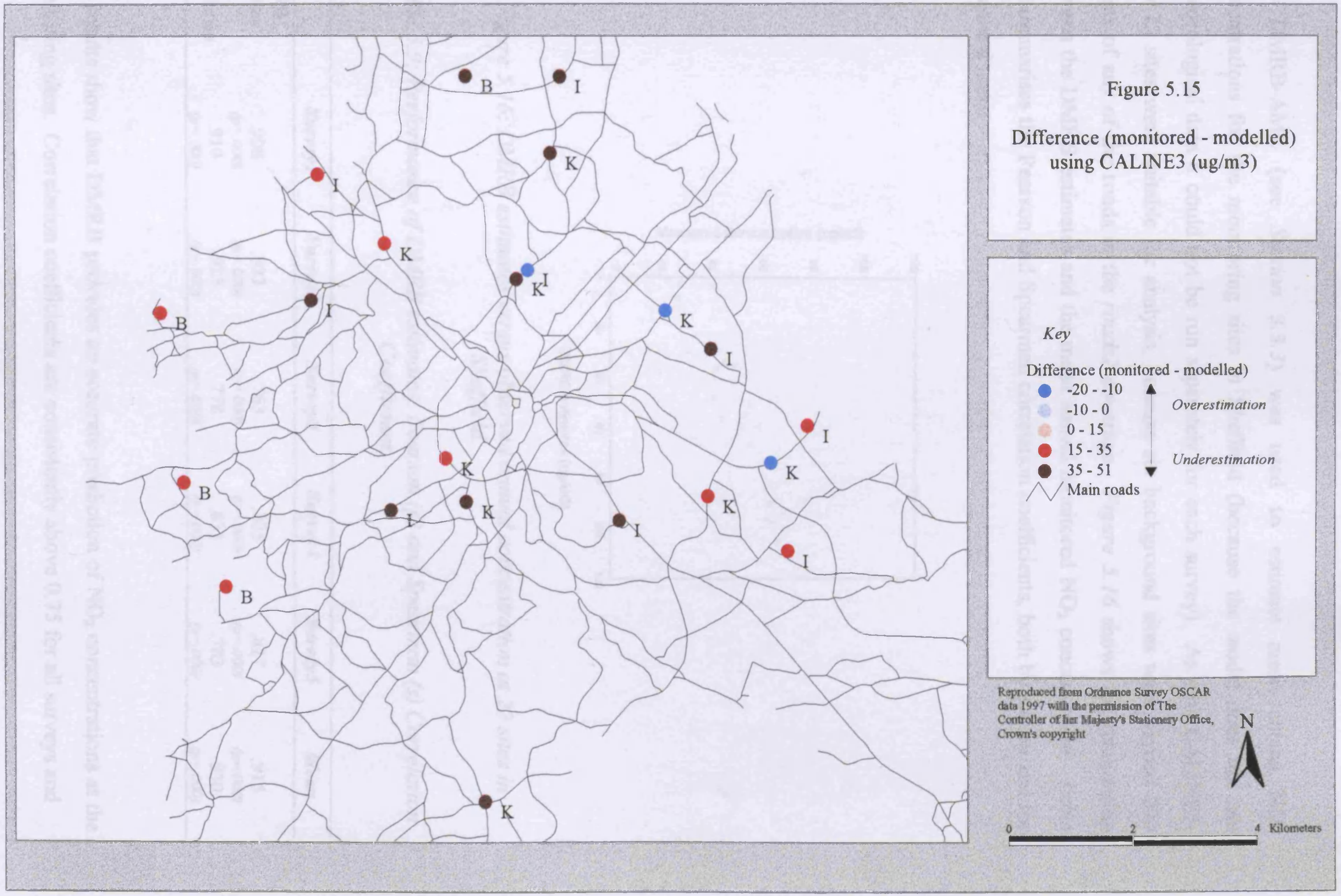
Figure 5.15
Difference (monitored - modelled) using CALINE3 (ug/m3)
Key
Difference (monitored - modelled)
-20 - -10
-10 - 0
0 - 15
15 - 35
35 - 51
Main roads
Overestimation
Underestimation
Reproduced from Ordnance Survey OSCAR data 1997 with the permission of The Controller of her Majesty's Stationery Office, Crown's copyright
N
0
2
4 Kilometers

5.6.3 DMRB

The DMRB-AML (see *Section 3.3.3*) was used to estimate mean annual NO_2 concentrations for the monitoring sites in Sheffield (because the model does not use meteorological data it could not be run separately for each survey). As with CALINE3, only 22 sites were suitable for analysis, because six background sites were beyond 200 metres of any of the roads in the *roads2* coverage. *Figure 5.16* shows the relationship between the DMRB estimates and the mean annual monitored NO_2 concentration. *Table 5.9* summarises the Pearson and Spearman correlation coefficients, both by survey and for the annual mean.

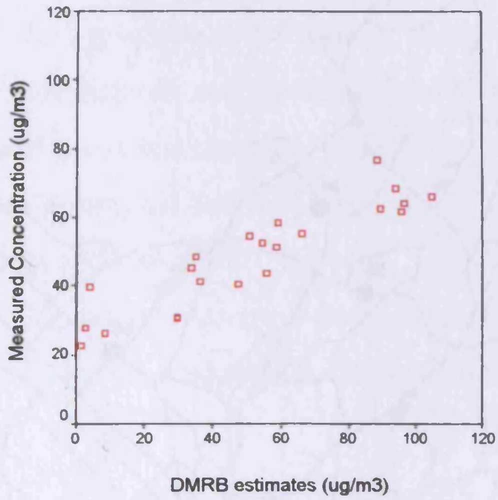

Figure 5.16: DMRB estimates versus observed annual concentration at 22 sites in Sheffield.

Table 5.9: Performance of DMRB estimates: Pearson (p) and Spearman (s) Correlation Coefficient.

	Survey1	***Survey2***	***Survey3***	***Survey4***	***Survey5***	***Mean***
DMRB						
Pearson	.908 *(p=.000)*	.922 *(p=.000)*	.763 *(p=.000)*	.805 *(p=.000)*	.817 *(p=.000)*	.915 *(p=.000)*
Spearman	.910 *(p=.000)*	.923 *(p=.000)*	.778 *(p=.000)*	.831 *(p=.000)*	.783 *(p=.000)*	.930 *(p=.000)*

The results show that DMRB provides an accurate prediction of NO_2 concentrations at the monitoring sites. Correlation coefficients are consistently above 0.75 for all surveys and

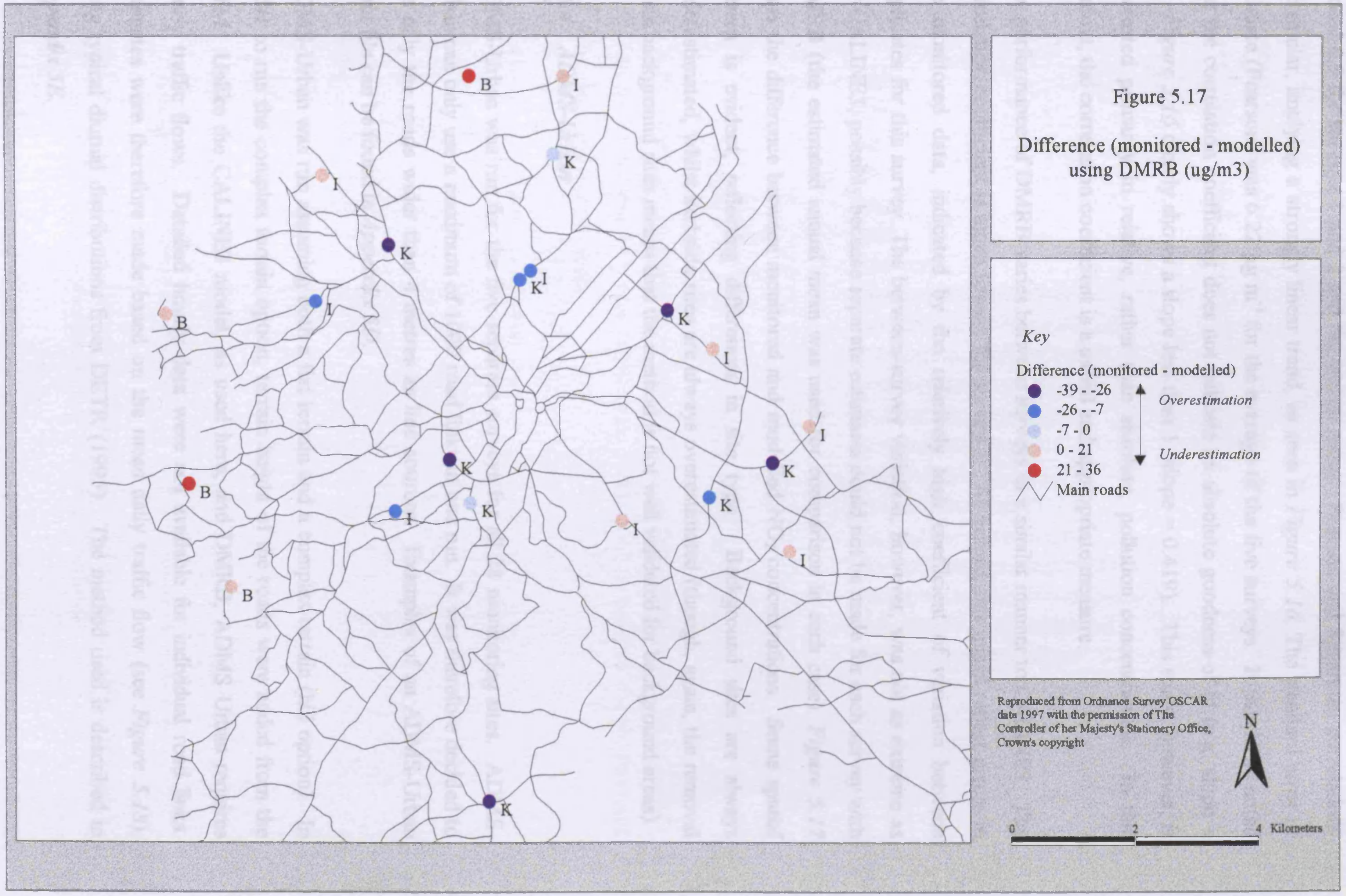

Figure 5.17

Difference (monitored - modelled) using DMRB (ug/m3) exceed 0.9 for surveys 1 and 2 and the annual mean. Pearson and Spearman correlations are similar, implying a strongly linear trend, as seen in *Figure 5.16*. The standard error of estimate (Pearson) was 6.22 μg m^{-3} for the average of the five surveys. It should be noted that the correlation coefficient does not indicate an absolute goodness-of fit (e.g. slope = 1). *Figure 5.16* clearly shows a slope less than 1 (slope = 0.419). This study, however, is interested primarily in relative, rather than absolute, pollution concentrations. In this context, the correlation coefficient is a useful and appropriate measure.

The performance of DMRB varies between surveys in a similar manner to CALINE3. The correlation coefficient is again lowest for survey 3. As before, this might reflect errors in the monitored data, indicated by the relatively high coefficient of variation between duplicates for this survey. The between-survey variation, however, was not as extreme as for CALINE3, possibly because separate estimates could not be made for each survey with DMRB (the estimated annual mean was used for comparison in each case). *Figure 5.17* maps the difference between monitored and modelled NO_2 concentrations. Some spatial pattern is evident, reflecting differences in site type. Background sites are always underestimated, whilst kerbside sites are always overestimated (though, again, the removal of six background sites means that the method is not well validated for background areas).

5.6.4 ADMS-Urban

ADMS-Urban was run for the five separate surveys for all 28 monitoring sites. ADMS-Urban can only use a maximum of 1000 road links in one run. It was therefore decided to use only the roads wider than 4 metres as line sources. Examples of an ADMS-Urban input file can be found in *Appendix 5D*.

ADMS-Urban was run assuming both a flat terrain and a complex terrain (hill option). In order to run the complex terrain option, terrain height of the roads were added from the DTM. Unlike the CALINE3 model, as used here, and DMRB, ADMS Urban requires hourly traffic flows. Detailed hourly data were not available for individual road links. Estimates were therefore made based on the mean daily traffic flow (see *Figure 5.18*), using typical diurnal distributions from DETR (1995). The method used is described in *Appendix 5E*.

ADMS-Urban can be applied using different meteorological variables (i.e. on the basis of the Monin-Obukhov length, cloud cover or the surface sensible heat flux). Due to limitations in the availability of meteorological data from the Meteorological Office for this study area, only the cloud cover method was used in this study.

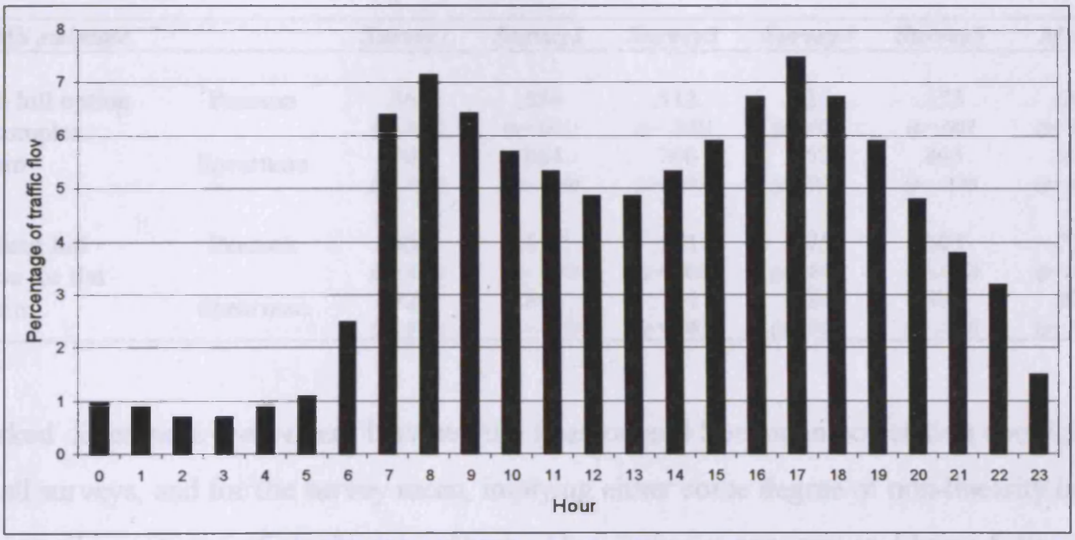

Figure 5.18: Distribution of traffic flow in percentage.

Figure 5.19 shows the relationship between the mean estimates derived from ADMS-Urban and the monitored NO_2 concentrations. *Table 5.10* summarises the Pearson and Spearman correlation coefficients.

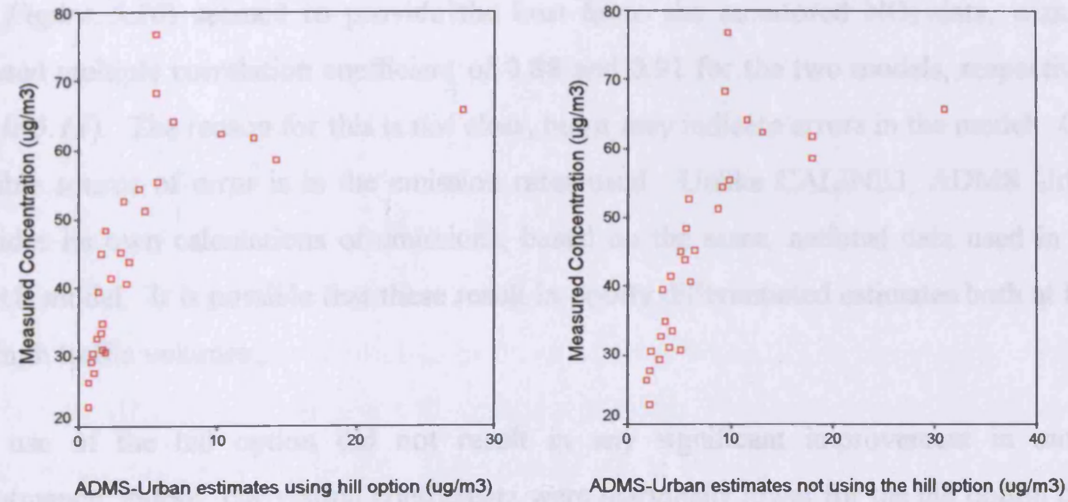

Figure 5.19: ADMS-Urban estimates with and without the hill option versus observed annual concentration at 28 sites in Sheffield.

The standard error of estimate (Pearson) was 11.45 μg m^{-3} for ADMS with the hill option and 10.23 μg m^{-3} for flat terrain.

Table 5.10 Performance of ADMS-urban with (+) and without (-) the hill option: Pearson and Spearman Correlation Coefficients.

ADMS estimate		Survey1	Survey2	Survey3	Survey4	Survey5	Mean
With hill option for complex terrain	Pearson	.561 *(p=.002)*	.584 *(p=.001)*	.512 *(p=.005)*	.735 *(p=.000)*	.555 *(p=.002*	.646 *(p=.000)*
	Spearman	.902 *(p=.000)*	.864 *(p=.000)*	.766 *(p=.000)*	.852 *(p=.000)*	.845 *(p=.000)*	.906 *(p=.000)*
Without hill option for flat terrain	Pearson	.557 *(p=.002)*	.657 *(p=.000)*	.571 *(p=.002)*	.775 *(p=.000)*	.605 *(p=.000)*	.731 *(p=.000)*
	Spearman	.929 *(p=.000)*	.864 *(p=.000)*	.744 *(p=.000)*	.828 *(p=.000)*	.888 *(p=.000)*	.928 *(p=.000)*

Marked differences are evident between the Pearson and Spearman correlation coefficients for all surveys, and for the survey mean, implying either some degree of non-linearity in the data, or the presence of significant outliers. One outlier is apparent in *Figure 5.19*. This relates to site 24, a kerbside site. The analysis for this site was rechecked and found to be correct. The site was therefore investigated in more detail, but no reason for the discrepancy could be found.

Possible non-linearity in the relationship was investigated by reanalysis of the data using curve-fitting methods in SPSS, for both the hill option and flat terrain results. An S-curve (see *Figure 5.20*) seemed to provide the best fit to the monitored NO_2 data, with an adjusted multiple correlation coefficient of 0.88 and 0.91 for the two models, respectively (*Table 5.11*). The reason for this is not clear, but it may indicate errors in the model. One possible source of error is in the emission rates used. Unlike CALINE3, ADMS Urban provides its own calculations of emissions, based on the same, national data used in the DMRB model. It is possible that these result in poorly differentiated estimates both at low and high traffic volumes.

The use of the hill option did not result in any significant improvement in model performance: indeed, correlation coefficients were marginally lower for the hill option than for flat terrain. This suggests that the version of the model available at the time of this study does not provide a fully realistic simulation of dispersion in complex terrain.

Table 5.11: Correlation coefficients and standard error of the two S-curves.

	ADMS with hill option	ADMS without hill option
Multiple R	.883	.891
R square	.780	.794
Adjusted square	.771	.786
Standard error	.159	.154

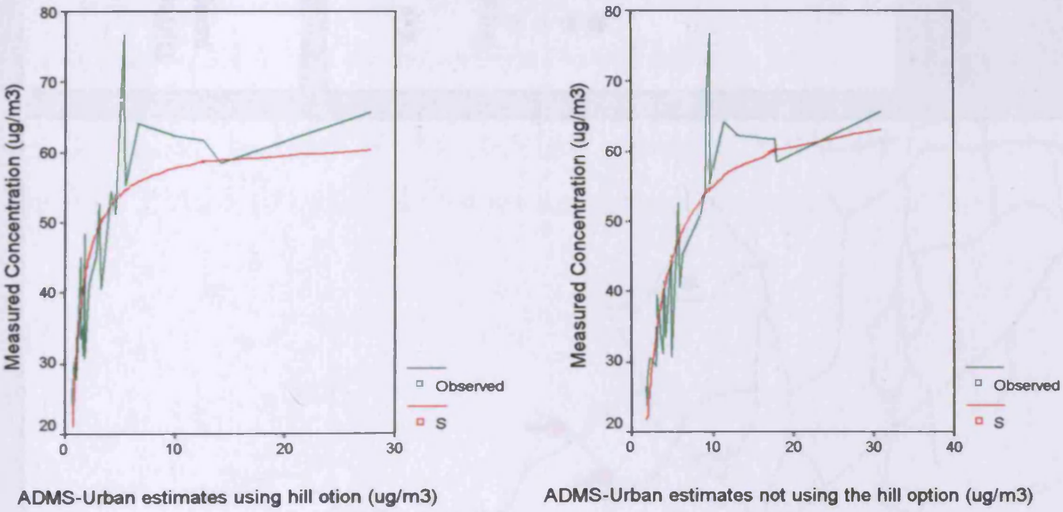

Figure 5.20: S-curves of ADMS-Urban estimates versus observed annual NO_2 concentrations

Another striking observation is the level of underestimation of ADMS-Urban (see *Figure 5.21*): the mean modelled NO_2 concentration from ADMS for the 28 monitoring sites was 4.6 μg m^{-3} (complex terrain) and 7.5 μg m^{-3} (flat terrain); the mean monitored concentration was 45.5 μg m^{-3}. Thus, the model is under-estimating monitored concentrations by about a factor of 0.10-0.16. As *Figure 5.21* shows, the underestimation is greatest at kerbside sites, whilst background sites tend to be equally over- and underestimated. Underestimation also tends to increase towards the city centre. Similar results have recently been obtained in applying ADMS-Urban in Northampton (Gulliver, pers. comm., Briggs *et al.* 1998). The reasons are at present unknown, but appear to relate either to the emissions rates generated by the model, or to the way in which the model simulates dispersion, especially in the near-source zone.

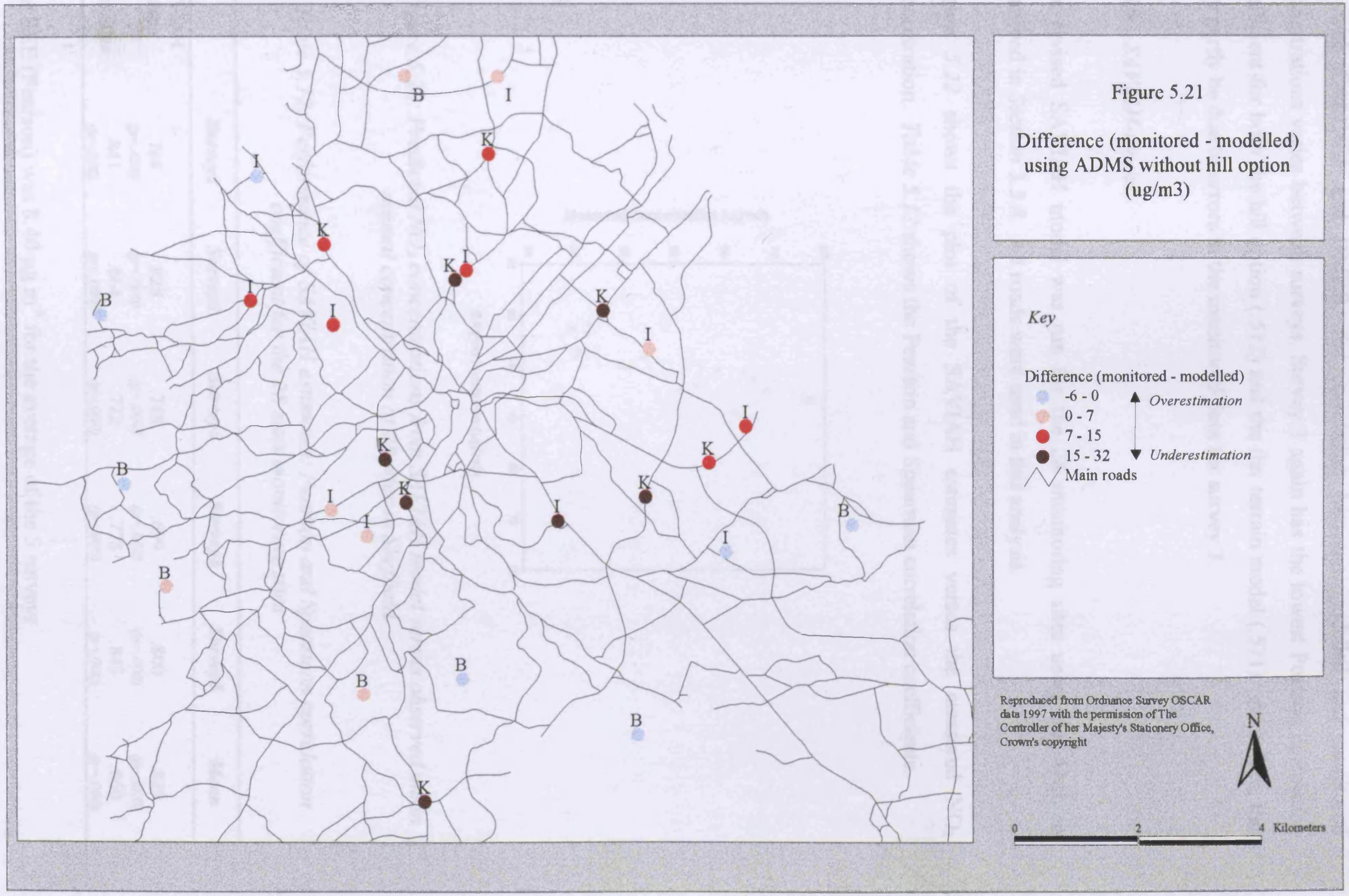

Figure 5.21

Difference (monitored - modelled) using ADMS without hill option (ug/m3)

As with CALINE3 and DMRB, the correlation between modelled and monitored concentrations varies between surveys. Survey 3 again has the lowest Pearson correlation coefficient for both the hill option (.512) and the flat terrain model (.571). As before, this may partly be due to errors in the monitored data for survey 3.

5.6.5 SAVIAH-model

The revised SAVIAH model was run for the 28 monitoring sites using the AML as described in *Section 3.3.8*. All roads were used in this analysis.

Figure 5.22 shows the plot of the SAVIAH estimates versus the measured NO_2 concentration. *Table 5.12* shows the Pearson and Spearman correlation coefficients.

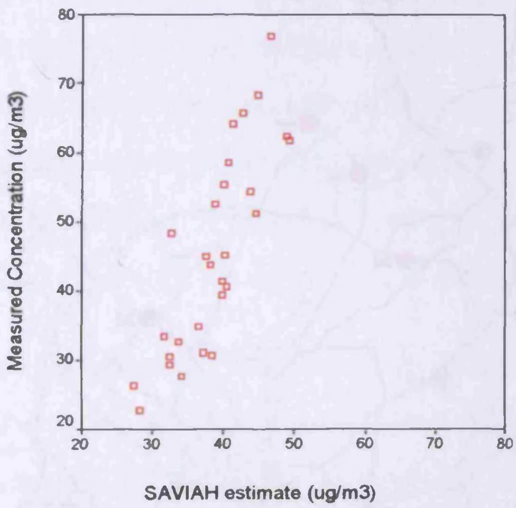

Figure 5.22: Predicted NO_2 concentrations from SAVIAH model versus observed mean annual concentration at 28 sites in Sheffield.

Table 5.12: Performance of SAVIAH estimates: Pearson and Spearman correlation coefficient for the 28 sites monitoring sites

	Survey1	***Survey2***	***Survey3***	***Survey4***	***Survey5***	***Mean***
SAVIAH						
Pearson	.784 *(p=.000)*	.825 *(p=.000)*	.718 *(p=.000)*	.699 *(p=.000)*	.800 *(p=.000)*	.829 *(p=.000)*
Spearman	.841 *(p=.000)*	.864 *(p=.000)*	.722 *(p=.000)*	.778 *(p=.000)*	.843 *(p=.000)*	.860 *(p=.000)*

The SEE (Pearson) was 8.40 $\mu g\ m^{-3}$ for the average of the 5 surveys

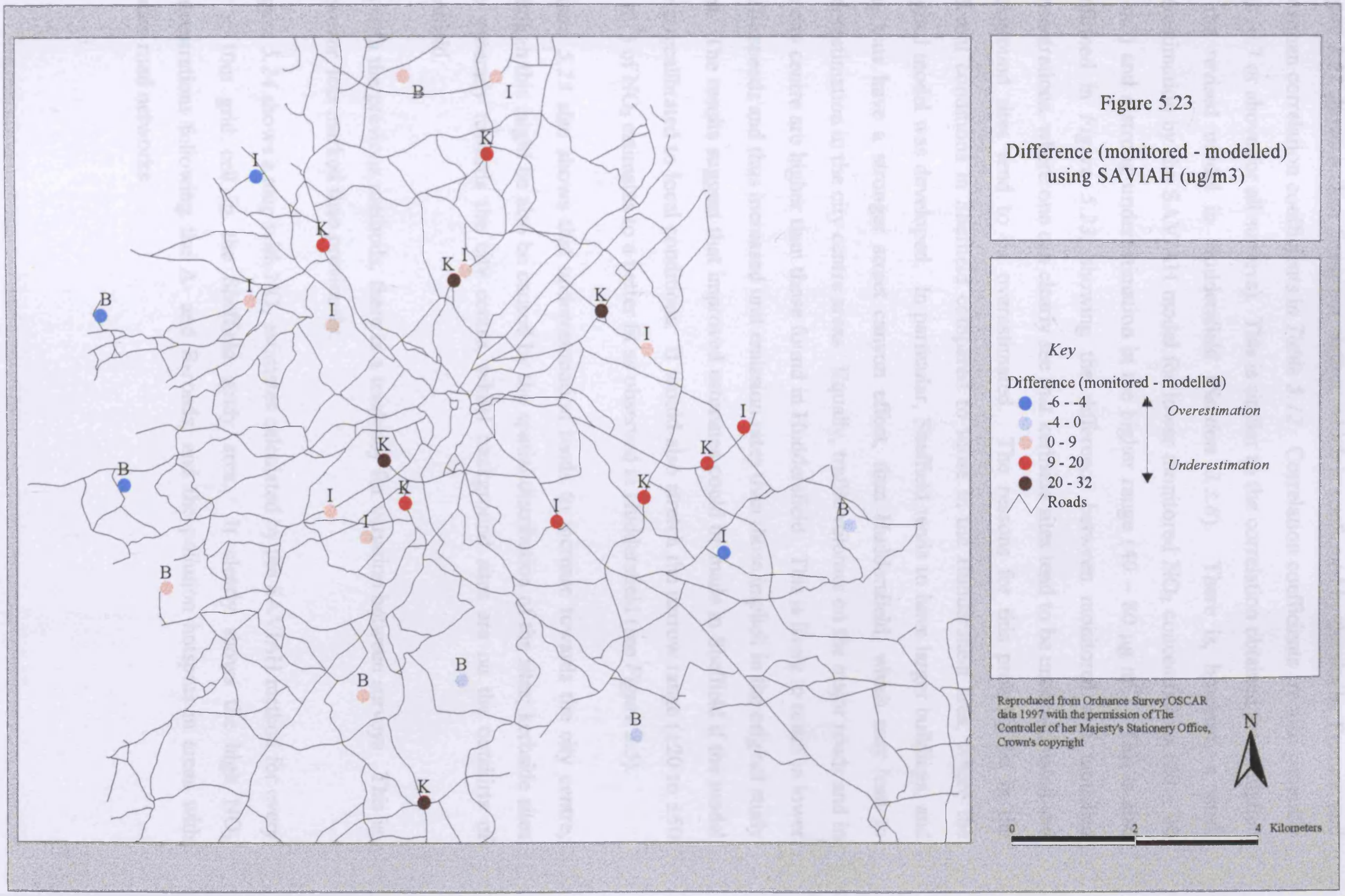

Figure 5.23

Difference (monitored - modelled) using SAVIAH (ug/m3)

Figure 5.22 shows a clear linear correlation, which is confirmed by the similar Pearson and Spearman correlation coefficients in *Table 5.12*. Correlation coefficients are also generally high (0.7 or above for all surveys). This is similar to the correlation obtained for validation of the revised model in Huddersfield (*Section 3.3.8*). There is, however, a small overestimation by the SAVIAH model for lower monitored NO_2 concentrations (20 – 30 $\mu g\ m^{-3}$) and a strong underestimation in the higher range (40 – 80 $\mu g\ m^{-3}$). This is also confirmed in *Figure 5.23*, showing the difference between monitored and modelled concentrations, where one can clearly see that kerbside sites tend to be underestimated and background sites tend to be overestimated. The reasons for this probably lie in the different conditions in Sheffield compared to those in the Huddersfield area, where the original model was developed. In particular, Sheffield tends to have larger buildings, and may thus have a stronger street canyon effect, than Huddersfield, which may lead to underestimation in the city centre areas. Equally, traffic volumes on the major roads and in the city centre are higher than those found in Huddersfield. This is likely to result in lower traffic speeds and thus increased unit emission rates than those implicit in the original study area. The results suggest that improved estimates could be made in Sheffield if the model were recalibrated to local conditions. It would also stretch the narrow range (±20 to ±50 $\mu g\ m^{-3}$) of NO_2 estimates to a better fit as observed in Huddersfield (see *Figure 3.5*).

Figure 5.23 also shows that underestimation tends to increase towards the city centre, although this might be also be caused by the spatial distribution of the sites; kerbside sites are generally towards the city centre, whilst background sites are on the outskirts of Sheffield.

As with the previous methods, there is a tendency for variation between surveys. This is, however, less marked than previously.

Figure 5.24 shows a map with NO_2 estimates calculated by the SAVIAH method for every 10 x 10m grid cell in the Sheffield study area. It clearly shows the high NO_2 concentrations following the A- and B-roads, and the pollution hotspots in areas with denser road networks.

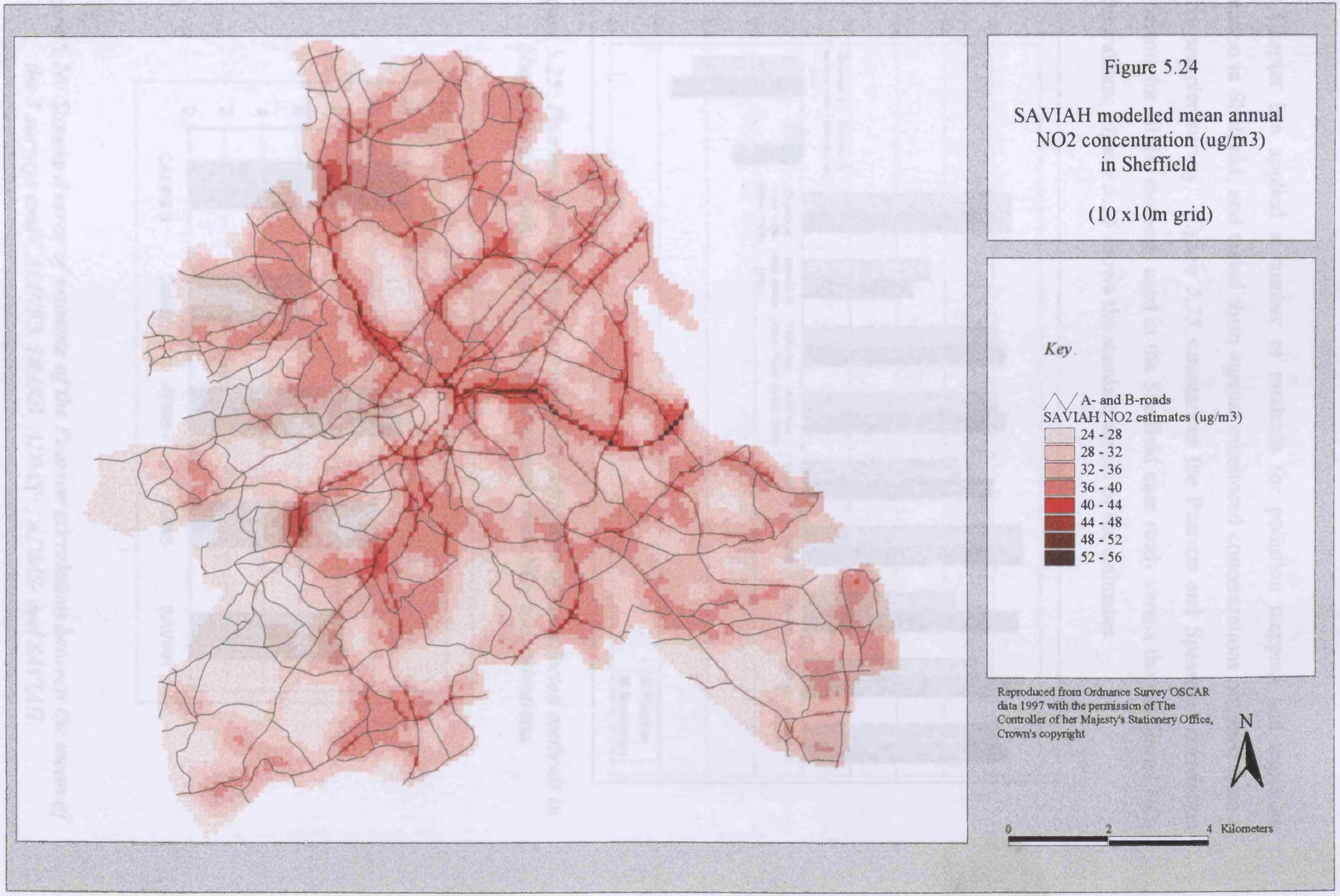

Figure 5.24

SAVIAH modelled mean annual NO_2 concentration (ug/m3) in Sheffield

(10 x10m grid)

5.7 SUMMARY

This Chapter has applied a number of methods for pollution mapping and exposure estimation in Sheffield, and tested them against monitored concentrations obtained from a passive sampler survey. *Figure 5.25* summarises the Pearson and Spearman correlation coefficients for all the methods used in the Sheffield case study versus the monitored NO_2 concentrations; *Figure 5.26* shows the standard errors of the estimates.

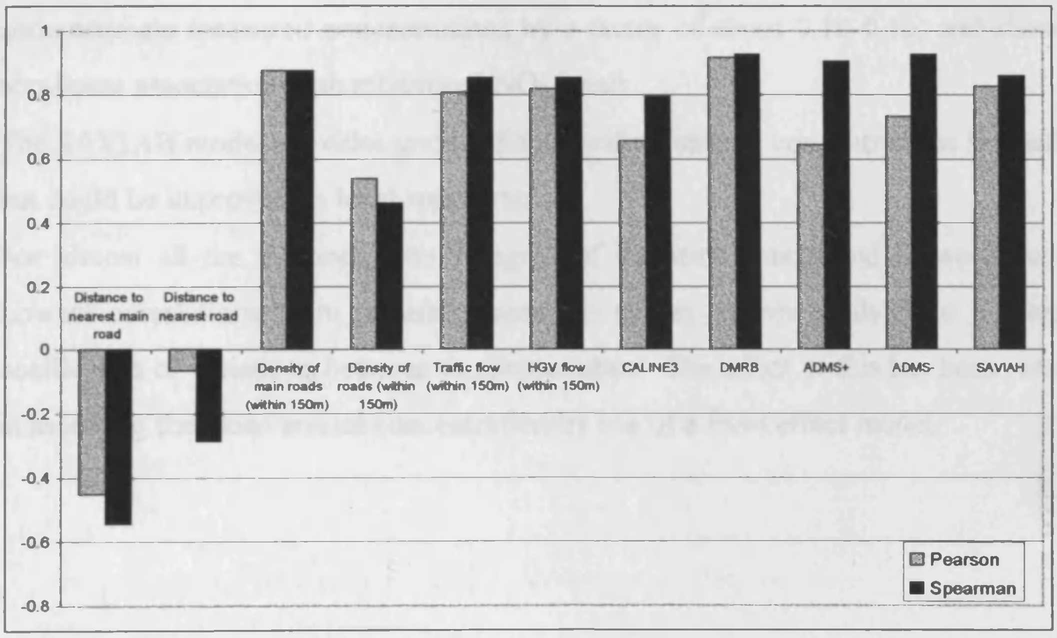

Figure 5.25: Pearson and Spearman correlation coefficients of the selected methods in Sheffield case study, versus monitored annual mean NO_2 concentrations.

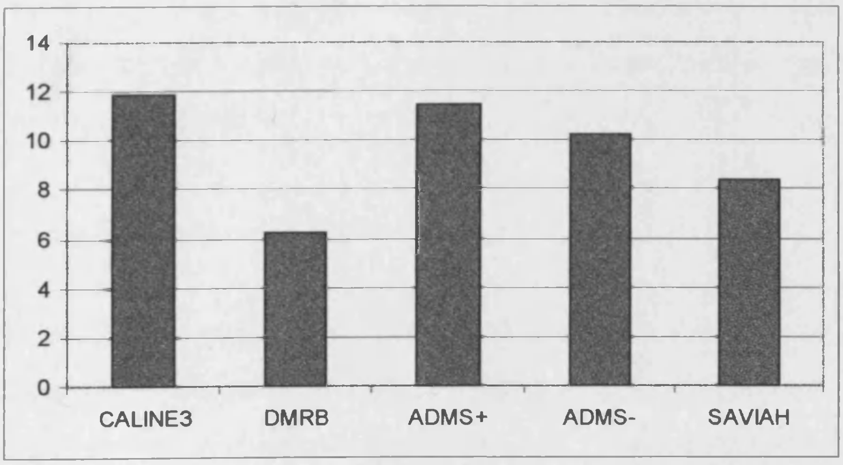

Figure 5.26: Standard error of estimate of the Pearson correlation between the mean of the 5 surveys and CALINE3, DMRB, ADMS+, ADMS- and SAVIAH.

Results may be summarised as follows:

- The indicators 'density of main roads', 'traffic flow' and 'HGV flow' (all within 150m), the air pollution dispersion model, DMRB and the regression model, SAVIAH, clearly are the best predictors of the NO_2 concentration at the monitoring sites.
- The indicators work better when using main roads. This confirms that main roads, which are mostly also the busy roads, have the largest impact on the NO_2 concentration
- CALINE3 and ADMS-Urban had similar performances. ADMS-Urban tends to underestimate measured concentrations by a factor of about 0.10-0.16, and showed a non-linear association with monitored NO_2 levels.
- The SAVIAH model provides good estimates of monitored concentrations in Sheffield, but could be improved by local recalibration.
- For almost all the methods, some degree of variation was found between surveys. Lowest correlations were generally seen for survey 3, which also had the highest coefficients of variations between duplicate tubes. The effect of this has been removed in assessing the mean annual concentration by use of a fixed effect model.

6 COMPARISON AND EVALUATION

6.1 INTRODUCTION

The previous two chapters have applied a range of methods to assess and map air pollution and exposure in Greater London and Sheffield, with varying results. The aim of this chapter is to review and evaluate the results in order to:

- compare the performance of the various methods;
- identify the most effective methods;
- investigate factors which determine the performance of the different methods; and
- assess the implications for the use of the methods for exposure and air pollution assessment.

6.2 COMPARATIVE PERFORMANCE OF EXPOSURE MEASURES

Six indicators and five modelling methods have been applied in the London and Sheffield case studies. The performance of the various methods can be evaluated by comparing the results with monitored NO_2 data. The results of the methods are summarised as Pearson correlation coefficients (by survey) in *Table 6.1* and through multiple regression analysis (for the survey mean) in *Table 6.2*.

6.2.1 Reliability of monitored NO_2 data

Before examining these results, it is important to assess the reliability of the monitored NO_2 concentrations, which were used as reference data for this analysis. These NO_2 concentrations were derived from passive samplers. As mentioned previously, a number of studies have cast doubt on the accuracy of these samplers - e.g. due to effects of chemical interference (Heal and Cape 1997) and wind speed and turbulence (Gair and Penkett 1995).

Table 6.1: Summary of Pearson (r) correlation coefficients in both Greater London and Sheffield for the different methods.

Methods	London			Sheffield					
	1993	*1994*	*1995*	*Survey1*	*Survey2*	*Survey3*	*Survey4*	*Survey5*	*Mean*
Indicators									
Distance main road				-0.405	-0.447	-0.341	-0.460	-0.455	-0.453
Distance road				-0.001	-0.184	-0.053	-0.116	0.055	-.0.062
Density main road				0.876	0.815	0.715	0.822	0.82	0.873
Density roads				0.604	0.490	0.387	0.459	0.522	0.536
Traffic volume				0.847	0.794	0.595	0.699	0.778	0.807
HGV volume				0.858	0.794	0.56	0.741	0.825	0.820
Dispersion models									
CALINE3	0.325			0.718	0.693	0.291	0.646	0.694	0.657
DMRB	0.277	0.281	0.233	0.908	0.922	0.763	0.805	0.817	0.915
ISC3	0.343	0.330	0.274						
ADMS+				0.561	0.584	0.512	0.735	0.555	0.646
ADMS-				0.557	0.657	0.571	0.775	0.605	0.731
Geostatistical									
Kriging									
All sites	-	0.449	0.429						
Background sites	0.573	0.710	0.684						
Cokriging									
Background sites	0.585	0.703	0.675						
SAVIAH				0.784	0.825	0.718	0.699	0.800	0.829

Table 6.2: Summary of Statistics for Greater London and Sheffield

Methods	*Location*	*R2*	*Constant*	*Slope*	*SEE*
Indicators					
Distance main road	Sheffield	.206			
Distance road	Sheffield	.004			
Density main road	Sheffield	.548			
Density roads	Sheffield	.145			
Traffic volume	Sheffield	.651			
HGV volume	Sheffield	.672			
Dispersion models					
CALINE3	London 93	.106	21.53	.172	5.02
	Sheffield	.417	40.80	.393	11.76
DMRB	London 93	.077	20.05	.069	5.3
	London 94	.079	21.66	.093	6.42
	London 95	.054	21.20	.082	7.19
	Sheffield	.837	26.89	.419	6.22
ISC3	London 93	.117	17.39	.096	5.05
	London 94	.109	20.09	.086	6.11
	London 95	.075	19.22	.076	6.60
ADMS+	Sheffield	.418	37.90	1.67	11.45
ADMS-	Sheffield	.535	32.79	1.70	10.23
Geostatistical					
Kriging					
All sites	London 94	.202	6.74	.704	5.83
	London 95	.184	9.43	.575	6.56
Background sites	London 93	.329	2.06	.873	2.89
	London 94	.504	.346	.967	2.91
	London 95	.468	.198	.978	3.08
Cokriging					
Background sites	London 93	.324	.953	.935	2.86
	London 94	.495	-.422	1.01	2.93
	London 95	.455	-.670	1.03	3.12
SAVIAH	Sheffield	.687	-33.07	2.13	8.40

Despite this, diffusion tubes are widely used, and various studies have shown that they provide consistent results, under a wide range of conditions (van Reeuwijk *et al.* 1998). Typically, coefficients of correlation (CVs) of 5-8% are found using duplicate tubes. Generally, NO_2 diffusion tubes also show consistent relationships with NO_2 monitored by other methods, such as automatic monitoring stations. It was possible in this study to test reliability of samplers further by examination of CVs from duplicates in Sheffield, and by comparison of the results between samplers and continuous monitors in Sheffield and London.

No duplicates were available for London sites, but CVs from Sheffield duplicates were generally 5-10% (see *Table 6.3*), similar to those reported elsewhere. There was therefore no reason to believe that the results from the NO_2 diffusion tubes in Sheffield were unreliable. The main exception were results from survey 3 in Sheffield. Possible explanations for this are considered in more detail below.

Table 6.3: Descriptive statistics for CV's of duplicates for the 5 surveys

CV	*Survey 1*	*Survey 2*	*Survey 3*	*Survey 4*	*Survey 5*	*Mean*
Mean	9.21	5.89	12.54	7.65	5.98	8.20
Standard Deviation	9.07	4.59	9.99	5.58	4.43	7.31
Confidence Level(95.0%)	4.83	1.94	4.03	2.30	1.75	1.33

Continuous monitoring NO_2 data in the Sheffield area were available for the Ladybower site, where NETCEN also run sampling tubes. This is a background rural site about 15 km west of Sheffield, in the Peak District. Figure 6.1 compares mean NO_2 concentrations of the background, intermediate and kerbside sites in the Sheffield study with Ladybower, Sheffield Centre and Sheffield Tinsley AUN sites. Results show a generally good correlation, though NO_2 concentrations measured by tubes tend to overestimate by 20-30%, compared to continuous monitored NO_2 data. This overestimation is confirmed when comparing average NO_2 concentrations during surveys 2 to 5 measured at Sheffield City Centre with NO_2 diffusion tubes, against NO_2 measured at the Sheffield City Centre AUN site during the same period (see *Table 6.4*).

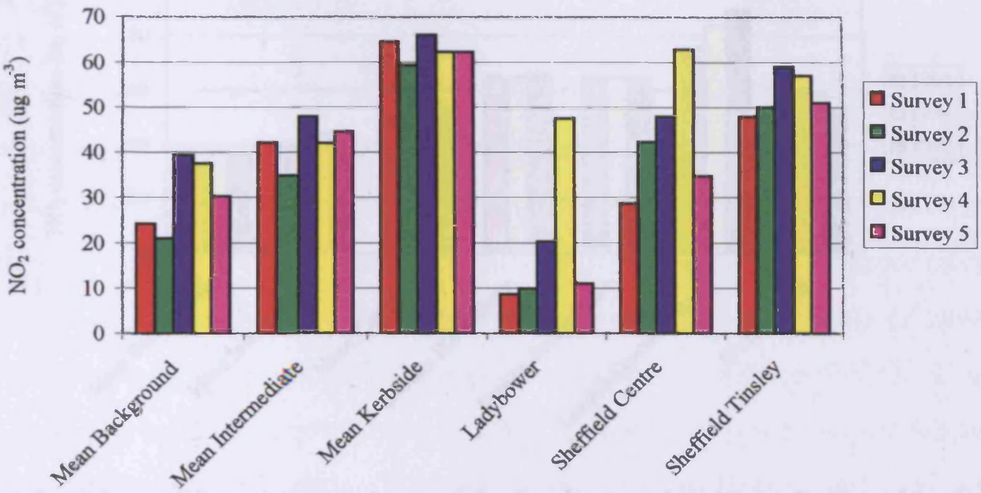

Figure 6.1: Mean NO_2 concentrations of the background, intermediate and kerbside monitoring sites compared with Ladybower, Sheffield Centre and Sheffield Tinsley AUN sites over the 5 monitoring periods.

Table 6.4: Continuous versus tube NO_2 annual mean (average over the Survey 2 to 5) results at Sheffield City Centre ($\mu g\ m^{-3}$)

	Continuous	Passive (Tube)	Overestimation
Sheffield City Centre	47	61	30%

Similarly, in London, it was possible to compare NO_2 concentrations from tubes with measured concentrations from nearby continuous sites, as part of NETCEN network. Again, *Figure 6.2* suggests a reasonable level of correlation, although NO_2 concentrations measured with diffusion tubes are under-estimates, in contrast with the over-estimation found in Sheffield. The discrepancy between London and Sheffield may be a 'laboratory effect'. Experience in London, for example, has shown that significant between-laboratory differences may occur in the absolute concentrations obtained by diffusion tubes (S. Beavers, South East Institute for Public Health, *pers. comm.*). The tubes from London used in this research were analysed through NETCEN as part of the national network; those in Sheffield were analysed by Kirklees Environmental Services specifically for this project.

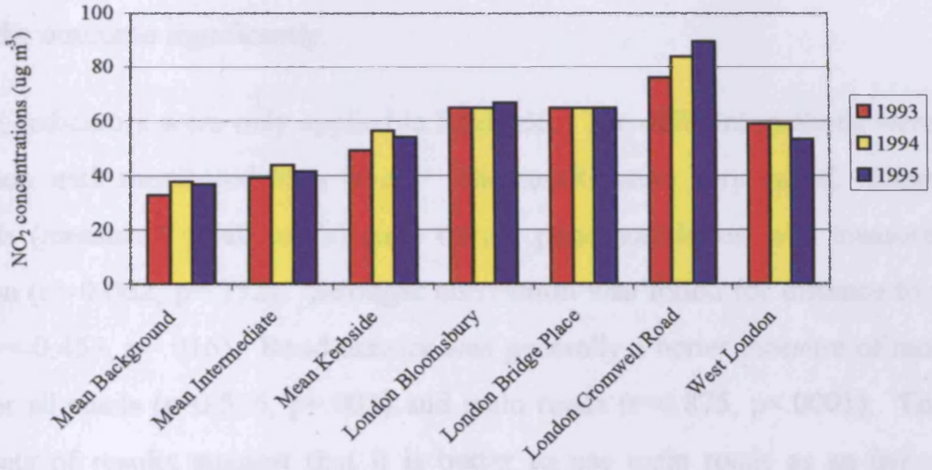

Figure 6.2: Mean NO_2 concentrations of the background, intermediate and kerbside monitoring sites compared with London AUN sites for 1993, 1994 and 1995.

Overall, however, results suggest that passive diffusion tubes can be assumed to be reliable as relative measures of NO_2 concentration, to an accuracy of +/- about 10%. This is well within the tolerance likely to be achieved by the methods used in this study. On this basis, NO_2 diffusion tubes can be considered to provide valid reference data, against which to assess the performance of the different measures used here. Nevertheless, in using monitored NO_2 as a 'golden mean' by which to judge these methods, it is important to recognise that this, itself, is only one possible marker of traffic-related pollution and is not necessarily the pollutant of most importance in terms of health effects.

6.2.2 *Indicators*

Indicators are widely used in epidemiological studies (Livingstone *et al.* 1996, Brunekreef *et al.* 1997, Wjst *et al.* 1993, Nitta *et al.* 1993), and have in a number of cases been shown to have associations with respiratory illness (Brunekreef *et al.* 1997, Wjst *et al.* 1993, Nitta *et al.* 1993). Major advantages in using indicators are the ease of computation, limited data requirements and apparent simplicity of interpretation. The extent, however, to which they provide a measure of pollution levels is largely unknown. Indicators provide only a non-specific measure of exposure. They are not indicative of any particular pollutant and they make no allowance for processes by which pollutants are dispersed through the environment. Measures are also highly sensitive to the definition of the indicator used.

For instance, the type of roads used to measure road density or distance from road, or type of vehicles used for traffic volumes (e.g. high duty vehicles., coaches, light duty vehicles) can change the outcome significantly.

In this study, indicators were only applied in Sheffield. The different methods were tested by comparison with monitored NO_2 levels. The results were very varied. Distance to nearest roads (measured as all roads) gave only a poor correlation with measured NO_2 concentration ($r=-0.062$, $p=.752$). Stronger correlation was found for distance to nearest main road ($r=-0.453$, $p=.016$). Road density was generally a better measure of monitored NO_2 both for all roads ($r=0.536$, $p=.003$) and main roads ($r=0.875$, $p<.0001$). Together, these two sets of results suggest that it is better to use main roads as an indicator of pollution levels rather than all roads. This reflects the concentration of traffic on the main roads. As this implies, measures based on traffic flow also give reasonably good correlations with measured NO_2: $r=0.807$ for traffic volume ($p<.0001$) within 150 metres of monitoring site and $r=0.820$ for HGV traffic within 150 metres ($p<.0001$).

6.2.3 CALINE3

CALINE3 has only rarely been used in relation with epidemiological studies, although Pershagen *et al.* (1995) applied the daughter model, CALINE4, to analyse relationships between traffic related pollution and health in Stockholm. A supposed advantage of using CALINE3 is its reported accuracy (Benson 1992). Disadvantages are the data requirements and the time consuming editing of input files. Another disadvantage in this study was the need to make various assumptions in order to cope with lack of data (see *Section 3.3.2*).

CALINE3 was used in both the Greater London (only for 1993) and Sheffield case studies. Results in Sheffield were much better than in Greater London: $r=0.657$, compared with $r=0.225$. Nevertheless, the SEE in Sheffield was 11.84 $\mu g\ m^{-3}$, which indicates that the estimated concentrations did not correspond well with the monitored levels. CALINE3 also seemed to underestimate the measured concentrations both in Greater London and Sheffield.

Differences in performance of CALINE3 between London and Sheffield can be largely attributed to differences in the spatial resolution and accuracy of the input data. The model very much depends on the accuracy of the location of the receptor in relation to the road(s). In Greater London, rounding of the co-ordinates for the receptors (monitoring sites) meant that their locations could be in error by as much as 140m. Receptors in Sheffield were much more accurate. The road data could also be an important factor. Traffic data in Greater London was sparse and resulted in omission of a large number of sites, the 200m buffer zones for which contained no roads with traffic flows (see *Section 3.3.2*). In Sheffield traffic data was available for a much more complete set of roads.

6.2.4 DMRB

DMRB is a methodology used primarily as an instrument for local authorities in the UK to assess the environmental impact of existing or proposed road schemes. Advantages in using DMRB are the ease of computation and the simple data requirements (no meteorological data are needed). A disadvantage of this technique is that the model can be applied only up to distances of 200 metres from any road. This makes DMRB unsuitable for predicting background concentrations.

DMRB was used in both the case studies. In Greater London the relation between the estimated and measured NO_2 concentrations was poor: 1993, r=.255 (p=.122); 1994, r=.431 (p=.001); and 1995, r=.382 (p=.007). In Sheffield the correlation was very high: r=.915 (p<.0001). This again probably reflects differences in the spatial resolution, accuracy and completeness of the input data.

6.2.5 ISC3

ISC3 was only used in the Greater London case study. Results of the ISC3 runs showed the best correlations with the monitored NO_2 concentrations compared with the other methods: r=.343 (p=.005) for 1993, r=.330 (p=.002) for 1994 and r=.274 (p=.014) for 1995. The main limitation on this methodology is clearly the spatial resolution of the emission inventory used. The consequence of using 1 km square grid cells as emission sources is that a single aggregated emission value is used to model concentrations at all locations in the grid cell, whether they be kerbside sites or background sites. The effect is thus greatly to attenuate variation in the predicted concentrations, and to smooth out local variation in the data. It also results in marked overestimation of concentrations at many sites, particularly those in background areas.

The extent to which this degree of smoothing matters in relation to exposure estimation nevertheless needs to be considered. Spatially precise models may give better estimates of concentrations at specific point locations, but human exposure to traffic-related pollution is integrated across a wide area. It is possible, therefore, that a more aggregated exposure score, obtained by averaging pollution levels across a grid cell, is in fact more realistic, at least as a *relative* measure of exposure than a specific point estimate. Unfortunately, without the capability to undertake personal monitoring, the effects of spatial resolution of the dispersion models on exposure assessment cannot be investigated.

6.2.6 ADMS-Urban

ADMS-Urban was only used in Sheffield, where it was applied both with and without the hill option. The Pearson correlation coefficient ($r=.646$, $p<.0001$ with the hill option and $r=.731$, $p<.0001$ without the hill option) was lower than the Spearman correlation coefficient ($r=.906$, $p<.0001$ with hill option and $r=.928$, $p<.0001$ without hill option), suggesting that the relationship between the estimates and monitored values was non-linear. The estimated concentrations were also not in the same range as the measured concentrations, illustrated by a SEE of 11.45 $\mu g\ m^{-3}$ for ADMS with the hill option and 10.23 $\mu g\ m^{-3}$ without the hill option.

A disadvantage of using this model is its long processing time. One run for ca. 600 sources and 28 receptors for 2 weeks, took ca. 8 hours on an NT workstation. Importing the roads data is also time-consuming. A further potential disadvantage is the relatively stringent requirement for meteorological data. The model is designed to run with data on the Monin Obukhov length which is derived from data on wind speed measured at two heights. This is rarely available and, where it is used, must usually be obtained from relatively distant monitoring stations. This was the reason why in this study cloud cover was used instead of the Monin Obukhov length. Together with temperature, cloud cover simulates the atmospheric stability and boundary layer conditions. The extent to which this degrades the accuracy of the model is not known. Further sensitivity analysis is therefore required to examine and compare the effects of using different boundary layer measures, and data from more or less remote sites.

6.2.7 Kriging and Co-Kriging

Kriging and co-kriging were only used in the Greater London case study. Kriging was performed using all sites, resulting in r=.449 (p<.0001) in 1994 and r=.429 (p<.0001). As such, it gave the best performance of any model, for the full data set, in London. When applied only to background sites significantly higher correlations were found: r=.573 (p=.001) for 1993, r=.710 (p<.0001) for 1994, and r=.684 (p<.0001) for 1995. Co-kriging gave no improvement on these results; used on the background sites, it gave r=.585 (p=.001) for 1993, r=.703 (p<.0001)for 1994 and r=.675 (p<.0001) for 1995.

It has to be noted that in the time available for this analysis it was impossible to evaluate all the available options in kriging and co-kriging. Results might be improved, for example, by applying different models to the semiovariograms, by using different window sizes or by applying different covariates in co-kriging. Nevertheless, the shape of the semiovariograms obtained for the full data set suggests that, at the density of sampling available, kriging is unlikely to provide a reliable means of modelling traffic related pollution across a complex area such as London. On the other hand, co-kriging or - as Knotters *et al.* (1996) used - kriging with regression, does seem to offer some potential for development if suitable co-variates can be found.

6.2.8 SAVIAH

SAVIAH is a recently developed methodology and therefore still relatively unknown. It was originally developed and tested in Huddersfield, Amsterdam and Prague (Briggs *et al.* 1997). As noted in *Chapter 3,* however, when attempts were made to apply it to Sheffield as part of this research, the original form of the model was found to be unstable at altitudes outside the range originally encountered in Huddersfield. For this reason, the original data were re-examined and a revised model, with a different altitudinal variable, was constructed. This has since also been applied in Northampton (Briggs *et al.* 1998) and

Hammersmith and Ealing (Wills 1998), where it has proved to be a reliable method in predicting NO_2 levels.

The revised SAVIAH was only used here in the Sheffield case study. A strong correlation was found between the monitored NO_2 data and the SAVIAH estimated NO_2 concentrations: $r=.829$ ($p<.0001$). Compared to the other models, this is the easiest model to apply with the least amount of input data and the shortest processing times. Nevertheless, the model seems to under-estimate concentrations at high concentrations and the slope of the relationship with measured concentrations is markedly greater than 1 (*Figure 5.22*). This probably reflects differences in factors such as traffic composition and speed, urban morphology and topography compared to the original study area in Huddersfield. It thus implies that, though the model gives good *relative* measures of NO_2 levels in Sheffield, to assess concentrations in absolute terms requires local recalibration. The results here suggest that this can be achieved using passive sampling at no more than about 20-30 sites, for about five periods over a year.

6.2.9 Effects of wind direction

Results presented in *Chapter 5* indicated that correlations between exposure measures used in the Sheffield case study and measured NO_2 tended to vary between the different surveys. Highest correlations tended to be found in surveys 1 and 5, lowest in surveys 3 and 4 (see *Table 5.7*). It was also notable that CVs between duplicates showed a similar pattern: least in surveys 1 and 5 and highest in survey 3 (see *Table 6.3*). A possible cause for these patterns was investigated.

One possible cause was problems with the diffusion tubes or the laboratory analysis for survey 3, and perhaps survey 4. To investigate this, contact was made with the laboratory, and checks were made on reported errors in the field and laboratory blanks. These gave no indication of any discrepancies for either of these surveys.

Another possible explanation was variation in meteorological conditions during the five surveys. *Table 6.5* shows the mean conditions for a number of meteorological parameters for each survey period in Sheffield, in relation to the mean monitored NO_2 concentration, the CV of duplicate tubes and r values for each measure.

Table 6.5: Means for meteorological conditions and r for methods

	Survey 1	*Survey 2*	*Survey 3*	*Survey 4*	*Survey 5*
Temperature (C)	17.59	13.09	8.34	4.35	7.07
Wind speed (m/s)	3.63	3.62	2.5	3.9	5.56
Cloud cover (Oktas)	4.92	5.19	6.47	5.88	5.97
Urban mixing height (m)	879.74	671.99	401.31	626.35	910.79
Precipitation, sum (mm)	35.8	4	25.8	31.6	47.8
modal wind direction	292.5	270	112.5	292.5	270
Mean NO_2	44	39	51	47	46
cv between samplers	9.21	5.89	12.54	7.65	5.98
r distance to main roads	-0.405	-0.447	-0.341	-0.46	-0.455
r distance to all roads	-0.001	-0.184	-0.053	-0.116	0.055
r density main roads	0.876	0.815	0.715	0.822	0.82
r density all roads	0.604	0.49	0.387	0.459	0.522
r traffic volume	0.847	0.794	0.595	0.699	0.778
r hgv volume	0.858	0.794	0.56	0.741	0.825
r CALINE3	0.718	0.693	0.291	0.646	0.694
r DMRB	0.908	0.922	0.763	0.805	0.817
r ADMS+	0.561	0.584	0.512	0.735	0.555
r ADMS-	0.557	0.657	0.571	0.775	0.605
r SAVIAH	0.784	0.825	0.718	0.699	0.8

Indications of some meteorological effects can be seen in this data. In particular, survey 3, which is characterised by the highest between-sampler CV, the highest mean NO_2 concentration and the lowest levels of correlation with most of the exposure estimates, also has the lowest mixing height, the lowest wind speed, the highest cloud cover and a markedly different wind direction.

Amongst these, the potential effects of wind direction is especially interesting, since it may relate to different weather patterns and the influence of different source areas. This can also be explored most readily, since it is likely to be reflected in the spatial patterns of pollution across the area. Wind roses for each survey are shown in *Appendix 5C*. Based on this it is possible to detect different pollution patterns.

Appendix 5C shows that during surveys 1 and 5, the wind primarily came from the west, while during survey 3 the wind primarily came from the east. Survey 2 has a tendency for winds from the west, but survey 4 has a variable wind direction pattern. There is a clear distinction between the west and the east of Sheffield. The Peak District, to the west of Sheffield, is an area of open moorland, without any major NO_2 sources and a relatively clean atmosphere. Measurements at Ladybower, about 15 km west of Sheffield, for example, show mean annual NO_2 concentrations of about 16 $\mu g\ m^{-3}$ (AEA 1994). This is in contrast to the urban areas of the Don Valley which stretch to the east of Sheffield. This means that when the wind consistently blows from the west, relatively clean air is blown into Sheffield, resulting in low NO_2 concentrations in the west and accumulation of NO_2 concentrations towards the east. Conversely, when the wind consistently comes from the east, the situation reverses. Heavily polluted air is blown into Sheffield from the east, which is then further polluted as it crosses the city, resulting in even higher concentrations in the west. This pattern can best be observed at the background sites used in the monitoring (see *Figure 5.4*). Survey 1 and 5 show relative low NO_2 concentrations at background sites in the west and higher in the east. This contrasts with survey 3, which shows significant higher NO_2 concentrations in the west. This pattern is more difficult to observe at kerbside and intermediate sites because pollution resulting from nearby roads tends to dominate.

Most models are not able to reflect these pollution patterns arising from prevailing wind directions. Neither DMRB nor SAVIAH use any meteorological data and are only able to predict annual mean NO_2 concentration. CALINE3 uses meteorological data and is able to predict NO_2 concentrations for every survey, but, as applied here, did not consider sources more than 200 m from any receptor point. Regional impacts were therefore not taken into account. Even if the 200 metre limit had not been imposed (which would greatly have added to processing times) it would not have been possible to extend the model sufficiently far afield to pick up these more remote effects. ADMS-Urban is also able to detect these patterns, in principle, but again to do so would require extending application of the model to an extremely large area. This would be prohibitive given the long processing times involved.

The inability of the models to detect these regional effects should be apparent when looking at the differences between estimated and observed NO_2 levels at the 28 monitoring sites. During survey 1 and 5, NO_2 levels in the east of Sheffield should be underestimated compared to the monitored NO_2 levels because of the accumulation of pollution eastwards as winds blow across the city. During survey 3, however, it should be expected that predicted NO_2 levels were underestimated at all sites in Sheffield, due to the ingress of polluted air from the east. *Figures 6.3* to *6.6* map the differences between the monitored

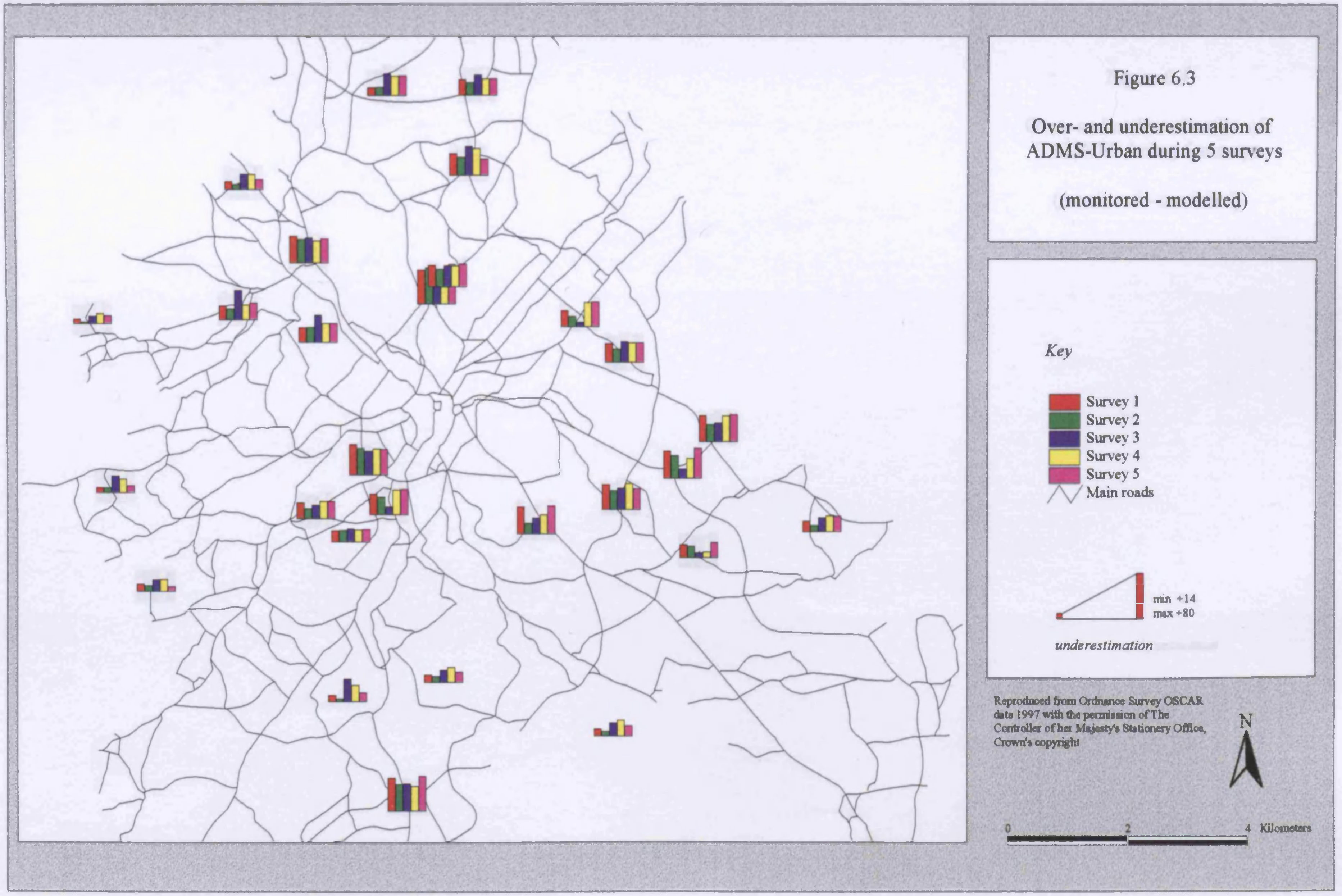

Figure 6.3

Over- and underestimation of ADMS-Urban during 5 surveys

(monitored - modelled)

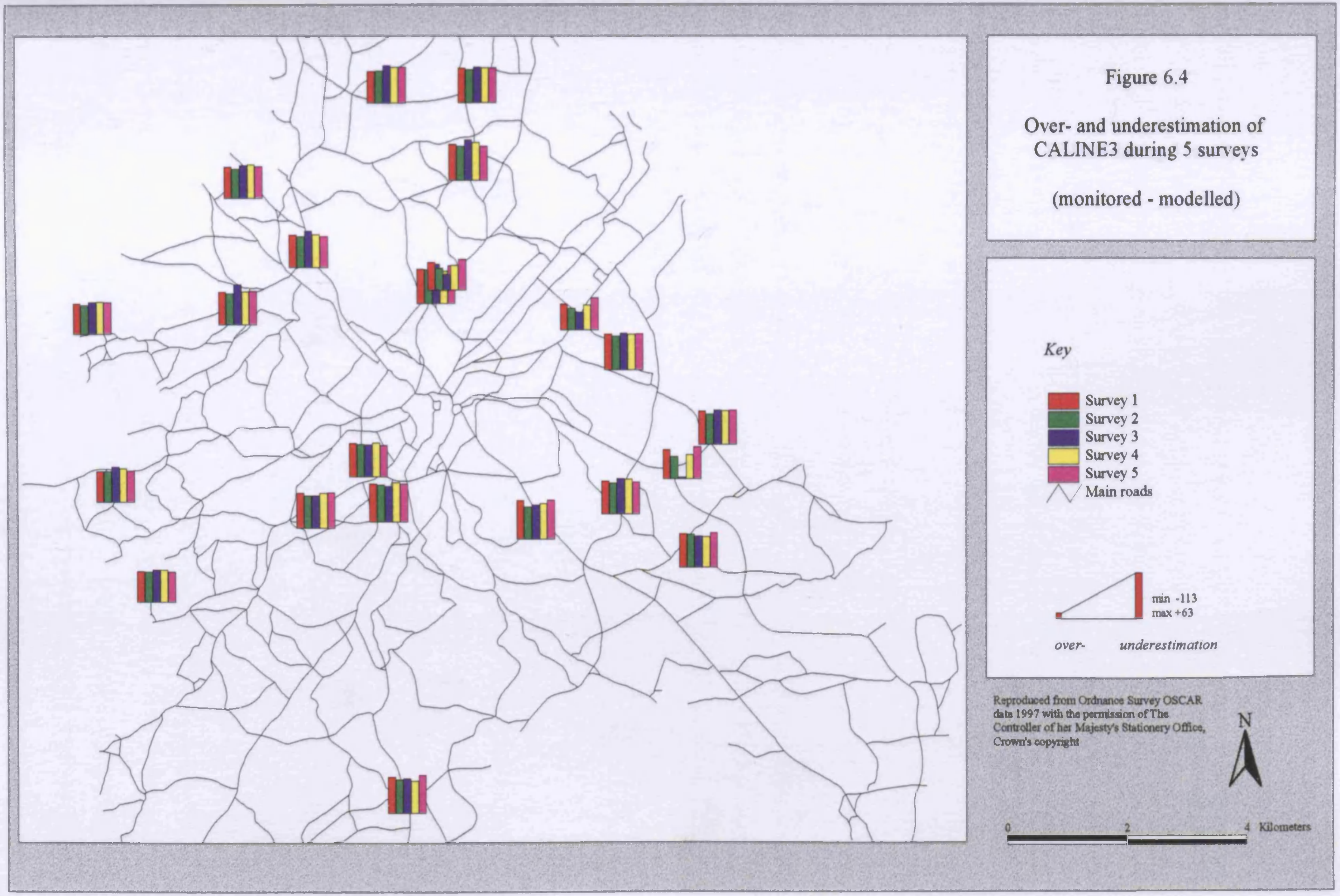

Figure 6.4

Over- and underestimation of CALINE3 during 5 surveys

(monitored - modelled)

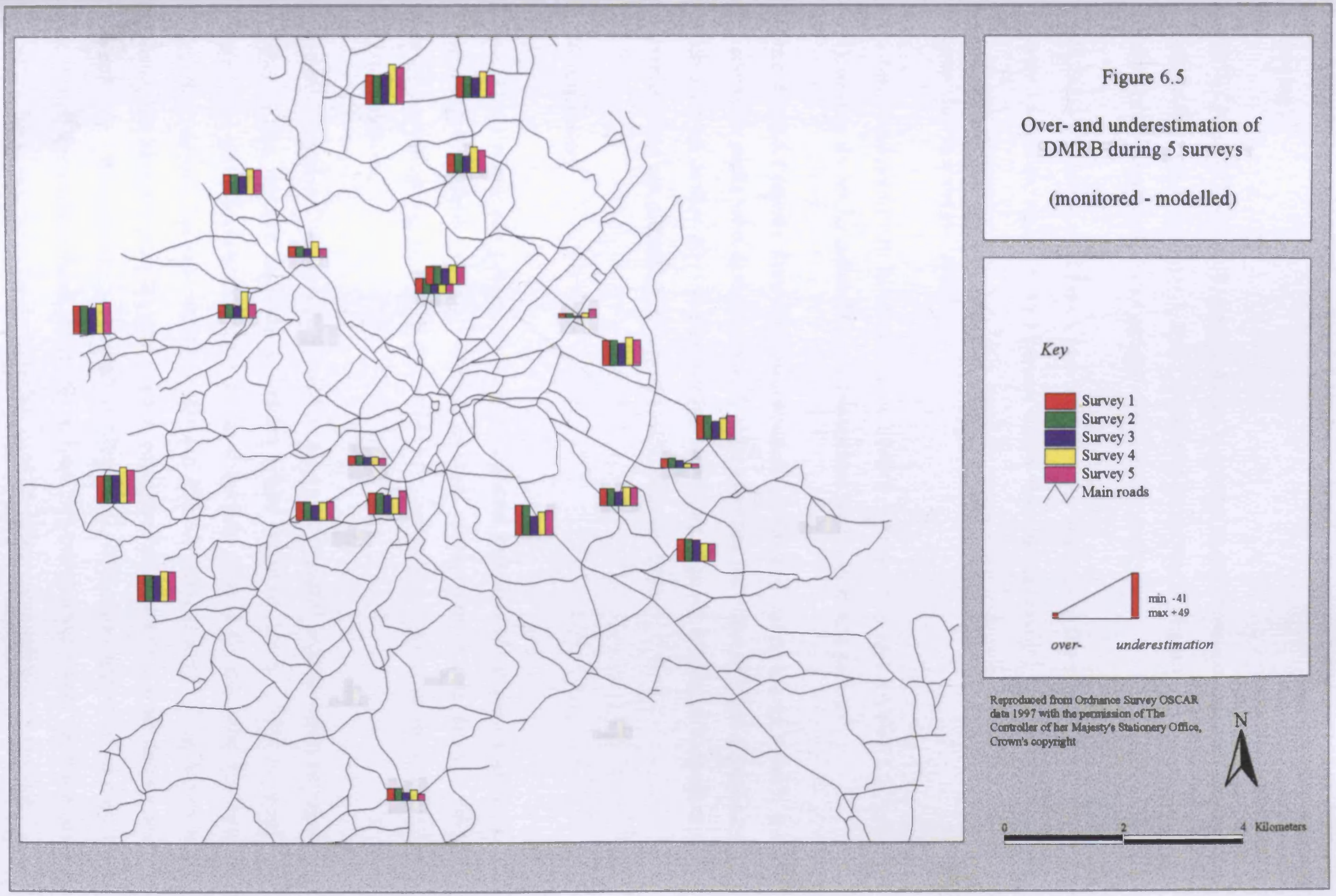

Figure 6.5

Over- and underestimation of DMRB during 5 surveys

(monitored - modelled)

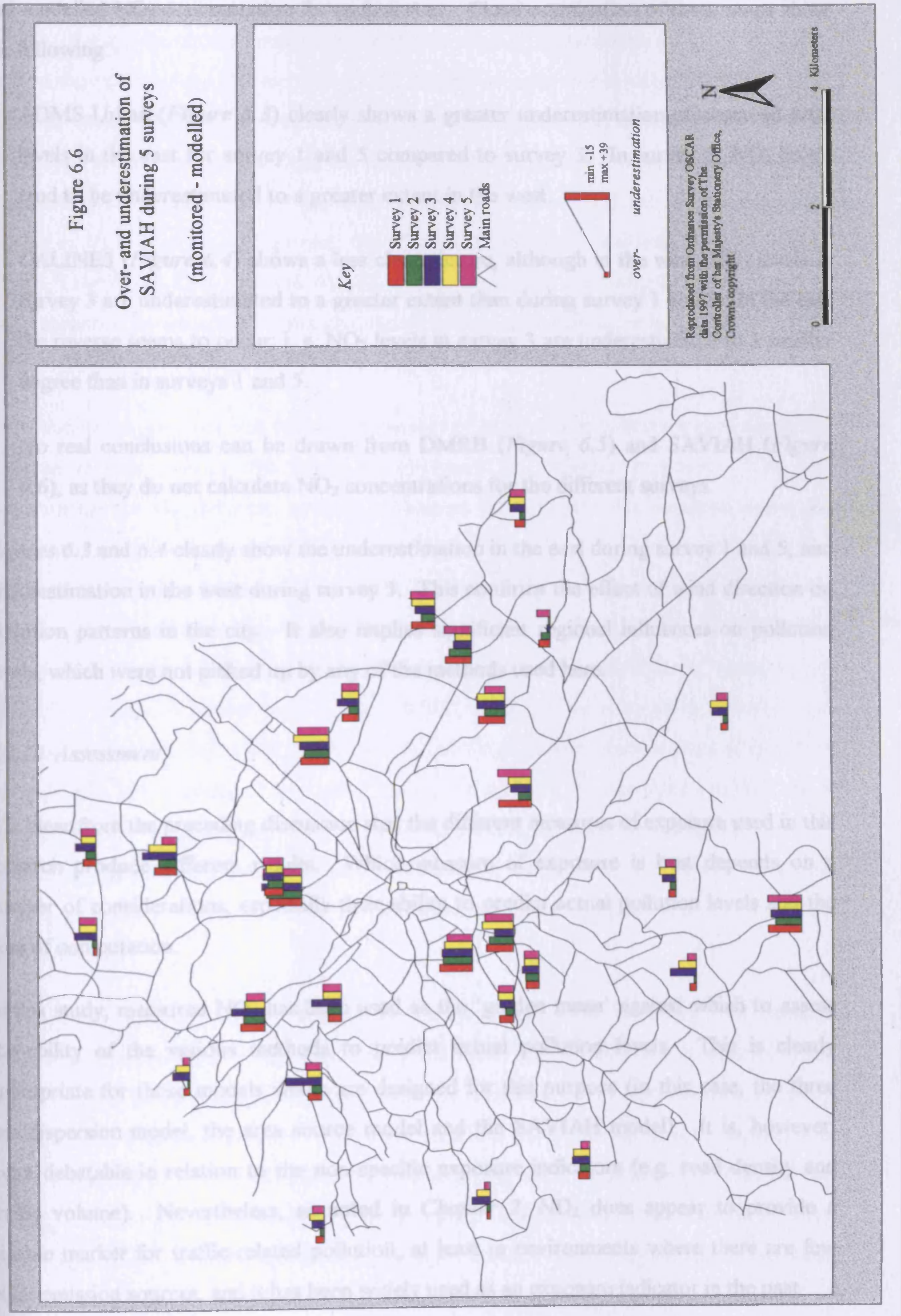

Figure 6.6
Over- and underestimation of SAVIAH during 5 surveys
(monitored - modelled)

and modelled NO_2 concentration for each survey. Close examination of these maps show the following:

- ADMS-Urban (*Figure 6.3*) clearly shows a greater underestimation of observed NO_2 levels in the east for survey 1 and 5 compared to survey 3. In survey 3, NO_2 levels tend to be underestimated to a greater extent in the west.

- CALINE3 (*Figure 6.4*) shows a less clear picture, although in the west, NO_2 levels in survey 3 are underestimated to a greater extent than during survey 1 and 5. In the east the reverse seems to occur: i. e. NO_2 levels in survey 3 are underestimated to a smaller degree than in surveys 1 and 5.

- No real conclusions can be drawn from DMRB (*Figure 6.5*) and SAVIAH (*Figure 6.6*), as they do not calculate NO_2 concentrations for the different surveys.

Figures 6.3 and *6.4* clearly show the underestimation in the east during survey 1 and 5, and underestimation in the west during survey 3. This confirms the effect of wind direction on pollution patterns in the city. It also implies significant regional influences on pollution levels, which were not picked up by any of the methods used here.

6.2.10 Assessment

It is clear from the preceding discussion that the different measures of exposure used in this research produce different results. Which measure of exposure is best depends on a number of considerations, especially their ability to predict actual pollution levels and the ease of computation.

In this study, measured NO_2 has been used as the 'golden mean' against which to assess the ability of the various methods to predict actual pollution levels. This is clearly appropriate for those models which are designed for this purpose (in this case, the three line dispersion model, the area source model and the SAVIAH model). It is, however, more debatable in relation to the non-specific exposure indicators (e.g. road density and traffic volume). Nevertheless, as noted in *Chapter 2*, NO_2 does appear to provide a reliable marker for traffic-related pollution, at least in environments where there are few other emission sources, and it has been widely used as an exposure indicator in the past.

In these terms, the best results are seen to be provided by the SAVIAH and DMRB models. Relatively strong associations with measured NO_2 were also provided by traffic flow in the surrounding 150 metres and the density of main roads within a 150 m buffer. These are also relatively easy measures to apply, making them all suitable for use both for simple screening applications (e.g. to help identify possible pollution hotspots) or for epidemiological studies, where exposure estimations are needed for a relatively large number of sites or areas. In general, the other methods performed less well. Several of these - notably the CALINE and ADMS models - are also relatively time-consuming to apply and have rigorous data demands. As such, they are likely to be less useful for many applications.

Nevertheless, in assessing the different measures of exposure, it is important to remember that the models used in this study are designed for different purposes. The data requirements for the different methods determine the output. Air pollution dispersion models generally use data on traffic, emission, meteorology and the road network as inputs in their calculations. Meteorological data for every hour, combined with hourly traffic volumes, give short-term air pollution dispersion models (e.g. CALINE3, ADMS-Urban) the ability to predict pollutant concentrations for every desired period (hour, week, month or year). Neither long-term models (e.g. DMRB, ISCLT3) nor regression methods have this temporal aspect built within their calculations (e.g. have no meteorological data) and are therefore only capable of predicting long term means. Geostatistical methods use a completely different approach. They use existing monitoring data, from which a surface is calculated. Depending on the monitored data used in the analysis (e.g. weekly or annual mean), geostatistical methods, like air pollution dispersion models, are able to model temporal effects.

Within these analyses, several sources of variation and error occurred. In London, monitored data provided good estimates of the mean annual NO_2 concentrations, albeit poorly located geographically. In Sheffield, the monitored data represented a temporal sample of five two-week periods. The extent to which these provide accurate measures of the mean annual NO_2 concentrations is unknown. The short-term model (CALINE3 and ADMS-Urban) might be expected to provide realistic estimates of concentrations for short time periods (e.g. for individual surveys) except that they could only be run in this study using long-term, mean traffic flows (adjusted to an hourly basis). The lack of real-time traffic measurements can be expected to contribute to errors in estimates for those models. In contrast, the long-term models (ISCLT3, DMRB, SAVIAH, kriging and co-kriging, as applied here) might be expected to perform badly as estimates for individual surveys, though to be relatively more accurate in assessing mean annual concentrations. In practise this seems not to have been fully borne out by the results of this study. As noted, none of the methods worked well in London, though ISC3 and kriging tended to be slightly more reliable. In Sheffield, the long-term models, DMRB and SAVIAH gave the best estimates of monitored pollution levels, both for individual surveys and for the mean annual concentrations. The implication is that limitations in the models themselves, or the available input data, mean that short-term models are as yet not capable of providing reliable pollution estimates at the temporal and spatial resolution needed for exposure assessment.

Finally, in both the Sheffield and Greater London case studies, digital data was used from different scales. In Sheffield, for example, 1:10,000 landuse data was used in conjunction with 1:1250 Ordnance Survey OSCAR road data. Mixing data of different scales in this way can clearly pose problems, for example by generating false silvers in areas where boundaries from different data sets, with different spatial scales, fail exactly to coincide. The spatial accuracy of any products generated by combining the different data sets will thus tend to be determined by the accuracy of the smallest data set used. Checks should therefore be made to ensure that significant errors do not occur when data sets of different scales are used together.

6.3 RELATIONSHIP BETWEEN EXPOSURE AND HEALTH

The previous analysis has considered the capability of various models and methods to provide a measure of monitored NO_2 concentrations, as a measure of exposure to traffic related pollution. It has suggested that the best measures were provided by the SAVIAH and DMRB models, and by the indicators of traffic flow, distance from main road and main road density. To date these methods were only evaluated in terms of their ability to predict monitored NO_2. In reality, however, this provides only a partial test of performance as a measure of exposure: it gives some indication of how well the methods predict actual pollution concentrations at specific sites, but it does not assess the extent to which this reflects the exposures experienced by either individuals or the population at large.

Ideally, this would be assessed by comparing modelled concentrations with measured exposures using personal monitoring techniques. Personal monitoring, however, is costly and logistically difficult, especially if a statistically representative sample of people is to be assessed. Several large scale studies are under way to investigate personal exposures (e.g. Jantunen *et al.* 1998) but data from these are as yet unavailable.

In the Sheffield case study, it was, however, possible to extend the assessment of these exposure measures by examining the extent to which they correlate with health outcome. Inevitably, this approach has some disadvantages, in that it cannot independently test the exposure estimation, and many other factors (including various confounders and other risk factors) may intrude on the relationship with health. Nevertheless, since the main purpose of these exposure measures is to provide a basis for examining links with health, this is likely to provide useful insight into, and an informative test of, the various methods.

For this analysis, only five measures were used: distance to nearest main road, main road density within 150 metres, traffic flow within 150 metres, HGVs within 150 metres and SAVIAH-modelled NO_2. These measures were selected because, as noted above, they gave the best predictions of measured NO_2 and were relatively easy to apply.

This section describes the health study conducted in Sheffield using these five exposure measures.

6.3.1 Locations of residence of school children and schools

Of the 18,203 respondents to the Sheffield Allergy Survey, 14,317 were selected for use in this project. Those excluded were omitted for various reasons, such as incomplete locational data or residence outside the study area (see *Figure 6.7*). The locations of residence of these respondents and the locations of the schools were obtained from the Central Postcode Directory (CPD) (see *Figure 6.8*).

The Ordnance Survey grid reference in the CPD represents the lower left corner of the 100m grid square, containing the first address in the postcode. This grid reference is supposed to be accurate to 100m. Evaluation of the CPD by Gatrell in 1989, however, showed that only 72 per cent of the grid references were accurate to within 100m and 97 per cent within 200m of the true location. Since then efforts to revising and correct the CPD data have improved the accuracy.

Reasons for the inaccuracy can be found in the fact that the grid reference on the CPD is of the first address in any unit postcode. This is not necessarily (and indeed is unlikely to be) the centroid of the postcode to which it relates. Martin (1996) therefore recommended adding 50m to both the x- and y-coordinates, in order to reduce the average spatial error of the CPD references.

23054 questionnaires distributed
(4851 not returned)
18203
(410 missing or invalid year of birth or gender)
17793
(190 no postcode)
17603
(16 postcodes mot found in CPD)
17587
(2764 postcode centroids outside the study region)
14823
(7 live in enumeration districts with no Carstairs score)
14816
(499 attend schools outside the study region)
14317 to be used in analysis

Figure 6.7: Data excluded from the full dataset.(Jeremy Bullard, 1998, pers. comm.)

This recommendation was followed in this research, and 50m was added to all the x- and y-coordinates of the respondents. The adjusted x- and y- coordinates were imported into ARCINFO where a point-coverage was created.

For 1,488 children in either the case-control study or the skin-prick test study, full postal addresses were available. With these postal addresses, accurate address point locations

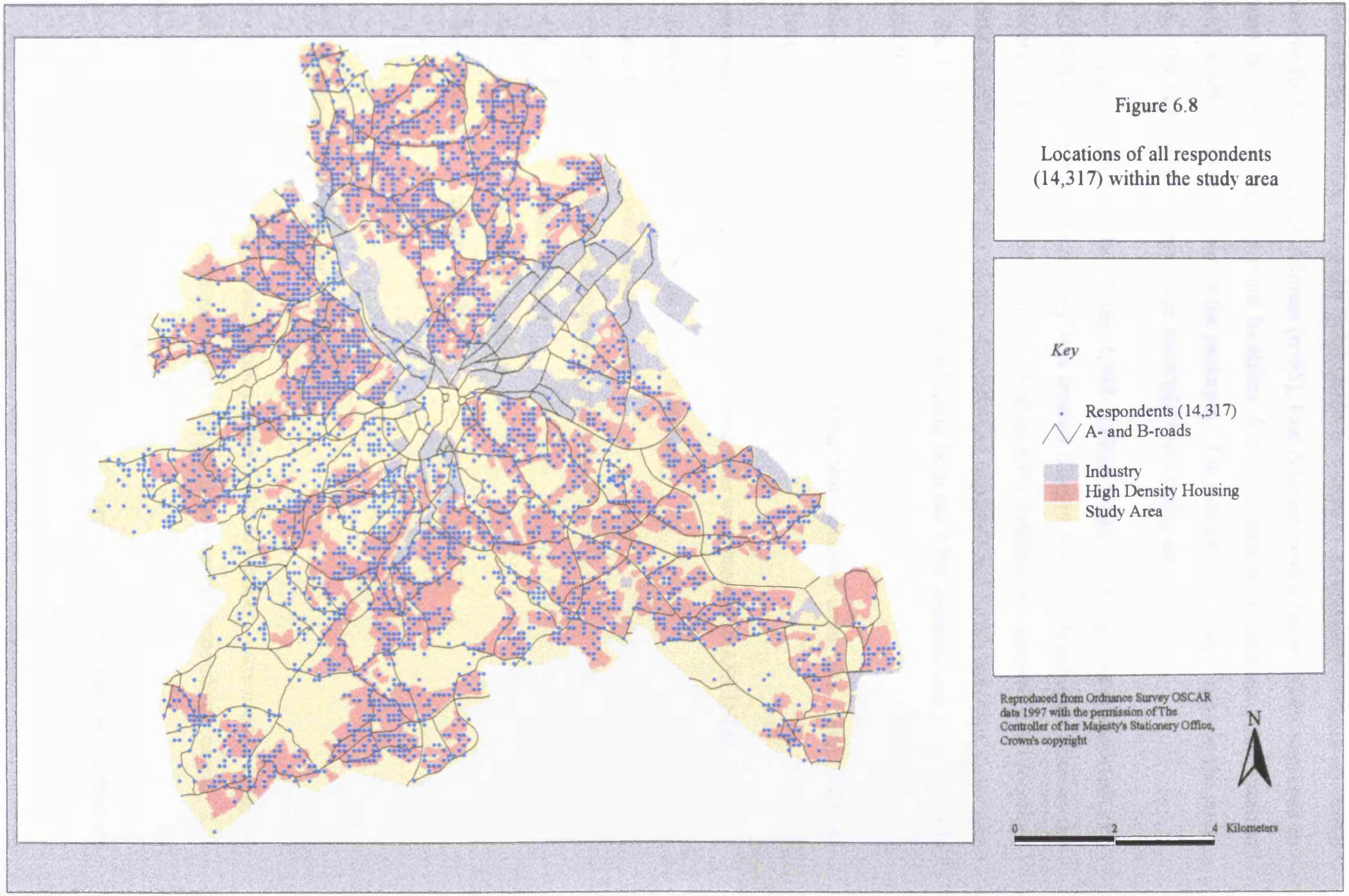

Figure 6.8

Locations of all respondents (14,317) within the study area could also be identified using the Quick Address system (10m accuracy). Where no match could be found with Quick Address (n=95), Fast Address, with a 1m accuracy, was used to obtain the missing address point locations. For 162 children no address point location could be obtained with either of the packages. The majority (152) were outside the study area. The remaining 10 were either incomplete or missing addresses.

The x- and y- coordinates of the 1,488 address point locations were imported into ARCINFO where a point-coverage was created (*Figure 6.9*). To investigate whether the different grid references (address point location, CPD location and adjusted CPD location) would affect analyses of the relationship between exposure and health outcome, coverages for the 1,488 children were also created using both the CPD location and adjusted CPD location.

Address point locations for the schools were also obtained using the Quick Address system.

In summary, therefore, the following point coverages were created in ARCINFO:

- Respondents adjusted postcode centroids
- Cases1 postcode centroids
- Cases2 adjusted postcode centroids
- Cases3 address point
- Schools1 postcode centroids
- Schools2 address point

6.3.2 Exposure estimates for the locations

The chosen methods - the three indicators and the SAVIAH model - were used to compute exposure measures for points in each of the six point-coverages (respondents, cases1, 2, 3 and schools1, 2).

Table 6.6 shows the median, range and 10^{th} and 90^{th} percentiles of the exposure estimates for the adjusted postcode centroids in the full dataset (respondents).

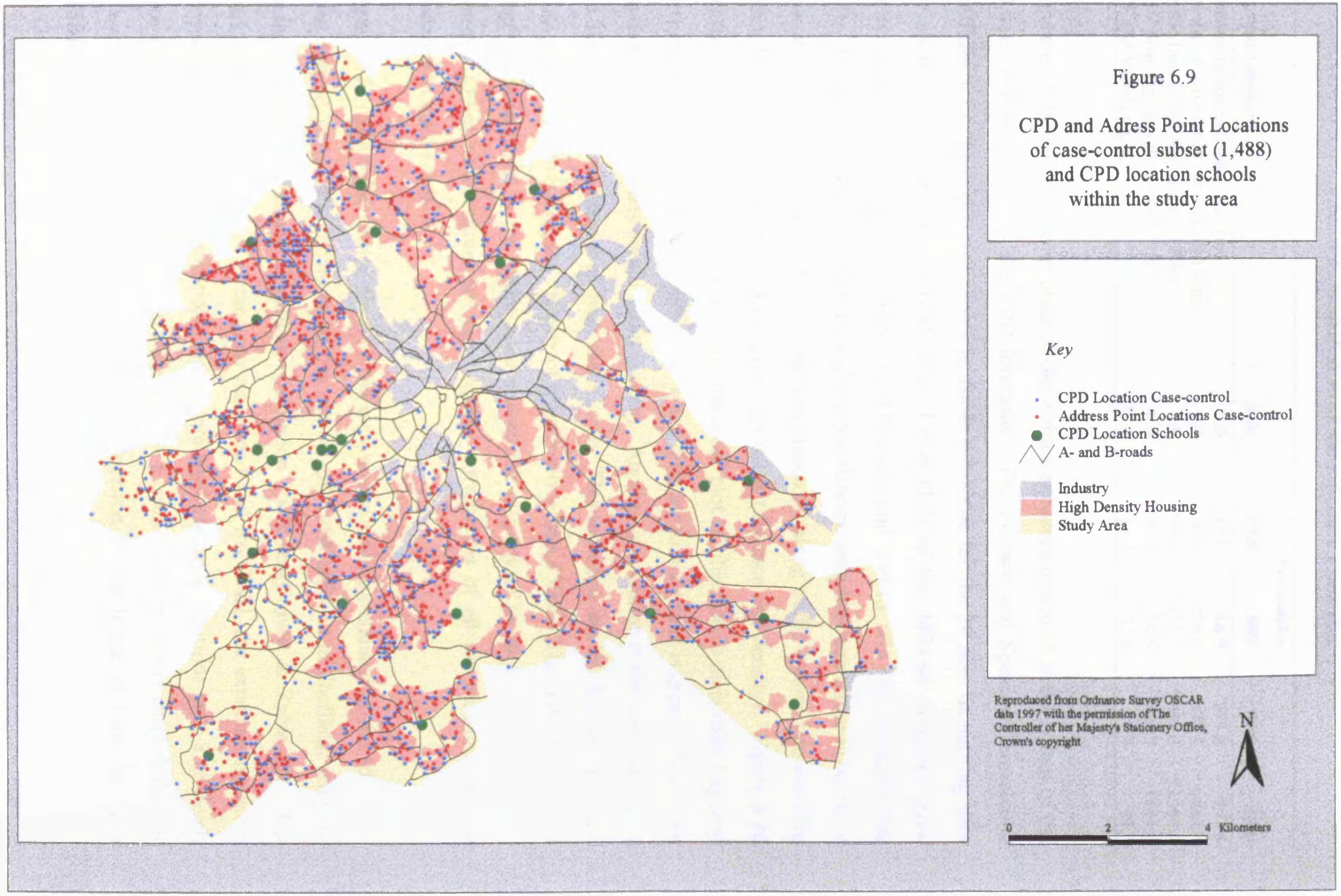

Figure 6.9

CPD and Adress Point Locations of case-control subset (1,488) and CPD location schools within the study area

Table 6.6: Distribution of the exposure estimates.

		Percentiles			
Exposure measure	***Min***	***10th***	***50th***	***90th***	***Max***
Distance to nearest main road (m)	0.0	15.5	88.9	275.8	957.8
Density of main roads (m) within 150m	0.0	0.0	255.4	475.1	888.4
Traffic flow (v km/day) within 150m	0.0	209.6	1356.5	5089.6	21064.0
HGV flow (hgv km/day) within 150m	0.0	6.7	58.6	368.7	1424.4
NO_2 (SAVIAH) $\mu g\ m^{-3}$	25.3	28.7	35.6	39.8	49.3

Figure 6.10 shows the scatter plots of the various exposure measures at the homes of the 14,816 children, based on the CPD locations. The Pearson and Spearman correlation coefficients for these sites are shown in *Table 6.7*; those for the 28 sites monitoring sites are shown for comparison in *Table 6.8*. Cross plots of the different measures show intercorrelations ranging from .261 to .937 (Pearson) and .249 to .974 (Spearman) (*Table 6.7*). At the 28 sites (*Table 6.8*) the highest correlations were between traffic flow, HGV flow and SAVIAH, showing the possible importance of taking traffic volume into account, rather than basing exposure measures only on roads (distance and density). *Figure 6.10* clearly shows the buffer zone of 150m in the cross plot of 'distance to main roads' against 'density of main roads within 150m' (e.g. when distance to main road is greater than 150m the density of main roads within 150m is zero). Another observation in the same cross plot is a 300m line on the density of main roads scale. This same line can be observed in all the other cross plots involving the 'density of main roads within 150m'. This indicates that the length of main roads in the buffer zone around the majority of locations is less than 300 metres. Other observations are the negative correlations of all the measures against 'distance to main roads'.

Figure 6.11 shows the scatter plots of the exposure measures evaluated at the address – point and adjusted CPD locations of the sub-set of 1,488 children in Sheffield, with the corresponding Pearson and Spearman correlation coefficients given in *Table 6.9*. The plots show that, apart from distance to main road and SAVIAH, the exposure measures between the address point locations and the adjusted postcode centroids have a relatively poor correlation. This suggests that there may be a considerable exposure misclassification in using postcode centroids as a measure of location of the home, at least for these measures.

Table 6.7: Pearson (p) and Spearman (s) correlation coefficients of exposure measures at the homes of 14,816 children (p=.000 for all correlations)

Measures		**Distance to main roads**	**Density of main roads within 150m**	**Traffic flow within 150m**	**HGV flow within 150m**	**SAVIAH modelled NO_2**
Distance to main roads	*Pearson*	1.000	-.707*	-.369*	-.374*	-.338*
	Spearman		-.841*	-.530*	-.537*	-.296*
Density of main roads within 150m	*Pearson*		1.000	.558*	.570*	.261*
	Spearman			.496*	.497*	.249*
Traffic flow within 150m	*Pearson*			1.000	.937*	.320*
	Spearman				.974*	.305*
HGV flow within 150m	*Pearson*				1.000	.355*
	Spearman					.333*
SAVIAH modelled NO_2	*Pearson*					1.000
	Spearman					

* Correlation is significant at the 0.01 level (2-tailed).

Table 6.8: Pearson (p) and Spearman (s) correlation coefficients of exposure measures at 28 monitoring sites

		Distance to main roads	**Density of main roads within 150m**	**Traffic flow within 150m**	**HGV flow within 150m**	**SAVIAH modelled NO_2**
Distance to main roads	*Pearson*	1.000	.050 *(p=.853)* *N=16*	-.419 *(p=.027)* *N=28*	-.419 *(p=.027)* *N=28*	-.601 *(p=.001)* *N=28*
	Spearman		-.206 *(p=.444)*	-.521 *(p=.004)*	-.516 *(p=.005)*	-.643 *(p=.000)*
Density of main roads within 150m	*Pearson*		1.000	.400 *(p=.125)* *N=16*	.466 *(p=.069)* *N=16*	.408 *(p=.408)* *N=16*
	Spearman			.350 *(p=.184)*	.450 *(p=.080)*	.538 *(p=.031)*
Traffic flow within 150m	*Pearson*			1.000	.957 *p=.000)* *N=28*	.813 *(p=.000)* *N=28*
	Spearman				.980 *(p=.000)*	.868 *(p=.000)*
HGV flow within 150m	*Pearson*				1.000	.790 *(p=.000)* *N=28*
	Spearman					.853 *(p=.000)*
SAVIAH modelled NO_2	*Pearson*					1.000
	Spearman					

Figure 6.10: Scatter plots of the various exposure measures evaluated at the homes of 14,816 children

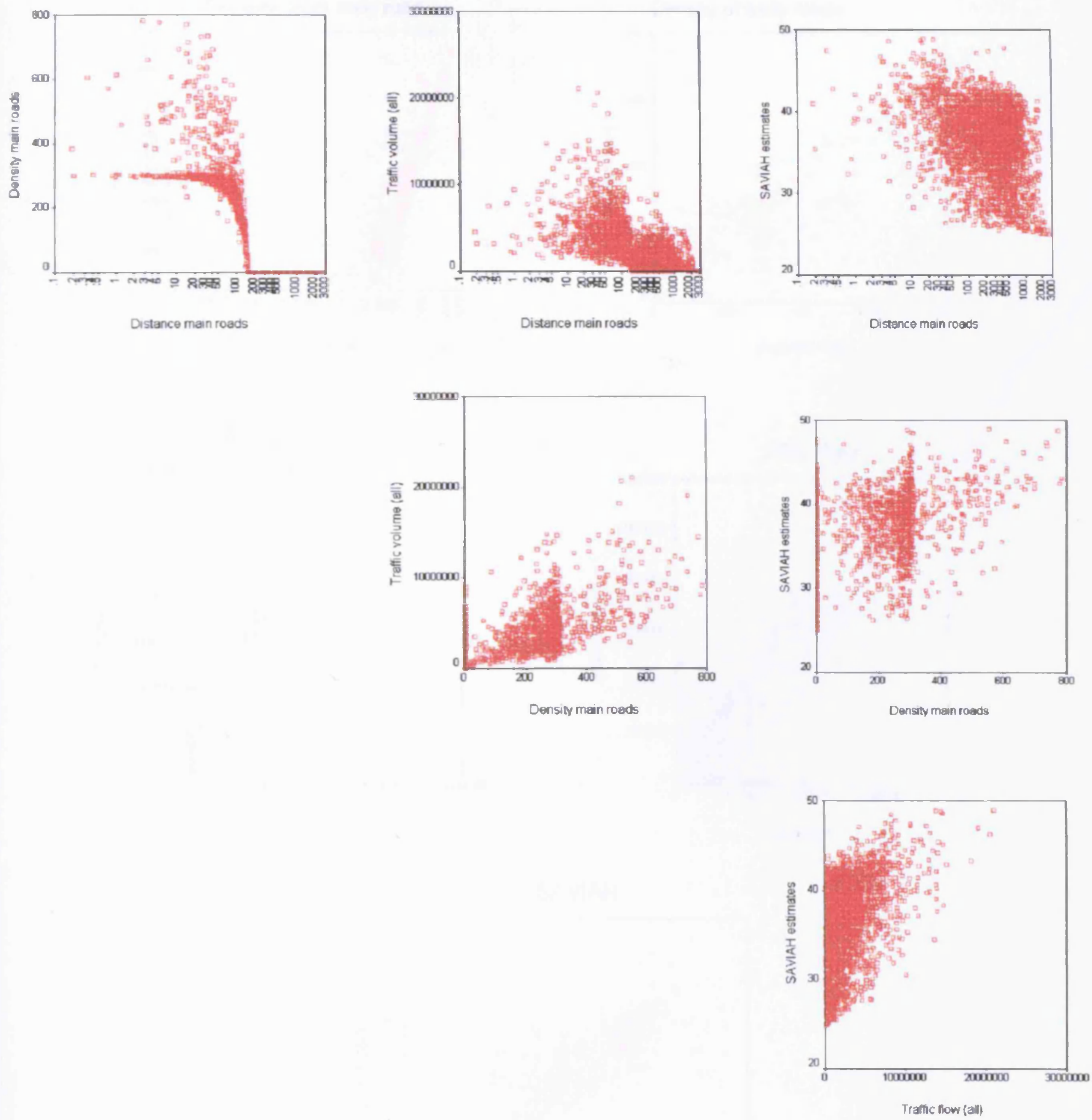

Figure 6.11: Scatter plots of exposure measures evaluated at he address-point and adjusted CPD location of 1,488 children in Sheffield.

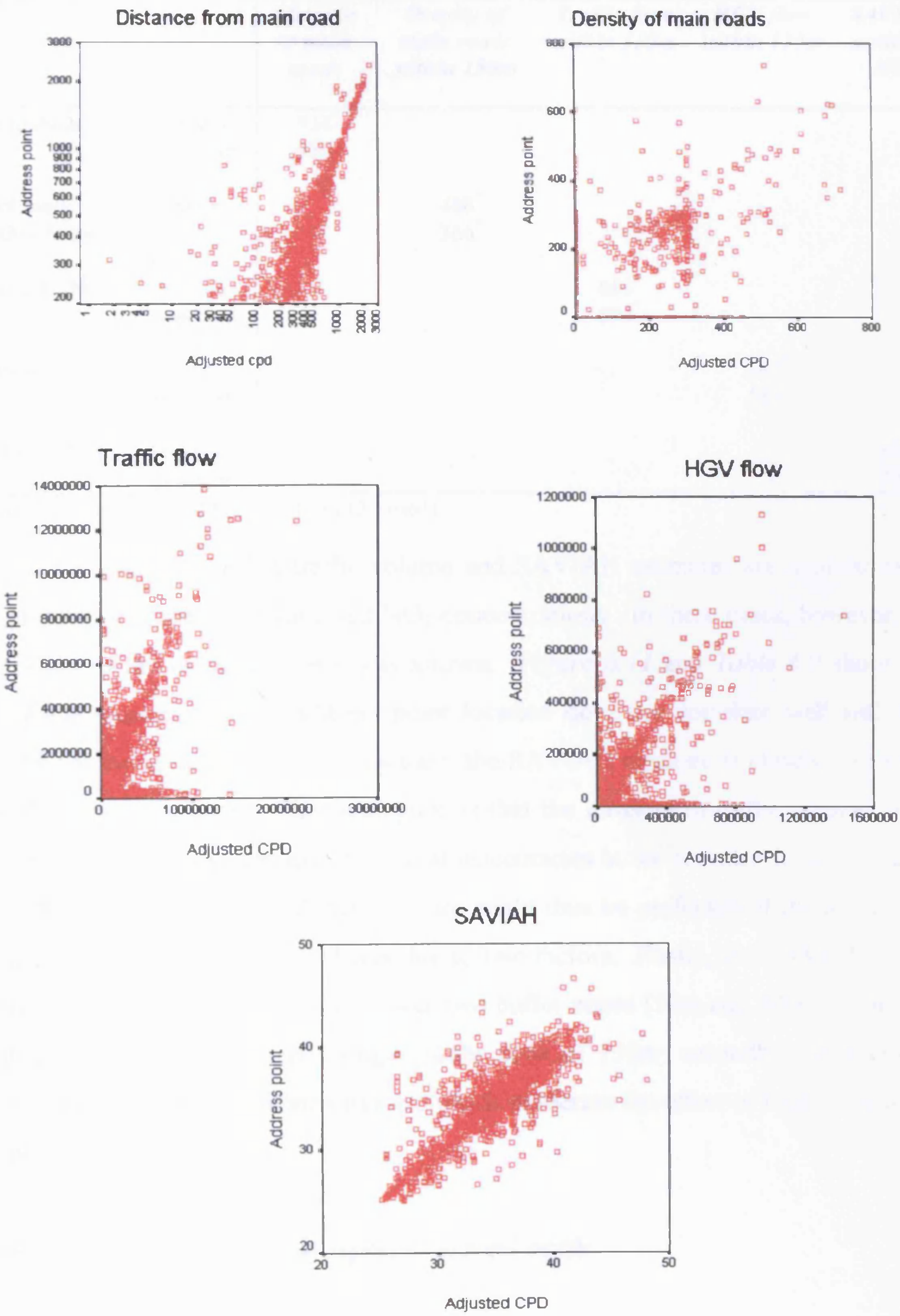

Table 6.9: Pearson and Spearman correlation coefficients of the exposure measures at the address-point (A) and adjusted CPD (B) location of the 1,488 children in Sheffield.

B	A	Distance to main roads	Density of main roads within 150m	Traffic flow within 150m	HGV flow within 150m	SAVIAH modelled NO_2
Distance to main roads	Pearson	.914*				
	Spearman	.816*				
Density of main roads within 150m	Pearson		.488*			
	Spearman		.366*			
Traffic flow within 150m	Pearson			.665*		
	Spearman			.594*		
HGV flow within 150m	Pearson				.662*	
	Spearman				.587*	
SAVIAH modelled NO_2	Pearson					.823*
	Spearman					.792*

* Correlation is significant at the 0.01 level (2-tailed).

In *Table 6.1* it was shown that traffic volume and SAVIAH estimates are approximately equally predictive of the true monitored NO_2 concentrations. In these cases, however, the exact location of the monitoring site was known. *Figure 6.11* and *Table 6.9* show that traffic volume measured for an address point location does not correlate well with that measured from the adjusted CPD. In contrast, the SAVIAH measure is closely correlated between these two estimates. The implication is that the measure of traffic volume in the nearest 150 metres is more sensitive to spatial inaccuracies in the receptor location than is the SAVIAH measure. The SAVIAH measure might thus be preferable if the location of the home is not precisely known. This is due to two factors. Firstly, the SAVIAH model incorporates measures of traffic volume over two buffer zones (50m and 300m), while the traffic flow measure is based on a single buffer zone of 150m; secondly, the SAVIAH model also uses land use and other variables which moderate the effect of traffic volume in the surrounding area.

6.3.3 Relating health outcome to exposure to road traffic

Analysis of the correlation between health outcome and the traffic-related exposure measures was carried out by Jeremy Bullard, of the Department of Epidemiology and Public Health at Imperial College in London. This section will summarise his analysis.

Relationships of the prevalence of allergic symptoms to estimated exposure measures were analysed at the individual level by fitting logistic regression models. These models were fitted with various degrees of adjustment for confounders:

- without adjustment for covariates;
- age adjusted;
- age and sex adjusted;
- age, sex and deprivation adjusted;
- and age, sex, deprivation and school adjusted.

The full tabulations of odds ratio estimates and 95% confidence intervals are included in *Appendix 6A*.

In order to investigate reports from earlier research (Oosterlee *et al.* 1996, Brunekreef *et al.* 1997) that adverse effects of road traffic are greater in girls, the models were repeated for each gender separately. It was also thought that a weighted average of the home exposure and the school exposure (exposure = 0.67 * home exposure + 0.33 * school exposure) might be a better estimate of personal exposure than place of residence alone. However, results of this analyses were not significantly different from those given in *Appendix 6A*.

In order to investigate the effects of road type, models were fitted that included separate terms for density of main roads and density of non-main roads over 4m wide. A similar method was applied to investigate the effects of HGV traffic with adjustment for the overall traffic volume. Neither of these additional models produced any more informative results.

The principal results are summarised in *Table 6.10*. No substantial or significant associations were found between any measure of local traffic density of traffic-related pollution exposure and any wheezing outcome. There was an adverse association between traffic exposure and hay fever, but the same indices were positively related to eczema.

Positive skin prick responses to three common aero-allergens were not related to traffic exposure.

Table 6.10: Results of age, gender, deprivation adjusted odds ratios and 95% CI for the effects of road traffic pollution on wheeze and sever wheeze

Exposure		*Wheeze* OR (95% CI)	*Severe Wheeze* OR (95% CI)
Distance to nearest main road	>150m	1	1
	50-150m	0.98 (0.87 - 1.10)	0.99 (0.81-1.22)
	<50m	1.03 (0.89 - 1.18)	1.07 (0.84 - 1.38)
Density of main roads within 150m	none	1	1
	up to 200m	1.01 (0.86 - 1.19)	0.94 (0.69 - 1.28)
	200-400m	1.00 (0.89 - 1.12)	1.04 (0.85 - 1.27)
	>400m	0.96 (0.73 - 1.25)	1.10 (0.85 - 1.74)
Traffic volume within 150m	<250 v km/day	1	1
	250-1000 v km/d	1.05 (0.91 - 1.21)	0.97 (0.75 - 1.26)
	1000-2500 v km/d	1.02 (0.88 - 1.17)	1.06 (0.82 - 1.36)
	>2500 v km/day	1.02 (0.89 - 1.18)	1.15 (0.89 - 1.48)
SAVIAH modelled NO_2	10th v 90th % ile	0.98 (0.84 - 1.15)	0.84 (0.63 - 1.11)

The possible positive or negative confounding of the above relationships by indoor environmental variables was studied in the case-control sample. Traffic exposure was weakly correlated with most indoor environmental variables, and the odds ratios relating pollution exposure to asthma symptoms were little changed after further adjustment for housing tenure, parental smoking, gas cooking, pet ownership, type of bedding and dampness in the home.

The case-control sample was also used to investigate whether the inaccuracy of the location of the home address using postcode might affected the associations with estimated pollution. The effects of estimated pollution exposure using the exact address did not differ greatly from those using postcodes.

6.4 INTERPRETATION

Analysis of the health data for Sheffield showed no correlation between any of the exposure measures and respiratory illness. This raises a number of important questions, both about the reliability of the exposure methods used and about the validity of assumed associations between traffic related pollution and health outcome.

Analysis of the associations between exposure and health outcome are based on three key assumptions:

1. The exposure measures used provide a reliable estimate of actual exposures in a population;

2. The health data provide a reliable measure of variations in the health outcome; and

3. The underlying aetiological hypothesis is valid.

Each of these will be considered in turn below.

6.4.1 Do the exposure measures provide a reliable estimate of differences in exposure in the population?

The extent to which any of the measures used here, and indeed in most previous epidemiological studies, provide a reliable measure of exposure is uncertain. Measures used here in practice only measure ambient NO_2 concentrations. As seen, they seem to be reliable in this respect. But this poses two questions:

1. Is NO_2 a good measure of traffic-related pollution?

2. Does ambient concentration provide a valid measure of personal exposure?

NO_2 and traffic-related pollution: In this study NO_2 is used as a marker for traffic-related pollution. Similar assumptions are made in number of other studies, based on the principle that most of the ambient NO_2, especially in urban areas, comes from traffic. Nevertheless, this assumption needs to be examined. In Sheffield, no major local NO_2 sources exist in Sheffield. Even in London, where such sources do clearly exist, transport accounts for 76% of the NO_2 emissions in the emissions inventory. In general, therefore, it does seem safe to assume that road traffic is the major source of NO_2, and that variations in NO_2 concentrations are largely associated with road traffic.

Even so, NO_2 does not necessarily provide a marker for all traffic-related pollutants. Relationships between NO_x emissions and ambient NO_2 is also complex, and varies both spatially and temporally depending on concentrations of ozone and other precursors. Patterns of emissions of different pollutants also vary in relation to traffic speed and composition. NO_x emissions for light duty vehicles are lowest at ca. 30 km/hr and peak at high speeds. CO emissions peak at low speeds and are lowest at 70 km/hr. Particulates emissions show similar trends to CO. These differences are likely to be exacerbated in urban areas, where speeds are relatively low. Given that particulates are most important in terms of their health effects (Pope 1991, Hoek and Brunekreef 1993, Jansen *et al.* 1997), it means that NO_2 may not be the best available measure of health risk. On the other hand, fine particulates are very difficult to measure reliably at a high spatial density. At the same time doubts still exist about what characteristic of fine particulates is of greatest health relevance (e.g. which size fraction, number or mass of particulates, particulate composition). For these reasons, NO_2 is likely to remain as a general marker for traffic-related pollution in epidemiological studies.

Relationship between ambient concentration and exposure: The extent to which ambient concentration provides a valid measure of personal exposure is highly doubtful. Exposure is often defined as "contact of a chemical, physical and biological agent with the outer boundary of an organism" (Corvalán *et al.* 1996). As such, exposure of individuals in a population depends not on average concentrations at fixed points, but on variations in pollution experienced as individuals move in real time through a spatially and temporally changing pollution field.

Nor is outdoor exposure the only source of relevance for health risk. People spend the majority of time indoors. In well-ventilated homes a correlation does exist between outdoor and indoor concentrations (Wallace 1996, Kingham *et al.* submitted). Most epidemiological studies (including time series studies), however, have assumed that ambient concentrations do provide a valid measure of total exposure. Nevertheless, for many people, indoor exposures - for instance to emissions from smoking, gas cooking, gas heating, furnishings and chemicals - are likely to be more important risk factors.

Which measure of exposure is most relevant in terms of health is also uncertain. Whether peak exposure, average exposure, or frequency of exposure to high concentrations are most relevant to health is as yet still unknown.

For all these reasons, it is clear that ambient pollution is not an ideal measure of total exposure to pollution. Nevertheless, if the focus of attention is on the effects of road traffic, as here, then the methods used here do give an indication of spatial variations in potential exposure to traffic-related pollution. There is, however, a real need to extend the methods used in this study to produce time-varying measures of pollution fields, which can be combined with data on time activity within a GIS. In this way, it would be possible to model actual levels of exposure as people move through an environment. In principle, dispersion models such as ADMS-Urban should provide the capability for this. In practice, though, this study has suggested that ADMS Urban does not provide reliable measures of NO_2 concentration under conditions studied here. This, together with the high processing times needed for ADMS-Urban runs, would make it impracticable for most purposes.

6.4.2 How reliable are the health data

The health data used in this study could be criticised in that it is based on a questionnaire. Various studies have suggested that questionnaire surveys are susceptible to inaccuracies because of the bias in reporting, inaccurate or inconsistent recall, and the misinterpretation of questions. On the other hand, the questionnaire allowed a large sample to be surveyed. Together with a response rate of 79% this should have reduced any potential bias. Follow-up studies, through skin-prick tests and re-contacting of 1409 children two years later, provided rigorous validation of the results.

The health study focused on secondary school children, which might also create problems. As children age, they tend to lose early respiratory sensitivity, but may become more likely to show respiratory effects due to smoking and other substance abuse. As in any health study, potential problems might exist due to confounding by other risk factors, such as exposure to smoking, damp, pets, gas cooking and bedding materials or parental history of atopy and number of younger or older siblings. These factors are strictly controlled for in this study. Associations were found between respiratory illness and non-feather bedding and ownership of furry pets either at the time of survey or at birth (Strachan and Carey

1995). It was also notable that no association between exposure to traffic-related pollution and health was found either with or without control for confounding. Uncertainties must be acknowledged about the reliability of the health data, but overall the data seemed at least as reliable as that used in other published studies and, in view of large sample, considerably more so.

6.4.3 Does a relationship between exposure to traffic-related pollution and chronic respiratory illness exist?

The motivation for this study was the concern about association between exposure to traffic-related pollution and chronic health effects. It is easy to consider the lack of such association in the Sheffield study as evidence for failings in the methodology or study design. Nevertheless, the results need to be put into context. Although a reasonably consistent story has emerged from acute studies (Schwartz *et al.* 1989, Pope *et al.* 1991, Schwartz 1993, Pope 1991) and a number of positive studies have been published for chronic effects, the picture in relation to chronic studies is far from conclusive. Several other published studies have shown no effect for chronic exposure: e.g. in Huddersfield, Prague, Amsterdam (Elliott *et al.*. 1995) Hammersmith (Wills 1998), Tower Hamlets (Livingstone *et al.* 1996), London (Wilkinson *et al.* unpub), Stockholm (Pershagen *et al.* 1995) and Haarlem (Oosterlee *et al.* 1997). Various reasons for this lack of detectable chronic effect may be suggested. One is the likelihood that the relative risks are low; thus extremely accurate exposure classification and health outcome data are needed over large populations to detect any effect. Few studies have achieved this: the study reported here is one of the more rigorous in these respects. Another possibility is that, although air pollution may trigger respiratory symptoms in those already suffering from the illness, long term exposures to relatively low levels of pollution may not increase susceptibility to respiratory morbidity.

It is also important to recognise the tendency for bias in reporting in literature, in that positive studies tend to get preferentially published. To this extent, results found here are consistent with this growing body of evidence.

This study also has analysed a number of different exposure measures, all validated as far as possible against monitored NO_2 concentrations. All give a consistent story for the large health study. The possibility thus remains that, at the range of exposures considered here, no detectable risk of traffic-related pollution for chronic respiratory illness exists.

7 SUMMARY AND CONCLUSIONS

7.1 SUMMARY OF MAIN FINDINGS AND CONCLUSIONS

The research presented here has provided a range of results and findings, which have general importance not only for further research in the areas of environmental epidemiology and exposure assessment, but also for the management and policy applications of the methods concerned.

The case study in Sheffield, for example, has confirmed that passive sampling of NO_2 provides a reliable measure of relative levels of air pollution across an urban area, with CVs between tubes of approximately 5-10%. This supports several earlier investigations of passive sampling tubes (e.g. van Reeuwijk *et al.* 1998) and raises some doubts about the practical importance of some of the supposed errors which are meant to affect diffusion tubes (e.g. Gair and Penkett 1995, Heal and Cape 1997). Despite the concern expressed about the use of passive samplers, therefore, they do provide reliable means of validating and calibrating pollution models. When used in conjunction with such models they also provide effective means of mapping relative spatial variations in air pollution. However they did not necessarily give reliable estimates in absolute terms.

ISC3 (used as an area source model) performed badly when applied in London, and did not give reliable estimates of measured NO_2. - though it did perform marginally better than the line dispersion models used. The reason for its poor performance was largely because the emissions data used in the model were based upon a relatively coarse (1 km^2) emissions inventory, which was unable to detect local variations in air pollution. Use of a finer emissions inventory, if available, would no doubt improve performance of the model. Another potential source of error was the inclusion of high level emissions (e.g. from industrial sources) as ground-level emissions. Better discrimination between sources would also have improved model performance. The construction of a detailed emissions inventory was, however, beyond the scope of this study, and indeed is rarely feasible for either research or management purposes.

Performance of a simple line dispersion model (DMRB) varied between London and Sheffield, due to differences in the quality of the input data. In Sheffield, where data was more reliable, it performed relatively well, and results were moderately strongly and linearly correlated with measured NO_2 concentrations within ca. 200 metres of main roads. Indeed, in terms of the level of correlation, it out-performed both the ADMS and CALINE models. To some extent this is surprising, for - unlike the other line source models used - it does not take account of meteorological conditions. This may be a chance finding. It may, alternatively, imply that short-term weather conditions are relatively unimportant in relation to longer-term patterns in concentrations of traffic-related pollution. Local, spatial variations in emissions probably account for the large proportion of the variation in concentrations. Moreover, where meteorological factors are significant, they are probably poorly represented by the line-source models which typically use weather data from only a few, relatively remote sites, and thus do not adequately characterise local meteorological conditions. However, the DMRB model did consistently over-estimate measured concentrations within the 200 metre zone, and application of the model is limited by fact that it does not provide estimates beyond 200m. In London, the model performed poorly, reflecting the limited spatial accuracy of the input data.

Results from the more sophisticated line source dispersion models (CALINE3 and ADMS Urban) also varied depending on quality of input data. In London, CALINE3 performed poorly, again due to the poor spatial resolution of the input data. In Sheffield, where the input data were more accurate, performance was better, although not as good as other methods. The model tended to underestimate measured concentrations at low levels,

ADMS-Urban was only used in Sheffield. Results showed a strong curvilinear relationship with measured NO_2, and the model under-estimated ambient levels to a large extent. The reasons for this are not wholly clear, but seem to relate to inadequate characterisation either of emissions or of dispersion in the near-source zone. The results agree with other recent evaluations of ADMS, which have also shown a tendency for significant under-estimation of pollution levels in kerbside and intermediate areas, both in Northampton (Briggs *et al.* 1998) and Bristol (Bull unpublished). Results thus suggest that the use of more sophisticated dispersion models, such as ADMS-Urban, for air pollution mapping may not be justified. Certainly, further validation of ADMS-Urban is advisable before it is widely used for Air Quality Management purposes.

Kriging and co-kriging were only used in London, where they gave reasonably reliable estimates of measured NO_2 for background sites, but failed to detect local hotspots and steep pollution gradients near to road sources. In the case of ordinary kriging, this was largely to be expected, for the method uses data only on measured concentrations, and can thus only detect spatial variations which are adequately sampled by the monitoring network. The network of sites in London was clearly inadequate for this purpose. More surprising was the finding that co-kriging, using traffic volume/distance to the nearest road as a covariate, did not improve this performance. Overall, the implication is that the existing passive sampling monitoring network is far too sparse to characterise spatial variation in NO_2 concentrations in London, and that without a much more intensive network of monitoring sites it cannot, of itself, provide a basis for air pollution mapping. More generally, of course, this raises the question of how representative the network is of air pollution conditions in London, and what inferences can be drawn from the measurements.

The SAVIAH model was only used in Sheffield. The original SAVIAH model (Briggs *et al.* 1997) was found not to work well in Sheffield, because of inadequate characterisation of the altitude factor. The original data from Huddersfield were therefore reanalysed, and a revised model developed. This gave comparable results to the original version in Huddersfield, but also performed well in Sheffield, where results correlated strongly with measured NO_2. The model did, however, tend to over-estimate at low concentrations and under-estimate at high concentrations. The capability of this model to produce a detailed map of the air pollution surface across the entire study area is a major advantage. Further application of the revised model in other areas (Northampton, Ealing and Hammersmith) has also shown that it also performs consistently. The results thus suggest that the model can be used to map NO_2 concentrations across an urban area, based on local calibration with a small number (20-30) of passive samplers, deployed over 4-5 two-weekly campaigns across one year. The SAVIAH method thus seems to provide a simple, low-cost screening method for traffic-related pollutants and for identifying pollution hotspots.

Correlation between modelled and observed concentrations from both dispersion models and statistical methods varied in Sheffield between surveys, depending upon wind direction. Results showed that NO_2 concentrations were raised downwind due to accumulation of pollution from the city. None of the models were able to detect this effect. The results thus suggest the need to incorporate into the models further parameters to characterise the regional contribution to pollution.

Traditional exposure indicators (e.g. road density, distance from road, traffic volume) were only used in Sheffield, where they performed with varying effect. None of the indicators based on all roads performed well compared to indicators based only on main roads. This indicates that main roads are the major sources of traffic-related pollutants. The most reliable indicators for measured NO_2 were density of main roads within 150 metres, traffic flow within 150 metres and HGV flow within 150 metres. These, and other, proxy indicators have been widely used in epidemiological studies in the past. The differential performance of the various indicators suggest that they are likely to produce different exposure estimates. Choice of indicator is thus likely to affect the outcome of any epidemiological application.

In general, the quality of all exposure measures was highly dependent on the quality of input data. Most of the variation in traffic related pollutants occurs close to main roads, so the spatial accuracy of the road coverage and the quality of traffic flow data on these roads are crucial. In London, clearly, these data were not adequate. In these cases, it remains difficult to provide reliable estimates of exposure. This greatly limits the viability and reliability of large area studies, and poses severe constraints on epidemiological investigations aimed at detecting small relative risks. On the one hand, these need to include large populations in order to attain sufficient power to detect any effects; on the other hand, as the size of the study area increases, so does the difficulty in obtaining accurate exposure measures.

Overall, the most reliable methods for mapping exposure to traffic-related pollutants were considered to be the SAVIAH model, DMRB, density of main roads within 150 metres, traffic flow within 150 metres and HGV flow within 150 metres.

The SAVIAH model, density of main roads within 150 metres, traffic flow within 150 metres and HGV flow within 150 metres were used in a detailed investigation of relationships between traffic related pollutants and respiratory health in a sample of 18,000 schoolchildren in Sheffield. None of the exposure measures showed significant relationships with respiratory health, either with or without control for confounding by age, sex, history of family atopy, smoking, pets, bedding and other domestic factors. Several reasons for this lack of correlation between exposure and health outcome in this study were considered.

Firstly, it is apparent that a pollution map does not give a direct measure of exposure, in that it does not take account of people's movements through an environment. Modelling outdoor exposures also fails to take full account of indoor exposures, which are quantitatively likely to dominate: a general correlation between outdoor and indoor concentrations can be assumed (e.g. Spengler *et al.* 1994, Wallace 1996), in that much of the indoor pollution is derived from outdoors, but other sources - such as home heating, cooking and smoking - will be locally important. Improved measures of exposure will need to take account of time activity patterns of the exposed population and of indoor as well as outdoor sources.

Secondly, NO_2 may not be an ideal marker for those traffic related pollutants which are of greatest health concern (e.g. fine particulates). General correlations do exist between NO_2 and other traffic-related pollutants (Kingham *et al.* submitted) but these tend to break down at the local level, because of the differential effects of traffic speed, traffic composition, meteorological conditions and chemical processes on different pollutants. Unfortunately, models which can provide reliable estimates of fine particulates and VOCs do not yet exist, and there are limited monitoring data on these pollutants to provide a basis for developing empirical methods.

In addition, doubts remain about the temporal character of exposures to traffic related pollution. The measures used here provide indications of long term exposures (averaged over weeks or years). These may give reasonable estimates of total, chronic exposure to traffic related pollution. Shorter term, high concentration exposures, however, may be more important both in generating sensitivity to traffic related pollution and - almost certainly - in triggering particular health events. Equally, exposures at particular times of life (e.g. in the first few months or years of life) may be especially important in sensitisation (Committee on Medical Effects of Atmospheric Pollution 1995). The extent to which any of the exposure indicators used here, and in other previous research, are capable of detecting these effects is open to doubt.

These various uncertainties also pose the question of what type of measure provides the best indicator of exposure to traffic-related pollution. The assumption in this research has been that a pollution-specific measure, such as NO_2 concentration, provides the best measure of exposure: measured NO_2 concentrations were thus used as the 'golden mean' to assess performance of the different methods. In practice, this may not be the case. Given the aetiological uncertainties, it may at present be more appropriate to use non-specific indicators (such as distance from road or traffic volume), which give some form of integrated measure of exposure to all traffic-related pollutants. The problems with this of course are that such measures do not help to identify the causal agents (and thus do not cast light on the aetiological processes) and are themselves subject to significant measurement error and inconsistency. Moreover, as shown here, they also do not necessarily show any correlation with health outcome.

At the same time, therefore, the possibility must be considered that there is no association between chronic exposure to traffic-related pollutants, at the levels considered here, and respiratory health. Certainly there is strong evidence in the epidemiological literature for an acute effect (Committee on Medical Effects of Atmospheric Pollution 1995). Evidence for a chronic effect remains equivocal. As noted in *Chapter 2*, several studies have suggested an association with chronic exposures, but many of these have been based either on small samples and/or on relatively weak and unverified exposure indicators. Larger and more rigorous studies, such as the SAVIAH study (Elliott and Briggs 1998), and those by Livingstone *et al.* (1996) and Wilkinson *et al.* (unpub) indicate no detectable effect. The results of the Sheffield study need to be seen in this context.

Finally, this research has demonstrated that GIS provides a powerful and useful tool for modelling and mapping traffic related pollutants and for exposure estimation. When used in conjunction with methods applied here, GIS clearly provides the capability to generate detailed maps of traffic related pollutants, as basis for epidemiological investigations, air quality management and traffic planning.

7.2 IMPLICATIONS FOR FURTHER RESEARCH

There is a major need to improve methods for modelling exposure to air pollution. As this research has implied, this requires considerable development and improvement on the methods used here. Detailed information is required, for example, not only on long-term average pollution levels at high spatial resolution, but also on time activity of individuals, as well as changes in pollution levels over time. Time activity data are traditionally obtained from questionnaires and time activity diaries (Jantunen in press), but improved information can be obtained by using Global Positioning Systems (GPS) to monitor movements of recruited volunteers. GIS provides the capability to download GPS data and relate it to modelled pollution levels. The use of personal samplers and monitors would also allow real-time exposure data to be gathered for these individuals to validate modelled exposures. Alternatively the opportunity exists to use population-level time activity data to simulate movements through a pollution field using 'random-walk' methods. In this way it might be possible to obtain estimates of exposure across an entire population.

A more difficult problem is to derive detailed air pollution maps for short-time periods, on the basis of existing technology and data. Methods such as SAVIAH and DMRB are only valid for long-term averages (minimum of ca. 2 weeks). Dispersion models such as ADMS-Urban have the capability to provide estimates for short-term averages (e.g. 1 hour), but these are less reliable than longer term averages. Moreover, large processing times are needed to run these models for a large number of receptors, sources and hours, which makes them impracticable for many purposes. In addition, traffic data is rarely available at sufficiently high spatial and temporal resolution to feed these models, though it is possible to generate estimates of hourly flows using traffic models such as the widely used local authority trip model SATURN. The use of parallel processing may help to resolve this dilemma by removing the constraint of processing times. There is a real need, however, to develop more efficient dispersion models, written to optimise processing times. The recent development of AERMOD (Perry *et al.* 1994) provides one example of this approach, which may provide a basis for faster, more practicable modelling in future.

Another important development will be to improve the ability to use available information and exploit different capabilities of different models, by linking them together within a GIS.

One such development within the scope of this research is combining spatial statistical methods (e.g. kriging) with dispersion modelling, to help derive detailed and spatially continuous pollution maps using both monitored and modelled data (Collins 1998a). Co-kriging seems to offer especial potential in this respect, since it allows incorporation of secondary variables, which may help in detecting local hotspots.

The relationship between traffic related pollutants and chronic health outcome, meanwhile, remains unresolved. Research to date has been inconsistent and inconclusive, partly because of the difficulties in obtaining reliable estimates of exposure. There is, perhaps, a need to move away from simple, indirect markers of exposure, such as NO_2 and obtain more direct measures of pollutants of health concern (e.g. fine particulates). This again requires improvements in dispersion models, which are not well adapted to fine particulates and volatile compounds (e.g. PAHs). There is also a need to consider the role of traffic related pollutants in a wider context of other exposures, including indoor pollution. This implies the need to estimate total exposure, and to be able to partition total exposure to different indoor and outdoor sources, on basis of time activity patterns. It also implies the need to consider synergistic effects of different pollutants, rather than the simple 'single pollutant' approach.

The methods used and tested here can thus help to investigate relationships between traffic related pollution and health, and to assess the risks of exposures to pollution from road traffic. GIS also provide a powerful environment within which to model exposures, as this research has shown. Nevertheless, major advances still remain to be made before we can obtain reliable estimates of exposure across large populations at a spatial and temporal level adequate to resolve the underlying question: to what extent does chronic exposure to traffic related pollution affect human health?

APPENDIX 3A

AML WRITTEN FOR USE IN ARC/INFO TO DERIVE INDICATORS

```
/*-----------------------------------------------------------
/*
/*      s1.aml;  calculates density of roads in
/*               a 150 meters buffer around individual points
/*
/*
/*      20/10/97  by C. de Hoogh
/*
/*-----------------------------------------------------------


&s file_id [open een.txt openstat -r]

&if %openstat% ne 0 &then
  &return &error Error in creating file
&else &type File is created

&s id [read %file_id% readstat]

&s file [open test.txt openstat -w]

&do &while %readstat% ne 102
  &call gamaar
&end

&s closestat [close %file%]
&s closestat [close %file_id%]

&return

/*--------------
&routine gamaar
/*--------------

reselect /home/kees/sheff/bigl temp point
res bigl-id = %id%
~
n
n

buffer temp temp_buf # # 150 # point

build temp_buf poly

intersect roads3 temp_buf sel_rds line

statistics sel_rds.aat sum.lut
sum length
~
n
n


&data arc info
ARC
SELECT SUM.LUT
EXPORT /HOME/KEES/SHEFF/OSCAR/TEMP.TXT SDF SUM-LENGTH
DELETE SUM.LUT
Y
Q STOP
```

```
&end

&s file1 [open temp.txt openstat -r]
&s x [read %file1% readstat]
&s closestat [close %file1%]
rm temp.txt

&s writestat [write %file% [quote %id%,%x%,]]
&s closestat [close %file1%]

kill temp
kill temp_buf
kill sel_rds
rm temp.txt

&s id [read %file_id% readstat]

&return



/*----------------------------------------------------------
/*
/*      sum.aml;  calculates weighted traffic volume in
/*          a 150 meters buffer around individual points
/*
/*      temporary coverages: temp, temp_buf, sel_rds
/*          temporary files: sum.lut,temp.txt
/*               final file: sum.txt
/*
/*      22/10/97  by C. de Hoogh
/*
/*----------------------------------------------------------


&s file_id [open een.txt openstat -r]

&if %openstat% ne 0 &then
  &return &error Error in creating file
&else &type File is created

&s id [read %file_id% readstat]

&s file [open test.txt openstat -w]

&do &while %readstat% ne 102
  &call gamaar
&end

&s closestat [close %file%]
&s closestat [close %file_id%]

&return

/*--------------
&routine gamaar
/*--------------

reselect /home/kees/sheff/big1 temp point
res big1-id = %id%
~
```

```
n
n

buffer temp temp_buf # # 150 # point

build temp_buf poly

intersect roads3 temp_buf sel_rds line

statistics sel_rds.aat sum.lut
sum length flow
~
n
n


&data arc info
ARC
SELECT SUM.LUT
EXPORT /HOME/KEES/SHEFF/OSCAR/TEMP.TXT SDF SUM-W-LENGTH
DELETE SUM.LUT
Y
Q STOP
&end

&s file1 [open temp.txt openstat -r]
&s x [read %file1% readstat]
&s closestat [close %file1%]
rm temp.txt

statistics sel_rds.aat sum.lut
sum length hgv2
~
n
n


&data arc info
ARC
SELECT SUM.LUT
EXPORT /HOME/KEES/SHEFF/OSCAR/TEMP.TXT SDF SUM-W-LENGTH
DELETE SUM.LUT
Y
Q STOP
&end
&s file1 [open temp.txt openstat -r]
&s y [read %file1% readstat]
&s writestat [write %file% [quote %id%,%x%,%y%]]
&s closestat [close %file1%]

kill temp
kill temp_buf
kill sel_rds
rm temp.txt

&s id [read %file_id% readstat]

&return
```

APPENDIX 3B

AML WRITTEN FOR USE IN ARC/INFO TO CREATE CALINE3 INPUT FILES

```
/*------------------------------------------------------
/*
/*          cal3shef.aml; writes a caline3 file from a
/*                        coord. text file
/*
/*          27/11/97  by C. de Hoogh
/*
/*------------------------------------------------------

&s file_xy [open sh_sites.txt openstat -r]
/*&s fi2 [open concall.txt openstat -w]

&s .file_bat [open mbat.bat openstat -w]

&if %openstat% ne 0 &then
  &return &error Error in creating file
&else &type File is created

&s line [read %file_xy% readstat]

&do &while %readstat% ne 102
  &call gamaar
&end

&s closestat [close %.file_bat%]

&return

/*--------------
&routine gamaar
/*--------------

&s .nr [extract 1 %line%]
&s .x [extract 2 %line%]
&s .y [extract 3 %line%]
&s .x [format '%1%' %.x%]
&s .y [format '%1%' %.y%]

create circle /home/kees/sheff/no2sites
generate circle
circles
1,%.x%,%.y%,200
end
quit

build circle polys

/* starline coverage is build, now buffer

intersect /home/kees/sheff/oscar/roads250 circle shef_circle1 line
build shef_circle1 node
addxy shef_circle1 node

&data arc info
ARC
SELECT SHEF_CIRCLE1.AAT
EXPORT /HOME/KEES/CAL3/CIRCLE_SDF SDF ROADS250#
Q STOP
&end

/*
```

```
&s file1 [open link_id openstat -w]
&s file2 [open link openstat -w]
/*&s file102 [open link_id2 openstat -w]
/*&s file103 [open link_id3 openstat -w]
/*&s file104 [open link_id4 openstat -w]
/*&s file105 [open link_id5 openstat -w]

&s fil1 [open flow openstat -w]
&s .circle_sdf [open circle_sdf openstat -r]

&s .id [read %.circle_sdf% readstat]
&s c = 1

ap

&do &while %readstat% ne 102
  &call link
  &s .id [read %.circle_sdf% readstat]
&end

&s writestat [write %fil1% [quote 0]]

quit

&s closestat [close %file1%]
&s closestat [close %file2%]
&s closestat [close %fil1%]
&s closestat [close %.circle_sdf%]

&call write

kill circle
kill shef_circle1

rm flow
rm link_id
rm link
rm circle_sdf

&s line [read %file_xy% readstat]

&return

/*-----------
&routine link
/*-----------

reselect shef_circle1 arcs roads250# = %.id%
writeselect kees.sel
clearselect
arc reselect shef_circle1 shef_sel arcs kees.sel

&data arc info
ARC
SELECT SHEF_SEL.AAT
EXPORT /HOME/KEES/CAL3/SHEF_SDF SDF FLOW
SELECT SHEF_SEL.NAT
EXPORT /HOME/KEES/CAL3/SHEF_SDF2 SDF X-COORD,Y-COORD
Q STOP
&end
```

```
&s file4 [open shef_sdf openstat -r]
&s file3 [open shef_sdf2 openstat -r]

/*&s file5 [open flow openstat -w]

&if %openstat% ne 0 &then
  &return &error Error in creating file
&else &type File is created

&s r1 [read %file4% readstat]
&s r2 [read %file3% readstat]
&s r3 [read %file3% readstat]


&s writestat [write %fil1% %r1%]
&format 0
&s fx [before %r2% ,]
&s fx [format '%1%' %fx%]
&s fy [after %r2% ,]
&s fy [format '%1%' %fy%]
&s tx [before %r3% ,]
&s tx [format '%1%' %tx%]
&s ty [after %r3% ,]
&s ty [format '%1%' %ty%]
&s writestat [write %file1% [format '%1,-20%AG%2,-7%%3,-7%%4,-7%%5,-
7%%6,-8%100.0.0010.0' %.id% %fx% %fy% %tx% %ty% %r1%]]

&s closestat [close %file4%]
&s closestat [close %file3%]
/*&s closestat [close %file4%]
/*&s closestat [close %file5%]

&s d [delete shef_sdf]
&s d [delete shef_sdf2]
arc kill shef_sel
&s d [delete kees.sel]



&s writestat [write %file2% [quote link%c%]]

/*&call write

/*&s .id [read %.id_sdf% readstat]
&s c = %c% + 1

&return

/*------------
&routine write
/*------------

/*------------------------
/*WRITE THE CALINE3 DAT FILE
/*------------------------

&s file10 [open sh1_%.nr%.dat openstat -w]

&if %openstat% ne 0 &then
  &return &error Error in creating file
&else &type File is created
```

```
&s .a %c% - 1
&s ti caline3run
&s writestat [write %file10% [format '%1,-
40%60.0150..000015.00011.00000000' %ti%]]

/* writes nr 1,2,3,... in input file
&s b = 1

/*&s writestat [write %file1% %b%]

/* writes receptorpoints to inputfile
&s .z = 2
&s writestat [write %file10% [format '%1,-20%%2,-10%%3,-10%%4,-10%'
%.nr% %.x% %.y% %.z%]]
&s met 336
&s writestat [write %file10% [format '
%1,-3%%2,-3%' %.a% %met%]]

/* writes link coordinates to inputfile

&s file12 [open link_id openstat -r]
&s nam [read %file12% readstat]

&do &while %readstat% ne 102
  &s writestat [write %file10% %nam%]
  &s nam [read %file12% readstat]
&end

&s closestat [close %file12%]
&s closestat [close %file10%]

&r shefcal.aml

&return
```

APPENDIX 3C

AMLS WRITTEN FOR USE IN ARC/INFO TO RUN DMRB

```
/*------------------------------------------------------------
/*
/*          DMRB_plus.aml;  Runs the DMRB-model for a number
/*                          of receptors and a road network
/*
/*          13/2/97  by C. de Hoogh
/*
/*------------------------------------------------------------

&s file_xy [open coord.txt openstat -r]
&s fi2 [open concall.txt openstat -w]

&if %openstat% ne 0 &then
  &return &error Error in creating file
&else &type File is created

&s line [read %file_xy% readstat]

&do &while %readstat% ne 102
  &call gamaar
&end

&type kees

&s closestat [close %fi2%]

&type kees

&r recal

&return

/*--------------
&routine gamaar
/*--------------

&s .nr [extract 1 %line%]
&s .x [extract 2 %line%]
&s .y [extract 3 %line%]
/*&s .speed [extract 4 %line%]
/*&s .speed [calc %.speed% * 1.609344]
&s .speed 25

create circle /home/kees/sheff/no2sites
generate circle
circles
1,%.x%,%.y%,200
end
quit

create dmrb_point /home/kees/sheff/no2sites
generate dmrb_point
points
1,%.x%,%.y%
end
quit

build circle polys
build dmrb_point points
/* starline coverage is build, now buffer
```

```
intersect /home/kees/sheff/oscar/r2_gen3 circle she_circle1 line

&data arc info
ARC
SELECT SHE_CIRCLE1.AAT
EXPORT /HOME/KEES/DMRB/CIRCLE_SDF SDF R2_GEN3-ID
Q STOP
&end

/*
&s file1 [open link_id openstat -w]
&s file2 [open link openstat -w]
&s fill [open flow openstat -w]
&s .circle_sdf [open circle_sdf openstat -r]
&s .file_conc [open conc%.nr%.txt openstat -w]

&if %openstat% ne 0 &then
  &return &error Error in creating file
&else &type File is created

&s .id [read %.circle_sdf% readstat]
&s c = 1

ap
/*display 9999
/*mape circle
/*arcs circle
/*linecolor yellow
/*arcs ken_traffic
/*markercolor green
/*nodes ken_traffic

&do &while %readstat% ne 102
  &call link
  &s .id [read %.circle_sdf% readstat]
&end

quit

&s writestat [write %.file_conc% [quote 0,0]]

&s closestat [close %file1%]
&s closestat [close %file2%]
&s closestat [close %fill%]
&s closestat [close %.circle_sdf%]
&s closestat [close %.file_conc%]



kill circle
kill she_circle1
rm flow
rm link_id
rm link
rm circle_sdf
kill dmrb_point

&call write

&s line [read %file_xy% readstat]
```

```
&return

/*-----------
&routine link
/*-----------

linecolor red

reselect /home/kees/sheff/oscar/r2_gen3 arcs r2_gen3-id = %.id%

/*arcs ken_traffic

writeselect kees.sel
clearselect
arc reselect /home/kees/sheff/oscar/r2_gen3 she_sel arcs kees.sel

/*arcs ken_sel

arc near dmrb_point she_sel line 200 she_near

&data arc info
ARC
SELECT SHE_SEL.AAT
EXPORT /HOME/KEES/DMRB/SHE_SDF SDF FLOW
SELECT SHE_NEAR.PAT
EXPORT /HOME/KEES/DMRB/SHE2_SDF SDF DISTANCE
Q STOP
&end

&s file4 [open she_sdf openstat -r]
&s file3 [open she2_sdf openstat -r]

/*&s file5 [open flow openstat -w]

&if %openstat% ne 0 &then
  &return &error Error in creating file
&else &type File is created

&s .flow [read %file4% readstat]
&s .dist [read %file3% readstat]

&s closestat [close %file4%]
&s closestat [close %file3%]

&s d [delete she_sdf]
&s d [delete she2_sdf]
arc kill she_sel
arc kill she_near
&s d [delete kees.sel]


&s c = %c% + 1

&type distance = %.dist% and traffic-volume = %.flow%

&r speed1

&r speed2

&r calcul
```

```
&return

/*----------------------
&routine write
/*----------------------

&s fi [open conc%.nr%.txt openstat -r]
&s line [read %fi% readstat]
&s a [extract 2 %line%]
&s line [read %fi% readstat]
&s b [extract 2 %line%]
&s a [calc %a% + %b%]

&do &while %b% ne 0
  &call een
&end

&call twee

&return

&routine een

&s line [read %fi% readstat]
&s b [extract 2 %line%]
&s a [calc %a% + %b%]

&return

&routine twee

&s writestat [write %fi2% [quote %.nr%,%a%]]
&s closestat [close %fi%]
/*&s closestat [close %fi2%]

&return
```

```
/*------------------------------------
/*
/*  recal.aml; calculates the 98%ile of
/*             hourly NO2 (ppb), is called
/*             up by DMRB_PLUS.aml
/*
/*  19/6/97 by C. de Hoogh
/*------------------------------------

&s file1 [open concall.txt openstat -r]
&s file2 [open ppb.txt openstat -w]

&if %openstat% ne 0 &then
  &return &error Error in creating file
&else &type File's are created

&s record [read %file1% readstat]
&s id [extract 1 %record%]
&s peak [extract 2 %record%]

&do &while %readstat% ne 102
  &call calc
  &s writestat [write %file2% [quote %id%,%y%]]
  &s record [read %file1% readstat]
  &s id [extract 1 %record%]
  &s peak [extract 2 %record%]
&end

&s closestat [close %file1%]
&s closestat [close %file2%]

&return

/*---------------------------
&routine calc
/*---------------------------

&if %peak% >= 200 &then
  &call three
&else
  &if %peak% <= 20 &then
    &call one
  &else &call two

&return

/*---------------------------
&routine one
/*---------------------------

&s y [calc 1.65 * %peak%]
&return

/*---------------------------
&routine two
/*---------------------------

&s y2 [calc %peak% * %peak%]
&s y3 [calc %peak% * %y2%]
&s x1 [calc 0.3712 * %peak%]
&s x2 [calc 0.0014 * %y2%]
```

```
&s x3 [calc 0.0000029 * %y3%]
&s y [calc 26.2967 + %x1% - %x2% + %x3%]
&return

/*---------------------------
&routine three
/*---------------------------

&s y [calc 0.0984 * %peak%]
&s y [calc 49.11 + %y%]
&return


/*------------------------------------------------
/*
/*      calcul.aml; calculates  NOX_PPB for a given
/*                  distance (DMRB; figure 2b)
/*
/*      10-2-97  by  C. de Hoogh
/*
/*------------------------------------------------

&s x %.dist%

&if %x% <= 47.5 &then
  &call close
&else &call far

/*&type NOX_PPB = %y%
&s ph [calc %.flow% * 0.05]

&s li [calc 0.84 * %ph%]
&s li [calc 0.81 * %.lv% * %li%]
&s he [calc 0.16 * %ph%]
&s he [calc 4.15 * %.hv% * %he%]
&s tot [calc %li% + %he%]
&s con [calc %y% * %tot%]
&s con [calc %con% / 1000]

&type Total contribution for section %.id% = %con% ppb NOx

&s writestat [write %.file_conc% [quote %.id%,%con%]]

&return

/*--------------
&routine close
/*--------------

&s y2 [calc %x% * %x%]
&s y3 [calc %x% * %y2%]
&s x1 [calc 4.519 * %x%]
&s x2 [calc 0.032 * %y2%]
&s x3 [calc 0.00008 * %y3%]
&s y [calc 219.738 - %x1% + %x2% - %x3%]

&return

/*--------------
&routine far
/*--------------
```

```
&s y2 [calc -0.0199 * %x%]
&s y3 [calc 2.7182818 ** %y2%]
&s y [calc 166.886 * %y3%]

&return

/*--------------------------------------------------
/*
/*     calcul2.aml; calculates  98%ile 1-hour conc
/*                  (ppb) from average peak hour NOx
/*                  conc (ppm);(DMRB; figure 6b)
/*
/*     15-2-97  by  C. de Hoogh
/*
/*--------------------------------------------------

&s file1 [open concall.txt openstat -r]
&s file2 [open no2ppb.txt openstat -w]

&if %openstat% ne 0 &then
  &return &error Error in creating file
&else &type file is created

&s rec [read %file1% readstat]

&do &while %readstat% ne 102
  &call loops
&end

&s closestat [close %file1%]
&s closestat [close %file2%]

/*---------------
&routine loops
/*---------------

&s id [extract 1 %rec%]
&s conc [extract 2 %rec%]

&if %conc% < 40 &then
  &do
    &call call1
  &end
&else
  &do
    &if %conc% >= 40 & %conc% < 100 &then
      &do
        &call call2
      &end
    &else
      &do
        &if %conc% >= 100 & %conc% < 200 &then
          &do
            &call call3
          &end
        &else
          &do
            &if %conc% >= 200 &then
              &do
                &call call4
```

```
              &end
            &else
              &do
                &goto eind
              &end
          &end
      &end
  &end

&label eind

&s writestat [write %file2% [quote %id%,%conc%,%a%]]

&s rec [read %file1% readstat]

&return

/*-------------
&routine call1
/*-------------

&s a [calc 1.6 * %conc%]

&return

/*-------------
&routine call2
/*-------------

&s a [calc 0.239 * %conc%]
&s a [calc %a% + 28]

&return

/*-------------
&routine call3
/*-------------

&s a [calc 0.1475 * %conc%]
&s a [calc %a% + 37]

&return

/*-------------
&routine call4
/*-------------

&s a [calc 0.098 * %conc%]
&s a [calc %a% + 48]

&return

/*----------------------------
/* for light duty vehicles
/*----------------------------

&if %.speed% <= 55 &then
  &call inv
&else &call qua

&return
```

```
/*-----------
&routine inv
/*-----------

&s y [calc 15.6485 / %.speed%]
&s .lv [calc 0.4008 + %y%]

&return

/*-----------
&routine qua
/*-----------

&s y2 [calc %.speed% * %.speed%]
&s x1 [calc  -0.0158 * %.speed%]
&s x2 [calc 0.0001 * %y2%]
&s .lv [calc 1.1272 + %x1% + %x2%]
&return


/*-----------------------------
/* for heavy duty vehicles
/*-----------------------------

&if %.speed% <= 70 &then
  &call cub2
&else &call qua2

&return

/*-----------
&routine cub2
/*-----------

&s y2 [calc %.speed% * %.speed%]
&s y3 [calc %.speed% * %y2%]
&s x1 [calc -0.0720 * %.speed%]
&s x2 [calc 0.0011 * %y2%]
&s x3 [calc -0.000006 * %y3%]
&s .hv [calc 2.4888 + %x1% + %x2% + %x3%]
&return

/*-----------
&routine qua2
/*-----------

&s y2 [calc %.speed% * %.speed%]
&s x1 [calc  -0.0561 * %.speed%]
&s x2 [calc 0.0004 * %y2%]
&s .hv [calc 2.6593 + %x1% + %x2%]
&return
```

APPENDIX 3D

DMRB GRAPHS

98th Percentile of 1 hour average Nitrogen dioxide concentration of total oxides of nitrogen in the peak traffic hour

Distance	*NO_x (ppb)*
5	200.4
10	189.1
15	162.2
20	138.7
25	119.3
30	103.2
35	89.8
40	78.4
45	68.8
50	60.6
55	53.4
60	47.3
65	41.9
70	37.2
75	33.1
80	29.5
85	26.4
90	23.6
95	21.2
100	19.1
105	17.2
110	15.5
115	14.1
120	12.8
125	11.7
130	10.7
135	9.8
140	9.1
145	8.4
150	7.8
155	7.3
160	6.8
165	6.4
170	6
175	5.7
180	5.3
185	5.1
190	4.8
195	4.5
200	4.2

(Department of Transport, 1994)

Total oxides of nitrogen concentration produced by 1000 veh hour^{-1} travelling at a speed of 100 km hr^{-1} as a function of distance from a road and the curve estimations

Average Peak Hour NO_x concentration (ppm)	*98%ile 1-hour NO_2 concentration (ppm)*
0	0
20	33
40	39.3
60	44.2
80	48.3
100	51.9
120	55.2
140	58.3
160	61.2
180	63.9
200	66.5
220	69.1
240	71.5
260	73.9
280	76.3
300	78.5
320	80.8
340	83
360	85.1
380	87.3
400	89.4
420	91.5
440	93.5
460	95.6
480	97.6
500	99.6
520	101.5
540	103.5
560	105.5
580	107.4
600	109.3
620	111.2
640	113.1
660	115
680	116.9
700	118.8
720	120.7
740	122.5
760	124.4
780	126.2
800	128
820	129.9
840	131.7
860	133.5
880	135.3
900	137.1
920	138.9
940	140.7
960	142.5
980	144.3
1000	146

APPENDIX 3E

AMLs WRITTEN FOR USE IN ARC/INFO TO CREATE ISC3 INPUT FILES AND TO CONVERT OUTPUT FILES INTO ARC/INFO COVERAGES

WR_POINT.aml; writes 6 input files for ISC3 for one specified receptor point. It was necessary to create 6 input files, because the number of area sources exceeded the maximum number of sources allowed for one run.

ADDCONC.aml; after running ISC3 for the 6 input files, ADDCONC.aml then reads the output files (plt files) and adds up the concentration for the one receptor.

```
/*---------------------------------------------------------------------
/*
/*        wr_point.aml; writes input files for isc3 with only one
/*                      receptor point
/*
/*        28/9/96     C. de Hoogh
/*
/*---------------------------------------------------------------------

&s f1 [open a1.inp openstat -r]
&s f7 [open /home/kees/isc_files/%.new%1.inp openstat -w]
&s no a1

&if %openstat% ne 0 &then
  &return &error Error in creating file1
&else &type file1 is created

&call write

&s closestat [close %f1%]
&s closestat [close %f7%]
&s f1 [open a2.inp openstat -r]
&s f7 [open /home/kees/isc_files/%.new%2.inp openstat -w]
&s no a2

&if %openstat% ne 0 &then
  &return &error Error in creating file2
&else &type file2 is created

&call write

&s closestat [close %f1%]
&s closestat [close %f7%]
&s f1 [open a3.inp openstat -r]
&s f7 [open /home/kees/isc_files/%.new%3.inp openstat -w]
&s no a3

&if %openstat% ne 0 &then
  &return &error Error in creating file3
&else &type file3 is created

&call write

&s closestat [close %f1%]
&s closestat [close %f7%]
&s f1 [open a4.inp openstat -r]
&s f7 [open /home/kees/isc_files/%.new%4.inp openstat -w]
&s no a4
```

```
&if %openstat% ne 0 &then
  &return &error Error in creating file4
&else &type file4 is created

&call write

&s closestat [close %f1%]
&s closestat [close %f7%]
&s f1 [open a5.inp openstat -r]
&s f7 [open /home/kees/isc_files/%.new%5.inp openstat -w]
&s no a5

&if %openstat% ne 0 &then
  &return &error Error in creating file5
&else &type file5 is created

&call write

&s closestat [close %f1%]
&s closestat [close %f7%]
&s f1 [open a6.inp openstat -r]
&s f7 [open /home/kees/isc_files/%.new%6.inp openstat -w]
&s no a6

&if %openstat% ne 0 &then
  &return &error Error in creating file6
&else &type file6 is created

&call write

&return
/*---------------
&routine write
/*---------------

&s writestat [write %f7% 'CO STARTING']
&s writestat [write %f7% 'CO TITLEONE TEST FOR THE AREA SOURCES']
&s writestat [write %f7% 'CO MODELOPT DFAULT CONC URBAN']
&s writestat [write %f7% 'CO AVERTIME ANNUAL']
&s writestat [write %f7% 'CO POLLUTID NOX']
&s writestat [write %f7% 'CO FLAGPOLE 1.5']
&s writestat [write %f7% 'CO RUNORNOT RUN']
&s writestat [write %f7% 'CO FINISHED']
&s writestat [write %f7% ' ']
&s writestat [write %f7% 'SO STARTING']
&s writestat [write %f7% ' ']

&s record [read %f1% readstat]

&do &while %readstat% ne 102
  &s writestat [write %f7% %record%]
  &s record [read %f1% readstat]
&end

&s writestat [write %f7% ' ']
&s writestat [write %f7% '** TO CONVERT THE M2 INTO M2 CONCENTRATIONS ']
&s writestat [write %f7% 'SO EMISUNIT 1.0E6  GRAMS/(SEC-M**2)
MICROGRAMS/CUBIC-METER ']
&s writestat [write %f7% ' ']
&s writestat [write %f7% 'SO SRCGROUP ALL ']
&s writestat [write %f7% 'SO FINISHED ']
```

```
&s writestat [write %f7% ' ']
&s writestat [write %f7% 'RE STARTING ']
/*&s writestat [write %f7% ' ']
&s writestat [write %f7% [quote RE DISCCART %.xcoord% %.ycoord%]]
&s writestat [write %f7% 'RE FINISHED ']
&s writestat [write %f7% ' ']
&s writestat [write %f7% 'ME STARTING']
&s writestat [write %f7% 'ME INPUTFIL /home/kees/isc_files/lon100.sta']
&s writestat [write %f7% 'ME ANEMHGHT  10.0 METERS']
&s writestat [write %f7% 'ME SURFDATA  1 1991 london']
&s writestat [write %f7% 'ME UAIRDATA  1 1991 london']
&s writestat [write %f7% 'ME STARDATA ANNUAL']
&s writestat [write %f7% 'ME AVESPEED 1.0 1.8 3.4 5.5 8.4 10.0 ']
&s writestat [write %f7% 'ME AVETEMPS ANNUAL 288 288 288 288 288 288']
&s writestat [write %f7% 'ME AVEMIXHT ANNUAL A 6*1300.0']
&s writestat [write %f7% 'ME AVEMIXHT ANNUAL B 6*900.0']
&s writestat [write %f7% 'ME AVEMIXHT ANNUAL C 6*850.0']
&s writestat [write %f7% 'ME AVEMIXHT ANNUAL D 6*800.0']
&s writestat [write %f7% 'ME AVEMIXHT ANNUAL E 6*400.0']
&s writestat [write %f7% 'ME AVEMIXHT ANNUAL F 6*100.0']
/*&s writestat [write %f7% '   STARTEND  1995 10 30 1 1995 11 12 24']
&s writestat [write %f7% 'ME FINISHED']
&s writestat [write %f7% ' ']
&s writestat [write %f7% 'OU STARTING']
&s writestat [write %f7% 'OU RECTABLE SRCGRP INDSRC']
&s writestat [write %f7% 'OU MAXTABLE 10 INDSRC SRCGRP SOCONT']
&s writestat [write %f7% [quote OU PLOTFILE ANNUAL ALL
/home/kees/isc_files/%no%.plt]]
&s writestat [write %f7% 'OU FINISHED']

&return

/*-----------------------------------------------------
/*
/*       addconc.aml
/*
/*       reads plt files and adds up concentrations
/*       OUTPUT: pointfile with 1 point and 1 conc
/*
/*       26/9/96   C. de Hoogh
/*
/*-----------------------------------------------------

&s fil1 [open /home/kees/isc_files/a1.plt openstat -r]
&s fil2 [open /home/kees/isc_files/a2.plt openstat -r]
&s fil3 [open /home/kees/isc_files/a3.plt openstat -r]
&s fil4 [open /home/kees/isc_files/a4.plt openstat -r]
&s fil5 [open /home/kees/isc_files/a5.plt openstat -r]
&s fil6 [open /home/kees/isc_files/a6.plt openstat -r]
&s file2 [open /home/kees/isc_files/%.new%.txt openstat -w]

&if %openstat% ne 0 &then
  &return &error Error in creating file
&else &type File is created

&do I := 1 &to 8
  &s record := [read %fil1% readstat]
&end

&s record := [read %fil1% readstat]
&s con1 [substr %record% 30 13]
```

```
&s xcoord [substr %record% 3 6]
&s ycoord [substr %record% 17 6]
&type %xcoord%,%ycoord%,%con1%

&do I := 1 &to 8
  &s record := [read %fil2% readstat]
&end

&s record := [read %fil2% readstat]
&s con2 [substr %record% 30 13]
&type con2 = %con2%

&do I := 1 &to 8
  &s record := [read %fil3% readstat]
&end

&s record := [read %fil3% readstat]
&s con3 [substr %record% 30 13]
&type %con3%

&do I := 1 &to 8
  &s record := [read %fil4% readstat]
&end

&s record := [read %fil4% readstat]
&s con4 [substr %record% 30 13]
&type %con4%

&do I := 1 &to 8
  &s record := [read %fil5% readstat]
&end

&s record := [read %fil5% readstat]
&s con5 [substr %record% 30 13]
&type %con5%

&do I := 1 &to 8
  &s record := [read %fil6% readstat]
&end

&s record := [read %fil6% readstat]
&s con6 [substr %record% 30 13]
&type %con6%

&s closestat [close %fil1%]
&s closestat [close %fil2%]
&s closestat [close %fil3%]
&s closestat [close %fil4%]
&s closestat [close %fil5%]
&s closestat [close %fil6%]

&s 1 [trim %con1% -both ' ']
&s 2 [trim %con2% -both ' ']
&s 3 [trim %con3% -both ' ']
&s 4 [trim %con4% -both ' ']
&s 5 [trim %con5% -both ' ']
&s 6 [trim %con6% -both ' ']


&s conc [abs [calc %1% + %2% + %3% + %4% + %5% + %6%]]
&type %conc%
```

```
/*&s file2 [open t2.txt openstat -w]

&if %openstat% ne 0 &then
  &return &error Error in creating file
&else &type file is created

/*&s writestat [write %file2% 'Dit is de eerste lijn']
&s writestat [write %file2% [quote 1,%xcoord%,%ycoord%,%conc%]]

&s closestat [close %file2%]

&return
```

APPENDIX 3F

AMLS WRITTEN FOR USE IN ARC/INFO TO CROSS VALLIDATE THE COKB3DM-PROGRAMME AND TO CONVERT OUTPUT FILES INTO ARC/INFO COVERAGE

```
/*--------------------------------
/*
/*  cokr.aml; performs cokriging
/*            cross-validation
/*
/*  C. de Hoogh, 20/4/98
/*
/*---------------------------------

&s file7 [open b95b3.out openstat -w]
&s file6 [open xy94.txt openstat -r]

&s a 11
&s b 42
&s counter 1

&label again

&s file1 [open 95b2.dat openstat -r]
&s file2 [open 95_tem.dat openstat -w]

&do I = 1 &to %a%
 &s line [read %file1% readstat]
 &s writestat [write %file2% %line%]
&end

&s line [read %file1% readstat]

&do I = 1 &to %b%
 &s line [read %file1% readstat]
 &s writestat [write %file2% %line%]
&end

&s closestat [close %file1%]
&s closestat [close %file2%]

&call par

&call run

&call out

&s a %a% + 1
&s b %b% - 1
&s counter %counter% + 1

&if %counter% = 43 &then
 &goto finish
&else
 &goto again

/*&do &until %a% eq 46
/* &goto again
/*&end

&label finish

&s file1 [open 95b2.dat openstat -r]
&s file2 [open 95_tem.dat openstat -w]

&do I = 1 &to 53
```

```
 &s line [read %file1% readstat]
 &s writestat [write %file2% %line%]
&end

&s closestat [close %file1%]
&s closestat [close %file2%]


&call par

&call run

&call out

&s closestat [close %file6%]
&s closestat [close %file7%]
rm 95_tem.dat


&return



/*----------
&routine run
/*----------

&data cokb3dm
95cok.par
y
&end

&return

/*----------
&routine par
/*----------

&s file5 [open 95cok.par openstat -w]
&s file3 [open bit1.txt openstat -r]
&s file4 [open bit2.txt openstat -r]


&do I = 1 &to 10
 &s l [read %file3% readstat]
 &s writestat [write %file5% %l%]
&end


&s xy [read %file6% readstat]
&s x [extract 1 %xy%]
&s y [extract 2 %xy%]

&type %x%,%y%

&s writestat [write %file5% [quote 1   %x%   0.1]]
&s writestat [write %file5% [quote 1   %y%   0.1]]

&do I = 1 &to 16
 &s m [read %file4% readstat]
 &s writestat [write %file5% %m%]
```

```
&end

&s closestat [close %file3%]
&s closestat [close %file4%]
&s closestat [close %file5%]

&return

/*----------
&routine out
/*----------

&s file8 [open 953.out openstat -r]

&do I = 1 &to 4
 &s n [read %file8% readstat]
&end

&s n [read %file8% readstat]
&s writestat [write %file7% %n%]

&s closestat [close %file8%]

rm 95cok.par
rm 953.out

&return



/*-------------------------------------------------------------
/*
/*      plt_cov.aml; converts output file from COKB3DM into
/*                   a point coverage in ARC/INFO.
/*
/*      20/4/98    by C. de Hoogh
/*
/*-------------------------------------------------------------

&r write.aml

/*&r write2.aml

/*create lut-table in tables


tables
DEFINE %.name%.LUT
%.name%-ID,4,5,B
X_COORD,10,11,N,0
Y_COORD,10,11,N,0
NOX_COKR,14,15,N,6
VARIANCE,14,15,N,6
~
ADD FROM %.name%.TEX
q

rm *.tex

/*create sdf-file in INFO
```

```
&data arc info
ARC
SELECT %.name%.LUT
EXPORT /HOME/KEES/METHODS/GSLIB2/BIN/%.name%_SDF SDF %.name%-
ID,X_COORD,Y_COORD
Q STOP
&end


&r write3.aml

create %.name% /home/kees/phd/l_dist2

generate %.name%
input %.name%_sdf2
points
quit
build %.name% points
joinitem %.name%.pat %.name%.lut %.name%.pat %.name%-id %.name%-id

/*pointgrid %.name% %.name%_g nox_cokr
/*500
/*y
/*NODATA

/*grid
/*%.name%_gr = int(%.name%_g)
/*quit

/*kill %.name%_g
/*kill %.name%
rm *sdf
/*&r point_lat.aml


&return

/*--------------------------------------------------------------
/*
/*      write.aml;reads and write for plt_cov.aml
/*
/*      20/4/98    by C. de Hoogh
/*
/*--------------------------------------------------------------

&s fileunit1 [open %.filename% openstat -r]
&s fileunit2 [open %.name%.tex openstat -w]

&if %openstat% ne 0 &then
  &return &error Error in creating file
&else &type File is created

&s counter  1
&s id = 1
&s record  [read %fileunit1% readstat]
&s no2 [extract 1 %record%]
&s var [extract 2 %record%]
&s x = 526000
&s y = 176900

&do &while %readstat% ne 102
```

```
  &s writestat  [write %fileunit2% %id%,%x%,%y%,%no2%,%var%]
  &s record  [read %fileunit1% readstat]
  &s no2 [extract 1 %record%]
  &s var [extract 2 %record%]
  &s x = %x% + 14
  &s counter  %counter% + 1
  &s id %id% + 1
  &if %counter% > 50 &then
    &call calculate
  &else
    &s k = 1
&end

&s closestat [close %fileunit1%]
&s closestat [close %fileunit2%]

&return

&routine calculate

&s y = %y% + 14
&s x = 526000
&s counter = 1

&return


/*-------------------------------------------------------------
/*
/*      write2.aml;reads and write for plt_cov.aml
/*
/*      20/4/98    by C. de Hoogh
/*
/*-------------------------------------------------------------

&s fileunit3 [open %.name%.tex openstat -r]
&s fileunit4 [open %.name%2.tex openstat -w]

&if %openstat% ne 0 &then
  &return &error Error in creating file
&else &type File2 is created

&s counter := 1
&s record := [read %fileunit3% readstat]
&s goed := [subst %record%  .00000 , ]

&do &while %readstat% ne 102
  &s writestat := [write %fileunit4% %counter%,%goed%]
/*  &s writestat := [write %fileunit2% %counter%,%record%]
  &s record := [read %fileunit3% readstat]
  &s goed := [subst %record% .00000 ,]
  &s counter := %counter% + 1

&end

&s closestat [close %fileunit3%]
&s closestat [close %fileunit4%]

&return
```

```
/*------------------------------------------------------------
/*
/*      write3.aml;reads and write for plt_cov.aml
/*
/*      20/4/98     by C. de Hoogh
/*
/*------------------------------------------------------------


&s fileunit5 [open %.name%_sdf openstat -r]
&s fileunit6 [open %.name%_sdf2 openstat -w]

&if %openstat% ne 0 &then
  &return &error Error in creating file
&else &type File3 is created

&s record := [read %fileunit5% readstat]

&do &while %readstat% ne 102
  &s writestat := [write %fileunit6% %record%]
  &s record := [read %fileunit5% readstat]
&end

&s writestat := [write %fileunit6% END]

&s closestat [close %fileunit5%]
&s closestat [close %fileunit6%]

&return
```

APPENDIX 3G

AMLS WRITTEN FOR USE IN ARC/INFO RUN THE SAVIAH EQUATION IN SHEFFIELD

```
/*--------------------------------------------------------
/*
/*  Saviah.aml; estimates NO2-conc using the SAVIAH-model
/*
/*  by C. de Hoogh  16/11/97
/*
/* parameters: Tvol0-40 = d40
/*             Tvol40-300 = d300
/*             Tvol300 = v300
/*             HDC0-300 = h300
/*             Ind0-300 = i300
/*             Land300 = l300
/*             Logalt = logalt
/*             MeanNO2 = no2
/*--------------------------------------------------------

&s file_id [open shcon.txt openstat -r]

&if %openstat% ne 0 &then
  &return &error Error in creating file
&else &type File is created

&s line [read %file_id% readstat]

&s file [open shconout.txt openstat -w]

&s writestat [write %file% [quote id,Tvol300,Land300,Altitude,MeanNO2]]

&do &while %readstat% ne 102
  &s id [extract 1 %line%]
  &s x [extract 2 %line%]
  &s y [extract 3 %line%]
  &s h [extract 4 %line%]
  &call gamaar
&end

&s closestat [close %file%]
&s closestat [close %file_id%]

&return

/*---------------
&routine gamaar
/*---------------

reselect /home/kees/sheff/big_all temp point
res big_all-id = %id%
~
n
n

&call create

/*checking whether there are any roads within 300 metres of the point

&call checkl

/*checking whether there are any urban areas within 300 m of the point

/*reselect /home/kees/sheff/digit/shlc_int sel_lc poly
/*res lc = 'U'
```

```
/*~
/*n
/*n

near temp sel_lu line 5000

&data arc info
ARC
SELECT TEMP.PAT
EXPORT /HOME/KEES/SAVIAH/DIST2.TXT SDF DISTANCE
Q STOP
&end

&s dist2 [open dist2.txt openstat -r]
&s dist [read %dist2% readstat]
&s closestat [close %dist2%]
rm dist2.txt
&if %dist% < 297.0 &then
  &call landu
&else
  &s h300 = 0

/*kill sel_lc

/*checking whether there are any industrial areas within 300 m of the
point

/*reselect /home/kees/sheff/digit/shlc_int sel_lc poly
/*res lc = 'I'
/*~
/*n
/*n

near temp sel_li line 15000

&data arc info
ARC
SELECT TEMP.PAT
EXPORT /HOME/KEES/SAVIAH/DIST3.TXT SDF DISTANCE
Q STOP
&end

&s dist3 [open dist3.txt openstat -r]
&s dist [read %dist3% readstat]
&s closestat [close %dist3%]
rm dist3.txt
&if %dist% < 297.0 &then
  &call landi
&else
  &s i300 = 0

/*kill sel_lc

&call rsalt

&call equation

&s line [read %file_id% readstat]

&return
```

```
/*---------------
&routine create
/*---------------

create circle40 /home/kees/sheff/net_p3
generate circle40
circles
1,%x%,%y%,40
end
quit

build circle40

create circle300 /home/kees/sheff/net_p3
generate circle300
circles
1,%x%,%y%,300
end
quit

build circle300

&return

/*---------------
&routine check1
/*---------------
near temp /home/kees/sheff/oscar/roads3 line 5000

&data arc info
ARC
SELECT TEMP.PAT
EXPORT /HOME/KEES/SAVIAH/DIST.TXT SDF DISTANCE
Q STOP
&end

&s dist11 [open dist.txt openstat -r]
&s dist [read %dist11% readstat]
&s closestat [close %dist11%]
rm dist.txt
&if %dist% < 300 &then
  &if %dist% < 40 &then
    &call tvol40
  &else
    &call tvol300
&else
  &call zero

&return

/*-----------
&routine zero
/*-----------

&s v300 = 0
&s d300 = 0
&s d40 = 0

&return
```

```
/*----------------
&routine tvol40
/*----------------

/* calculates the parameters Tvol0-40 and Tvol40-300

intersect /home/kees/sheff/oscar/roads3 circle40 sel_rds40 line
intersect /home/kees/sheff/oscar/roads3 circle300 sel_rds300 line

statistics sel_rds40.aat sum40.lut
sum length flow18
~
n
n

statistics sel_rds300.aat sum300.lut
sum length flow18
~
n
n

&data arc info
ARC
SELECT SUM40.LUT
EXPORT /HOME/KEES/SAVIAH/TEMP40.TXT SDF SUM-W-LENGTH
DELETE SUM40.LUT
Y
Q STOP
&end

&data arc info
ARC
SELECT SUM300.LUT
EXPORT /HOME/KEES/SAVIAH/TEMP300.TXT SDF SUM-W-LENGTH
DELETE SUM300.LUT
Y
Q STOP
&end

&s file1 [open temp40.txt openstat -r]
&s d40 [read %file1% readstat]
&s closestat [close %file1%]
/*rm temp40.txt

&s file2 [open temp300.txt openstat -r]
&s d300 [read %file2% readstat]
&s closestat [close %file2%]
/*rm temp300.txt

&s d300 [calc %d300% - %d40%]

&type Tvol0-40 = %d40% and Tvol40-300 = %d300%

&s v300 [calc 15 * %d40% + %d300%]

&s v300 [calc %v300% / 1000 ]

&type Tvol300 = %v300%

/*kill circle40
/*kill circle300
```

```
kill sel_rds40
kill sel_rds300
rm temp40.txt
rm temp300.txt

/*&s writestat [write %file% [quote %id%,%d40%,%d300%]]

&return
/*----------------
&routine tvol300
/*----------------

/* calculates the parameter Tvol40-300

intersect /home/kees/sheff/oscar/roads3 circle300 sel_rds300 line

statistics sel_rds300.aat sum300.lut
sum length flow18
~
n
n

&data arc info
ARC
SELECT SUM300.LUT
EXPORT /HOME/KEES/SAVIAH/TEMP300.TXT SDF SUM-W-LENGTH
DELETE SUM300.LUT
Y
Q STOP
&end

&s file2 [open temp300.txt openstat -r]
&s d300 [read %file2% readstat]
&s closestat [close %file2%]
/*rm temp300.txt

&type Tvol0-40 = 0 and Tvol40-300 = %d300%

&s d40 = 0

&s v300 %d300%

&s v300 [calc %v300% / 1000 ]

&type Tvol300 = %v300%

/*kill circle300
kill sel_rds300
/*rm temp40.txt
rm temp300.txt

/*&s writestat [write %file% [quote %id%,%d40%,%d300%]]

&return


/*----------------
&routine landu
/*----------------

intersect /home/kees/sheff/digit/shlc_int circle300 sel_lc300 poly
```

```
/*intersect /home/kees/sheff/digit/lc circle300 sel_lc300 poly

tables
select sel_lc300.pat
reselect lc = 'U'
statistics lc lch.lut
sum area
end

aselect
quit

&data arc info
ARC
SELECT LCH.LUT
EXPORT /HOME/KEES/SAVIAH/LCH.TXT SDF SUM-AREA
DELETE LCH.LUT
Y
Q STOP
&end

&s file3 [open lch.txt openstat -r]
&s h300 [read %file3% readstat]
&s closestat [close %file3%]
rm lch.txt

&s h300 = [calc %h300% / 10000]


&type HDC0-300 = %h300%

kill sel_lc300

&return

/*--------------
&routine landi
/*--------------

intersect /home/kees/sheff/digit/shlc_int circle300 sel_lc300 poly
/*intersect /home/kees/sheff/digit/lc circle300 sel_lc300 poly

tables
select sel_lc300.pat
reselect lc = 'I'
statistics lc lci.lut
sum area
end

aselect
quit

&data arc info
ARC
SELECT LCI.LUT
EXPORT /HOME/KEES/SAVIAH/LCI.TXT SDF SUM-AREA
DELETE LCI.LUT
Y
Q STOP
&end
```

```
&s file4 [open lci.txt openstat -r]
&s i300 [read %file4% readstat]
&s closestat [close %file4%]
rm lci.txt

&s i300 = [calc %i300% / 10000]

&type Ind0-300 = %i300%

kill sel_lc300

&return

/*--------------
&routine rsalt
/*--------------
&s logalt [log10 %h%]



&type logalt = %logalt%
&return

/*----------------
&routine equation
/*----------------

/* saviah equation
/* chosen sample height = 2 metres; so 22.424 * 1/2 = 11.212

&s l300 = [calc 1.8 * %h300% + %i300%]
&type Land300 = %l300%

&s r [calc 0.003705 * %v300%]
&s s [calc 0.232 * %l300%]
&s t [calc 5.673 * %logalt%]
&s u 11.212

&s no2 [calc 49.732 + %r% + %s% - %t% - %u%]
&type/*---------------
&type
&type MeanNO2 = %no2% ug/m3
&type
&type/*---------------

&s writestat [write %file% [quote %id%,%v300%,%l300%,%h%,%no2%]]

kill circle40
kill circle300
kill temp

&return
```

APPENDIX 4A

EXAMPLE OF TEXT FILE WITH TRAFFIC COUNTS FOR EALING AND THE AMLS WRITTEN FOR USE IN ARC/INFO TO CONVERT THE TEXT FILES INTO ARC/INFO COVERAGES

1 DEPARTMENT OF TRANSPORT

REGION: GREATER LONDON LOCAL AUTHORITY: EALING

ROAD: A3005 CLASS: PRINCIPAL BUILT-UP

ROAD BETWEEN JUNCTIONS LOCATED AT OSGR 513264E 178365N IE THE JUNCTION OF NORWOOD RD/TENTELOW RD
AND 512835E 180387N IE THE JUNCTION OF SOUTH RD/THE BROADWAY/HIGH STREET, UXBRIDGE
(DTp NODE NOS 52701110 52701113)

LINK LENGTH: 2.6KM CARRIAGEWAYS: 1 LANES: 2 SPEED LIMIT: 30 MPH

						HEAVY GOODS VEHICLES							
	PEDAL CYCLES	MOTOR CYCLES	CARS AND TAXIS	BUS AND COACH	LIGHT GOODS VEHS	RIGID 2 AXLE	RIGID 3 AXLE	RIGID 4 OR MORE AXLE	ARTIC 4 OR LESS AXLE	ARTIC 5 OR MORE AXLE	TOTAL HGV	ALL MOTOR VEHS	HGV %
OBSERVED 12 HR FLOW (7AM TO 7PM)	183	82	8783	630	1055	721	43	43	36	59	902	11452	7.9
ESTIMATED ANNUAL AVERAGE FLOW 1995													
AV. DAILY (7) 24HR FLOW	160	100	12100	700	1000	680	30	40	30	50	840	14700	5.7
AV. WEEKDAY(5) 24HR FLOW	190	100	12300	775	1175	810	40	50	40	70	1010	15400	6.6
AV. WEEKDAY(5) 16HR FLOW (6AM-10PM)	180	100	11000	725	1125	770	40	50	40	60	950	13900	6.9
AV. WEEKDAY(5) 12HR FLOW (7AM-7PM)	150	75	8700	600	1000	680	40	40	30	60	850	11200	7.6

THESE FLOWS HAVE BEEN CALCULATED FROM THE FOLLOWING DATA

ROTATING CENSUS COUNT at OS GRID REF 512617E 179800N on Tuesday 10 May 1994 (Census Point No. 47610)

ESTIMATED DAILY FLOWS BASED ON OBSERVED COUNTS MADE PRIOR TO 1992 HAVE BEEN SCALED UP USING NATIONAL SCALING FACTORS: THEY DO NOT NECESSARILY REFLECT LOCAL CIRCUMSTANCES

NOTE: ALL ESTIMATED FLOWS HAVE BEEN INDIVIDUALLY ROUNDED, THUS TOTALS FOR ALL MOTOR VEHICLES OR HEAVY GOODS VEHICLES MAY NOT ALWAYS BE THE SUM OF THE SEPARATE VEHICLE CLASSES

1 DEPARTMENT OF TRANSPORT

REGION: GREATER LONDON LOCAL AUTHORITY: EALING

ROAD: A4127 CLASS: PRINCIPAL BUILT-UP

ROAD BETWEEN JUNCTIONS LOCATED AT OSGR 513264E 178365N IE THE JUNCTION OF NORWOOD RD/TENTELOW RD
AND 514267E 180233N IE THE JUNCTION OF WINDMILL LANE/UXBRIDGE RD/GREENFORD RD

(DTp NODE NOS 52701110 52701114)

LINK LENGTH: 2.3KM CARRIAGEWAYS: 1 LANES: 4 SPEED LIMIT: 30 MPH

	PEDAL CYCLES	MOTOR CYCLES	CARS AND TAXIS	BUS AND COACH	LIGHT GOODS VEHS	HEAVY GOODS VEHICLES: RIGID 2 AXLE	RIGID 3 AXLE	RIGID 4 OR MORE AXLE	ARTIC 4 OR LESS AXLE	ARTIC 5 OR MORE AXLE	TOTAL HGV	ALL MOTOR VEHS	HGV %
OBSERVED 12 HR FLOW (7AM TO 7PM)	166	203	18899	8	2151	499	43	62	41	137	782	22043	3.5
ESTIMATED ANNUAL AVERAGE FLOW 1995													
AV. DAILY (7) 24HR FLOW	170	225	25300	0	1975	460	30	50	40	120	700	28200	2.5
AV. WEEKDAY(5) 24HR FLOW	190	275	25700	0	2350	550	40	70	40	150	850	29200	2.9
AV. WEEKDAY(5) 16HR FLOW (6AM-10PM)	180	250	22900	0	2225	510	40	60	40	140	800	26200	3.1
AV. WEEKDAY(5) 12HR FLOW (7AM-7PM)	150	200	18200	0	1950	460	40	60	40	130	710	21000	3.4

THESE FLOWS HAVE BEEN CALCULATED FROM THE FOLLOWING DATA

ROTATING CENSUS COUNT at OS GRID REF 514270E 180050N on Friday 22 April 1994 (Census Point No. 47708)

ESTIMATED DAILY FLOWS BASED ON OBSERVED COUNTS MADE PRIOR TO 1992 HAVE BEEN SCALED UP USING NATIONAL SCALING FACTORS: THEY DO NOT NECESSARILY REFLECT LOCAL CIRCUMSTANCES

NOTE: ALL ESTIMATED FLOWS HAVE BEEN INDIVIDUALLY ROUNDED, THUS TOTALS FOR ALL MOTOR VEHICLES OR HEAVY GOODS VEHICLES MAY NOT ALWAYS BE THE SUM OF THE SEPARATE VEHICLE CLASSES

1 DEPARTMENT OF TRANSPORT

```
/*--------------------------------------------------------------
/*
/*      traffic.aml; reads files from the department of transport
/*                   (word6 -> text only format) into an input file
/*                   for generate and a lut file with traffic
/*                   volume data
/*
/*      26/6/96    by C. de Hoogh   I.E.P.A.
/*
/*--------------------------------------------------------------

&s file1 [open %.text% openstat -r]
&s file2 [open %.name%.inp openstat -w]
&s file3 [open %.name%.tex openstat -w]

&if %openstat% ne 0 &then
  &return &error Error in creating file
&else &type File1 and File2 are created

/* read the first 7 lines of the file but doesn't writes it away

&do I := 1 &to 7
  &s record := [read %file1% readstat]
&end
&s no = 1

&label read

&s record = [read %file1% readstat]
&s road = [substr %record% 8 5]
&s record = [read %file1% readstat]
&s record = [read %file1% readstat]
&s xcoord = [substr %record% 41 6]
&s ycoord = [substr %record% 49 6]
&s writestat = [write %file2% %no%]
&s writestat = [write %file2% %xcoord%,%ycoord%]
&s record = [read %file1% readstat]
&s xcoord = [substr %record% 41 6]
&s ycoord = [substr %record% 49 6]
&s writestat = [write %file2% %xcoord%,%ycoord%]
&s writestat = [write %file2% 'END']

&do I := 1 &to 10
  &s record := [read %file1% readstat]
&end

&s record = [read %file1% readstat]
/*   &s m1 = [substr %record% 46 4]
/*   &s c1 = [substr %record% 52 6]
/*   &s b1 = [substr %record% 61 4]
/*   &s l1 = [substr %record% 67 5]
&s h1 = [substr %record% 109 5]
&s t1 = [substr %record% 115 6]
&s record = [read %file1% readstat]
&s record = [read %file1% readstat]
&s h2 = [substr %record% 109 5]
&s t2 = [substr %record% 115 6]
&s record = [read %file1% readstat]
&s h3 = [substr %record% 109 5]
&s t3 = [substr %record% 115 6]
&s record = [read %file1% readstat]
```

```
&s h4 = [substr %record% 109 5]
&s t4 = [substr %record% 115 6]
&s record = [read %file1% readstat]
&s h5 = [substr %record% 109 5]
&s t5 = [substr %record% 115 6]

&s writestat = [write %file3%
%no%,%road%,%h1%,%t1%,%h2%,%t2%,%h3%,%t3%,%h4%,%t4%,%h5%,%t5%]

/*read the next 18 lines and but doesn't writes it away

&do I := 1 &to 18
  &s record := [read %file1% readstat]
&end

&s no = %no% + 1

&do &while %readstat% ne 102
  &goto read
&end

&s writestat = [write %file2% END]
/*&s writestat = [write %file3% END]

&s closestat [close %file1%]
&s closestat [close %file2%]
&s closestat [close %file3%]

&return


/*-------------------------------------------------------------
/*
/*      plt_cov.aml; creates a line coverage in ARC/INFO form input file
/*.                    created with traffic.aml
/*
/*      27/6/96    by C.de Hoogh    I.E.P.A.
/*
/*-------------------------------------------------------------

/*create lut-table in tables

tables
DEFINE %.name%.LUT
%.name%-ID,4,5,B
ROAD_TYPE,7,6,C
H1,8,7,N,0
T1,8,7,N,0
H2,8,7,N,0
T2,8,7,N,0
H3,8,7,N,0
T3,8,7,N,0
H4,8,7,N,0
T4,8,7,N,0
H5,8,7,N,0
T5,8,7,N,0
~
ADD FROM %.name%.TEX
q

rm *.tex
```

```
/*&r write3.aml

create %.name% /homelx/kees/phd/lonnox_poly

generate %.name%
input %.name%.inp
lines
quit
build %.name% lines
joinitem %.name%.aat %.name%.lut %.name%.aat %.name%-id %.name%-id

&return
```

APPENDIX 4B

EXAMPLE OF A CALINE3 INPUT FILE

```
caline3run60.0150..000015.00011.00000000
                     9    526256    177315         2
                                         11360
                    18AG 526406 177446 526369 177433   22900  4.0.0010.0
                     1AG 526321 177504 526369 177433   19300  4.0.0010.0
                     2AG 526369 177433 526250 177374   27800  4.0.0010.0
                     3AG 526170 177495 526250 177374   20500  4.0.0010.0
                    10AG 526250 177374 526282 177325   20000  4.0.0010.0
                     6AG 526369 177433 526455 177302   16900  4.0.0010.0
                     4AG 526250 177374 526083 177270   32300  4.0.0010.0
                     7AG 526083 177270 526066 177256   32300  4.0.0010.0
                    12AG 526282 177325 526395 177256   20000  4.0.0010.0
                    11AG 526447 177257 526395 177256   20000  4.0.0010.0
                     8AG 526083 177270 526146 177149    6000  4.0.0010.0
  3 1004   5120.03
  3  904   4980.03
  3 1304   5120.03
  2 2005   3000.03
  2 1304   4940.03
  2 1403   4460.03
  2 1503   4510.03
  2  803   4790.03
  3 1303   5770.03
  3 1103   6860.03
  3 1103   7860.03
  3  803   8860.03
  3 1303   9660.03
  4 1203  10470.03
  5  804  11210.03
  4  803  12050.03
  6  704  12900.03

...............etc

  3  103  10840.03
  3  603  10710.03
  3  503  10410.03
  2  205   3810.03
  3  204   5700.03
  3  504   5830.03
  3  705   4450.03
```

APPENDIX 4C

EXAMPLE OF AN ISC3 INPUT FILE

```
CO STARTING
CO TITLEONE TEST FOR THE AREA SOURCES
CO MODELOPT DFAULT CONC URBAN
CO AVERTIME ANNUAL
CO POLLUTID NOX
CO FLAGPOLE 1.5
CO RUNORNOT RUN
CO FINISHED

SO STARTING

SO LOCATION 261 AREA 516000 159000
SO LOCATION 316 AREA 510000 160000
.............................. etc
SO LOCATION 2459 AREA 518000 195000
SO LOCATION 2460 AREA 519000 195000

SO SRCPARAM 261 0.920572E-06 1.0  1000  1000
SO SRCPARAM 316 1.330889E-06 1.0  1000  1000
.............................. etc
SO SRCPARAM 2459 0.868627E-06 1.0  1000  1000
SO SRCPARAM 2460 2.182305E-06 1.0  1000  1000

** TO CONVERT THE M2 INTO M2 CONCENTRATIONS
SO EMISUNIT 1.0E6  GRAMS/(SEC-M**2) MICROGRAMS/CUBIC-METER

SO SRCGROUP ALL
SO FINISHED

RE STARTING
RE DISCCART 526472 175519
RE FINISHED

ME STARTING
ME INPUTFIL /homelx/kees/isc_files/london.sta
ME ANEMHGHT  10.0 METERS
ME SURFDATA  1 1991 london
ME UAIRDATA  1 1991 london
ME STARDATA ANNUAL
ME AVESPEED 1.0 1.8 3.4 5.5 8.4 10.0
ME AVETEMPS ANNUAL 288 288 288 288 288 288
ME AVEMIXHT ANNUAL A 6*1300.0
ME AVEMIXHT ANNUAL B 6*900.0
ME AVEMIXHT ANNUAL C 6*850.0
ME AVEMIXHT ANNUAL D 6*800.0
ME AVEMIXHT ANNUAL E 6*400.0
ME AVEMIXHT ANNUAL F 6*100.0
ME FINISHED

OU STARTING
OU RECTABLE SRCGRP INDSRC
OU MAXTABLE 10 INDSRC SRCGRP SOCONT
OU PLOTFILE ANNUAL ALL /homelx/kees/isc_files/a2.plt
OU FINISHED
```

APPENDIX 4D

METEOROLOGICAL DATA USED FOR ISC3 IN GREATER LONDON

Station: London Weather Centre

Data collection period: 1 January 1982 to 31 December 1991

Wind direction frequencies expressed as percentages (HMIP, 1993)

Pasquill Stability Category: A

		Sector number / wind direction (degrees)												
Wind speed	Calm	01	02	03	04	05	06	07	08	09	10	11	12	All
($m\ s^{-1}$)	0	345	015	045	075	105	135	165	195	225	255	285	315	
		015	045	075	105	135	165	195	225	255	285	315	345	
< 1.0	.001	.000	.000	.000	.000	.000	.000	.000	.000	.000	.000	.000	.000	.00
1.0 - 2.5	.000	.010	.007	.014	.011	.008	.017	.007	.009	.005	.006	.011	.001	.10
2.5 - 4.25	.000	.000	.000	.000	.000	.000	.000	.000	.000	.000	.000	.000	.000	.00
4.25 - 6.75	.000	.000	.000	.000	.000	.000	.000	.000	.000	.000	.000	.000	.000	.00
6.75 - 10.0	.000	.000	.000	.000	.000	.000	.000	.000	.000	.000	.000	.000	.000	.00
>10.0	.000	.000	.000	.000	.000	.000	.000	.000	.000	.000	.000	.000	.000	.00
All	.001	.010	.007	.014	.011	.008	.017	.007	.009	.005	.006	.011	.001	.10

Pasquill Stability Category: B

		Sector number / wind direction (degrees)												
Wind speed	Calm	01	02	03	04	05	06	07	08	09	10	11	12	All
($m\ s^{-1}$)	0	345	015	045	075	105	135	165	195	225	255	285	315	
		015	045	075	105	135	165	195	225	255	285	315	345	
< 1.0	.019	.000	.000	.000	.000	.000	.000	.000	.000	.000	.000	.000	.000	.01
1.0 - 2.5	.000	.186	.292	.219	.063	.072	.148	.146	.149	.153	.162	.183	.124	1.89
2.5 - 4.25	.000	.092	.123	.135	.062	.063	.071	.084	.070	.083	.096	.104	.074	1.05
4.25 - 6.75	.000	.003	.025	.033	.033	.019	.005	.015	.017	.018	.024	.015	.001	.20
6.75 - 10.0	.000	.000	.000	.000	.000	.000	.000	.000	.000	.000	.000	.000	.000	.00
>10.0	.000	.000	.000	.000	.000	.000	.000	.000	.000	.000	.000	.000	.000	.00
All	.019	.282	.440	.387	.157	.154	.224	.245	.236	.254	.282	.301	.200	3.18

Pasquill Stability Category: C

		Sector number / wind direction (degrees)												
Wind speed	Calm	01	02	03	04	05	06	07	08	09	10	11	12	All
($m\ s^{-1}$)	0	345	015	045	075	105	135	165	195	225	255	285	315	
		015	045	075	105	135	165	195	225	255	285	315	345	
< 1.0	.009	.000	.000	.000	.000	.000	.000	.000	.000	.000	.000	.000	.000	.00
1.0 - 2.5	.000	.096	.121	.054	.013	.023	.079	.041	.040	.023	.031	.038	.042	.59
2.5 - 4.25	.000	.378	.590	.549	.151	.240	.363	.373	.415	.497	.479	.474	.314	4.82
4.25 - 6.75	.000	.560	.740	.665	.318	.338	.324	.647	.750	.973	.856	.690	.488	7.35
6.75 - 10.0	.000	.005	.030	.084	.072	.008	.006	.010	.002	.010	.005	.008	.000	.24
>10.0	.000	.000	.001	.011	.005	.000	.000	.001	.000	.002	.001	.000	.000	.02
All	.009	1.038	1.482	1.363	.558	.608	.771	1.073	1.207	1.506	1.371	1.209	.844	13.04

Pasquill Stability Category: D

		Sector number / wind direction (degrees)												
Wind speed	Calm	01	02	03	04	05	06	07	08	09	10	11	12	All
($m\ s^{-1}$)	0	345	015	045	075	105	135	165	195	225	255	285	315	
		015	045	075	105	135	165	195	225	255	285	315	345	
< 1.0	.025	.000	.000	.000	.000	.000	.000	.000	.000	.000	.000	.000	.000	.02
1.0 - 2.5	.000	.172	.294	.192	.048	.086	.169	.099	.107	.075	.118	.124	.123	1.60
2.5 - 4.25	.000	.366	.594	.593	.171	.249	.357	.388	.529	.455	.455	.399	.274	4.83
4.25 - 6.75	.000	1.136	1.746	1.594	.728	.752	.834	1.677	2.642	2.835	2.089	1.320	.866	18.22
6.75 - 10.0	.000	1.642	2.714	2.014	.926	.494	.671	2.747	6.059	5.842	3.750	1.939	1.100	29.89
>10.0	.000	.273	.694	.422	.072	.029	.079	.950	2.300	1.664	1.225	.420	.155	8.28
All	.025	3.589	6.043	4.815	1.945	1.609	2.110	5.862	11.638	10.871	7.638	4.202	2.518	62.86

Pasquill Stability Category: E

		Sector number / wind direction (degrees)												
Wind speed	Calm	01	02	03	04	05	06	07	08	09	10	11	12	All
($m\ s^{-1}$)	0	345	015	045	075	105	135	165	195	225	255	285	315	
		015	045	075	105	135	165	195	225	255	285	315	345	
< 1.0	.000	.000	.000	.000	.000	.000	.000	.000	.000	.000	.000	.000	.000	.00
1.0 - 2.5	.000	.000	.000	.000	.000	.000	.000	.000	.000	.000	.000	.000	.000	.00
2.5 - 4.25	.000	.242	.410	.489	.148	.165	.225	.212	.379	.392	.371	.272	.224	3.52
4.25 - 6.75	.000	.251	.406	.443	.211	.199	.143	.237	.469	.711	.620	.389	.242	4.32
6.75 - 10.0	.000	.000	.000	.000	.000	.000	.000	.000	.000	.000	.000	.000	.000	.00
>10.0	.000	.000	.000	.000	.000	.000	.000	.000	.000	.000	.000	.000	.000	.00
All	.000	.493	.816	.932	.359	.364	.367	.450	.848	1.103	.990	.661	.466	7.84

Pasquill Stability Category: F+G

		Sector number / wind direction (degrees)												
Wind speed	Calm	01	02	03	04	05	06	07	08	09	10	11	12	All
($m\ s^{-1}$)	0	345	015	045	075	105	135	165	195	225	255	285	315	
		015	045	075	105	135	165	195	225	255	285	315	345	
< 1.0	.088	.000	.000	.000	.000	.000	.000	.000	.000	.000	.000	.000	.000	.08
1.0 - 2.5	.000	.418	.580	.509	.130	.172	.391	.273	.363	.306	.325	.367	.261	4.09
2.5 - 4.25	.000	.097	.232	.282	.087	.071	.098	.096	.209	.187	.173	.131	.111	1.77
4.25 - 6.75	.000	.000	.000	.000	.000	.000	.000	.000	.000	.000	.000	.000	.000	.00
6.75 - 10.0	.000	.000	.000	.000	.000	.000	.000	.000	.000	.000	.000	.000	.000	.00
>10.0	.000	.000	.000	.000	.000	.000	.000	.000	.000	.000	.000	.000	.000	.00
All	.088	.515	.811	.791	.217	.243	.489	.369	.572	.493	.499	.499	.372	5.95

APPENDIX 5A

NO_2 MONITORING RESULTS + MIXED EFFECT MODEL

Table 1: NO_2 concentration ($\mu g\ m^{-3}$) measured with diffusion tubes in Sheffield

	Survey 1		*Survey 2*		*Survey 3*		*Survey 4*		*Survey 5*	
Site-id	***Tube1***	***Tube2***	***Tube1***	***Tube2***	***Tube1***	***Tube2***	***Tube1***	***Tube2***	***Tube1***	***Tube2***
1	70	66	66	58	42	70	50	58	76	62
2	[1]	[1]	45	43	46	61	59	57	55	63
3	32	32	25	24	40	39	39	41	38	41
4	39	32	33	32	[2]	[2]	[2]	[2]	40	38
5	62	55	55	43	55	66	61	60	48	50
6	[2]	[2]	31	34	43	[2]	46	[2]	[2]	[2]
7	24	24	22	21	34	39	39	42	34	26
8	79	70	64	62	57	84	63	55	72	78
9	23	24	17	19	43	64	46	36	28	28
10	24	24	20	23	31	36	38	[2]	28	30
11	60	60	56	56	43	53	66	67	62	62
12	70	68	63	66	62	71	62	63	62	55
13	30	32	29	36	33	41	32	36	34	34
14	[1]	[1]	33	[2]	42	39	46	41	45	42
15	24	24	21	23	32	34	35	30	20	22
16	21	19	19	21	43	39	36	32	24	22
17	36	38	36	39	57	66	45	44	47	42
18	36	39	32	32	53	87	45	33	40	43
19	21	19	[2]	[2]	27	25	31	26	24	27
20	26	26	22	21	37	46	42	34	28	29
21	62	64	59	58	78	74	54	63	59	52
22	79	70	77	79	83	85	65	66	77	88
23	[2]	[2]	[2]	[2]	56	53	50	50	51	55
24	70	58	53	62	56	74	71	77	70	66
25	[2]	[2]	39	34	50	54	45	48	46	47
26	47	55	[2]	[2]	69	66	63	55	41	39
27	39	39	34	36	50	50	45	38	41	42
28	34	19	29	24	45	60	44	47	42	50

[1] location not used
[2] tube lost

Table 2: NO_2 concentrations ($\mu g\ m^{-3}$) after using the fixed-effect model

Site-id	Survey 1	Survey 2	Survey 3	Survey 4	Survey 5	Average
1	68	62	56	54	69	62
2	58	44	53	58	59	54
3	32	25	39	40	39	35
4	36	33	24	22	39	31
5	58	49	60	60	49	55
6	60	32	43	46	61	48
7	24	21	37	40	30	31
8	74	63	70	59	75	68
9	24	18	53	41	28	33
10	24	22	34	38	29	29
11	60	56	48	66	62	59
12	69	64	66	62	59	64
13	31	32	37	34	34	34
14	42	33	41	44	43	41
15	24	22	33	32	21	26
16	20	20	41	34	23	28
17	37	38	61	45	45	45
18	38	32	70	39	41	44
19	20	14	26	29	25	23
20	26	21	42	38	28	31
21	63	59	76	58	55	62
22	74	78	84	66	82	77
23	52	47	54	50	53	51
24	64	58	65	74	68	66
25	45	36	52	46	46	45
26	51	45	68	59	40	53
27	39	35	50	42	42	41
28	26	27	53	46	46	40

Table 3: Fixed-effect model (*Baseline - site 1, survey 1 = 36*)

		Model components (fixed effect)			
Site	**Survey**	**Site**	**Survey**	**Interaction**	**Mean NO2**
1	1	0	0	0	36
2	1	-5.085	0	0	30.915
3	1	-19	0	0	17
4	1	-17	0	0	19
5	1	-5	0	0	31
6	1	-4.215	0	0	31.785
7	1	-23	0	0	13
8	1	3.5	0	0	39.5
9	1	-23.5	0	0	12.5
10	1	-23	0	0	13
11	1	-4	0	0	32
12	1	0.5	0	0	36.5
13	1	-19.5	0	0	16.5
14	1	-13.59	0	0	22.41
15	1	-23	0	0	13
16	1	-25.5	0	0	10.5
17	1	-16.5	0	0	19.5
18	1	-16	0	0	20
19	1	-25.5	0	0	10.5
20	1	-22	0	0	14
21	1	-2.5	0	0	33.5
22	1	3.5	0	0	39.5
23	1	-8.22	0	0	27.78
24	1	-2	0	0	34
25	1	-12.045	0	0	23.955
26	1	-9	0	0	27
27	1	-15	0	0	21
28	1	-22	0	0	14
1	2	0	-3.045	0	32.955
2	2	-5.085	-3.045	-4.46	23.41
3	2	-19	-3.045	-0.885	13.07
4	2	-17	-3.045	1.43	17.385
5	2	-5	-3.045	-1.75	26.205
6	2	-4.215	-3.045	-11.625	17.115
7	2	-23	-3.045	1.47	11.425
8	2	3.5	-3.045	-2.98	33.475
9	2	-23.5	-3.045	0.01	9.465
10	2	-23	-3.045	1.49	11.445
11	2	-4	-3.045	0.83	29.785
12	2	0.5	-3.045	0.77	34.225
13	2	-19.5	-3.045	3.74	17.195
14	2	-13.59	-3.045	-1.675	17.69
15	2	-23	-3.045	1.595	11.55
16	2	-25.5	-3.045	3.195	10.65
17	2	-16.5	-3.045	3.62	20.075
18	2	-16	-3.045	0.14	17.095
19	2	-25.5	-3.045	0	7.455
20	2	-22	-3.045	0.3	11.255
21	2	-2.5	-3.045	0.81	31.265
22	2	3.5	-3.045	5.045	41.5
23	2	-8.22	-3.045	0	24.735

		Model components (fixed effect)			
Site	Survey	Site	Survey	Interaction	Mean NO2
24	2	-2	-3.045	-0.275	30.68
25	2	-12.045	-3.045	-1.505	19.405
26	2	-9	-3.045	0	23.955
27	2	-15	-3.045	0.575	18.53
28	2	-22	-3.045	3.325	14.28
1	3	0	-6.31	0	29.69
2	3	-5.085	-6.31	3.675	28.28
3	3	-19	-6.31	10.175	20.865
4	3	-17	-6.31	0	12.69
5	3	-5	-6.31	7.475	32.165
6	3	-4.215	-6.31	-2.695	22.78
7	3	-23	-6.31	12.755	19.445
8	3	3.5	-6.31	4.175	37.365
9	3	-23.5	-6.31	22.03	28.22
10	3	-23	-6.31	11.165	17.855
11	3	-4	-6.31	0.01	25.7
12	3	0.5	-6.31	5.14	35.33
13	3	-19.5	-6.31	9.575	19.765
14	3	-13.59	-6.31	5.49	21.59
15	3	-23	-6.31	10.825	17.515
16	3	-25.5	-6.31	17.82	22.01
17	3	-16.5	-6.31	19.495	32.685
18	3	-16	-6.31	23.49	37.18
19	3	-25.5	-6.31	9.68	13.87
20	3	-22	-6.31	14.43	22.12
21	3	-2.5	-6.31	13.41	40.6
22	3	3.5	-6.31	11.5	44.69
23	3	-8.22	-6.31	7.36	28.83
24	3	-2	-6.31	6.925	34.615
25	3	-12.045	-6.31	10.07	27.715
26	3	-9	-6.31	15.24	35.93
27	3	-15	-6.31	11.89	26.58
28	3	-22	-6.31	20.41	28.1
1	4	0	-7.175	0	28.825
2	4	-5.085	-7.175	7	30.74
3	4	-19	-7.175	11.365	21.19
4	4	-17	-7.175	0	11.825
5	4	-5	-7.175	8.165	31.99
6	4	-4.215	-7.175	0	24.61
7	4	-23	-7.175	15.555	21.38
8	4	3.5	-7.175	-1.02	31.305
9	4	-23.5	-7.175	16.555	21.88
10	4	-23	-7.175	14.195	20.02
11	4	-4	-7.175	10.48	35.305
12	4	0.5	-7.175	3.88	33.205
13	4	-19.5	-7.175	8.51	17.835
14	4	-13.59	-7.175	8.02	23.255
15	4	-23	-7.175	11.38	17.205
16	4	-25.5	-7.175	14.925	18.25
17	4	-16.5	-7.175	11.43	23.755
18	4	-16	-7.175	7.785	20.61
19	4	-25.5	-7.175	11.92	15.245
20	4	-22	-7.175	13.28	20.105

		Model components (fixed effect)			
Site	Survey	Site	Survey	Interaction	Mean NO2
21	4	-2.5	-7.175	4.77	31.095
22	4	3.5	-7.175	2.55	34.875
23	4	-8.22	-7.175	6.09	26.695
24	4	-2	-7.175	12.695	39.52
25	4	-12.045	-7.175	7.79	24.57
26	4	-9	-7.175	11.605	31.43
27	4	-15	-7.175	8.28	22.105
28	4	-22	-7.175	17.39	24.215
1	5	0	0.54	0	36.54
2	5	-5.085	0.54	0	31.455
3	5	-19	0.54	3.255	20.795
4	5	-17	0.54	1.27	20.81
5	5	-5	0.54	-5.555	25.985
6	5	-4.215	0.54	0	32.325
7	5	-23	0.54	2.545	16.085
8	5	3.5	0.54	0.02	40.06
9	5	-23.5	0.54	1.825	14.865
10	5	-23	0.54	1.925	15.465
11	5	-4	0.54	0.345	32.885
12	5	0.5	0.54	-5.755	31.285
13	5	-19.5	0.54	0.995	18.035
14	5	-13.59	0.54	0	22.95
15	5	-23	0.54	-2.57	10.97
16	5	-25.5	0.54	1.3	12.34
17	5	-16.5	0.54	3.7	23.74
18	5	-16	0.54	1.335	21.875
19	5	-25.5	0.54	2.495	13.535
20	5	-22	0.54	0.515	15.055
21	5	-2.5	0.54	-4.615	29.425
22	5	3.5	0.54	3.81	43.85
23	5	-8.22	0.54	0	28.32
24	5	-2	0.54	1.6	36.14
25	5	-12.045	0.54	0	24.495
26	5	-9	0.54	-6.1	21.44
27	5	-15	0.54	0.545	22.085
28	5	-22	0.54	10.035	24.575

APPENDIX 5B

ROAD TRAFFIC DATA FOR SHEFFIELD

1996 24HR AADF ESTIMATES DERIVED FROM 1995 GMTU DAY/MONTH FACTORS

TPU CENSUS	*LOCATION*	*LINK*	*DoT CENSUS*		*ALL*	*% HEAVY*
88211A	ABBEY LANE	WHIRLOWDALE RD - ECCLESALL RD STH			8747	2
90226	ABBEY LANE	CHESTERFIELD RD - HUTCLIFFE WOOD RD			7442	5
90252	ABBEY LANE	ABBEYDALE RD STH - HUTCLIFFE WOOD RD			12335	4
90252	ABBEY LANE	ABBEYDALE RD STH - WHIRLOWDALE RD			11605	4
96134	ABBEYDALE RD	WOLSELEY RD - BROADFIELD RD	27381	DoT	19028	9
89244	ABBEYDALE RD	CARTER KNOWLE RD - ARCHER RD			24203	7
91159	ABBEYDALE RD	WOLSELEY RD - LONDON RD			13081	8
92213	ABBEYDALE RD	BROADFIELD RD - CARTER KNOWLE RD			23963	7
94122	ABBEYDALE RD STH	GLOVER RD - TWENTYWELL LANE	8710	DoT	14084	6
90252	ABBEYDALE RD STH	ABBEY LANE - DORE RD			16974	5
90252	ABBEYDALE RD STH	ABBEY LANE - MILLHOUSES LANE			13334	6
96217	ALMA ST	GREEN LANE - CORPORATION ST		TPP	2261	6
95114	ANGEL ST (ONE WAY)	CASTLE SQUARE - CASTLE ST	8274	DoT	3698	76
89106	ARCHER RD	ULVERSTON RD - HUTCLIFFE WOOD RD			12521	3
95242	ARUNDEL GATE	FURNIVAL SQUARE - CHARLES ST			13864	19
95139	ARUNDEL GATE	CHARLES ST - CASTLE SQUARE	18447	DoT	18444	18
96142	ATTERCLIFFE COMMON	MEADOW HALL RETAIL PARK - WEEDON ST	37441	DoT	27910	9
96124	ATTERCLIFFE COMMON	JANSON ST - BROUGHTON LANE	38549	DoT	31703	10
96227	ATTERCLIFFE COMMON	BROUGHTON LANE - MEADOW HALL RETAIL PARK		TPP	31892	9
ATC	ATTERCLIFFE COMMON	NEWHALL RD - JANSON ST		ATC	15658	11
95109	ATTERCLIFFE RD	WORKSOP RD - NEWHALL RD	7380	DoT	24885	11
96140	ATTERCLIFFE RD	SUTHERLAND ST - STEVENSON RD	27393	DoT	8593	18
94171	ATTERCLIFFE RD	STEVENSON RD - EFFINGHAM RD			16594	16
87252	BACK LANE	STEPHEN HILL - BOLE HILL RD			4233	2
93208	BANNERDALE RD	CARTER KNOWLE RD - ABBEYDALE RD			5907	2
93208	BANNERDALE RD	CARTER KNOWLE RD - ARCHER LANE			4792	2
93210	BANNERDALE RD	ARCHER LANE - BRINCLIFFE EDGE RD			3246	2
ATC	BARNSLEY RD	DEERLANDS AVE - HIGH GREAVE		ATC	13273	7
94127	BARNSLEY RD	HATFIELD HOUSE LANE - DEERLANDS AVE	57875	DoT	13681	6
88138	BARNSLEY RD	HERRIES RD - HUCKLOW RD			14132	5
88138	BARNSLEY RD	HERRIES RD - NORWOOD RD			17913	7
88201	BARNSLEY RD	NORWOOD RD - BURNGREAVE RD			23048	7
89202	BARNSLEY RD	HUCKLOW RD - LONGLEY LANE			8583	5
90164	BARNSLEY RD	HATFIELD HOUSE LANE - STUBBIN LANE			15851	7
90117	BASLOW RD	GLOVER RD - OWLER BAR	57365	DoT	4415	7
95113	BAWTRY RD	M1 JUNCTION 34 STH - WEST BAWTRY RD	17332	DoT	14720	7
87243	BEAVER HILL RD	MARKET ST - RETFORD RD			4873	4
94264	BEIGHTON RD	MOSBOROUGH PARKWAY - STATION RD			6752	11
90162	BELLHOUSE RD	SHIREGREEN LANE - ECCLESFIELD RD			6653	7
90162	BELLHOUSE RD	SHIREGREEN LANE - FIRTH PARK RD			7025	7
86235	BEN LANE	RODNEY HILL - FAR LANE			3216	8
89301	BERNARD RD	BERNARD ST - EFFINGHAM RD			12412	9
96178	BERNARD ST	BERNARD RD - DUKE ST			12330	7
96138	BIRLEY MOOR RD	HOLLINSEND RD - OCCUPATION LANE	37419	DoT	13324	8
87325	BIRLEY MOOR RD	OCCUPATION LANE - SHEFFIELD RD			11385	9
87220	BIRLEY SPA LANE	OCCUPATION LANE - DYKE VALE RD			2817	12
89289	BLACKSTOCK RD	GLEADLESS RD - NORTON LANE			6360	5
96166	BLONK ST (ONE WAY)	WICKER - CASTLEGATE			31643	7
ATC	BOCHUM PARKWAY	NORTON LANE - MEADOW HEAD		ATC	25657	3
95117	BOCHUM PARKWAY	JORDANTHORPE PARKWAY - LIGHTWOOD LANE	7818	DoT	23993	6
89165	BOCKING LANE	ABBEY LANE - GREENHILL AVE			20260	5
87314A	BOLE HILL RD	HAGG HILL - COMPTON ST			724	3

1996 24HR AADF ESTIMATES DERIVED FROM 1995 GMTU DAY/MONTH FACTORS

TPU			*DoT*			*%*
CENSUS	*LOCATION*	*LINK*	*CENSUS*		*ALL*	*HEAVY*
87252	BOLE HILL RD	BACK LANE - HAGG HILL			4233	2
96220	BOLSOVER ST	BROOK HILL RBT - WINTER ST		TPP	12899	5
96144	BOYNTON RD	HERRIES RD - SHIRECLIFFE RD	967077	DoT	1716	2
96123	BRADFIELD RD	PENISTONE RD - OWLERTON GREEN	27821	DoT	8188	3
89107	BRADWAY RD	TWENTYWELL LANE - LOWEDGES RD			10254	7
94140	BRAMALL LANE	WOODHEAD RD - JOHN ST	47393	DoT	17795	5
96211	BRAMALL LANE	ST MARYS GATE - JOHN ST		TPP	23557	5
96168	BRIDGE ST (ONE WAY)	LADYS BRIDGE - SNIG HILL			19494	6
95116	BRIGHTSIDE LANE	UPWELL ST - NEWHALL RD	17718	DoT	12579	12
96226	BRIGHTSIDE LANE	WEEDON ST - UPWELL ST		TPP	20168	11
89241	BRINCLIFFE EDGE RD	NETHER EDGE RD - ASHLAND RD			2498	1
89241	BRINCLIFFE EDGE RD	NETHER EDGE RD - UNION RD			1460	1
89250	BRINCLIFFE EDGE RD	UNION RD - ECCLESALL RD STH			1627	1
96264	BROAD LANE	ROCKINGHAM ST - TENTER ST			23375	3
96263	BROAD LANE	BROOK HILL RBT - MAPPIN ST			20984	4
96263	BROAD LANE	MAPPIN ST - ROCKINGHAM ST			18340	4
96202	BROAD ST	PARK SQUARE - CRICKET INN RD		TPP	7344	12
92213	BROADFIELD RD	ABBEYDALE RD - LONDON RD			7964	3
88218	BROCCO BANK	HUNTERS BAR - CLARKEHOUSE RD			20395	4
96203	BROOK HILL	BROOK HILL RBT - WESTERN BANK		TPP	26635	6
ATC	BROOKHOUSE HILL	FULWOOD RD - CRIMICAR LANE		ATC	10511	6
87315	BROOKLANDS AVE	CRIMICAR LANE - GREEN LANE			3462	3
96224	BROOMHALL ST (ONE WAY)	HANOVER WAY - BROOMHALL RD		TPP	1498	2
96221	BROOMSPRING LANE	GLOSSOP RD - UPPER HANOVER ST		TPP	1841	2
94130	BROUGHTON LANE	GREENLAND RD - ATTERCLIFFE COMMON	48804	DoT	12226	5
95242	BROWN ST	FURNIVAL ST - PATERNOSTER ROW			15797	9
96222	BRUNSWICK RD	SPITALFIELDS - BURNGREAVE RD		TPP	1994	3
94146	BURNCROSS RD	LOUNDSIDE - HALLWOOD RD	47405	DoT	11139	3
95136	BURNGREAVE RD	GOWER ST - PITSMOOR RD	17728	DoT	15683	13
89246	BUTTON HILL	CARTER KNOWLE RD - SPRINGFIELD RD			3253	1
90115	CARLISLE ST	SUTHERLAND ST - SPITAL HILL			5396	9
90115	CARLISLE ST EAST	SUTHERLAND ST - NEWHALL RD			10048	9
90220	CARLISLE ST EAST	UPWELL ST - NEWHALL RD			13417	10
89291	CARR RD, STOCKSBRIDGE	MANCHESTER RD - ROYD LANE			4102	4
90179	CARSICK HILL RD	SANDYGATE RD - TOM LANE			3474	2
95183	CARTER KNOWLE RD	ARCHER LANE - BANNERDALE RD			5480	5
95183	CARTER KNOWLE RD	ARCHER LANE - SPRINGFIELD AVE			5119	5
89246	CARTER KNOWLE RD	ECCLESALL RD STH - BUTTON HILL			7988	2
96148	CARTMELL RD	TODWICK RD - ULVERSTON RD	967075	DoT	198	3
87137	CASTLEBECK AVE	HASTILAR RD STH - PRINCE OF WALES RD			3829	5
96167	CASTLEGATE (ONE WAY)	BLONK ST - LADYS BRIDGE			30861	8
96158	CATCH BAR LANE	MIDDLEWOOD RD - LEPPINGS LANE			12574	5
96158	CATCH BAR LANE	LEPPINGS LANE - PARKSIDE RD			14623	5
93233	CATLEY RD	MAIN RD - GREENLAND RD			7135	9
92132	CAUSEWAY HEAD RD	BRICKHOUSE LANE - HIGH ST			2904	5
89224	CEMETERY RD	PSALTER LANE - WASHINGTON RD			8811	3
91161	CEMETERY RD	WASHINGTON RD - NAPIER ST			5776	6
89161	CHAPELTOWN RD/ECCLESFIELD RD	NETHER LANE - BURNCROSS RD			12345	8
93211	CHARLOTTE RD	QUEENS RD - HEELEY BANK RD			9684	15
93211	CHARLOTTE RD	QUEENS RD - SHOREHAM ST			7987	13
96139	CHARTER ROW	FITZWILLIAM ST - CHARTER SQUARE	38227	DoT	20165	10
96215	CHATHAM ST (ONE WAY)	ROCK ST - NURSERY ST		TPP	3859	7
92128	CHAUCER RD	YEW LANE - DEERLANDS AVE			6215	6
ATC	CHESTERFIELD RD	SCARSDALE RD - LITTLE LONDON RD		ATC	17724	9

1996 24HR AADF ESTIMATES DERIVED FROM 1995 GMTU DAY/MONTH FACTORS

TPU CENSUS	LOCATION	LINK	DoT CENSUS		ALL	% HEAVY
95111	CHESTERFIELD RD	LITTLE LONDON RD - QUEENS RD	16581	DoT	24134	7
89105	CHESTERFIELD RD	SCARSDALE RD - ABBEY LANE			22779	8
94119	CHESTERFIELD RD STH	MEADOW HEAD RBT - SHEFFIELD RD	48531	DoT	33291	6
88132	CHURCH LANE, DORE	TOWNHEAD RD - OLD HAY LANE			2879	2
96147	CHURCH LANE, HACKENTHORPE	BEIGHTON RD - DELVES RD	967083	DoT	287	3
87123	CHURCH ST, ECCLESFIELD	MILL RD - ST MARYS LANE			8052	7
87226	CHURCH ST, ECCLESFIELD	STOCKS HILL - ST MARYS LANE			3528	6
96178	CITY RD	DUKE ST - GRANVILLE RD			7529	9
94138	CITY RD	MANOR TOP - PARK GRANGE RD	27373	DoT	10738	15
88218	CLARKEHOUSE RD	BROCCO BANK - CLARKEGROVE RD			20395	4
95172	CLARKEHOUSE RD	GLOSSOP RD - CLARKEGROVE RD			13350	2
90179	COLDWELL LANE	SANDYGATE RD - MANCHESTER RD			3811	3
94168A	COMMERCIAL ST	HAYMARKET - PARK SQUARE		10hr	11544	12
96115	COMMONSIDE	SCHOOL RD - BARBER RD			2806	3
88133	COMMONSIDE	HOWARD RD - BARBER RD			7725	8
96114	CONDUIT RD	CROOKESMOOR RD - SCHOOL RD			1588	1
92195	COOKS WOOD RD	SHIRECLIFFE RD - RUTLAND RD			13460	6
95184	CORPORATION ST (ONE WAY)	WEST BAR - BRIDGE ST			18658	6
95184	CORPORATION ST (ONE WAY)	BRIDGE ST - NURSERY ST			20327	6
90163	COWLEY HILL	NETHER LANE - M1 JUNCTION 35			13625	7
94123	COWLEY LANE	STATION RD - NETHER LANE	56862	DoT	9542	5
87234	COWLISHAW RD	PSALTER LANE - JUNCTION RD			10789	3
96202	CRICKET INN RD	BROAD ST - BERNARD RD		TPP	7344	12
86261	CRICKET INN RD	WOODBOURN RD - BERNARD RD			9813	12
88179	CRIMICAR LANE	REDMIRES RD - BROOKLANDS AVE			1945	8
94174	CROOKES	LYDGATE LANE - NORTHFIELD RD			11847	6
96117	CROOKES RD	LYDGATE LANE - CROOKESMOOR RD			12543	6
96117	CROOKES RD	WHITHAM RD - CROOKESMOOR RD			14024	6
96220	CROOKES VALLEY RD	WINTER ST - CROOKESMOOR RD		TPP	12899	5
96114	CROOKESMOOR RD	CONDUIT RD - CROOKES RD			4903	2
96114	CROOKESMOOR RD	CONDUIT RD - CROOKES VALLEY RD			5960	2
ATC	CROSS HILL	HIGH GREAVE - GREEN LANE		ATC	13273	7
96120	CROSS LANE	LYDGATE LANE - ARRAN RD			2876	2
87240	DARESBURY RD	EAST BANK RD - GLEADLESS RD			8317	7
93233	DARNALL RD	WORKSOP RD - MAIN RD			7135	9
89201	DEEP LANE	ECCLESFIELD RD - GRANGE LANE			4352	3
88248	DEERLANDS AVE	WORDSWORTH AVE - CHAUCER RD			9362	7
89330	DEERLANDS AVE	BARNSLEY RD - WORDSWORTH AVE			4602	5
90105	DERBYSHIRE LANE	SCARSDALE RD - COBNAR RD			6384	6
96260	DEVONSHIRE ST	FITZWILLIAM ST - DIVISION ST			2228	2
96260	DIVISION ST	DEVONSHIRE ST - ROCKINGHAM ST			2228	2
89120	DORE RD	HIGH ST - ABBEYDALE RD STH			3053	3
96200	DUKE ST	PARK SQUARE - BERNARD ST		TPP	8128	8
96178	DUKE ST	BERNARD ST - CITY RD			7529	9
86323	DYCHE LANE	BOCHUM PARKWAY - JORDANTHORPE PARKWAY			3814	7
ATC	EAST BANK RD	HURLFIELD RD - DARESBURY RD		ATC	11246	10
90176	EAST BANK RD	NORFOLK PARK RD - OLIVE GROVE RD			11568	6
88223	EAST BANK RD	EAST RD - MYRTLE RD			16225	8
96165	EAST COAST RD	BRIGHTSIDE LANE - FARADAY RD	969228	DoT	1114	11
96212	ECCLESALL RD	SUMMERFIELD ST - MOORE ST		TPP	33000	4
94287	ECCLESALL RD	PSALTER LANE - BROCCO BANK			20994	5
96174	ECCLESALL RD	BROCCO BANK - SUMMERFIELD ST			20553	6
90183	ECCLESALL RD STH	CARTER KNOWLE RD - RINGINGLOW RD			26143	6
90190	ECCLESALL RD STH	KNOWLE LANE - CARTER KNOWLE RD			20791	6

1996 24HR AADF ESTIMATES DERIVED FROM 1995 GMTU DAY/MONTH FACTORS

TPU CENSUS	*LOCATION*	*LINK*	*DoT CENSUS*		*ALL*	*% HEAVY*
90233	ECCLESALL RD STH	WHIRLOWDALE RD - ABBEY LANE			8847	5
93325	ECCLESALL RD STH	BENTS RD - ABBEY LANE			20586	3
93325	ECCLESALL RD STH	BENTS RD - KNOWLE LANE			17847	4
94143	ECCLESALL RD STH	PSALTER LANE - RINGINGLOW RD	47396	DoT	32398	4
ATC	ECCLESFIELD RD	FIFE ST - DEEP LANE		ATC	11295	5
92196	ECCLESFIELD RD	GREEN LANE - BELLHOUSE RD			9671	6
89161	ECCLESFIELD RD/CHAPELTOWN RD	NETHER LANE - BURNCROSS RD			12345	8
87361	ECKINGTON RD	ORCHARD LANE - OWLTHORPE GREENWAY			7769	6
87361	ECKINGTON RD	WEST ST - ORCHARD LANE			6463	7
96201	EDMUND RD	ST MARYS RD - CHARLOTTE RD		TPP	2785	4
96204	EFFINGHAM RD	EFFINGHAM ST - BERNARD RD		TPP	5606	10
96204	EFFINGHAM ST	FURNIVAL RD - EFFINGHAM RD		TPP	5606	10
94126	EXCHANGE ST	PARK SQUARE - FURNIVAL RD	48076	DoT	43455	9
96167	EXCHANGE ST	BLONK ST - FURNIVAL RD			52134	8
95137	EYRE ST	ST MARYS GATE - CUMBERLAND ST	17317	DoT	19297	7
95242	EYRE ST	FURNIVAL SQUARE - CUMBERLAND ST			14720	15
96151	FARADAY RD	WASHFORD RD - EAST COAST RD	967080	DoT	532	26
96218	FARM RD (ONE WAY)	GRANVILLE SQUARE - DUCHESS RD		TPP	4207	7
96260	FITZWILLIAM ST	DEVONSHIRE ST - WELLINGTON ST			2801	3
96261	FITZWILLIAM ST	WELLINGTON ST - CHARTER ROW			5114	3
96193	FITZWILLIAM ST (ONE WAY)	DEVONSHIRE ST - WEST ST			3362	2
90253	FLAT ST	POND ST - FITZALAN SQUARE			2435	71
92122	FOSTER WAY	THOMPSON HILL - GREEN GATE LANE			1399	14
87130	FOX HILL RD	PARSON CROSS RD - HALIFAX RD			3060	6
87130	FOX HILL RD	PARSON CROSS RD - SALT BOX LANE			3498	6
ATC	FULWOOD RD	MANCHESTER RD - BROOKHOUSE HILL		ATC	10511	6
89123	FULWOOD RD	MANCHESTER RD - GLOSSOP RD			20304	7
87233	FURNACE LANE	RETFORD RD - JUNCTION RD			4464	10
95245	FURNIVAL GATE	PINSTONE ST - FURNIVAL SQUARE			22580	8
95245	FURNIVAL GATE	PINSTONE ST - CHARTER SQUARE			24657	10
96204	FURNIVAL RD	EXCHANGE ST - EFFINGHAM ST		TPP	5606	10
95242	FURNIVAL ST	FURNIVAL SQUARE - BROWN ST			15797	9
95218	GIBRALTER ST (MID SUPERTRAM)	MOORFIELDS - WEST BAR			18139	15
ATC	GLEADLESS RD	BLACKSTOCK RD - HOLLINSEND RD		ATC	10515	2
96146	GLEADLESS RD	CARRFIELD RD - DARESBURY RD	967078	DoT	12176	4
90229	GLEADLESS RD	CARRFIELD RD - LONDON RD			5780	3
96188	GLEADLESS RD	RIDGEWAY RD - HOLLINSEND RD			7643	4
96188	GLEADLESS RD (ONE WAY)	RIDGEWAY RD - WHITE LANE			10740	5
96213	GLOSSOP RD	UPPER HANOVER ST - CLARKSON ST		TPP	11638	7
89297	GLOSSOP RD	FULWOOD RD - NEWBOULD LANE			7681	6
89297	GLOSSOP RD	NEWBOULD LANE - CLARKEHOUSE RD			9654	7
96193	GLOSSOP RD	REGENT ST - GELL ST			9062	17
96191	GLOSSOP RD	UPPER HANOVER ST - GELL ST			8824	13
90115	GOWER ST	CARLISLE ST - BURNGREAVE RD			11655	8
89201	GRANGE LANE	DEEP LANE - UPPER WORTLEY RD			4352	3
96208	GRANVILLE RD	CITY RD - GRANVILLE ST		TPP	10130	7
96177	GRANVILLE RD	GRANVILLE ST - GRANVILLE SQUARE			13214	8
96177	GRANVILLE ST	SHREWSBURY RD - GRANVILLE RD			4774	7
92196	GREEN LANE, ECCLESFIELD	THE COMMON - ECCLESFIELD RD			9671	6
96217	GREEN LANE, SHALESMOOR	PENISTONE RD - ALMA ST		TPP	2261	6
90175	GREENHILL AVE	GREENHILL MAIN RD - BOCKING LANE			12436	5
90175	GREENHILL MAIN RD	GREENHILL AVE - MEADOW HEAD			16508	6
90175	GREENHILL MAIN RD	GREENHILL AVE - GREENHILL PARKWAY			9384	7
90175	GREENHILL PARKWAY	GREENHILL MAIN RD - RENEY RD			9384	7

1996 24HR AADF ESTIMATES DERIVED FROM 1995 GMTU DAY/MONTH FACTORS

TPU CENSUS	*LOCATION*	*LINK*	*DoT CENSUS*		*ALL*	*% HEAVY*
90182	GREENHILL PARKWAY	LOWEDGES RD - RENEY RD			10004	8
94120	GREENLAND RD	CATLEY RD - SHEPCOTE LANE	18721	DoT	23521	7
94130	GREENLAND RD	SHEPCOTE LANE - BROUGHTON LANE	48804	DoT	12226	5
90127	GREENLAND RD (PRE ORR)	MAIN RD - CATLEY RD	57716	DoT	22789	10
86274	GREYSTONES RD	ECCLESALL RD - HIGHCLIFFE RD			4498	4
96149	GRIMESTHORPE RD	CARWOOD RD - BOTHAM ST	967079	DoT	1788	5
90227	HAGG LANE	MANCHESTER RD - LONG LANE			692	1
87259	HAGG STONES RD	WORRALL RD - BURTON LANE			1382	8
87332	HALIFAX RD	SOUTHEY GREEN RD - CHAUCER RD			23584	9
87332	HALIFAX RD	SOUTHEY GREEN RD - FOX HILL RD			27871	9
90204	HALIFAX RD	SALT BOX LANE - DEERLANDS AVE			19920	8
96154	HANDSWORTH AVE	HANDSWORTH RD - LOUND RD			1009	4
96154	HANDSWORTH RD	PRINCE OF WALES RD - HANDSWORTH AVE			13742	8
96154	HANDSWORTH RD	HANDSWORTH AVE - SHEFFIELD PARKWAY			13655	8
88237	HANGINGWATER RD	NETHERGREEN RD - FULWOOD RD			7853	2
88237	HANGINGWATER RD	NETHERGREEN RD - HIGHCLIFFE RD			7064	1
96191	HANOVER WAY	UPPER HANOVER ST - MOORE ST RBT			31036	4
87333	HARBOROUGH AVE	PRINCE OF WALES RD - WOODROVE AVE			3231	8
87333	HARBOROUGH AVE	PRINCE OF WALES RD - MANOR LANE			4383	9
89330	HARTLEY BROOK RD	BARNSLEY RD - SICEY AVE			4096	5
87137	HASTILAR RD STH	NODDER RD - CASTLEBECK AVE			3829	5
87137	HASTILAR RD STH	RICHMOND RD - NODDER RD			5601	7
94134	HATHERSAGE RD	STONY RIDGE RD - WHIRLOWDALE RD	57320	DoT	5021	8
96130	HAWKE ST	BRIGHTSIDE LANE - JANSON ST	37902	DoT	12149	9
87147	HEAVYGATE RD	NORTHFIELD RD - COMPTON ST			8476	6
87147	HEAVYGATE RD	NORTHFIELD RD - UPPERTHORPE RD			923	3
86352	HEELEY BANK RD	CHARLOTTE RD - EAST RD			7583	10
90254	HEMSWORTH RD	WARMINSTER RD - DERBYSHIRE LANE			5426	5
90254	HEMSWORTH RD	WARMINSTER RD - NORTON LANE			8329	5
96189	HERDINGS RD	NORTON AVE - HERDINGS VIEW			298	4
88175	HERRIES DRIVE	HERRIES RD - LONGLEY LANE			3871	7
96137	HERRIES RD	MOONSHINE LANE - WORDSWORTH AVE	27859	DoT	17095	6
88138	HERRIES RD	BARNSLEY RD - NORWOOD RD			9626	14
89229	HERRIES RD	MOONSHINE LANE - HERRIES DRIVE			14870	9
96157	HERRIES RD	HERRIES RD STH - LEPPINGS LANE			8549	10
96159	HERRIES RD STH	PENISTONE RD - HERRIES RD			12103	5
ATC	HIGH GREAVE	BARNSLEY RD - CROSS HILL		ATC	13273	7
94168A	HIGH ST	HAYMARKET - CASTLE SQUARE		10hr	14551	25
87248	HIGH ST, ECCLESFIELD	WORDSWORTH AVE - ST MICHAELS RD			3499	11
87248	HIGH ST, ECCLESFIELD	ST MARYS LANE - WORDSWORTH AVE			4652	10
88107	HIGH ST, MOSBOROUGH	STATION RD - SHEFFIELD RD			8512	8
89331	HIGH ST, MOSBOROUGH	MOSBOROUGH MOOR - STATION RD			13760	7
86273	HIGH STORRS RD	RINGINGLOW RD - HIGHCLIFFE RD			6815	2
88237	HIGHCLIFFE RD	HANGINGWATER RD - GREYSTONES RD			7064	1
90181	HIGHFIELD LANE	ORGREAVE LANE - ORGREAVE RD			8025	11
88132	HILLFOOT RD, DORE	OLD HAY LANE - BASLOW RD			2879	2
96187	HOLLINSEND RD	RIDGEWAY RD - MANSFIELD RD			5961	3
96187	HOLLINSEND RD	RIDGEWAY RD - GLEADLESS COMMON			4361	5
89194	HOLLOW GATE, BURNCROSS	BURNCROSS RD - POTTER HILL RD			4784	7
95173	HOLME LANE (MID SUPERTRAM)	BRADFIELD RD - RIVELIN VALLEY RD			14574	6
96230	HOLYWELL RD	UPWELL ST - JENKIN RD		TPP	11468	9
88133	HOWARD RD	SOUTH RD - COMMONSIDE			7725	8
95243	HOWARD ST	SHEAF SQUARE - ARUNDEL GATE			1747	34
95218	HOYLE ST (MID SUPERTRAM)	PENISTONE RD - MEADOW ST			26208	5

1996 24HR AADF ESTIMATES DERIVED FROM 1995 GMTU DAY/MONTH FACTORS

TPU CENSUS	*LOCATION*	*LINK*	*DoT CENSUS*		*ALL*	*% HEAVY*
89202	HUCKLOW RD	BARNSLEY RD - STUBBIN LANE			4488	10
88136	HUTCLIFFE WOOD RD	ABBEY LANE - ARCHER RD			11211	3
96130	JANSON ST	HAWKE ST - ATTERCLIFFE COMMON	37902	DoT	12149	9
ATC	JENKIN RD	HOLYWELL RD - NEWMAN RD		ATC	5917	3
92192	JORDANTHORPE PARKWAY	BOCHUM PARKWAY - DYCHE LANE			17655	3
92192	JORDANTHORPE PARKWAY	DYCHE LANE - CHESTERFIELD RD STH			8487	4
87234	KINGFIELD RD	PSALTER LANE - ST ANDREWS RD			7778	4
86307	KIRK EDGE RD	LONG LANE - BURNT HILL LANE			275	4
96166	LADYS BRIDGE	BRIDGE ST - NURSERY ST			14294	27
89104	LANE END	LOUND SIDE - MORTOMLEY LANE			8576	6
96225	LANGSETT RD	HOLME LANE - RIPLEY ST		TPP	6306	22
ATC	LANGSETT RD NTH	MAIN RD - CHURCH ST		ATC	9348	4
96158	LANGSETT RD STH	MIDDLEWOOD RD NTH - FORGE HILL			12574	5
87210	LANGSETT RD STH (ONE WAY)	FORGE HILL - CHURCH ST			7221	13
95243	LEADMILL RD	SHEAF SQUARE - SUFFOLK RD			29114	9
96157	LEPPINGS LANE	PENISTONE RD NTH - CATCH BAR LANE			14931	7
96158	LEPPINGS LANE (ONE WAY)	CATCH BAR LANE - MIDDLEWOOD RD			6118	6
96206	LONDON RD	ST MARYS GATE - BOSTON ST		TPP	18301	10
86282	LONDON RD	WOLSELEY RD - ABBEYDALE RD			7393	9
93328	LONDON RD	SHARROW LANE - ABBEYDALE RD			16767	10
93328	LONDON RD	WOODHEAD RD - BOSTON ST			15759	10
89137	LONG LANE, STANNINGTON	OLDFIELD RD - ROSCOE BANK			219	3
88148	LONGLEY LANE	HERRIES RD - HERRIES DRIVE			2634	12
89104	LOUND SIDE	BURNCROSS RD - LANE END			8576	6
92156	LOWEDGES RD	CHESTERFIELD RD STH - GREENHILL PARKWAY	90915	DoT	2945	14
90185	LOXLEY RD	RODNEY HILL - STUDFIELD HILL			3185	5
90185	LOXLEY RD	RODNEY HILL - LONG LANE			3944	6
96152	LUMLEY ST	BERNARD RD - WORTHING RD	967081	DoT	4452	14
96119	LYDGATE LANE	NAIRN ST - CROOKES			5103	2
96119	LYDGATE LANE	NAIRN ST - CROSS LANE			4428	2
96120	LYDGATE LANE	CROSS LANE - MANCHESTER RD			5784	2
ATC	M1 JUNCTION 34 STH ENTRY			ATC	11357	21
ATC	M1 JUNCTION 34 STH EXIT			ATC	11612	21
96141	M1 MOTORWAY	M1 JUNCTION 34 NTH - M1 JUNCTION 34 STH	28052	DoT	64762	14
93233	MAIN RD	DARNALL RD - CATLEY RD			7135	9
94125	MAIN RD, WHARNCLIFFE SIDE	VAUGHTON HILL - LANGSETT RD NTH	57418	DoT	8987	8
90205	MAIN ST, GRENOSIDE	NORFOLK HILL - SALT BOX LANE			3397	8
90205	MAIN ST, GRENOSIDE	NORFOLK HILL - WOODHEAD RD			2578	3
95112	MANCHESTER RD	RIVELIN VALLEY RD - COLDWELL LANE	6565	DoT	6229	5
96125	MANCHESTER RD	LADYBOWER - RIVELIN VALLEY RD	26576	DoT	5800	6
89123	MANCHESTER RD	FULWOOD RD - LYDGATE LANE			10263	7
90227	MANCHESTER RD	COLDWELL LANE - LYDGATE LANE			8753	5
89291	MANCHESTER RD, STOCKSBRIDGE	VAUGHTON HILL - STOCKSBRIDGE BY PASS			8660	8
88178	MANOR LANE	MALTRAVERS RD - SHEFFIELD PARKWAY SLIP RD			7881	6
88178	MANOR LANE	MALTRAVERS RD - HARBOROUGH AVE			9211	9
90177	MANOR WAY	WOODBOURN RD - SHEFFIELD PARKWAY SLIP RD			10657	8
95118	MANSFIELD RD	WOODHOUSE RD - HURLFIELD RD	7355	DoT	19720	8
96265	MAPPIN ST	PORTOBELLO ST - WEST ST			3868	3
96263	MAPPIN ST	BROAD LANE - PORTOBELLO ST			4582	3
91126	MEADOW HALL RD	MEADOW HALL WAY - TRANSPORT INTERCHANGE	47826	DoT	15502	14
94145	MEADOW HEAD	MEADOW HEAD RBT - ABBEY LANE	46620	DoT	19840	8
96205	MEADOW ST	WATERY ST - HOYLE ST		TPP	4582	5
91114	MICKLEY LANE	ROD MOOR RD - BASLOW RD			4678	3
96158	MIDDLEWOOD RD	CATCH BAR LANE - MIDDLEWOOD RD NTH			12574	5

1996 24HR AADF ESTIMATES DERIVED FROM 1995 GMTU DAY/MONTH FACTORS

TPU CENSUS	LOCATION	LINK	DoT CENSUS		ALL	% HEAVY
96158	MIDDLEWOOD RD NTH	MIDDLEWOOD RD - LANGSETT RD STH			12574	5
89238	MONTGOMERY RD	RUNDLE RD - KENWOOD PARK RD			5893	5
89238	MONTGOMERY RD	RUNDLE RD - MACHON BANK RD			2229	6
89229	MOONSHINE LANE	HERRIES RD - SOUTHEY GREEN RD			8212	8
89331	MOOR VALLEY	QUARRY HILL - SHEFFIELD RD			8611	8
96212	MOORE ST	ECCLESALL RD - HANOVER WAY		TPP	33000	4
88232	MOORE ST	HANOVER WAY - FITZWILLIAM ST			25458	5
95218	MOORFIELDS (MID SUPERTRAM)	SHALESMOOR - GIBRALTER ST			18139	15
86327	MORTOMLEY LANE	WORTLEY RD - LANE END			3858	11
89331	MOSBOROUGH MOOR	QUARRY HILL - HIGH ST			13760	7
ATC	MOSBOROUGH PARKWAY II	SHEFFIELD PARKWAY - COISLEY HILL		ATC	24808	10
94264	MOSBOROUGH PARKWAY IIIB	BEIGHTON RD - ASTON RELIEF RD			11036	8
94264	MOSBOROUGH PARKWAY IIIA	BEIGHTON RD - ECKINGTON WAY			9906	7
96216	MOWBRAY ST	PITSMOOR RD - HARVEST LANE		TPP	11386	10
91112	MYRTLE RD	PROSPECT RD - QUEENS RD			11495	5
96119	NAIRN ST	LYDGATE LANE - BUTE ST			953	1
90163	NETHER LANE	THE COMMON - COWLEY LANE			7796	8
87349	NETHER SHIRE LANE	BELLHOUSE RD - HARTLEY BROOK RD			1712	4
88237	NETHERGREEN RD	HANGINGWATER RD - FULWOOD RD			5457	3
95218	NETHERTHORPE RD (MID SUPERTRAM)	MEADOW ST - BROOK HILL RBT			26208	5
87149	NEWHALL RD	BRIGHTSIDE LANE - CARLISLE ST			6832	10
92219	NEWHALL RD	ATTERCLIFFE RD - BRIGHTSIDE LANE			9651	11
91142	NEWMAN RD	BARROW RD - MERTON LANE			2825	4
91142	NEWMAN RD	MERTON LANE - JENKIN RD			5960	8
90205	NORFOLK HILL	MAIN ST - PENISTONE RD			2186	13
90187	NORTHFIELD RD	HEAVYGATE RD - CROOKES			9900	10
96114	NORTHUMBERLAND RD	WHITHAM RD - CROOKESMOOR RD			2911	2
88173	NORTON AVE	HEMSWORTH RD - LIGHTWOOD LANE			6802	5
96188	NORTON AVE	GLEADLESS RD - WHITE LANE			33688	7
96189	NORTON AVE	LIGHTWOOD LANE - WHITE LANE			34132	7
88173	NORTON LANE	HEMSWORTH RD - BOCHUM PARKWAY			7791	4
90255	NORTON LEES LANE	WARMINSTER RD - SCARSDALE RD			3739	4
90255	NORTON LEES LANE	WARMINSTER RD - UPPER ALBERT RD			5495	4
96166	NURSERY ST (ONE WAY)	SPITALFIELDS - WICKER			22725	8
88237	OAKBROOK RD	HANGINGWATER RD - RUSTLINGS RD			7138	3
87128	OCCUPATION LANE	SHEFFIELD RD - BIRLEY MOOR RD			2359	5
88132	OLD HAY LANE, DORE	CHURCH LANE - HILLFOOT RD			2879	2
90184	OLDFIELD RD	STANNINGTON RD - LONG LANE			2280	7
90181	ORGREAVE LANE	HIGH FIELD LANE - END			867	18
90181	ORGREAVE LANE	HANDSWORTH RD - HIGH FIELD LANE			5742	9
90181	ORGREAVE RD	HIGHFIELD LANE - POPLAR WAY			8025	11
92210	OSBORNE RD	UNION RD - ST ANDREWS RD			8350	2
92210	OSBORNE RD	UNION RD - BARKERS RD			7798	3
87253	OWLER LANE	FIRVALE JUNCTION - RUSHBY ST			15015	12
87253	OWLER LANE	RUSHBY ST - UPWELL ST			15015	12
88177	PAGE HALL RD	FIRTH PARK RD - OWLER LANE			5797	9
96118	PARKERS RD	CROOKES RD - WHITHAM RD			1005	0
96122	PARKSIDE RD	CATCH BAR LANE - PENISTONE RD	28172	DoT	10256	4
93103	PARKWAY AVE	WOODBOURN RD - PARKWAY DRIVE			8149	11
95243	PATERNOSTER ROW	SHEAF SQUARE - BROWN ST			15747	11
96133	PENISTONE RD	HALLWOOD RD - NORFOLK HILL	56624	DoT	21531	6
96229	PENISTONE RD	BRADFIELD RD - MCDONALDS		TPP	44822	6
96209	PENISTONE RD	HOYLE ST - RUTLAND RD		TPP	39917	7
96160	PENISTONE RD	BRADFIELD RD - PARKSIDE RD			48759	6

1996 24HR AADF ESTIMATES DERIVED FROM 1995 GMTU DAY/MONTH FACTORS

TPU CENSUS	*LOCATION*	*LINK*	*DoT CENSUS*		*ALL*	*% HEAVY*
94144	PENISTONE RD	BAMFORTH ST - MCDONALDS	46619	DoT	34027	10
96128	PENISTONE RD	HALLWOOD RD - WESTWOOD NEW RD	56597	DoT	18028	6
90206	PENISTONE RD (A629)	WESTWOOD NEW RD - STOCKSBRIDGE BY PASS			4972	8
96157	PENISTONE RD NTH	LEPPINGS LANE - FOX HILL RD			36897	7
96157	PENISTONE RD NTH	HERRIES RD STH - LEPPINGS LANE			27057	7
96159	PENISTONE RD NTH	PARKSIDE RD - HERRIES RD STH			37496	7
95245	PINSTONE ST	FURNIVAL GATE - CHARLES ST			7968	26
96215	PITSMOOR RD	RUTLAND RD - ROCK ST		TPP	8066	6
96215	PITSMOOR RD (ONE WAY)	MOWBRAY ST - ROCK ST		TPP	4207	6
95243	POND ST	SHEAF SQUARE - FLAT ST			3943	59
92123	POTTER HILL LANE	POTTER HILL RD - THOMPSON HILL			814	27
92123	POTTER HILL RD	HOLLOW GATE - POTTER HILL LANE			814	27
ATC	PRINCE OF WALES RD	MAIN RD - SHEFFIELD PARKWAY		ATC	28240	8
96131	PRINCE OF WALES RD	SHEFFIELD PARKWAY - MANOR TOP	27822	DoT	25064	8
91112	PROSPECT RD	SPENCER RD - MYRTLE RD			11495	5
87153	PROSPECT RD, BRADWAY	BRADWAY RD - WOODLAND PLACE			4388	4
89227	PSALTER LANE	ECCLESALL RD - OSBORNE RD			8728	2
96126	QUEENS RD	LONDON RD - MYRTLE RD	37898	DoT	26088	7
96132	QUEENS RD	CHARLOTTE RD - DUCHESS RD	27857	DoT	14229	10
96223	QUEENS RD	GRANVILLE SQUARE - DUCHESS RD		TPP	19818	11
93211	QUEENS RD	CHARLOTTE RD - MYRTLE RD			15329	9
87249	REDMIRES RD	SANDYGATE RD - CRIMICAR LANE			5765	8
96193	REGENT ST (ONE WAY)	GLOSSOP RD - PORTOBELLO ST			1999	3
94133	RETFORD RD	ORGREAVE LANE - ROTHERHAM RD	46585	DoT	15165	9
91112	RICHARDS RD	GLEADLESS RD - SPENCER RD			11495	5
88219	RICHMOND PARK RD	HANDSWORTH RD - RICHMOND RD			5942	7
88164	RICHMOND RD	HASTILAR RD STH - STRADBROKE RD			12745	5
88164	RICHMOND RD	STRADBROKE RD - RICHMOND PARK RD			10369	5
88224	RICHMOND RD	NORMANTON HILL - HASTILAR RD STH			10710	5
96187	RIDGEWAY RD	HOLLINSEND RD - HURLFIELD RD			25117	7
96187	RIDGEWAY RD	HOLLINSEND RD - GLEADLESS RD			26514	7
ATC	RINGINGLOW RD	HOUNDKIRK RD - BENTS RD		ATC	4661	2
93324	RINGINGLOW RD	BENTS RD - HIGH STORRS RD			5753	3
94135	RIVELIN VALLEY RD	MANCHESTER RD - HOLLINS LANE	47822	DoT	3032	7
95173	RIVELIN VALLEY RD (MID SUPERTRAM)	HOLME LANE - WATERSMEET RD			15168	3
96194	ROCKINGHAM ST	WEST ST - TRIPPET LANE			7366	3
96264	ROCKINGHAM ST	BROAD LANE - TRIPPET LANE			7823	3
96194	ROCKINGHAM ST (ONE WAY)	WEST ST - DIVISION ST			5330	3
87153	ROD MOOR RD	BRADWAY RD - MICKLEY LANE			4172	6
90196	RODNEY HILL	LOXLEY RD - BEN LANE			2312	6
90181	ROTHERHAM RD, HANDSWORTH	ORGREAVE LANE - RETFORD RD			8504	11
91119	ROTHERHAM RD, MOSBOROUGH	STATION RD - LITTLEMOOR RD			12554	5
87253	RUSHBY ST	OWLER LANE - OWLER LANE			15015	12
91210	RUSHBY ST	OWLER LANE - OWLER LANE			13306	9
86287	RUSTLINGS RD	ECCLESALL RD - OAKBROOK RD			7872	4
89197	RUTLAND RD	COOKS WOOD RD - BOYLAND ST			15231	7
96120	RYEGATE CRESCENT	LYDGATE LANE - RYEGATE RD			635	1
90179	SANDYGATE RD	COLDWELL LANE - MANCHESTER RD			6858	5
90179	SANDYGATE RD	COLDWELL LANE - REDMIRES RD			7872	4
91127	SAVILE ST	ATTERCLIFFE RD - WICKER	56863	DoT	20294	15
87255	SAVILE ST EAST	ATTERCLIFFE RD - BRIGHTSIDE LANE			8372	11
89109	SCARSDALE RD	CHESTERFIELD RD - DERBYSHIRE LANE			6820	5
96115	SCHOOL RD	CROOKES - CONDUIT RD			3288	3
96115	SCHOOL RD	CONDUIT RD - COMMONSIDE			2806	3

1996 24HR AADF ESTIMATES DERIVED FROM 1995 GMTU DAY/MONTH FACTORS

TPU CENSUS	*LOCATION*	*LINK*	*DoT CENSUS*		*ALL*	*% HEAVY*
96153	SCHOOL RD, CHAPELTOWN	GREENGATE LANE - WORRALL RD	967076	DoT	679	29
95218	SHALESMOOR (MID SUPERTRAM)	HOYLE ST - MOORFIELDS			18139	15
92212	SHARROW LANE	PSALTER LANE - WASHINGTON RD			6071	3
92212	SHARROW LANE	WASHINGTON RD - LONDON RD			9266	2
96136	SHEAF ST	SHEAF SQUARE - PARK SQUARE	36625	DoT	39978	8
94147	SHEFFIELD PARKWAY	MANOR LANE SLIP RD - PRINCE OF WALES RD	47855	DoT	49007	6
96129	SHEFFIELD PARKWAY	HANDSWORTH RD - MOSBOROUGH PARKWAY	36588	DoT	55112	7
96210	SHEFFIELD PARKWAY	PARK SQUARE - MANOR LANE SLIP RD		TPP	49936	6
88107	SHEFFIELD RD, MOSBOROUGH	HIGH ST - ROTHERHAM RD			8512	8
94136	SHEFFIELD RD, TINSLEY	M1 JUNCTION 34 STH - CENTENARY WAY	57330	DoT	12618	14
88204	SHEFFIELD RD, WOODHOUSE	WOLVERLEY RD - TANNERY ST			6971	7
96228	SHEPCOTE LANE	GREENLAND RD - M1 JUNCTION 34 STH		TPP	12506	11
92195	SHIRECLIFFE RD	HERRIES RD - COOKS WOOD RD			13460	6
90162	SHIREGREEN LANE	BELLHOUSE RD - WINCOBANK AVE			6222	6
96214	SHOREHAM ST	ST MARYS RD - CHARLOTTE RD		TPP	10481	9
95244	SHOREHAM ST	ST MARYS RD - LEADMILL RD			16858	5
96219	SHREWSBURY RD	GRANVILLE ST- TALBOT ST		TPP	10429	9
96177	SHREWSBURY RD (ONE WAY)	GRANVILLE SQUARE - GRANVILLE ST			5283	10
88176	SICEY AVE	GREGG HOUSE RD - HATFIELD HOUSE LANE			3352	8
88176	SICEY AVE	GREGG HOUSE RD - NETHERSHIRE LANE			2405	5
95185	SNIG HILL	BRIDGE ST - BANK ST			4684	41
88133	SOUTH RD	WALKLEY RD - HOWARD RD			7725	8
88249	SOUTHEY GREEN RD	HALIFAX RD - WORDSWORTH AVE			7539	7
92125	SOUTHEY HILL	WORDSWORTH AVE - MOONSHINE LANE			1091	5
91112	SPENCER RD	RICHARDS RD - PROSPECT RD			11495	5
87225	SPITAL HILL	GOWER ST - HALLCAR ST			8664	13
90247	SPITAL HILL	CARLISLE ST - HALLCAR ST			9386	14
96116	SPRINGVALE RD	CROOKES - WESTERN RD			2219	3
96116	SPRINGVALE RD	WESTERN RD - COMMONSIDE			2263	3
96192A	ST GEORGES TERRACE (ONE WAY)	BROOK HILL RBT - PORTOBELLO ST			3084	2
95132	ST MARYS GATE	LONDON RD - BRAMALL LANE	57861	DoT	45048	5
88232	ST MARYS GATE	HANOVER WAY - LONDON RD			45251	6
87248	ST MARYS LANE, ECCLESFIELD	YEW LANE - CHURCH ST			4652	10
95244	ST MARYS RD	SHOREHAM ST - EDMUND RD			15865	7
95244	ST MARYS RD	SHOREHAM ST - BRAMALL LANE			31490	8
90197	STANIFORTH RD	MAIN RD - WOODBOURN RD	64064	DoT	11427	15
91118	STANNINGTON RD	LIBERTY HILL - HOLLINS LANE			7349	6
93155	STANNINGTON RD	LIBERTY HILL - OLDFIELD RD			6539	6
95173	STANNINGTON RD (MID SUPERTRAM)	HOLME LANE - WOOD LANE			10758	7
95134	STATION RD, CHAPELTOWN	COWLEY LANE - WHITE LANE	7758	DoT	7260	4
87252	STEPHEN HILL	MANCHESTER RD - BACK LANE			4233	2
90205	STEPHEN LANE	MAIN ST - SKEW HILL			1649	3
94171	STEVENSON RD	ATTERCLIFFE RD - WOODBINE RD			3876	16
90225	STOCKSBRIDGE BY PASS	WESTWOOD MAIN RD - M1 JUNCTION 35A			11823	25
90225	STOCKSBRIDGE BY PASS	WESTWOOD MAIN RD - ROUGH LANE			12455	24
91105	STRADBROKE RD	RICHMOND RD - SHEFFIELD RD			5272	13
94132	SUFFOLK RD	FORNHAM ST - LEADMILL RD	8758	DoT	9757	18
96174	SUMMERFIELD ST	ECCLESALL RD - CEMETERY RD			14723	2
90115	SUTHERLAND ST	CARLISLE ST - SAVILE ST			11965	8
96178	TALBOT ST	DUKE ST - SHREWSBURY RD			9145	8
89118	TANNERY ST	BEAVER HILL RD - STRADBROKE RD			9395	9
96119	TAPTON CRESCENT RD	LYDGATE LANE - RYEGATE RD			1318	1
96264	TENTER ST	BROAD LANE - WEST BAR GREEN			23375	3
92196	THE COMMON, ECCLESFIELD	GREEN LANE - NETHER LANE			18130	6

1996 24HR AADF ESTIMATES DERIVED FROM 1995 GMTU DAY/MONTH FACTORS

TPU CENSUS	*LOCATION*	*LINK*	*DoT CENSUS*		*ALL*	*% HEAVY*
87226	THE WHEEL, ECCLESFIELD	TOWNEND RD - WHEEL LANE			3528	6
92127	THOMPSON HILL	WESTWOOD NEW RD - WORTLEY RD			4872	2
96135	TINSLEY VIADUCT (LOWER DECK)	M1 JUNCTION 34 NTH - M1 JUNCTION 34 STH	37913	DoT	22450	12
90199	TOM LANE	FULWOOD RD - STUMPERLOWE HALL RD			1004	2
87226	TOWN END RD, ECCLESFIELD	THE WHEEL - STOCKS HILL			3528	6
88132	TOWN HEAD RD, DORE	CHURCH LANE - NEWFIELD LANE			1378	5
87150	TWENTYWELL LANE	ABBEYDALE RD STH - BRADWAY RD			5523	2
96191	UPPER HANOVER ST	GLOSSOP RD - BROOK HILL RBT			29495	5
96191	UPPER HANOVER ST	GLOSSOP RD - HANOVER WAY			31036	4
87253	UPWELL ST	OWLER LANE - HOLYWELL RD			15015	12
ATC	UPWELL ST	BRIGHTSIDE LANE - HOLYWELL RD		ATC	16611	10
96168	WAINGATE	BRIDGE ST - COMMERCIAL ST			3620	74
88217	WALKLEY RD	BURNABY CRESCENT - WHITEHOUSE LANE			2734	7
88217	WALKLEY RD	WALKLEY LANE - BURNABY CRESCENT			2873	6
96151	WASHFORD RD	ATTERCLIFFE RD - FARADAY RD	967080	DoT	532	26
92212	WASHINGTON RD	SHARROW LANE - CEMETERY RD			10026	3
96261	WELLINGTON ST	FITZWILLIAM ST - ROCKINGHAM ST			2581	3
95185	WEST BAR	SNIG HILL - CORPORATION ST			20878	14
95218	WEST BAR (MID SUPERTRAM)	GIBRALTER ST - CORPORATION ST			18139	15
96264	WEST BAR GREEN	TENTER ST - WEST BAR			23375	3
96193	WEST ST	FITZWILLIAM ST - MAPPIN ST			7342	20
96194	WEST ST	ROCKINGHAM ST - CARVER ST			7020	22
96194	WEST ST	ROCKINGHAM ST - ELDON ST			7138	22
96265	WEST ST	ELDON ST - MAPPIN ST			9631	15
87241	WESTBOURNE RD	GLOSSOP RD - CLARKEHOUSE RD			4536	2
96203	WESTERN BANK	BROOK HILL - CLARKSON ST		TPP	26635	6
95135	WESTERN BANK	CLARKSON ST - WHITHAM RD	8144	DoT	15039	8
96115	WESTERN RD	SCHOOL RD - SPRINGVALE RD			1250	2
96116	WESTERN RD	SPRINGVALE RD - NORTHFIELD RD			958	3
90225	WESTWOOD MAIN RD, HIGH GREEN	STOCKSBRIDGE BY PASS - M1 JUNCTION 36			14286	10
90225	WESTWOOD MAIN RD, HIGH GREEN	STOCKSBRIDGE BY PASS - WORTLEY RD			11808	9
93162	WESTWOOD NEW RD	WORTLEY RD - PENISTONE RD (A629)	26607	DoT	12515	7
87226	WHEEL LANE, ECCLESFIELD	THE WHEEL - HALIFAX RD			3528	6
96101	WHIRLOWDALE RD	ECCLESALL RD STH - ABBEY LANE			2744	6
96189	WHITE LANE (ONE WAY)	NORTON AVE - GLEADLESS RD			10179	5
95134	WHITE LANE, CHAPELTOWN	STATION RD - M1 JUNCTION 36	7758	DoT	7260	4
95135	WHITHAM RD	WESTERN BANK - CROOKES RD	8144	DoT	15039	8
96207	WICKER	SPITAL HILL - STANLEY ST		TPP	32982	15
96166	WICKER	STANLEY ST - BLONK ST			30098	17
90162	WINCOBANK AVE	SHIREGREEN LANE - JENKIN RD			6222	6
88185	WINDMILL GREENWAY	SHEFFIELD RD - ROTHERHAM RD			1737	14
96220	WINTER ST	BOLSOVER ST - CROOKES VALLEY RD		TPP	12899	5
86282	WOLSELEY RD	QUEENS RD - ABBEYDALE RD			7383	14
88239	WOOD LANE, STANNINGTON	MYERS GROVE LANE - STANNINGTON RD (WEST)			3751	3
88239	WOOD LANE, STANNINGTON	STANNINGTON RD (EAST) - MYERS GROVE LANE			5593	3
94171	WOODBINE RD	STEVENSON RD - BRIGHTSIDE LANE			3876	16
93103	WOODBOURN RD	PARKWAY AVE - STANIFORTH RD			13318	10
93103	WOODBOURN RD	PARKWAY AVE - MANOR WAY			11713	10
94264	WOODHOUSE LANE	MOSBOROUGH PARKWAY - ROBIN LANE			6342	7
94264	WOODHOUSE LANE	ROBIN LANE - ROTHERHAM RD			3457	4
87333	WOODROVE AVE	HARBOROUGH AVE - NODDER RD			3231	8
89109	WOODSEATS RD	CHESTERFIELD RD - ABBEYDALE RD			4669	4
90103	WORDSWORTH AVE	SOUTHEY HILL - DEERLANDS AVE			8716	5
93233	WORKSOP RD	ATTERCLIFFE RD - DARNALL RD			7135	9

1996 24HR AADF ESTIMATES DERIVED FROM 1995 GMTU DAY/MONTH FACTORS

TPU CENSUS	*LOCATION*	*LINK*	*DoT CENSUS*		*ALL*	*% HEAVY*
96152	WORTHING RD	LUMLEY ST - WOODBOURN RD	967081	DoT	4452	14
90191	WORTLEY RD	WESTWOOD MAIN RD - MORTOMLEY LANE			2146	4
91214	WOSTENHOLME RD	SHARROW LANE - KENWOOD PARK RD			3985	6
92128	YEW LANE	CHAUCER RD - ST MARYS LANE			6215	6

APPENDIX 5C

WIND ROSES FOR THE 5 SURVEYS

Windrose Survey 1

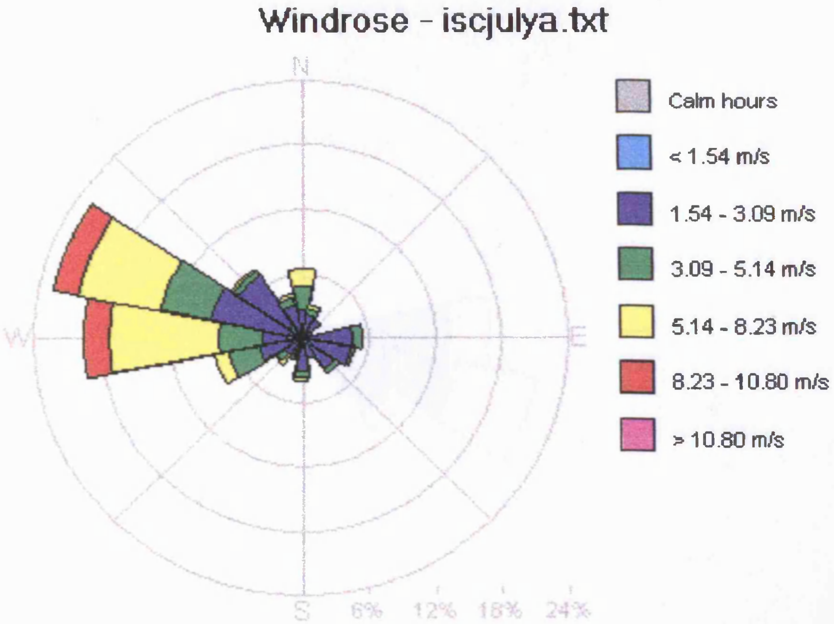

Windrose Survey 2

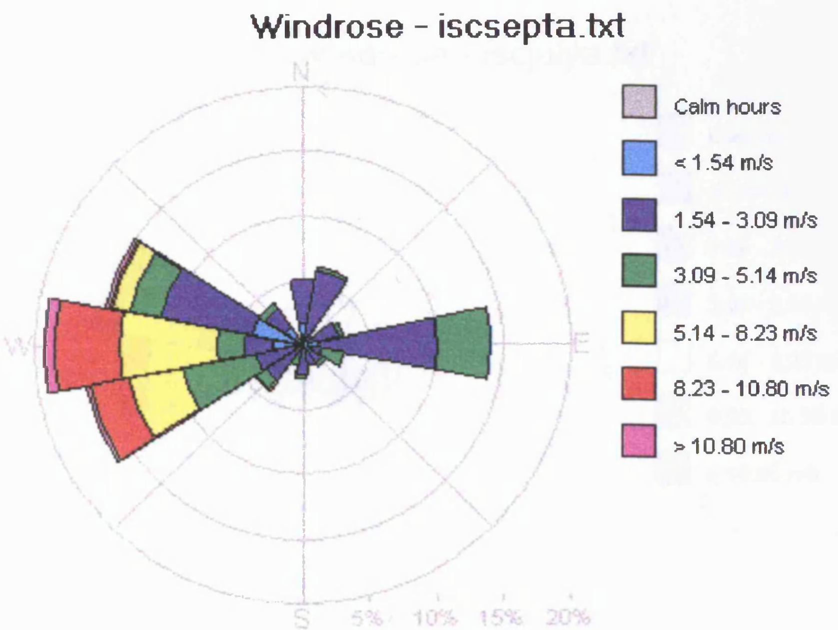

Windrose Survey 3

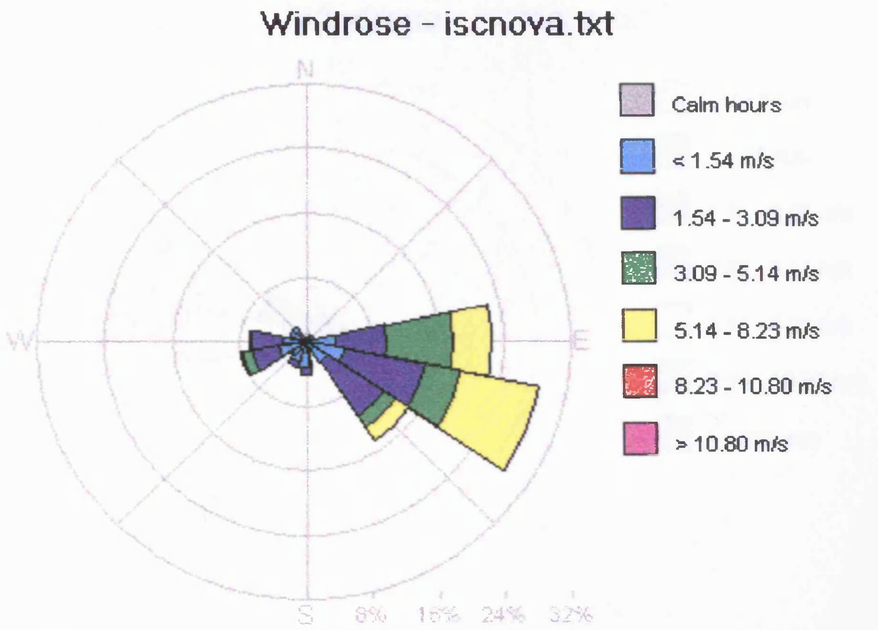

Windrose Survey 4

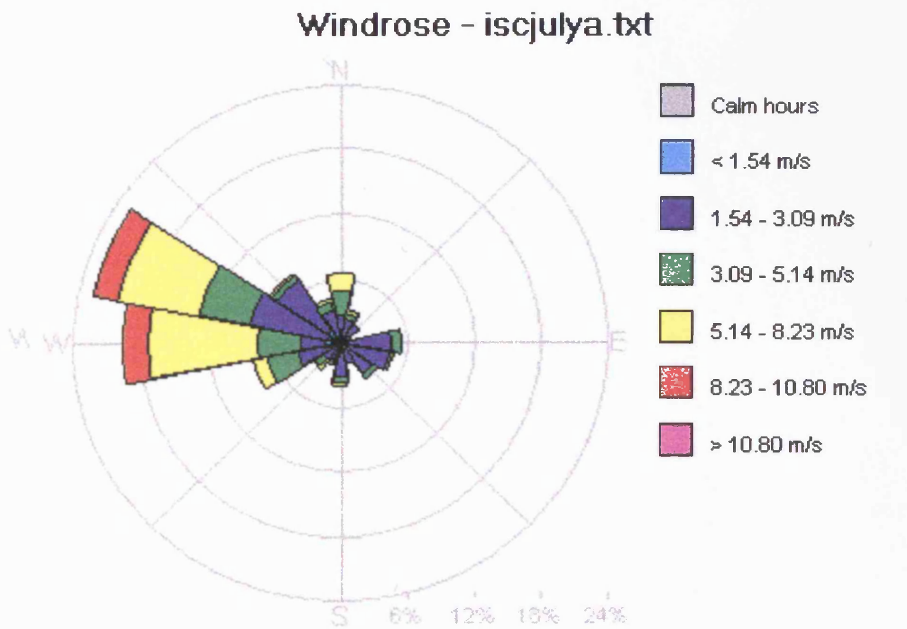

Windrose Survey 5

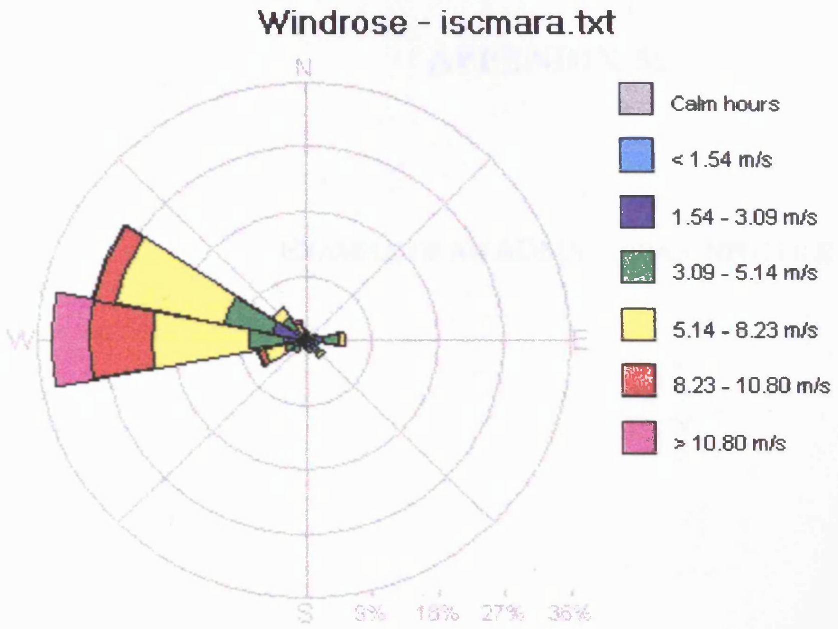

APPENDIX 5D

EXAMPLE OF AN ADMS-URBAN INPUT FILE

```
&ADMS_HEADER
Comment = 'This is an ADMS Urban Model parameter file
'
Model = 'ADMS-Urban'
Version = 1.4
Complete = 1
/

&ADMS_PARAMETERS_SUP
SupSiteName        = 'kees
'
SupProjectName     = 'kees
'
SupReleaseType     = 0
SupComplexEffects = 0
SupOther           = 0
SupRoughness       = 5.000000000000000e-001
SupLatitude        = 5.200000000000000e+001
SupPufType         = 0
SupCalcChm         = 0
SupCalcDryDep      = 0
SupCalcWetDep      = 0
SupUseHourlyEmissionFactors = 1
SupHourlyEmissionFactorWeekday =
      2.400000e-001  2.100000e-001  1.600000e-001  1.600000e-001
      2.100000e-001  2.600000e-001  6.000000e-001  1.540000e+000
      1.820000e+000  1.540000e+000  1.360000e+000  1.270000e+000
      1.160000e+000  1.160000e+000  1.270000e+000  1.410000e+000
      1.620000e+000  1.800000e+000  1.620000e+000  1.410000e+000
      1.150000e+000  9.100000e-001  7.600000e-001  3.600000e-001
SupHourlyEmissionFactorSaturday =
      2.400000e-001  2.100000e-001  1.600000e-001  1.600000e-001
      2.100000e-001  2.600000e-001  6.000000e-001  1.540000e+000
      1.820000e+000  1.540000e+000  1.360000e+000  1.270000e+000
      1.160000e+000  1.160000e+000  1.270000e+000  1.410000e+000
      1.620000e+000  1.800000e+000  1.620000e+000  1.410000e+000
      1.150000e+000  9.100000e-001  7.600000e-001  3.600000e-001
SupHourlyEmissionFactorSunday =
      2.400000e-001  2.100000e-001  1.600000e-001  1.600000e-001
      2.100000e-001  2.600000e-001  6.000000e-001  1.540000e+000
      1.820000e+000  1.540000e+000  1.360000e+000  1.270000e+000
      1.160000e+000  1.160000e+000  1.270000e+000  1.410000e+000
      1.620000e+000  1.800000e+000  1.620000e+000  1.410000e+000
      1.150000e+000  9.100000e-001  7.600000e-001  3.600000e-001
/
&ADMS_PARAMETERS_MET
MetDataSource              = 0
MetDataFileWellFormedPath = 'c:\adms-urb\metdata\admsjuly.met
'
MetFileWindHeight          = 1.000000000000000e+001
MetWindSectorSize          = 0
MetLateralSpreadType       = 0
MetLateralSpreadStdDev     = 0.000000000000000e+000
MetDataIsSequential        = 1
MetSiteIsRepr              = 1
MetUsePrecipFactor         = 0
MetPrecipFactor            = 0.000000000000000e+000
MetUseRoughChanges         = 0
MetSurfRough               = 0.000000000000000e+000
MetHandWindHeight          = 1.000000000000000e+001
MetHeatFluxType            = 0
MetInclBoundaryLyrHt       = 1
MetInclSurfaceTemp         = 0
MetInclLateralSpread       = 0
MetHandNumEntries          = 0
/
&ADMS_PARAMETERS_BLD
BldNumBuildings = 0
/
&ADMS_PARAMETERS_HIL
HilGridSize     = 1
HilRoughInput   = 0
HilTerrainPath = 'c:\adms-urb\data\terrain.ter
'
HilRoughPath    = 'c:\adms-urb\data\roughnes.ruf
'
/
```

```
&ADMS_PARAMETERS_FLC
FlcAvgTime            = 0.000000000000000e+000
FlcCalcToxicResponse  = 0
FlcToxicExp           = 1.000000000000000e+000
FlcCalcPercentiles    = 0
FlcNumPercentiles     = 0
FlcCalcPDF            = 0
FlcPDFMode            = 0
FlcNumPDF             = 0
/
&ADMS_PARAMETERS_GRD
GrdType                  = 1
GrdSpacingType           = 0
GrdRegularMin =
  -1.000000e+003
  -1.000000e+003
GrdRegularMax =
  1.000000e+003
  1.000000e+003
GrdVarSpaceNumPointsX  = 0
GrdVarSpaceNumPointsY  = 0
GrdGriddedZ            = 0.000000e+000
GrdPtsNumPoints        = 28
GrdPtsPointNames =
      '2                  '  '6                  '  '7                  '  '8
'
      '9                  '  '10                 '  '11                 '  '12
'
      '13                 '  '14                 '  '15                 '  '16
'
      '17                 '  '18                 '  '19                 '  '20
'
      '21                 '  '22                 '  '23                 '  '24
'
      '25                 '  '26                 '  '27                 '  '28
'
      '1                  '  '3                  '  '4                  '  '5
'
GrdPtsPointsX =
      4.403720e+005  4.373320e+005  4.386220e+005  4.351740e+005
      4.341850e+005  4.357860e+005  4.348740e+005  4.345390e+005
      4.342420e+005  4.336590e+005  4.309920e+005  4.303140e+005
      4.337090e+005  4.323750e+005  4.299440e+005  4.324850e+005
      4.335620e+005  4.356840e+005  4.358620e+005  4.380720e+005
      4.388110e+005  4.362250e+005  4.363750e+005  4.348660e+005
      4.397780e+005  4.421000e+005  4.400520e+005  4.387550e+005
GrdPtsPointsY =
      3.871960e+005  3.857240e+005  3.823120e+005  3.812480e+005
      3.829450e+005  3.831950e+005  3.860070e+005  3.866820e+005
      3.854750e+005  3.858760e+005  3.846540e+005  3.862870e+005
      3.887650e+005  3.891430e+005  3.889350e+005  3.910910e+005
      3.900230e+005  3.894730e+005  3.896170e+005  3.889910e+005
      3.883930e+005  3.914320e+005  3.926400e+005  3.926440e+005
      3.866340e+005  3.856580e+005  3.852380e+005  3.861020e+005
GrdPtsPointsZ =
      2.500000e+000  2.500000e+000  2.500000e+000  2.500000e+000
      2.500000e+000  2.500000e+000  2.500000e+000  2.500000e+000
      2.500000e+000  2.500000e+000  2.500000e+000  2.500000e+000
      2.500000e+000  2.500000e+000  2.500000e+000  2.500000e+000
      2.500000e+000  2.500000e+000  2.500000e+000  2.500000e+000
      2.500000e+000  2.500000e+000  2.500000e+000  2.500000e+000
      2.500000e+000  2.500000e+000  2.500000e+000  2.500000e+000
/
&ADMS_PARAMETERS_PUF
PufStart            = 1.000000000000000e+002
PufStep             = 1.000000000000000e+002
PufNumSteps         = 10
/
&ADMS_PARAMETERS_GAM
GamCalcDose            = 0
GamNumOutputPoints     = 0
/
&ADMS_PARAMETERS_OPT
OptNumOutputs          = 1
OptPolName =
      'NO2                '
OptInclude =
```

```
      1
OptShortOrLong =
      0
OptSamplingTime =
      3.600000e+003
OptUseRollingAvg =
      1
OptPercentile1 =
      0.000000e+000
OptPercentile2 =
      0.000000e+000
OptUnits =
      'ug/m³'
OptGroupsOrSource     = 0
OptNumGroups          = 1
OptIncludedGroups =
      'All sources          '
OptIncludedSource     = '                     '
/
&ADMS_PARAMETERS_CHM
ChmLevelsKnown = 1
ChmNumLevels   = 6
ChmPolNames =
      'NO                      ' 'NOx                     ' 'SO2                     ' 'VOC
'
      'CO                      ' 'O3                      '
ChmLevels =
      0.000000e+000  0.000000e+000  0.000000e+000  0.000000e+000
      0.000000e+000  0.000000e+000
/
&ADMS_PARAMETERS_ETC
SrcNumSources    = 649
PolNumPollutants = 6
PolNumIsotopes   = 1
/

    &ADMS_POLLUTANT_DETAILS
    PolName                   = 'NO                      '
    PolPollutantType          = 0
    PolGasDepVelocityKnown    = 1
    PolGasDepositionVelocity  = 0.000000000000000e+000
    PolGasType                = 0
    PolParDepVelocityKnown    = 1
    PolParTermVelocityKnown   = 1
    PolParNumDepositionData   = 1
    PolParDepositionVelocity =
      0.000000e+000
    PolParTerminalVelocity =
      0.000000e+000
    PolParDiameter =
      1.000000e-006
    PolParDensity =
      1.000000e+003
    PolParMassFraction =
      1.000000e+000
    PolWetWashoutKnown = 1
    PolWetWashout      = 0.000000000000000e+000
    PolWetWashoutA     = 1.000000000000000e-004
    PolWetWashoutB     = 6.400000000000000e-001
    PolConvFactor      = 8.000000000000000e-001
    /

    &ADMS_POLLUTANT_DETAILS
    PolName                   = 'NO2                     '
    PolPollutantType          = 0
    PolGasDepVelocityKnown    = 1
    PolGasDepositionVelocity  = 0.000000000000000e+000
    PolGasType                = 0
    PolParDepVelocityKnown    = 1
    PolParTermVelocityKnown   = 1
    PolParNumDepositionData   = 1
    PolParDepositionVelocity =
      0.000000e+000
    PolParTerminalVelocity =
      0.000000e+000
    PolParDiameter =
      1.000000e-006
```

```
PolParDensity =
  1.000000e+003
PolParMassFraction =
  1.000000e+000
PolWetWashoutKnown = 1
PolWetWashout      = 0.000000000000000e+000
PolWetWashoutA     = 1.000000000000000e-004
PolWetWashoutB     = 6.400000000000000e-001
PolConvFactor      = 5.200000000000000e-001
/

&ADMS_POLLUTANT_DETAILS
PolName                  = 'SO2                  '
PolPollutantType         = 0
PolGasDepVelocityKnown   = 1
PolGasDepositionVelocity = 0.000000000000000e+000
PolGasType               = 0
PolParDepVelocityKnown   = 1
PolParTermVelocityKnown  = 1
PolParNumDepositionData  = 1
PolParDepositionVelocity =
  0.000000e+000
PolParTerminalVelocity =
  0.000000e+000
PolParDiameter =
  1.000000e-006
PolParDensity =
  1.000000e+003
PolParMassFraction =
  1.000000e+000
PolWetWashoutKnown = 1
PolWetWashout      = 0.000000000000000e+000
PolWetWashoutA     = 1.000000000000000e-004
PolWetWashoutB     = 6.400000000000000e-001
PolConvFactor      = 3.500000000000000e-001
/

&ADMS_POLLUTANT_DETAILS
PolName                  = 'VOC                  '
PolPollutantType         = 0
PolGasDepVelocityKnown   = 1
PolGasDepositionVelocity = 0.000000000000000e+000
PolGasType               = 0
PolParDepVelocityKnown   = 1
PolParTermVelocityKnown  = 1
PolParNumDepositionData  = 1
PolParDepositionVelocity =
  0.000000e+000
PolParTerminalVelocity =
  0.000000e+000
PolParDiameter =
  1.000000e-006
PolParDensity =
  1.000000e+003
PolParMassFraction =
  1.000000e+000
PolWetWashoutKnown = 1
PolWetWashout      = 0.000000000000000e+000
PolWetWashoutA     = 1.000000000000000e-004
PolWetWashoutB     = 6.400000000000000e-001
PolConvFactor      = 3.000000000000000e-001
/

&ADMS_POLLUTANT_DETAILS
PolName                  = 'PM                   '
PolPollutantType         = 1
PolGasDepVelocityKnown   = 1
PolGasDepositionVelocity = 0.000000000000000e+000
PolGasType               = 0
PolParDepVelocityKnown   = 0
PolParTermVelocityKnown  = 0
PolParNumDepositionData  = 1
PolParDepositionVelocity =
  1.000000e+000
PolParTerminalVelocity =
  3.000000e+000
PolParDiameter =
```

```
    1.000000e-005
  PolParDensity =
    1.000000e+003
  PolParMassFraction =
    1.000000e+000
  PolWetWashoutKnown = 1
  PolWetWashout      = 0.000000000000000e+000
  PolWetWashoutA     = 1.000000000000000e-004
  PolWetWashoutB     = 6.400000000000000e-001
  PolConvFactor      = 1.000000000000000e+000
  /

  &ADMS_POLLUTANT_DETAILS
  PolName                  = 'CO                    '
  PolPollutantType         = 0
  PolGasDepVelocityKnown   = 1
  PolGasDepositionVelocity = 0.000000000000000e+000
  PolGasType               = 0
  PolParDepVelocityKnown   = 1
  PolParTermVelocityKnown  = 1
  PolParNumDepositionData  = 1
  PolParDepositionVelocity =
    0.000000e+000
  PolParTerminalVelocity =
    0.000000e+000
  PolParDiameter =
    1.000000e-006
  PolParDensity =
    1.000000e+003
  PolParMassFraction =
    1.000000e+000
  PolWetWashoutKnown = 1
  PolWetWashout      = 0.000000000000000e+000
  PolWetWashoutA     = 1.000000000000000e-004
  PolWetWashoutB     = 6.400000000000000e-001
  PolConvFactor      = 8.600000000000000e-001
  /

  &ADMS_ISOTOPE_DETAILS
  IsoName                  = '(unnamed-isotope)     '
  IsoPollutantType         = 0
  IsoGasDepVelocityKnown   = 1
  IsoGasDepositionVelocity = 0.000000000000000e+000
  IsoGasType               = 0
  IsoParDepVelocityKnown   = 1
  IsoParTermVelocityKnown  = 1
  IsoParNumDepositionData  = 1
  IsoParDepositionVelocity =
    0.000000e+000
  IsoParTerminalVelocity =
    0.000000e+000
  IsoParDiameter =
    1.000000e-006
  IsoParDensity =
    1.000000e+003
  IsoParMassFraction =
    1.000000e+000
  IsoWetWashoutKnown = 1
  IsoWetWashout      = 0.000000000000000e+000
  IsoWetWashoutA     = 1.000000000000000e-004
  IsoWetWashoutB     = 6.400000000000000e-001
  IsoConvFactor      = 1.000000000000000e+000
  /

&ADMS_SOURCE_DETAILS
SrcName          = '1                    '
SrcHeight        = 0.000000000000000e+000
SrcDiameter      = 1.000000000000000e+000
SrcVolFlowRate   = 0.000000000000000e+000
SrcVertVeloc     = 0.000000000000000e+000
SrcTemperature   = 1.500000000000000e+001
SrcMolWeight     = 2.896000000000000e+001
SrcDensity       = 1.225000000000000e+000
SrcSpecHeatCap   = 1.012000000000000e+003
SrcSourceType    = 4
SrcReleaseAtNTP  = 0
SrcVolFlowKnown  = 0
```

```
  SrcDensityKnown   = 0
  SrcX1             = 0.000000000000000e+000
  SrcY1             = 0.000000000000000e+000
  SrcL1             = 4.000000000000000e+000
  SrcL2             = 1.000000000000000e+001
  SrcNumGroups      = 1
  SrcGroup =
      'All sources          '
  SrcTraEmissionsMode = 0
  SrcTraYear          = 1995
  SrcNumVertices = 2
  SrcTraNumTrafficFlows = 2
  SrcNumPollutants      = 5
  SrcPollutants =
      'NO                   '  'NO2                      '  'VOC                      '  'PM
'
      'CO                   '
  SrcPolEmissionRate =
      6.769300e-001  3.562790e-002  3.951750e-001  3.271670e-002
      3.736260e+000
  SrcPolTotalemission =
      1.000000e+000  1.000000e+000  1.000000e+000  1.000000e+000
      1.000000e+000
  SrcPolStartTime =
      0.000000e+000  0.000000e+000  0.000000e+000  0.000000e+000
      0.000000e+000
  SrcPolDuration =
      0.000000e+000  0.000000e+000  0.000000e+000  0.000000e+000
      0.000000e+000
  SrcNumIsotopes        = 0
  /

    &ADMS_SOURCE_VERTEX
    SourceVertexX = 4.336130000000000e+005
    SourceVertexY = 3.941980000000000e+005
    /

    &ADMS_SOURCE_VERTEX
    SourceVertexX = 4.335880000000000e+005
    SourceVertexY = 3.943180000000000e+005
    /

    &ADMS_TRAFFICFLOW_DETAILS
    TraVehicleCategory     = 'light duty vehicle  '
    TraAverageSpeed        = 2.500000000000000e+001
    TraVehicleCount        = 690
    TraNumRoadPollutants   = 4
    TraPolName =
      'NOx                   '  'VOC                      '  'PM                       '  'CO
'
    TraEmissionFactor =
      2.499000e+000  2.005000e+000  5.000000e-002  1.900500e+001
    /

    &ADMS_TRAFFICFLOW_DETAILS
    TraVehicleCategory     = 'heavy duty vehicle  '
    TraAverageSpeed        = 2.500000000000000e+001
    TraVehicleCount        = 60
    TraNumRoadPollutants   = 4
    TraPolName =
      'NOx                   '  'VOC                      '  'PM                       '  'CO
'
    TraEmissionFactor =
      1.401500e+001  6.530000e-001  1.388000e+000  5.618000e+000
    /
```

(NB Only one source was printed. In the real input file there are another 648 roads with source-details)

APPENDIX 5E

CALCULATION OF THE HOURLY VARIATION IN TRAFFIC

The hourly variation of traffic low was calculated using figures presented in the 'London Traffic Monitoring Report', 1995. Percentages were calculated for the different periods (see *Tabel 1*). ADMS-Urban needed hourly variations in traffic flow (see *Figure 1*). The percentages for the periods (red dots in *Figure 1*) were therefore converted into hourly percentages (yellow bars in *Figure 1*) by smoothing.

Table 1: Percentage of traffic flow at different times of the day (based on figures presented in 'London Traffic Monitoring Report', 1995)

Period	*Time*	*Traffic Flow (percentage)*
Night	0 – 7hr	8
Morning Peak	7 – 10hr	20
Off Peak	10 – 16hr	32
Evening Peak	16 – 19hr	21
Late Evening	19 –24hr	19

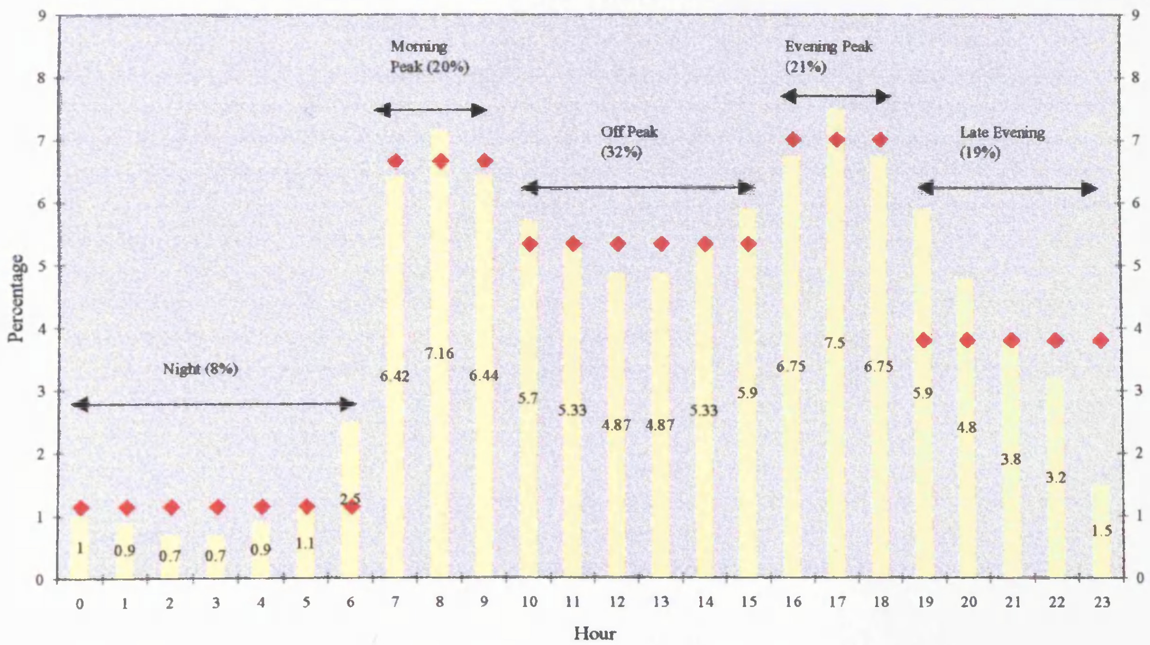

Figure 1: Converting percentages per period to percentages per hour

APPENDIX 6A

ODDS RATIOS RELATING ASTHMA AND ALLERGIC DISEASE TO VARIOUS EXPOSURE MEASURES

The following tabulations present the odds ratios and 95% confidence intervals relating a range of indicators of road traffic exposure to each disease outcome. Exposure measures shown here are based on the postcode of residence in the full dataset. The number of affected children (cases) and unaffected children (controls) within each exposure category is shown.

The odds ratios are presented before and after adjustment for age, sex, deprivation score and school attended. Where continuously distributed exposure measures are used, the odds ratio is calculated for the comparison between the 90th and 10th percentiles of the relevant exposure distribution.

Tables

1. Wheeze in the last year
2. Severe wheeze in the last year (compared to no wheeze)
3. Severe wheeze in the last year (compared to milder wheeze)
4. Wheeze in the last year among "atopic" children (those with a history of doctor-diagnosed hay fever, allergic rhinitis or eczema at any age)
5. Wheeze in the last year among "non-atopic" children
6. Non-infective rhinitis in the last year
7. Flexural eczema in the last year

SPECIAL NOTE

This item is tightly bound and while every effort has been made to reproduce the centres force would result in damage.

able 1: Wheeze in the last year

	Cases	Controls	Unadjusted OR	Unadjusted 95%CI	Adjusted for age-sex OR	Adjusted for age-sex 95%CI	Adjusted for age-sex-dep OR	Adjusted for age-sex-dep 95%CI	Adjusted for age-sex-dep-schoo OR	Adjusted for age-sex-dep-schoo 95%CI
tance - roads										
50m	685	3272	1.00		1.00		1.00		1.00	
-150m	906	4190	1.03	(0.93- 1.15)	1.03	(0.93- 1.15)	1.03	(0.92- 1.15)	1.02	(0.91- 1.14)
0m	741	3274	1.08	(0.96- 1.21)	1.08	(0.96- 1.21)	1.08	(0.96- 1.21)	1.05	(0.94- 1.18)
root dist			1.07	(0.96- 1.20)	1.07	(0.96- 1.20)	1.07	(0.96- 1.21)	1.05	(0.94- 1.18)
tance - mainroads										
50m	1589	7334	1.00		1.00		1.00		1.00	
-150m	463	2162	0.99	(0.88- 1.11)	0.99	(0.88- 1.10)	0.98	(0.87- 1.10)	0.99	(0.88- 1.11)
0m	280	1240	1.04	(0.91- 1.20)	1.04	(0.90- 1.19)	1.03	(0.89- 1.18)	1.02	(0.88- 1.18)
root dist			1.05	(0.96- 1.15)	1.04	(0.95- 1.14)	1.04	(0.94- 1.14)	1.03	(0.94- 1.13)
ngth of roads within 150m										
ne	685	3272	1.00		1.00		1.00		1.00	
to 200m	267	1255	1.02	(0.87- 1.19)	1.01	(0.86- 1.17)	1.00	(0.86- 1.17)	0.99	(0.85- 1.16)
0-400m	993	4465	1.06	(0.95- 1.18)	1.06	(0.96- 1.18)	1.06	(0.95- 1.18)	1.05	(0.94- 1.17)
00m	387	1744	1.06	(0.92- 1.22)	1.05	(0.92- 1.21)	1.05	(0.92- 1.21)	1.03	(0.89- 1.18)
ad length 10th V 90th %			1.05	(0.93- 1.17)	1.04	(0.93- 1.17)	1.04	(0.93- 1.17)	1.02	(0.90- 1.15)
ngth of main roads within 150m										
ne	1589	7334	1.00		1.00		1.00		1.00	
to 200m	184	839	1.01	(0.86- 1.20)	1.01	(0.86- 1.20)	1.01	(0.85- 1.19)	1.02	(0.86- 1.21)
0-400m	491	2243	1.01	(0.90- 1.13)	1.01	(0.90- 1.12)	1.00	(0.89- 1.12)	1.00	(0.89- 1.12)
00m	68	320	0.98	(0.75- 1.28)	0.97	(0.74- 1.27)	0.96	(0.73- 1.25)	0.95	(0.72- 1.26)
ad length 10th V 90th %			1.00	(0.91- 1.10)	1.00	(0.91- 1.10)	0.99	(0.90- 1.09)	0.99	(0.89- 1.09)
ffic flow within 150m - total										
50km/day	361	1709	1.00		1.00		1.00		1.00	
0-1000km/day	637	2868	1.05	(0.91- 1.21)	1.05	(0.91- 1.21)	1.05	(0.91- 1.21)	1.03	(0.89- 1.19)
00-2500km/day	680	3160	1.02	(0.89- 1.17)	1.03	(0.89- 1.18)	1.02	(0.88- 1.17)	1.00	(0.87- 1.16)
500km/day	654	2999	1.03	(0.90- 1.19)	1.03	(0.90- 1.19)	1.02	(0.89- 1.18)	1.01	(0.87- 1.17)
ntinuous flow 10 V 90 %			0.99	(0.90- 1.08)	0.99	(0.90- 1.08)	0.98	(0.89- 1.08)	0.99	(0.89- 1.09)
ffic flow within 150m - HGV										
0km/day	593	2798	1.00		1.00		1.00		1.00	
-50km/day	473	2116	1.05	(0.92- 1.20)	1.05	(0.92- 1.20)	1.05	(0.92- 1.20)	1.03	(0.89- 1.18)
-150km/day	632	2844	1.05	(0.93- 1.19)	1.05	(0.93- 1.19)	1.05	(0.93- 1.19)	1.03	(0.91- 1.17)
50km/day	634	2978	1.00	(0.89- 1.14)	1.00	(0.89- 1.14)	0.99	(0.88- 1.12)	0.98	(0.86- 1.11)
ntinuous flow 10 V 90 %			0.97	(0.88- 1.07)	0.97	(0.88- 1.06)	0.96	(0.87- 1.05)	0.97	(0.88- 1.07)
AH NO2 model										
ug/m3	617	2847	1.00		1.00		1.00		1.00	
37ug/m3	878	4139	0.98	(0.87- 1.10)	0.98	(0.88- 1.10)	0.96	(0.85- 1.09)	0.94	(0.83- 1.07)
ug/m3	837	3750	1.03	(0.92- 1.15)	1.03	(0.92- 1.15)	1.00	(0.88- 1.14)	0.96	(0.83- 1.10)
2 concentration			1.02	(0.89- 1.17)	1.02	(0.89- 1.17)	0.98	(0.84- 1.15)	0.94	(0.79- 1.12)

Table 2: Severe wheeze v no wheeze

			Unadjusted		Adjusted for age-sex		Adjusted for age-sex-dep		Adjusted for age-sex-dep-schoo	
	Cases	Controls	OR	95%CI	OR	95%CI	OR	95%CI	OR	95%CI
stance - roads										
50m	180	3272	1.00		1.00		1.00		1.00	
-150m	257	4190	1.11	(0.92- 1.36)	1.12	(0.92- 1.36)	1.12	(0.92- 1.36)	1.11	(0.91- 1.36)
0m	201	3274	1.12	(0.91- 1.37)	1.11	(0.91- 1.37)	1.12	(0.91- 1.37)	1.08	(0.88- 1.34)
v root dist			1.03	(0.84- 1.27)	1.04	(0.84- 1.27)	1.04	(0.84- 1.28)	1.01	(0.82- 1.24)
stance - mainroads										
50m	432	7334	1.00		1.00		1.00		1.00	
-150m	127	2162	1.00	(0.81- 1.22)	1.00	(0.81- 1.22)	0.99	(0.81- 1.22)	0.99	(0.80- 1.22)
0m	79	1240	1.08	(0.84- 1.38)	1.08	(0.85- 1.39)	1.07	(0.84- 1.38)	1.03	(0.80- 1.33)
v root dist			1.05	(0.89- 1.23)	1.05	(0.89- 1.24)	1.04	(0.89- 1.23)	1.02	(0.86- 1.21)
ngth of roads within 150m										
ne	180	3272	1.00		1.00		1.00		1.00	
to 200m	73	1255	1.06	(0.80- 1.40)	1.04	(0.78- 1.37)	1.04	(0.78- 1.37)	1.02	(0.77- 1.36)
0-400m	269	4465	1.10	(0.90- 1.33)	1.10	(0.91- 1.34)	1.10	(0.91- 1.34)	1.10	(0.90- 1.34)
00m	116	1744	1.21	(0.95- 1.54)	1.21	(0.95- 1.54)	1.21	(0.95- 1.54)	1.16	(0.91- 1.48)
ad length 10th V 90th %			1.10	(0.89- 1.35)	1.10	(0.90- 1.36)	1.10	(0.90- 1.36)	1.07	(0.86- 1.32)
ngth of main roads within 150m										
ne	432	7334	1.00		1.00		1.00		1.00	
to 200m	47	839	0.95	(0.70- 1.30)	0.94	(0.69- 1.28)	0.94	(0.69- 1.28)	0.94	(0.69- 1.29)
0-400m	138	2243	1.04	(0.86- 1.27)	1.05	(0.86- 1.28)	1.04	(0.85- 1.27)	1.02	(0.83- 1.25)
00m	21	320	1.11	(0.71- 1.75)	1.12	(0.71- 1.76)	1.10	(0.70- 1.74)	1.08	(0.68- 1.72)
ad length 10th V 90th %			1.02	(0.86- 1.20)	1.02	(0.86- 1.21)	1.01	(0.85- 1.20)	0.99	(0.83- 1.18)
affic flow within 150m - total										
250km/day	97	1709	1.00		1.00		1.00		1.00	
50-1000km/day	158	2868	0.97	(0.75- 1.26)	0.97	(0.75- 1.26)	0.97	(0.75- 1.26)	0.96	(0.74- 1.25)
000-2500km/day	188	3160	1.05	(0.81- 1.35)	1.06	(0.82- 1.37)	1.06	(0.82- 1.36)	1.08	(0.82- 1.38)
2500km/day	195	2999	1.15	(0.89- 1.47)	1.15	(0.90- 1.48)	1.15	(0.89- 1.48)	1.12	(0.87- 1.45)
ntinuous flow 10 V 90 %			1.08	(0.91- 1.26)	1.08	(0.92- 1.27)	1.07	(0.91- 1.27)	1.07	(0.90- 1.27)
affic flow within 150m - HGV										
10km/day	155	2798	1.00		1.00		1.00		1.00	
-50km/day	126	2116	1.07	(0.84- 1.37)	1.07	(0.84- 1.36)	1.07	(0.84- 1.37)	1.05	(0.81- 1.34)
-150km/day	180	2844	1.14	(0.92- 1.42)	1.15	(0.92- 1.44)	1.15	(0.92- 1.44)	1.15	(0.92- 1.44)
150km/day	177	2978	1.07	(0.86- 1.34)	1.08	(0.86- 1.35)	1.07	(0.86- 1.34)	1.04	(0.83- 1.30)
ntinuous flow 10 V 90 %			1.04	(0.88- 1.22)	1.04	(0.89- 1.22)	1.03	(0.87- 1.22)	1.03	(0.87- 1.22)
VIAH NO2 model										
3ug/m3	179	2847	1.00		1.00		1.00		1.00	
-37ug/m3	233	4139	0.90	(0.73- 1.09)	0.90	(0.74- 1.10)	0.87	(0.70- 1.09)	0.88	(0.70- 1.10)
7ug/m3	226	3750	0.96	(0.78- 1.17)	0.96	(0.79- 1.18)	0.92	(0.73- 1.16)	0.93	(0.73- 1.19)
2 concentration			0.89	(0.70- 1.13)	0.90	(0.71- 1.15)	0.84	(0.63- 1.11)	0.84	(0.63- 1.14)

Table 3: Severe wheeze v mild wheeze

	Cases	Controls	Unadjusted		Adjusted for age-sex		Adjusted for age-sex-dep		Adjusted for age-sex-dep-schoo	
			OR	95%CI	OR	95%CI	OR	95%CI	OR	95%CI
istance - roads										
150m	180	505	1.00		1.00		1.00		1.00	
0-150m	257	649	1.11	(0.89- 1.39)	1.13	(0.90- 1.41)	1.13	(0.90- 1.42)	1.14	(0.91- 1.44)
50m	201	540	1.04	(0.83- 1.32)	1.05	(0.83- 1.33)	1.06	(0.83- 1.34)	1.09	(0.85- 1.38)
v root dist			0.95	(0.75- 1.20)	0.94	(0.75- 1.19)	0.94	(0.75- 1.19)	0.95	(0.75- 1.21)
istance - mainroads										
150m	432	1157	1.00		1.00		1.00		1.00	
0-150m	127	336	1.01	(0.80- 1.28)	1.01	(0.80- 1.28)	1.01	(0.80- 1.28)	0.99	(0.78- 1.26)
50m	79	201	1.05	(0.79- 1.40)	1.05	(0.79- 1.39)	1.05	(0.79- 1.40)	1.05	(0.78- 1.41)
v root dist			1.00	(0.84- 1.20)	0.99	(0.83- 1.19)	1.00	(0.83- 1.20)	0.99	(0.82- 1.19)
ength of roads within 150m										
one	505	180	1.00		1.00		1.00		1.00	
to 200m	194	73	1.06	(0.77- 1.45)	1.08	(0.79- 1.49)	1.09	(0.79- 1.50)	1.08	(0.78- 1.50)
00-400m	724	269	1.04	(0.84- 1.30)	1.05	(0.84- 1.31)	1.06	(0.85- 1.32)	1.09	(0.87- 1.36)
400m	271	116	1.20	(0.91- 1.58)	1.21	(0.92- 1.60)	1.22	(0.92- 1.61)	1.22	(0.91- 1.63)
oad length 10th V 90th %			1.07	(0.85- 1.36)	1.08	(0.85- 1.37)	1.08	(0.85- 1.37)	1.09	(0.85- 1.40)
ength of main roads within 150m										
one	1157	432	1.00		1.00		1.00		1.00	
to 200m	137	47	0.92	(0.65- 1.30)	0.93	(0.66- 1.33)	0.94	(0.66- 1.33)	0.92	(0.64- 1.31)
00-400m	353	138	1.05	(0.84- 1.31)	1.04	(0.83- 1.31)	1.05	(0.83- 1.31)	1.03	(0.82- 1.31)
400m	47	21	1.20	(0.71- 2.03)	1.16	(0.68- 1.97)	1.16	(0.68- 1.98)	1.14	(0.66- 1.98)
oad length 10th V 90th %			1.02	(0.84- 1.24)	1.01	(0.83- 1.23)	1.01	(0.83- 1.23)	1.00	(0.81- 1.22)
raffic flow within 150m - total										
250km/day	264	97	1.00		1.00		1.00		1.00	
50-1000km/day	479	158	0.90	(0.67- 1.20)	0.89	(0.66- 1.20)	0.90	(0.67- 1.21)	0.91	(0.67- 1.24)
000-2500km/day	492	188	1.04	(0.78- 1.39)	1.04	(0.78- 1.39)	1.05	(0.79- 1.40)	1.08	(0.80- 1.45)
2500km/day	459	195	1.16	(0.87- 1.54)	1.16	(0.87- 1.54)	1.17	(0.87- 1.56)	1.18	(0.87- 1.60)
ontinuous flow 10 V 90 %			1.14	(0.94- 1.37)	1.14	(0.94- 1.38)	1.14	(0.94- 1.39)	1.14	(0.94- 1.40)
raffic flow within 150m - HGV										
10km/day	438	155	1.00		1.00		1.00		1.00	
0-50km/day	347	126	1.03	(0.78- 1.35)	1.03	(0.78- 1.36)	1.04	(0.78- 1.37)	1.05	(0.79- 1.40)
0-150km/day	452	180	1.13	(0.87- 1.45)	1.13	(0.88- 1.46)	1.14	(0.89- 1.47)	1.19	(0.92- 1.55)
150km/day	457	177	1.09	(0.85- 1.41)	1.10	(0.85- 1.42)	1.11	(0.86- 1.43)	1.13	(0.87- 1.47)
ontinuous flow 10 V 90 %			1.10	(0.91- 1.33)	1.10	(0.91- 1.33)	1.10	(0.91- 1.34)	1.11	(0.91- 1.36)
AVIAH NO2 model										
33ug/m3	179	438	1.00		1.00		1.00		1.00	
-37ug/m3	233	645	0.88	(0.70- 1.11)	0.88	(0.70- 1.11)	0.87	(0.68- 1.12)	0.94	(0.72- 1.23)
37ug/m3	226	611	0.91	(0.72- 1.14)	0.90	(0.72- 1.14)	0.88	(0.68- 1.15)	0.97	(0.73- 1.29)
O2 concentration 10 V 90%			0.83	(0.63- 1.09)	0.83	(0.63- 1.09)	0.78	(0.57- 1.08)	0.87	(0.62- 1.24)

Table 4: Wheeze in "atopic" children

	Cases	Controls	Unadjusted OR	Unadjusted 95%CI	Adjusted for age-sex OR	Adjusted for age-sex 95%CI	Adjusted for age-sex-dep OR	Adjusted for age-sex-dep 95%CI	Adjusted for age-sex-dep-school OR	Adjusted for age-sex-dep-school 95%CI
istance - roads										
150m	376	682	1.00		1.00		1.00		1.00	
0-150m	523	831	1.14	(0.97- 1.35)	1.13	(0.96- 1.34)	1.12	(0.94- 1.32)	1.10	(0.92- 1.31)
50m	417	663	1.14	(0.96- 1.36)	1.13	(0.95- 1.35)	1.14	(0.95- 1.36)	1.10	(0.92- 1.32)
v root dist			1.10	(0.92- 1.31)	1.11	(0.93- 1.32)	1.12	(0.94- 1.34)	1.09	(0.91- 1.31)
istance - mainroads										
150m	891	1510	1.00		1.00		1.00		1.00	
0-150m	277	424	1.11	(0.93- 1.32)	1.10	(0.92- 1.31)	1.07	(0.90- 1.28)	1.07	(0.90- 1.28)
50m	148	242	1.04	(0.83- 1.29)	1.02	(0.82- 1.27)	0.98	(0.78- 1.23)	0.94	(0.75- 1.19)
v root dist			1.06	(0.92- 1.21)	1.05	(0.91- 1.21)	1.02	(0.88- 1.17)	0.99	(0.85- 1.15)
ngth of roads within 150m										
ne	376	682	1.00		1.00		1.00		1.00	
p to 200m	155	247	1.14	(0.90- 1.44)	1.11	(0.88- 1.41)	1.10	(0.86- 1.39)	1.07	(0.84- 1.36)
0-400m	575	895	1.17	(0.99- 1.37)	1.16	(0.99- 1.37)	1.16	(0.98- 1.37)	1.14	(0.96- 1.35)
400m	210	352	1.08	(0.88- 1.34)	1.06	(0.86- 1.31)	1.07	(0.86- 1.33)	1.02	(0.82- 1.27)
ad length 10th V 90th %			1.08	(0.90- 1.29)	1.07	(0.89- 1.28)	1.08	(0.90- 1.30)	1.04	(0.87- 1.26)
ngth of main roads within 150m										
ne	891	1510	1.00		1.00		1.00		1.00	
p to 200m	113	177	1.08	(0.84- 1.39)	1.08	(0.84- 1.39)	1.06	(0.82- 1.36)	1.08	(0.83- 1.40)
0-400m	277	433	1.08	(0.91- 1.29)	1.07	(0.90- 1.28)	1.04	(0.87- 1.24)	1.02	(0.85- 1.22)
400m	35	56	1.06	(0.69- 1.63)	1.02	(0.66- 1.57)	0.97	(0.62- 1.50)	0.88	(0.56- 1.39)
ad length 10th V 90th %			1.06	(0.91- 1.23)	1.05	(0.90- 1.22)	1.01	(0.87- 1.18)	0.98	(0.84- 1.15)
affic flow within 150m - total										
250km/day	207	384	1.00		1.00		1.00		1.00	
50-1000km/day	353	581	1.13	(0.91- 1.40)	1.15	(0.92- 1.42)	1.12	(0.90- 1.39)	1.11	(0.89- 1.39)
000-2500km/day	390	639	1.13	(0.92- 1.40)	1.15	(0.93- 1.42)	1.12	(0.90- 1.39)	1.10	(0.88- 1.38)
2500km/day	366	572	1.19	(0.96- 1.47)	1.20	(0.97- 1.48)	1.16	(0.93- 1.44)	1.13	(0.91- 1.42)
ontinuous flow 10 V 90 %			1.03	(0.89- 1.20)	1.03	(0.89- 1.19)	1.00	(0.86- 1.16)	1.01	(0.86- 1.18)
affic flow within 150m - HGV										
10km/day	332	610	1.00		1.00		1.00		1.00	
0-50km/day	271	429	1.16	(0.95- 1.42)	1.15	(0.94- 1.41)	1.16	(0.94- 1.42)	1.15	(0.93- 1.42)
0-150km/day	356	585	1.12	(0.93- 1.35)	1.11	(0.92- 1.34)	1.10	(0.91- 1.33)	1.08	(0.88- 1.31)
150km/day	357	552	1.19	(0.98- 1.43)	1.18	(0.98- 1.43)	1.14	(0.94- 1.38)	1.12	(0.92- 1.37)
ontinuous flow 10 V 90 %			1.06	(0.91- 1.23)	1.06	(0.91- 1.22)	1.01	(0.87- 1.18)	1.01	(0.86- 1.19)
AVIAH NO2 model										
3ug/m3	358	616	1.00		1.00		1.00		1.00	
3-37ug/m3	502	842	1.03	(0.86- 1.22)	1.03	(0.87- 1.23)	0.97	(0.80- 1.17)	0.94	(0.77- 1.14)
7ug/m3	456	718	1.09	(0.92- 1.30)	1.10	(0.93- 1.32)	1.00	(0.82- 1.22)	0.95	(0.76- 1.17)
O2 concentration			1.12	(0.91- 1.37)	1.14	(0.92- 1.40)	1.00	(0.78- 1.27)	0.94	(0.72- 1.22)

Table 5: Wheeze in "non-atopic" children

	Cases	Controls	Unadjusted OR	Unadjusted 95%CI	Adjusted for age-sex OR	Adjusted for age-sex 95%CI	Adjusted for age-sex-dep OR	Adjusted for age-sex-dep 95%CI	Adjusted for age-sex-dep-school OR	Adjusted for age-sex-dep-school 95%CI
istance - roads										
>150m	309	2590	1.00		1.00		1.00		1.00	
0-150m	383	3359	0.96	(0.82- 1.12)	0.96	(0.82- 1.12)	0.97	(0.82- 1.13)	0.98	(0.82- 1.13)
50m	324	2611	1.04	(0.88- 1.23)	1.04	(0.88- 1.23)	1.06	(0.89- 1.25)	1.03	(0.87- 1.22)
v root dist			1.04	(0.88- 1.24)	1.04	(0.88- 1.23)	1.05	(0.89- 1.25)	1.03	(0.87- 1.22)
istance - mainroads										
150m	698	5824	1.00		1.00		1.00		1.00	
0-150m	186	1738	0.89	(0.75- 1.06)	0.89	(0.75- 1.06)	0.88	(0.74- 1.04)	0.89	(0.75- 1.06)
50m	132	998	1.10	(0.91- 1.34)	1.10	(0.90- 1.34)	1.08	(0.88- 1.32)	1.09	(0.89- 1.33)
v root dist			1.08	(0.95- 1.23)	1.08	(0.94- 1.23)	1.06	(0.93- 1.21)	1.07	(0.93- 1.22)
ength of roads within 150m										
one	309	2590	1.00		1.00		1.00		1.00	
p to 200m	112	1008	0.93	(0.74- 1.17)	0.93	(0.74- 1.16)	0.93	(0.74- 1.17)	0.93	(0.74- 1.17)
00-400m	418	3570	0.98	(0.84- 1.15)	0.98	(0.84- 1.15)	1.00	(0.85- 1.17)	0.99	(0.84- 1.16)
400m	177	1392	1.07	(0.88- 1.30)	1.06	(0.88- 1.30)	1.08	(0.89- 1.32)	1.06	(0.87- 1.29)
oad length 10th V 90th %			1.03	(0.87- 1.22)	1.04	(0.88- 1.23)	1.05	(0.89- 1.25)	1.03	(0.87- 1.22)
ength of main roads within 150m										
one	698	5824	1.00		1.00		1.00		1.00	
p to 200m	71	662	0.89	(0.69- 1.16)	0.90	(0.69- 1.16)	0.88	(0.68- 1.14)	0.90	(0.69- 1.17)
00-400m	214	1810	0.99	(0.84- 1.16)	0.98	(0.84- 1.16)	0.97	(0.82- 1.14)	0.97	(0.82- 1.15)
400m	33	264	1.04	(0.72- 1.51)	1.05	(0.72- 1.52)	1.01	(0.70- 1.47)	1.05	(0.72- 1.54)
oad length 10th V 90th %			1.01	(0.88- 1.16)	1.01	(0.88- 1.15)	0.99	(0.86- 1.13)	1.00	(0.87- 1.15)
raffic flow within 150m - total										
<250km/day	154	1325	1.00		1.00		1.00		1.00	
250-1000km/day	284	2287	1.07	(0.87- 1.31)	1.07	(0.87- 1.32)	1.08	(0.87- 1.32)	1.06	(0.86- 1.32)
1000-2500km/day	290	2521	0.99	(0.81- 1.22)	1.00	(0.81- 1.23)	1.00	(0.81- 1.23)	0.98	(0.80- 1.22)
>2500km/day	288	2427	1.02	(0.83- 1.26)	1.02	(0.83- 1.26)	1.01	(0.82- 1.24)	1.00	(0.81- 1.24)
ontinuous flow 10 V 90 %			1.01	(0.88- 1.16)	1.01	(0.88- 1.16)	1.00	(0.87- 1.14)	1.00	(0.87- 1.16)
raffic flow within 150m - HGV										
<10km/day	261	2188	1.00		1.00		1.00		1.00	
10-50km/day	202	1687	1.00	(0.83- 1.22)	1.01	(0.83- 1.23)	1.04	(0.85- 1.26)	1.02	(0.83- 1.25)
50-150km/day	276	2259	1.02	(0.86- 1.22)	1.03	(0.86- 1.24)	1.04	(0.87- 1.25)	1.02	(0.85- 1.22)
>150km/day	277	2426	0.96	(0.80- 1.14)	0.96	(0.81- 1.15)	0.95	(0.79- 1.13)	0.93	(0.78- 1.12)
ontinuous flow 10 V 90 %			0.98	(0.86- 1.12)	0.98	(0.86- 1.12)	0.95	(0.83- 1.09)	0.96	(0.84- 1.11)
AVIAH NO2 model										
33ug/m3	259	2231	1.00		1.00		1.00		1.00	
3-37ug/m3	376	3297	0.98	(0.83- 1.16)	0.98	(0.83- 1.16)	0.93	(0.78- 1.12)	0.91	(0.76- 1.10)
37ug/m3	381	3032	1.08	(0.92- 1.28)	1.08	(0.92- 1.28)	1.01	(0.83- 1.22)	0.96	(0.78- 1.17)
O2 concentration			1.10	(0.90- 1.34)	1.10	(0.90- 1.34)	1.01	(0.80- 1.27)	0.96	(0.75- 1.23)

Table 6: Non-infective rhinitis in the last year

			Unadjusted		Adjusted for age-sex		Adjusted for age-sex-dep		Adjusted for age-sex-dep-school	
	Cases	Controls	OR	95%CI	OR	95%CI	OR	95%CI	OR	95%CI
Distance - roads										
>150m	731	2985	1.00		1.00		1.00		1.00	
50-150m	847	3945	0.88	(0.79- 0.98)	0.88	(0.79- 0.98)	0.86	(0.77- 0.97)	0.87	(0.77- 0.97)
<50m	679	3066	0.90	(0.81- 1.02)	0.90	(0.80- 1.01)	0.87	(0.78- 0.98)	0.88	(0.78- 0.99)
Inv root dist			0.97	(0.87- 1.10)	0.97	(0.86- 1.09)	0.94	(0.84- 1.06)	0.96	(0.85- 1.08)
Distance - mainroads										
>150m	1621	6770	1.00		1.00		1.00		1.00	
50-150m	405	2051	0.82	(0.73- 0.93)	0.82	(0.73- 0.92)	0.84	(0.75- 0.95)	0.85	(0.75- 0.96)
<50m	231	1175	0.82	(0.71- 0.95)	0.81	(0.70- 0.95)	0.86	(0.74- 1.00)	0.86	(0.74- 1.01)
Inv root dist			0.88	(0.80- 0.97)	0.87	(0.79- 0.96)	0.91	(0.82- 1.01)	0.92	(0.83- 1.02)
Length of roads within 150m										
None	731	2985	1.00		1.00		1.00		1.00	
Up to 200m	248	1158	0.87	(0.75- 1.02)	0.87	(0.74- 1.02)	0.86	(0.73- 1.01)	0.86	(0.73- 1.01)
200-400m	937	4216	0.91	(0.82- 1.01)	0.91	(0.82- 1.01)	0.89	(0.80- 0.99)	0.89	(0.80- 1.00)
>400m	341	1637	0.85	(0.74- 0.98)	0.84	(0.73- 0.97)	0.82	(0.71- 0.94)	0.83	(0.72- 0.96)
Road length 10th V 90th %			0.87	(0.77- 0.98)	0.86	(0.76- 0.97)	0.83	(0.74- 0.94)	0.85	(0.75- 0.96)
Length of main roads within 150m										
None	1621	6770	1.00		1.00		1.00		1.00	
Up to 200m	153	792	0.81	(0.67- 0.97)	0.80	(0.67- 0.96)	0.82	(0.69- 0.99)	0.83	(0.69- 0.99)
200-400m	433	2126	0.85	(0.76- 0.96)	0.84	(0.75- 0.95)	0.88	(0.78- 0.98)	0.88	(0.78- 0.99)
>400m	50	308	0.68	(0.50- 0.92)	0.67	(0.50- 0.90)	0.73	(0.53- 0.99)	0.73	(0.54- 1.00)
Road length 10th V 90th %			0.82	(0.74- 0.91)	0.81	(0.73- 0.90)	0.85	(0.76- 0.94)	0.85	(0.76- 0.94)
Traffic flow within 150m - total										
<250km/day	393	1521	1.00		1.00		1.00		1.00	
250-1000km/day	645	2658	0.94	(0.82- 1.08)	0.93	(0.81- 1.07)	0.93	(0.81- 1.08)	0.95	(0.82- 1.10)
1000-2500km/day	650	3019	0.83	(0.73- 0.96)	0.84	(0.73- 0.96)	0.85	(0.73- 0.97)	0.86	(0.75- 1.00)
>2500km/day	569	2798	0.79	(0.68- 0.91)	0.78	(0.68- 0.90)	0.81	(0.70- 0.93)	0.82	(0.70- 0.95)
Continuous flow 10 V 90 %			0.82	(0.74- 0.91)	0.81	(0.73- 0.90)	0.84	(0.76- 0.94)	0.83	(0.75- 0.93)
Traffic flow within 150m - HGV										
<10km/day	638	2557	1.00		1.00		1.00		1.00	
10-50km/day	485	1907	1.02	(0.89- 1.16)	1.02	(0.89- 1.16)	0.97	(0.85- 1.11)	0.99	(0.86- 1.13)
50-150km/day	582	2745	0.85	(0.75- 0.96)	0.85	(0.75- 0.97)	0.85	(0.75- 0.96)	0.86	(0.76- 0.98)
>150km/day	552	2787	0.79	(0.70- 0.90)	0.79	(0.70- 0.89)	0.82	(0.72- 0.93)	0.82	(0.72- 0.94)
Continuous flow 10 V 90 %			0.81	(0.73- 0.89)	0.80	(0.72- 0.89)	0.85	(0.77- 0.95)	0.85	(0.76- 0.94)
AVIAH NO2 model										
<33ug/m3	641	2598	1.00		1.00		1.00		1.00	
33-37ug/m3	889	3840	0.94	(0.84- 1.05)	0.93	(0.83- 1.04)	1.05	(0.92- 1.18)	1.06	(0.93- 1.20)
>37ug/m3	727	3558	0.83	(0.74- 0.93)	0.82	(0.73- 0.92)	0.96	(0.84- 1.10)	1.00	(0.87- 1.15)
NO2 concentration			0.76	(0.66- 0.87)	0.75	(0.66- 0.87)	0.91	(0.78- 1.07)	0.95	(0.80- 1.12)

Table 7: Flexural eczema in the last year

			Unadjusted		Adjusted for age-sex		Adjusted for age-sex-dep		Adjusted for age-sex-dep-school	
	Cases	Controls	OR	95%CI	OR	95%CI	OR	95%CI	OR	95%CI
Distance - roads										
>150m	220	3629	1.00		1.00		1.00		1.00	
50-150m	351	4563	1.27	(1.07- 1.51)	1.27	(1.06- 1.51)	1.26	(1.06- 1.51)	1.26	(1.06- 1.51)
<50m	285	3605	1.30	(1.09- 1.56)	1.31	(1.09- 1.57)	1.28	(1.06- 1.54)	1.25	(1.04- 1.51)
Inv root dist			1.24	(1.04- 1.47)	1.24	(1.04- 1.48)	1.21	(1.02- 1.44)	1.18	(0.99- 1.41)
Distance - mainroads										
>150m	577	8089	1.00		1.00		1.00		1.00	
50-150m	177	2339	1.06	(0.89- 1.26)	1.06	(0.89- 1.27)	1.11	(0.93- 1.32)	1.12	(0.94- 1.34)
<50m	102	1369	1.04	(0.84- 1.30)	1.05	(0.84- 1.30)	1.11	(0.89- 1.39)	1.16	(0.92- 1.45)
Inv root dist			1.04	(0.90- 1.20)	1.04	(0.90- 1.20)	1.09	(0.95- 1.26)	1.12	(0.97- 1.29)
Length of roads within 150m										
none	220	3629	1.00		1.00		1.00		1.00	
up to 200m	100	1367	1.21	(0.95- 1.54)	1.20	(0.94- 1.53)	1.20	(0.94- 1.53)	1.18	(0.92- 1.51)
200-400m	393	4926	1.32	(1.11- 1.56)	1.31	(1.11- 1.56)	1.30	(1.10- 1.55)	1.30	(1.09- 1.54)
>400m	143	1875	1.26	(1.01- 1.56)	1.27	(1.02- 1.58)	1.24	(1.00- 1.55)	1.22	(0.98- 1.52)
Road length 10th V 90th %			1.25	(1.05- 1.49)	1.26	(1.05- 1.51)	1.24	(1.03- 1.48)	1.21	(1.01- 1.46)
Length of main roads within 150m										
none	577	8089	1.00		1.00		1.00		1.00	
up to 200m	75	910	1.16	(0.90- 1.48)	1.14	(0.89- 1.47)	1.18	(0.92- 1.52)	1.19	(0.93- 1.54)
200-400m	182	2449	1.04	(0.88- 1.24)	1.05	(0.88- 1.25)	1.10	(0.92- 1.31)	1.13	(0.94- 1.35)
>400m	22	349	0.88	(0.57- 1.36)	0.89	(0.57- 1.38)	0.99	(0.63- 1.53)	1.03	(0.66- 1.61)
Road length 10th V 90th %			1.01	(0.87- 1.17)	1.02	(0.88- 1.18)	1.07	(0.92- 1.25)	1.09	(0.94- 1.28)
Traffic flow within 150m - total										
<250km/day	122	1872	1.00		1.00		1.00		1.00	
250-1000km/day	218	3169	1.06	(0.84- 1.32)	1.05	(0.84- 1.32)	1.07	(0.85- 1.35)	1.04	(0.82- 1.31)
1000-2500km/day	281	3486	1.24	(1.00- 1.54)	1.23	(0.99- 1.53)	1.27	(1.02- 1.58)	1.26	(1.01- 1.59)
>2500km/day	235	3270	1.10	(0.88- 1.38)	1.10	(0.88- 1.38)	1.17	(0.93- 1.47)	1.14	(0.90- 1.44)
Continuous flow 10 V 90 %			0.96	(0.83- 1.11)	0.96	(0.83- 1.12)	1.01	(0.87- 1.18)	1.01	(0.86- 1.18)
Traffic flow within 150m - HGV										
<10km/day	193	3091	1.00		1.00		1.00		1.00	
10-50km/day	185	2311	1.28	(1.04- 1.58)	1.28	(1.04- 1.58)	1.24	(1.00- 1.53)	1.15	(0.93- 1.43)
50-150km/day	244	3162	1.24	(1.02- 1.50)	1.23	(1.01- 1.49)	1.24	(1.02- 1.51)	1.23	(1.01- 1.51)
>150km/day	234	3233	1.16	(0.95- 1.41)	1.16	(0.96- 1.42)	1.23	(1.01- 1.51)	1.20	(0.98- 1.48)
Continuous flow 10 V 90 %			0.89	(0.76- 1.03)	0.89	(0.76- 1.04)	0.96	(0.82- 1.12)	0.97	(0.82- 1.13)
SAVIAH NO2 model										
<33ug/m3	227	3081	1.00		1.00		1.00		1.00	
33-37ug/m3	336	4520	1.01	(0.85- 1.20)	1.01	(0.85- 1.21)	1.18	(0.98- 1.43)	1.19	(0.98- 1.45)
>37ug/m3	293	4196	0.95	(0.79- 1.13)	0.95	(0.80- 1.14)	1.20	(0.98- 1.47)	1.15	(0.93- 1.43)
NO2 concentration			0.88	(0.72- 1.09)	0.89	(0.72- 1.10)	1.16	(0.91- 1.49)	1.11	(0.86- 1.44)

REFERENCES

Adema, E. H., 1989, *Inleiding in de luchthygiëne. Diktaat DA-College H100-601.* (Wageningen, Vakgroep Luchthygiëne en –verontreiniging)

AEA, 1994, *Air pollution in the UK: 1994.* AEA/RAMP/200015001/1 (Abingdon, AEA).

Ahmed, S. and De Marsily, G., 1987, Comparison of geostatistical methods for estimating transmissivity using data on transmissivity and specific capacity. *Water Resources Research,* 23, 9, 1717-1737.

Anderson, P. M., 1970, The uses and limitations of trend surface analysis in studies of urban air pollution. *Atmospheric Environment,* 4, 129-147.

Anh, V., Duc, H. and Shannon, I., 1997, Spatial variability of Sydney air quality by cumulative semivariogram. *Atmospheric Environment,* Vol. 31, No. 24, 4073-4080.

Atkins, D. H. F., Sandalls, J., Law, D. V., Hough, A. M. and Stevenson, K., 1986, *The measurement of nitrogen dioxide in the outdoor environment using passive diffusion tube samplers AERA R12133.* Environmental and Medical Sciences Division, Harwell Laboratory, Oxfordshire.

Bailey , T. C. and Gatrell, A. C., 1995, *Interactive spatial data analysis.* (Harlow, Longman Scientific & Technical)

Benson, P.E, 1979, *CALINE3 – A versatile dispersion model for predicting air pollutant levels near highways and arterial streets.* Report No. FHWA/CA/TL-79/23

Benson, P. E., 1989, CALINE4 – *A dispersion model for predicting air pollutant concentrations near roadways.* Report No. FHWA/CA/TL-84/15

Benson, P. E, 1992, A review of the development and application of the CALINE3 and CALINE4 models. *Atmospheric Environment,* 26B, 3, pp 379 – 390.

Bly, P. H. and Dasgupta, M., 1995, Urban travel demand: a growing business, but can it last? in: Sucharov, L. J. (Ed), *Urban Transport and the Environment for the 21st Century.* (Southampton Boston, Computational Mechanics Publications) 89-97.

Boubel, R. A., Fox, D. L., Turner, D.B. and Stern, A. C., 1994, *Fundamentals of Air Pollution Third Edition* (U.S.A., Academic Press)

Briggs, D. J. and Elliot, P., 1995, GIS methods for the analysis of relationships between environment and health. *World Health Statistics Quarterly,* 48, 85-94.

Briggs, D. J., Collins, S., Elliott, P., Fischer, P., Kingham, S., Lebret, E., Pryl, K., Reeuwijk, H. van, Smallbone, K. and Veen, A. van de, 1997, Mapping urban air pollution using GIS: a regression-based approach. *Int. J. Geographical Information Science,* 11, 7, 699-718.

Briggs, D. J., Ashmore, M., Bell, M. and Elliott, P., 1998, Coming up for air. *The Surveyor* 1 October 1998, 22-24.
Brunekreef, B., Janssen, N. A. H., Hartog, J. de, Harssema, H., Knape, M. and Vliet, P. van, 1997, Air pollution from truck traffic and lung function in children living near motorways. *Epidemiology*, 8, 3, 298-303.

Buckingham, C. et al, 1998, *London Atmospheric Emissions Inventory*. (London, London Research Centre).

Bull, M. (unpublished) *A user's experience of dispersion models*. Unpublished paper, Arup Environmental Ltd.

Burden, N. C., Whitwell, I. And Longhurst, J. W. S. (unpublished) *Testing the tools for air quality management: A comparison of predictions of nitrogen dioxide concentrations by CALINE4 and the DMRB models with monitored levels at the M4/M5 interchange in Bristol, UK*. Department of Environmental Health and Science, University of the West of England, Bristol.

Burrough, P. A. and McDonnel, R. A., 1998, *Principles of geographical information systems*. (Oxford, Oxford University Press)

Burrough, P. A., 1986, *Principles of geographical information systems for land resources assessment*. (Oxford, Clarendon Press)

CERC, 1998, ADMS-Urban An urban air quality management system. User guide. (Cambridge, CERC)

Collins, S., 1997, Modelling urban air pollution using GIS. In: Craglia, M. and Couclesis, H. (Eds.). *Geographic Information research. Bridging the Atlantic*. (London, Taylor & Francis), 427-440.

Collins, S., 1998a, *A GIS approach to modelling traffic-related air pollution*. Ph. D. Thesis, The University of Huddersfield.

Collins, S., 1998b, Modelling spatial variations in air quality using GIS, in: Gatrell, A. C. and Löytönen, M. (Eds), *GIS and Health*. (London, Taylor & Francis Ltd) 81-95.

Commission on the European Communities, 1995, *CORINAIR*. (Luxembourg, Office for Official Publications of the European Communities.

Committee of the Environmental and Occupational Health Assembly of the American Thoracic Society 1996 Health effects of outdoor pollution. *American Journal of Respiratory Critical Care Medicine* 153, 3-50.

Committee on Medical Effects of Air Pollutants, 1995, *Asthma and outdoor air pollution*. (London: HMSO)

Cornelius, J. M. and Reynolds, J. F., 1991, On determining the statistical significance of discontinuities within ordered ecological data. *Ecology* 72, 6, 2057-60.

Corvalán, C., Briggs, D. and Kjellström, T., 1996, Development of environmental health indicators, in: Briggs, D. J., Corvalán, C. and Nurminen M. (Eds) *Linkage methods for environment and health analysis: general guidelines. A report of the Health and Environment Analysis for Decision-making Project (HEADLAMP)*. UNEP, ESEPA & WHO. Geneva: Office of Global and Integrated Environmental Health, WHO. 19-54.

Cronshey, R. G., Theurer, F. D. and Glenn R. L., 1996, GIS water-quality model interface: a prototype, in: Goodchild, M. F., Steyaert, L. T., Park, B. O., Johnston, C., Maidment, D., Crane, M. and Glendinning, S. (Eds) *GIS and Environmental Modelling: Progress and research issues*, (Ford Collins: GIS World Books) 287-291.

D'Agnese, F. A., Turner, A. K. and Faunt, C. C., 1996, Using geoscientific information systems for three-dimensional regional groundwater flow modelling: Death Valley region, Nevada and California, in: Goodchild, M. F., Steyaert, L. T., Park, B. O., Johnston, C., Maidment, D., Crane, M. and Glendinning, S. (Eds) *GIS and Environmental Modelling: Progress and research issues*, (Ford Collins: GIS World Books) 265-270.

Dalbokova, D. L., Dimitrova, R. S., Boeva, B. P., Henriques, W. D. and Briggs, D. J., 1999, Tools for risk assessment: Geographic Information Systems, in: Briggs, D. J., Stern, R and Tinker, T. (Eds) *Environmental Health for All. Risk assessment and risk communication for National Environmental Health Action Plans.* NATO Sciences Series. (Dordrecht, Kluwer Academic Publishers), 133-146.

Danard, M. B., 1972, Numerical modelling of carbon monoxide concentrations near a highway. *Journal Applied Meteorology*, 11, 947

Department of the Environment, the Scottish Office and the Welsh Office, 1998, *Review and Assessment: Pollutant -Specific Guidance. Part IV of the Environment Act 1995 Local Air Quality Management*. (London: The Stationary Office)

Department of the Environment and the Scottish Office (1997) *The United Kingdom National Air Quality Strategy*, (London: The Stationery Office)

Department of the Environment, 1996, *Expert Panel on Air Quality Standards, Nitrogen Dioxide*. (London: The Stationery Office)

Department of Transport, 1994, *Design manual for roads and bridges, Vol 11: Environmental assessment, Section 3, Part 1 – Air Quality*. (London: HMSO)

DETR, 1997a, *Transport statistics Great Britain* (London, The Stationery Office)

DETR, 1997b, *Air Quality and traffic management*. (London: The Stationery Office)

DETR, 1995, *London Traffic Monitoring Report: 1995*. (London, HMSO)

DETR, 1998a, *A new deal for transport: Better for everyone. The government's white paper on the future of transport* (London, The Stationery Office)

DETR, 1998b, *Review of the United Kingdom national air quality strategy. A consultation document* (London, The Stationery Office)

Deutsch, C. V. and Journel, A. G., 1992, *GSLIB, Geostatistical Software Library and user's guide*. (Oxford, Oxford University Press)

Dockery, D. W., Pope, C. A. III, Xu, X., Spengler, J. D., Ware, J. H., Fay, M. E., Ferris, B. G. and Speizer, F. E., 1993. An association between air pollution and mortality in six U.S. cities. *The New England Journal of Medicine*, 329, 24, 1753-1759.

Duhme, H., Weiland, S. P., Keil, U., Kraemer, B., Schmid, M., Stender, M. and Chambless, L., 1996, The association between self-reported symptoms of asthma and allergic rhinitis and self-reported traffic density on street of residence in adolescents. *Epidemiology*, 7, 6, 578-582.

Edwards, J., Walters, S. and Griffiths, R. K., 1994, Hospital admissions for asthma in preschool children: Relationship to major roads in Birmingham, United Kingdom. *Archives of Environmental Health*, 49, 4, 223-227.

Eerens, H. C., Sliggers, C. J. and Hout, K. D. van, 1993, The CAR model: The Dutch method to determine city street air quality. *Atmospheric Environment*, 27B, 4, 389-399.

Elliott, P., Cuzick, J., English, D. and Stern, R. (eds.) 1992 *Geographical and environmental epidemiology: methods for small-area studies* (Oxford: Oxford University Press).

Elliott, P., Briggs, D. J., Lebret, E., Gorynski, P and Kriz, B., 1995, Small area variations in air quality and health (the SAVIAH study): design and methods. (Abstract) *Epidemiology*, 6, S32.

Elliott, P. and Briggs, D. J., 1998, Recent developments in the geographical analysis of small area health and environmental data, in: Scally, S. (Ed) *Progress in public health* (London: FT Healthcare) 101-125.

Elsom, D., 1987, *Atmospheric Pollution*. (Oxford: Blackwell)

Elsom, D., 1996, *Smog alert, Managing urban air quality*. (London: Earthscan)

Farrow, A., Taylor, H. and Golding, J., 1997, Time spent in the home by different family members. *Environmental Technology*, 18, 605-614.

French, D. P. and Reed, M., 1996, Integrated environmental impact model and GIS for oil and chemical spills, in Goodchild, M. F., Steyaert, L. T., Park, B. O., Johnston, C., Maidment, D., Crane, M. and Glendinning, S. (Eds) *GIS and Environmental Modelling: Progress and research issues*, (Ford Collins: GIS World Books) 197-198.

Gair , A. J. and Penkett, S. A., 1995 The effects of wind speed and turbulence on the performance of diffusion tube samplers. *Atmospheric Environment* 29, 2529-2533.

Gatrell, A. C., 1989, On the spatial representation and accuracy of address-based data in the United Kingdom. *Int, J. Geographic Information Systems*, 3, 4, 335-348.

Gatrell, A. C. and Dunn, C. E., 1995, Geographic information systems and spatial epidemiology: Modelling the possible association between cancer of the larynx and incineration in north-west England, in: Lepper de, M. J. C., Scholten, H. J. and Stern R. M. *The added value of geographic information systems in public and environmental health*. (Dordrecht, Kluwer Academic Publishers) 215-235.

Gatrell, A. C. and Löytönen, M. (Eds), 1998, *GIS and Health*. (London, Taylor & Francis Ltd).

Gifford, F. A. and Hanna, S. R., 1973, Modelling urban air pollution. *Atmospheric Environment*, 7, 131-136.

Gillham, C. A., Leech, P. K. and Egglestone, H. S., 1992, *National atmospheric emissions inventory*. (London, Department of Environment.)

Gladstone, K. P., Niki, H., Shepson, P. B., Bottenheim, J. W., Schiff, H. I. and Sandhu, H. S., 1991, Photochemical oxidant concentrations in two Canadian prairie cities: model evaluation. *Atmospheric Environment*, 27B, 1, 105-120

Goldsmith, A., 1986, *Measurements of nitrogen dioxide at rural sites using diffusion samplers*. Warren Spring Laboratory Report no LR 582 (AP)M.

Goodchild, M. F., Steyaert, L. T., Park, B. O., Johnston, C., Maidment, D., Crane, M. and Glendinning, S. (Eds), 1996, *GIS and Environmental Modelling: Progress and research issues*, (Ford Collins: GIS World Books).

Grønskei, K. E., Walker, S. E. and Gram, F., 1993, Evaluation of a model for hourly spatial concentration distributions. *Atmospheric Environment*, 26B, 1, 107-116.

Harrison, R. M. (ed), 1990, Pollution: causes, effects and control. (Cambridge, Royal Society of Chemistry) 201-219.

Harssema, H., 1987, *Berekenen en meten van de luchtkwaliteit. Dictaat DA-college H100-131*. (Wageningen, Vakgroep Luchthygiëne en –verontreiniging)

Hartog, K. D., 1995, *Laboratory procedures for measuring SO2 Willems-badges and NO2 Palmes tubes*. Wageningen Agricultural University, Department of Air Quality, Report No. IV-202.

Heal, M. R. and Cape, J. N., 1997, A numerical evaluation of chemical interferences in the measurements of ambient nitrogen dioxide by passive diffusion samplers. *Atmospheric Environment*, 31, 13, 1911-1923.

Heida, H., Jong, A. L. de and Huygen c., 1989, Model calculations of street-air concentrations for carbon monoxide and nitrogen dioxide in Amsterdam, in Brasser L. J.

and Mulder, W. C. (Eds) *Man and his Ecosystem. Proc. 8th World Clean Air Congress.* (Elsevier, Amsterdam) 3 233-238.

Henriques, W. D. and Briggs, D. J., 1998, Environmental modelling in the NEHAP process, in: Briggs, D. J., Stern, R and Tinker, T. (Eds) *Environmental Health for All. Risk assessment and risk communication for National Environmental Health Action Plans.* NATO Sciences Series. (Dordrecht, Kluwer Academic Publishers), 113-132.

Hernandez, E., Martin, F. and Valero, F., 1992, Statistical forecast models for daily air particulate iron and lead concentrations for Madrid, Spain, *Atmospheric Environment*, 12, 599-604.

HMIP, 1993, *An assessment of the effects of industrial releases of nitrogen oxides in the East Thames corridor*. (London: HMSO)

Hodgson, M. E., 1991, Characteristics of the window for neighbourhood analysis of nominal data. In: *Technical Papers of the ACSN-ASPRS Annual Convention, Baltimore. Vol. 3. Remote Sensing.* (Baltimore:ACSM/ASPRS), 206-214.

Hoek, G. and Brunekreef, B., 1993, Acute effects of a winter air pollution episode on pulmonary function and respiratory symptoms of children. *Archives of Environmental Health*, 48, 118-124.

Huang, G., 1992, A stepwise cluster analysis method for predicting air quality in an urban environment. *Atmospheric Environment*, 26B, 3, 349-357.

Hutchinson, M. F., 1984, A summary of some surface fitting and contouring programs for noisy data. *CSIRO Division of Mathematics and Statistics Consulting Report ACT84/6.* CSIRO Division of Mathematics and Statistics, Yarralumla, ACT, Australia.

Hutchinson, M. F., 1996, Thin plate spline interpolation of mean rainfall: Getting the temporal statistics correct, in Goodchild, M. F., Steyaert, L. T., Park, B. O., Johnston, C., Maidment, D., Crane, M. and Glendinning, S. (Eds) *GIS and Environmental Modelling: Progress and research issues*, (Ford Collins: GIS World Books) 85-90.

Indic, 1996, AirViro user's guide v2, Sweden

Inoue, T., Hoshi, M. and Taguri, M., 1986a, Regression analysis of nitrogen oxide concentration. *Atmospheric Environment*, 20, 1, 71-85.

Inoue, T., Hoshi, M. and Taguri, M., 1986b, Prediction of nitrogen oxide concentration by a regression model. *Atmospheric Environment*, 20, 12, 2325-2337.

Isaksen, I. S. A., Hesstvedt E. and Hov, O., 1978, A chemical model for urban plumes: test for ozone and particulate sulphur formation in St. Louis urban plume. *Atmospheric Environment*, 12, 599-604.

Jakeman, A. J., Bai, J. and Miles G. H., 1991, Prediction of seasonal extremes of one-hour average urban CO concentrations. *Atmospheric Environment*, 25B, 3, 219-229

Jansen, N. A. H., Hoek, G., Harssema, H. and Brunekreef, B., 1997, Childhood exposure to PM_{10}: relation between personal, classroom, and outdoor concentrations. *Occupational and Environmental Medicine*, 54, 888-894.

Jantunen M. J., Hanninen O., Katsouyanni K., Knoppel H., Lebret E., Maroni M., Saarela K., Sram R. and Zmirou D. (in press). Air pollution exposure in European cities: the 'EXPOLIS' study. *Journal of Exposure Analysis and Environmental Epidemiology*.

Jin, S. and Demerjian, K., 1993, A photochemical box model for urban air quality study. *Atmospheric Environment*, 27B, 4, 371-387.

Kingham, S. P., Gatrell, A. C. and Rowlingson, B., 1995, Testing for clustering of health events within a geographical information system framework. *Environment and Planning*, 27, 809-821.

Kingham, S., Briggs, D., Elliot, P., Fisher, P. and Lebret, E., submitted, Concentrations of traffic-related pollutants in indoor and outdoor air in relation to vehicles intensity in Huddersfield, England. *Atmospheric Environment.*

Knotters, M., Brus, D. J. and Oude Voshaar, J. H., 1995, A comparison of kriging, co-kriging and kriging combined with regression for spatial interpolation of horizon depth with censored observations. *Geoderma*, 67, 227-246.

Kono, H. and Ito, S., 1990a A comparison of concentrations estimates by the OMG VOLUME-SOURCE dispersion model with three line source dispersion models *Atmospheric Environment*, 24B, 2, 253-260.

Kono, H. and Ito, S., 1990b, A micro-scale dispersion model for motor vehicle exhaust gas in urban areas – OMG-VOLUME-SOURCE model. *Atmospheric Environment*, 24B, 2, 243-251.

Ku, J. Y., Rao, S. T. and Rao, K. S., 1987a, Numerical simulation of air pollution in urban areas: model development. *Atmospheric Environment*, 21, 1, 201-212.

Ku, J. Y., Rao, S. T. and Rao, K. S., 1987b, Numerical simulation of air pollution in urban areas: model performance. *Atmospheric Environment*, 21, 1, 201-212.

Lee, T. J. and Pielke, R. A., 1996, GIS and atmospheric modelling: a case study, in: Goodchild, M. F., Steyaert, L. T., Park, B. O., Johnston, C., Maidment, D., Crane, M. and Glendinning, S. (Eds) *GIS and Environmental Modelling: Progress and research issues*, (Ford Collins: GIS World Books) 239-242.

Leenearts, H., Okx, J. P. and Burrough, P. A., 1989, Co-kriging: and accurate and inexpensive means of mapping floodplain soil pollution by using elevation data. *Geostatistics*, 1, 371-382.

Lefohn, A. S., Knudsen, H. P. and McEvoy Jr, L. R., 1988, The use of kriging to estimate monthly ozon exposure parameters for the southeastern United States. *Environmental Pollution*, 53, 27-42.

Livingstone, A. E., Shaddick, G., Grundy, C. and Elliot, P., 1996, Do people living near inner city main roads have more asthma needing treatment? Case control study. *British Medical Journal*, 312, 676-677.

London Research Centre, 1993, *London Energy Study*. (London, London Research Centre).

Martin, D., 1996, *Geographic Information Systems: Socioeconomic applications*. (London, Routledge).

Matheron, G., 1971, The theory of regionalized variables and its applications. *Les Cahiers du Centre de Morphologie Mathematique de Fontainebleau*, No. 5, Paris.

Mattson, M. D. and Godfrey P. J., 1994, Identification of road salt contamination using multiple regression and GIS. *Environmental Management*, 18, 5, 767-773.

McBratney, A. B. and Webster, R., 1986, Choosing functions for semi-variograms of soil properties and fitting them to sampling estimates. *Journal of Soil Science*, 37, 617-639.

McRea, G. J., Goodin, W. R. and Seinfeld, J. H., 1982, Development of a second-generation mathematical model for urban air pollution – I. Model formulation. *Atmospheric Environment* 16, 4, 679-696.

McRea, and Seinfeld, J. H., 1983, Mathematical model for urban air pollution – II. Evaluation of model performance. *Atmospheric Environment* 17, 3, 501-522.

Moore, I. D., 1996, Hydrologic modelling and GIS, in: Goodchild, M. F., Steyaert, L. T., Park, B. O., Johnston, C., Maidment, D., Crane, M. and Glendinning, S. (Eds) *GIS and Environmental Modelling: Progress and research issues*, (Ford Collins: GIS World Books) 143-148.

Murakami, M., Ono, M. and Tamura. K., 1990, Health problems of residents along heavy-traffic roads. *Journal of Human Ergology*, 19, 101-106.

Mutius E von., Fritzsch, C., Weiland, S.K., Roll, G. and Magnussen, H. 1992 Prevalence of asthma and allergic disorders among children in the United Germany: a descriptive comparison. *British Medical Journal* 305, 1395-99.

Nakai, S., Nitta, H. and Maeda, K., 1995, Respiratory health associated with exposure to automobile exhaust II. Personal NO2 exposure levels according to distance from the roadside., *Journal of Exposure Analysis and Environmental Epidemiology*, 5, 2, 125-136.

Namdeo, A. K., and Colls, J. J., 1996, Development and evaluation of SBLINE, a suit of model for the prediction of pollution concentrations form vehicles in urban areas. *The Science of Total Environment*, 189/190, 311-320.

Nitta, H., Nakai, S., Maeda, K., Aoki, S. and Ono, M., 1993, Respiratory health associated with exposure to automobile exhaust. I. Results of cross-sectional studies in 1979, 1982 and 1983., *Archives of Environmental Health*, 48, 1, 53-58.

Noll, K. E., Miller, T. L. and Claggett, M., 1978, A comparison of three highway line source dispersion models. *Atmospheric Environment*, 12, 1323-1329.

Oliver, M. A. and Webster, R., 1990, Kriging: a method of interpolation for geographical information systems. *Int. J. Geographical Information Systems*, 4, 3, 313-332.

Onursal, B. and Gautam, S. P., 1997, *Vehicular air pollution. Experiences from seven Latin American urban centers*. World Bank technical paper no. 373 (Washington, D.C., The World Bank), p17.

Oosterlee, A., Drijver, M., Lebret, E. and Brunekreef, B., 1996, Chronic respiratory symptoms in children and adults living along streets with high traffic density. *Occupational and Environmental Medicine*, 53, 241-247.

OPCS (Office of Population Censuses and Surveys), 1991, *1991 census: preliminary report for England and Wales*, (London, HMSO)

Palmes, E. D., Gunnison, A. F., DiMattiio, J. and Tomczyk, C., 1976, Personal sampler for nitrogen dioxide, *Am. Ind. Hyg. Assoc. J.*, 37, 570-577

Pasquill, F., 1974, *Atmospheric diffusion*. 2nd ed.(New York, Halstead Press).

Perry, S. G., Cimorelli, A. J., Fee, R. F., Paine, R. J., Venkatram, A. and Weil, J. C., 1994, *AERMOD: A dispersion model for industrial source applications*. Boulder, USEPA report no 94-TA23.04.

Pershagen, G., Rylander, E., Norberg, S., Eriksson, M. and Nordvall, S.L., 1995, Air pollution involving nitrogen dioxide exposure and wheezing bronchitis in children. *International Journal of Epidemiology*, 24, 6, 1147-1153.

Pilnis, C., Kassomenos, P. and Kallos, G., 1993, Modelling of photochemical pollution in Athens, Greece. Application of the RAMS-CALGRID modelling system. *Atmospheric Environment*, 27B, 4, 353-370.

Pitts, R. O. and Lyons, T. J., 1992, A coupled mesoscale/particle model applied to an urban area. . *Atmospheric Environment*, 26B, 3, 279-289.

Pope, C. A. III, 1991, Respiratory hospital admissions associated with PM10 pollution in Utah, Salt Lake, and Cache valleys. *Archives of Environmental Health*, 46, 89-97.

Pope, C. A., Dockery, D. W., Spengler, J. D. and Raizenne, M. E., 1991, Repiratory health and PM10 pollution: A daily time series analysis. *American Revue of Respiratory Disease*, 144, 668-674

Pope C. A., Bates, D. A. and Raizenne, M. E., 1995. Health effects of particulate air pollution: time for reassessment? *Environmental Health Perspectives*, 103:472-480.

Pul, W. A. J. van, Zantvoort, E. D. G. van, Leeuw, F. A. A. M. de, and Sluyter, R. J. C. F., 1996, *Urban Air Quality Assessment Model UAQAM*. (Bilthoven, RIVM)

Rao, S. T., Sistla, G., Keenan, M. T. and Wilson, J. S., 1980, An evaluation of some commonly used highway dispersion models. *Journal of the Air Pollution Control Association*, 30, 3, 239-246

Rao, K. S., Ku, K. Y. and Rao, S. T., 1989, A comparison study of three urban air pollution models. *Atmospheric Environment*, 23, 4, 793-801.

van Reeuwijk, H., Fisher, P. H., Harssema, H., Briggs, D. J., Smallbone, K. and Lebret, E., 1998, Field comparison of two passive samplers to assess spatial variation. *Environmental Monitoring and Assessment*, 50, 37-51.

Robeson, S. M. and Steyn, D. G., 1990, Evaluation and comparison of statistical forecast models for daily maximum ozone concentrations. *Atmospheric Environment*, 24B, 2, 303-312.

Robeson, S. M. and Willmott, C. J., 1996, Spherical spatial interpolation and terrestrial air temperature variability. In Goodchild, M. F., Steyaert, L. T., Park, B. O., Johnston, C., Maidment, D., Crane, M. and Glendinning, S. (Eds), *GIS and Environmental Modelling: Progress and research issues*, (Ford Collins: GIS World Books) 111-115.

Rodden, J. B., Green, N. J., Messina, A. D. and Bullin, J. A., 1982, Comparison of roadway pollutant dispersion models using the Texas data. *Journal of the Air Pollution Control Association*, 32, 12, 1226-1228.

Roemer, M. G. M., 1989, *Box model calculations of emission abatement strategies in the greater Athens area.* (Delft (NL), TNO) Report No. R89/310.

Romieu, I., Weitzenfeld, H. and Finkelman, J., 1990, *Urban air pollution in Latin America and the Caribbean: Health perspectives.* World Health Statistics, Quarterly, 43, 153-167.

Royal Commission on Environmental Pollution, 1995, *Eighteenth report – Transport and the Environment.* (London, HMSO)

Sally Liu, L.-J. and Rossini, A. J., 1996, Use of kriging models to predict 12-hour mean ozone concentrations in metropolitan Toronto – a pilot study. *Environment International*, 22, 6, 677-692.

Scheffe, R. D. and Morris, R. E., 1993, A review of the development and evaluation of the urban airshed model. *Atmospheric Environment*, 24B, 1, 75-86.

Schwartz, J., Dockery, D. W., Ware, J. H., Sprengler, J. D., Wypij, D., Koutrakis, P., Speizer, F. E. and Ferris, B. G. Jr., 1989. *Acute effects of acid aerosols on respiratory symptoms reporting in children.* Air Pollution Control Association Paper, 89, 92.1.

Schwartz, J., 1993. Particulate air pollution and chronic respiratory disease. *Environmental Research*, 62, 7-13.

SEIPH, 1996, *Air quality in London 1995. The third report of the London Air Quality Network.* (Tunbridge Wells, SEIPH)

SEIPH, 1997, *The AIM project and air quality in London 1996. The fourth report of the London Air Quality Network.* (Tunbridge Wells, SEIPH)

Şen, Z., 1995, Regional air pollution assessment by cumulative semivariogram technique. *Atmospheric Environment*, 29, 4, 543-548.

Si, J. P., Harrison, R. M., 1997, Regression modelling of hourly NOx and NO2 concentrations in urban air in London. *Atmospheric Environment*, 31, 24, 4081-4094.

Simpson, R. W. and Miles, G., 1990, Controlling emissions to avoid violations of health standards for short term and long term exposures to TSP concentrations. *Atmospheric Environment*, 24B, 1, 75-86.

Souleyrette, R. R., Sathisan, S. K., James, D. E. and Lim, S., 1992, GIS for transportation and air quality analysis, in: Wayson, R. L. (Ed) Transportation planning and air quality. Proceedings of the national conference. (New York, American Society of Civil Engineers) 182-194.

Spengler, J. D., Schwab, M., Ryan, P. B., Billick, I. H., Colome, S., Wilson, A. L. and Becker, E., 1994, Personal exposure to nitrogen dioxide in the Los Angeles Basin. *Journal of Air and Waste Management Association*, 44, 39-47.

Stanners, D. and Bordeau, P. (eds). 1995 *Europe's environment. The Dobrís assessment.* Copenhagen: European Environment Agency.

Stein, A., Dooremolen, W. van, Bouma, J. and Bregt, A. K., 1988, Cokriging point data on moisture deficit. *Soil Science Society of America Journal*, 52, 1418-1423.

Strachan D. P., Taylor, E. M. and Carpenter, R.G., 1996, Family structure, neonatal infection, and hay fever in adolescence. *Archives of Disease in Childhood*, 74, 422-426.

Strachan, D. P. and Carey, I. M., 1995, Home environment and severe asthma in adolescence: a population based case-control study. *British Medical Journal*, 311, 1053-1056.

Strachan, D. P., Elliot, P. and Briggs, D., 1998, *Relationship of asthma and allergic rhinitis to local traffic density and ambient pollution modelled at a small area level.* Final Report STRACHAN/AIR/96/11.

Tartaglia, M., Giannone, A., Gualtieri, G. and Barbaro, A., 1995, Development and validation of an urban street canyon model based on carbon-monoxide experimental data measured in Firenze, in: Sucharov, L. J. (Ed) *Urban Transport and the Environment for the 21st Century.* (Southampton Boston, Computational Mechanics Publications) 173-182.

Teppo, L., 1998, Problems and possibilities in the use of cancer data by GIS – experience in Finland, in Gatrell, A. C. and Löytönen, M. (Eds), *GIS and Health.* (London, Taylor & Francis Ltd) 167-177

Trinca, S., 1998, GIS applications for environment and health in Italy, in Gatrell, A. C. and Löytönen, M. (Eds), *GIS and Health.* (London, Taylor & Francis Ltd) 113-123.

USEPA, 1995, *User's guide for the industrial source complex (ISC3) dispersion models. Volume I – User instructions.* Report No. EPA-454/B-95-003a

Vauclin, M., Vieira, S. R., Vachaud, G. and Nielsen, D. R., 1983, The use of co-kriging with limited field soil observations. *Soil Science Society of America Journal*, 47, 2, 175-183.

Venkatram, A., 1988, On the use of kriging in the spatial analysis of acid precipitation data. *Atmospheric Environment*, 22, 9, 1963-1975.

Vincent, P. and Gatrell, A. C., 1991, The spatial distribution of radon gas in Lancashire (UK). A kriging study, in: Harts, J, Ottens, H. F. L. and Scholten, H. J., *EGIS '91 Proceeding. Second European conference on geographical information systems.* (Utrecht: EGIS Foundation) 1179-1186.

Vincze, I., Elek, E. and Nàdor, G., 1999, Tools for risk assessment: statistical and spatial methods, in Briggs, D. J., Stern, R and Tinker, T. (Eds) *Environmental Health for All. Risk assessment and risk communication for National Environmental Health Action Plans.* NATO Sciences Series. (Dordrecht, Kluwer Academic Publishers), 97-111.

Vine, M. F., Degnan, D., Hanchette, C., 1997, Geographic information systems: their use in environmental epidemiological research. *Environ Health Perspect* 1997 Jun; 105, 6, 598-605.

Wallace, L., 1996, Indoor particles: a review. *Journal of the Air and Waste Management Association*, 46, 98-126.

Wang, X. and Stauffer B., 1995. Application of GIS for environmental impact analysis in a traffic relief study. *Comput. Environ. And Urban Systems*, 19, 4, 275-286.

Wartenberg, D., Uchrin, C. and Coogan, P., 1991, Estimating exposure using kriging: A simulation study. *Environmental Health Perspectives*, Vol. 94, 75-82.

Wartenberg, D., 1993 Some epidemiologic applications of kriging, in: Soares, A. (Ed), *Geostatistics Troia ' 92. Vol. 2.* 911-922.

Watson, D. F. and Philip, G. M., 1985, A Refinement of Inverse Distance Weighted Interpolation. *Geo-Processing*, 2, 315 – 327.

Weiland, S. K., Mundt, K. A., Ruckmann, A. and Keil, U., 1994, Self-reported wheezing and allergic rhinitis in children and traffic density on street of residence. *AEP*, 4, 3, 243-247.

WHO, 1992, *Our Planet Our Health. Report of the WHO Commission on Health and Environment.* Geneva, WHO.

Wilkingson, P., Elliot, P., Grundy, C., Shaddick, G., Thakrar, B., Walls, P. and Falconer, S., (unpublished), *Case-control study of hospital admission with asthma in children aged 5-14 years: relation with road traffic in north west London.*

Wills, J. T., 1998, *The development and use of environmental health indicators for epidemiology policy applications: a geographical analysis.* Ph. D. Thesis, University of Leicester.

Wjst, M., Reitmeir, P., Dold, S., Wulff, A., Nicolai, T., Freifrau von Loeffelholz-Colberg, E. and Mutius, E. von, 1993, Road traffic and adverse effects on respiratory health in children. *British Medical Journal*, 307, 596-600.

World Resources Institute (WRI), 1996, *World resources, a guide to the global environment - The urban environment.* (Oxford, The Oxford University Press)

Wu, H. M., 1998, Spatial modelling methods for environmental analysis. M. Phil., The University of Huddersfield.

Yamartino, R. J. and Wiegand, G., 1986, Development and evaluation of simple models for the flow, turbulence and pollutant concentration fields within an urban street canyon. *Atmospheric Environment*, 20, 11, 2137-2156.

van Zandvoort, E. D. G., Sluyter, R. J. C. F. and Larssen. S. (Eds), , 1995. *Air quality in major European cities. Part II: City report forms.* RIVM Rapport 722401009, Bithoven, RIVM.

Zellner, K. and Moussiopoulus, N., 1986, Simulations of the ozone formation caused by traffic in urban areas. *Atmospheric Environment*, 20, 8, 1589-1596.

Zimmerman, J. R. and Thompson R. S., 1974, *HIWAY: A Highway Air Pollution Model.* (North Carolina, Enviromental Protection Agency)